

Understanding Heavy and Light Quark Brownian Motion from AdS/CFT

Analytical Analysis of Open String Evolution in the Bulk

ALEXES K. MES

Supervisors: ASSOC. PROF. W. HOROWITZ AND DR. J. SHOCK

Department of Applied Mathematics, University of Cape Town

Abstract

A revised, consistent, pedagogical approach to studying the motion of heavy and light probe quarks in a thermal plasma using the AdS/CFT correspondence is explored. Two cases are considered: external heavy or light quarks undergoing Brownian motion in the plasma, and an external heavy quark moving through the field theory plasma with a constant velocity.

In the bulk theory, the dual description of these probe quarks are realised as test strings in an asymptotically anti-de Sitter-Schwarzschild background. An on-mass-shell, external heavy quark is modelled as an open string attached at the AdS boundary and hanging towards the horizon. In juxtaposition, an off-mass-shell, external light quark is modelled as an open string, initially stretched between the AdS boundary and just above the horizon, whose AdS boundary endpoint is released to fall at the local speed of light. In both cases, the Schwarzschild black hole excites the modes on the string – resulting in the string’s boundary (stationary or falling) endpoint enduring irregular motion. This corresponds respectively to the heavy or light probe quark in the gauge theory undergoing Brownian motion. For both cases, the mean-squared transverse displacement of the string’s boundary endpoint, $s^2(t; d)$ (equivalent to the mean-squared displacement travelled by the external quark in the thermal plasma) is computed. In the early time limit, the behaviour is found to be ballistic $s^2(t; d) \sim t^2$, while the late time dynamics are diffusive $s^2(t; d) = 2D(d)t$. The diffusion coefficient $D(d)$ is extricated for both the heavy and light quark’s test strings; first in AdS_3 -Schwarzschild and then generalised to AdS_d -Schwarzschild.

Further, an infinitely massive probe quark moving through the thermal plasma with a constant velocity is considered. An open string trailing out behind the quark (arcing down into AdS-Schwarzschild) is used to model the situation. From this, the drag force on the test string is calculated in the bulk and rewritten – via the AdS/CFT correspondence – in terms of relevant quantities in the gauge theory.

Contents

1	Introduction	1
1.1	Dissertation Structure	2
I	Theory	4
2	The Gauge/String Duality	4
2.1	Anti-de Sitter Spacetime as a limit of D3-brane Geometry	4
2.2	The AdS/CFT Conjecture	5
3	Brownian Motion: the Dynamics of Langevin's Model	7
3.1	The Non-retarded Langevin Model	7
3.2	The Generalised Langevin Model	11
II	Calculations in the Bulk	16
4	Analysing Heavy Quark Brownian Motion	16
4.1	Polyakov String Equations of Motion	16
4.2	Leading Order String Behaviour	20
4.2.1	Test Strings in $\mathbb{R}^{1,1}$	20
4.2.2	Test Strings in AdS ₃ -Schwarzschild	22
4.3	Fluctuating Test String Dynamics	24
4.3.1	Nambu-Goto String Equations of Motion for Transverse Fluctuations	25
4.3.2	Calculating the Heavy Quark's Mean-Squared Displacement $s^2(t)$ in AdS ₃ -Schwarzschild	27
4.3.3	The Limiting Cases of $s^2(t)$	34
4.4	Generalising to AdS _d -Schwarzschild	36
5	Analysing Light Quark Brownian Motion	37
5.1	Leading Order String Behaviour	37
5.1.1	Parameterising the Limp Noodle: The Bars <i>et al.</i> method	38
5.1.2	Test Strings in $\mathbb{R}^{1,1}$	42
5.1.3	Test Strings in AdS ₃ -Schwarzschild	47
5.2	Fluctuating Test String Dynamics	48
5.2.1	Calculating the Light Quark's Mean-Squared Displacement $s^2(t)$ in AdS ₃ -Schwarzschild	48
5.2.2	The Limiting Cases of $s^2(t)$	49
5.3	Generalising to AdS _d -Schwarzschild	55
5.3.1	Expanding the AdS ₃ -Schwarzschild Transverse Equations of Motion and its Solution in the Near-Horizon Region	57
5.3.2	Expanding the AdS ₃ -Schwarzschild Metric in the Near-Horizon Region	58
5.3.3	The Diffusion Constant in AdS _d -Schwarzschild	61
6	Drag Force in AdS/CFT	66
6.1	Test Strings in AdS ₅ -Schwarzschild	66
6.2	Generalising to AdS _d -Schwarzschild	72
7	Conclusions and Future Outlook	75
A	Appendix	77
A.1	Polyakov String Equations of Motion	77
A.2	The Virasoro Constraints and String Equations of Motion in Isothermal Coordinates	79
A.3	Energy of a Test String in an AdS-Schwarzschild Background	83
A.4	Nambu-Goto String Equations of Motion for Transverse Fluctuations	86
A.5	Canonical Commutation Relations and Normalised Basis	88
A.6	Leading Order Contributions of the Near-Horizon Tortoise Coordinate	91
A.7	Accessing the Mathematica Code	92

Note on Notation

Throughout this dissertation, lower-case *Latin alphabet* indices (e.g. a, b, c, d) index over the string's worldsheet parameter space, typically over the standard parameter variables (τ, σ) or the light-cone parameter variables (σ^+, σ^-) . Lower-case *Greek alphabet* indices (e.g. $\mu, \nu, \lambda, \gamma$) are used to index over the spacetime, typically in anti-de Sitter spacetime over the temporal t , radial r , and transverse directions X^I . The subspace of anti-de Sitter spacetime spanned by the transverse directions are always indexed by I, J . In some instances the Greek alphabet indices are enumerated – for example, the isothermal coordinate X^μ , where $\mu \in \{0, 1\}$ indexes over the first and second directions in a two-dimensional subspace of spacetime.

Note on Coloured Links

In this dissertation, citations are declared in **dark green**; while links to page numbers, figures, tables, sections and equations are designed to be less noticeable and are given in dark gray.

List of Figures

1	The spacetime around N_c D3-branes in type IIB theory	5
2	A fundamental open string of length ℓ_0 used as a probe in an AdS black hole background . .	16
3	Snapshots of a fundamental open string of length ℓ_0 used as a probe in an AdS black hole background, falling as time increases from left to right	37
4	Light-cone coordinate lattice structure imposed on the worldsheet parameter space in order to determine the general string solution using the Bars <i>et al.</i> method	38
5	The functions (i) $F(z)$ and (ii) $f(z)$ over the range $(-6\sigma_f, 6\sigma_f)$	44
6	The worldsheet parameter space and embedding functions in \mathbb{R}^{1+1}	45
7	The worldsheet parameter space in light-cone coordinates and isothermal embedding functions in \mathbb{R}^{1+1}	46
8	The worldsheet parameter space and embedding functions in AdS ₃ -Schwarzschild	47
9	A fundamental open string used as a probe in an AdS black hole background to model an infinitely massive quark moving through a thermal plasma at a constant velocity v on the boundary	66

List of Tables

1	The AdS/CFT dictionary - translating between quantities in the bulk and boundary theories	6
---	---	---

“These motions were such as to satisfy me, after frequently repeated observation, that they arose neither from currents in the fluid, nor from its gradual evaporation, but belonged to the particle itself.”

- **Robert Brown**

'A Brief Account of Microscopical Observations made in the Middle of June, July, and August, 1827, on the Particles Contained in the Pollen of Plants', Philosophical Magazine, 1828

1 Introduction

It is both experimentally pertinent and theoretically interesting to examine the movement of a quark undergoing Brownian motion in a hot plasma. The main aim of this work is to present an instructional or pedagogical approach to using the AdS/CFT correspondence to explore the dynamical behaviour of probe heavy and light quarks immersed in a thermal plasma.

The plasma in question, the quark-gluon plasma (QGP), is created by colliding lead and gold nuclei at high energies in the Large Hadron Collider (LHC) at CERN; and the Relativistic Heavy Ion Collider (RHIC) in Brookhaven National Laboratory (BNL). Before the first results from RHIC in 2000 it was expected that at high energy densities QCD asymptotic freedom would result in a weakly-coupled system exhibiting gas-like behaviour. However, the experimental results [1] indicated that the produced QGP (a deconfined state of matter consisting of quarks and gluons) does not expand isotropically and behaves, in-fact, as a strongly-coupled medium [2, 3]. The thermal plasma expands anisotropically in its azimuthal direction. The momentum anisotropy of the measured particles is known as *elliptic flow*¹. This discovery did not definitively settle the question as to whether the QGP is weakly- or strongly-coupled. There is evidence to support both. Weak coupling techniques from perturbative quantum chromodynamics (pQCD) have been successful in predicting the distributions of high transverse momentum observables [6–8]; while low transverse momentum observables described by near-ideal relativistic hydrodynamics [9–12] can be understood within a strong coupling paradigm [13, 14]. Further, jet suppression [15, 16] and heavy quark energy loss studies [17] support the theory of a strongly-coupled thermal plasma.

At strong coupling, the usual perturbation techniques are no longer applicable and many quantities in gauge theories become difficult to compute. In 1974, 't Hooft [18] postulated that the generalisation of the quantum chromodynamic $SU(3)$ gauge group (where $N_c = 3$ is the number of quark colours in the theory) would be an $SU(N_c)$ gauge group, where the large N_c limit is taken ($N_c \rightarrow \infty$ while $\lambda := g_{YM} N_c$ is kept fixed and large). The Yang-Mills coupling is denoted by g_{YM} , and the quantity λ is known as the 't Hooft coupling. The large N_c limit provides an approximation to compute the gauge theory at strong coupling². Inspired by 't Hooft's idea, a promising approach in studying the strong coupling limit of non-abelian quantum field theories (such as QCD) was formulated in 1999 by Juan Maldacena [21]. Known as the anti-de Sitter/Conformal Field Theory (AdS/CFT) correspondence, it is a study of the duality between bulk gravitational physics of a given d -dimensional spacetime and a $(d-1)$ -dimensional gauge theory on its boundary. Considering the phenomenologically relevant case, at finite temperature the equivalence exists between type IIB string theory on ten-dimensional spacetime approximated by Einstein's general relativity on a five-dimensional non-compact anti-de Sitter spacetime and a five-dimensional sphere ($AdS_5 \times S^5$) (referred to as either the *gravity* or *bulk* theory); and $\mathcal{N} = 4$ supersymmetric Yang-Mills theory (SYM) on four-dimensional Minkowski spacetime [20] (referred to as either the *gauge* or *boundary* theory). Quantities which are difficult to compute in a strongly-coupled gauge theory can be calculated in a weakly-coupled gravity theory, and translated back via the AdS/CFT dictionary (see table (1), page 6)³. After its initial discovery, generalisations of the AdS/CFT correspondence followed and the field is now grouped under *gauge/string dualities*. In the succeeding two decades since the initial publications of [21, 24–27] there has been much interest (and success) in using the gauge/string duality to determine properties of the given gauge theory's plasma state.

Propelled by experiments at RHIC and the LHC, theoretical developments in this regard have been inspired by an early calculation [28] which found the ratio of shear viscosity to volume entropy density (η/s) in the strong coupling regime using the AdS/CFT correspondence. This ratio is experimentally measurable, and data provided by RHIC supported the theoretical result [29, 30]. Building on this, Kovtun *et. al.* [31, 32]

¹For two comprehensive reviews on discoveries relating to the hydrodynamic description of relativistic heavy-ion collisions (specifically collective flow and viscosity), see [4, 5].

²In the large N_c limit, a topological factor N_c^ζ (where ζ is the Euler characteristic) is assigned to each Feynman graph. Summing over these graphs can be thought of as summing over the worldsheets of the supposed '*QCD string*' (the QCD string dual is unknown and is approximated by the $\mathcal{N} = 4$ SYM string dual) to yield the partition function for the large N_c theory [19, 20].

³There is a hitherto unaddressed assumption at play here – the theory of quantum chromodynamics is not exactly equivalent to $\mathcal{N} = 4$ supersymmetric Yang-Mills theory. The theories are however analogous: while the matter fields and quantum dynamics of the theories differ, their gauge fields and tree-level interactions are common [22]. Qualitatively the plasmas of QCD and $\mathcal{N} = 4$ SYM share many properties, such as Debye screening and finite spatial correlation lengths [23]. Hence, for studies in the high temperature regime it is assumed that the plasma of $\mathcal{N} = 4$ supersymmetric Yang-Mills is similar to the quark-gluon plasma of QCD.

discovered the shear viscosity/entropy density ratio is universal for a large class of these QFTs and, further, that this ratio is a universal lower bound for the viscosity in general⁴. This discovery was essential in understanding the elliptic flow that had been observed at RHIC, and sparked interest in the link between string theory and relativistic heavy-ion phenomenology⁵. Exploring this link, two pertinent examples this dissertation will focus on are (i) the dissipative and diffusive behaviour of a massive quark moving through a field theory plasma explained by studying trailing strings in the AdS spacetime [22, 35–41]; and (ii) heavy and light quarks undergoing Brownian motion studied by examining transverse fluctuations on open strings in an AdS black hole background [42–52].

Motivated by these past studies, this dissertation seeks to better understand the fluctuating energy loss of light and heavy quarks in a thermal medium. Specifically, heavy and light probe quarks in the gauge theory are considered to undergo Brownian motion⁶, and the mean-squared transverse displacement of the string’s boundary endpoint $s^2(t; d)$ (equivalent to the mean-squared displacement travelled by the external quark which is initially at rest in the thermal plasma) is computed. Functioning as a pedagogical work for these types of gauge/string calculations, this dissertation aims to present a consistent framework⁷ – providing insights into published results and including proofs of some of the more vague statements in the literature. In terms of original advancement, previous generalisations of $s^2(t; 3)$ in AdS₃-Schwarzschild to AdS_d-Schwarzschild for the light quark’s case are challenged and the method in which to generalise to $s^2(t; d)$ correctly given for the first time. Notwithstanding this, the other main contribution of the dissertation to this field is presenting a definitive, consolidated theoretical derivation – from which further research, including analytical calculations with different test string configurations or numerical analysis confirming previous analytic results, can be undertaken.

1.1 Dissertation Structure

This dissertation is organised in two parts. The first part provides some useful theoretical background needed to understand the bulk calculations in Part II. The central results of this dissertation are given in the second part.

In Part I:

First, the gauge/string duality is introduced in section (2). Particular attention is paid to the *throat* construction of anti-de Sitter spacetime as a limit of D3-brane geometry, and the justification of the AdS/CFT conjecture. In section (3) the basic theory of Brownian motion and the non-retarded and retarded Langevin models are explored. The first and second fluctuation-dissipation theorems are derived. The mean-squared displacement $s^2(t)$ is calculated and its behaviour in the early and late time limits are discussed. At early times, the Brownian particle’s behaviour is proportional to time and the motion is expected to be ballistic $s(t) \sim t$; while, at late times, the Brownian particle’s motion is diffusive, $s(t) \sim \sqrt{t}$.

In Part II:

To begin Part II, section (4) focuses on calculating an external heavy quark’s diffusion coefficient in the bulk AdS₃-Schwarzschild spacetime. The dual description of the on-mass-shell heavy quark exhibiting Brownian motion in the thermal plasma – an open string attached at the anti-de Sitter boundary⁸ and hanging towards the horizon undergoing transverse fluctuations – is used to compute the mean-squared transverse displacement of the string’s boundary endpoint $s^2(t; 3)$. The diffusion coefficient is extracted at late times. Similarly, in section (5) an off-mass-shell light quark exhibiting Brownian motion in the thermal plasma is modelled as an open string undergoing transverse fluctuations (initially stretched between the AdS bound-

⁴In addition, see Buchel *et al.*’s contributions [33, 34].

⁵A worthwhile review on the topic is given by Casalderrey-Solana *et al.* [14].

⁶Brownian motion [53] concerns the ceaseless, random motion of a given particle undergoing microscopic collisions with the constituent particles of the fluid it is immersed in. The motion is responsible for the dissipative nature of a system and its approach to thermal equilibrium. Any particle suspended in a finite temperature fluid undergoes this motion, and as such a probe quark immersed in the QGP behaves the same way. The AdS/CFT correspondence can be used to study the behaviour a probe quark exhibits while interacting with the strongly-coupled thermal plasma.

⁷A necessary pursuit considering how versatile the field is – publications on gauge/string dualities span all physics arXivs [20].

⁸The boundary of a D7-brane stretching from $r = \infty$ to the string’s boundary endpoint [54].

ary and just above the horizon) whose AdS boundary endpoint is released to fall at the local speed of light in the presence of a space filling D7-brane [54]. Initially this section focuses on calculating an external light quark's diffusion coefficient in the bulk AdS_3 -Schwarzschild spacetime. Then, importantly, the results are generalised to AdS_d -Schwarzschild by expanding and truncating the near-horizon metric. Further, in section (6), an infinitely massive probe quark moving through the thermal plasma with a constant velocity is considered. An open string trailing out behind the quark (arcing down into AdS-Schwarzschild) is used to model the situation. From this, the drag force on the test string is calculated in the bulk and rewritten – via the AdS/CFT correspondence – in terms of relevant quantities in the gauge theory⁹. The Langevin equation is then used to extricate the friction coefficient, and (by means of the Einstein-Sutherland relation) the diffusion coefficient for a heavy quark in AdS_d -Schwarzschild. Section (7) concludes the dissertation and proposes avenues for future research.

There are a number of appendices to this dissertation. Appendix (A.1) derives the string equations of motion by calculating the functional derivative of the Polyakov action with respect to the string worldsheet coordinates and setting this variation to zero. In an analogous fashion, the string equations of motion for the transverse fluctuations are found in appendix (A.4) by varying the Nambu-Goto action. The Virasoro constraints and string equations of motion in isothermal coordinates are given in appendix (A.2); while a derivation of the energy of a test string in an AdS-Schwarzschild background can be found in appendix (A.3). Appendix (A.5) aims to fix the normalization constant A_ω , thereby completely determining the general solution for the transverse equations of motion. As the penultimate, appendix (A.6) calculates the leading order contributions of the tortoise coordinate in the near-horizon region. Appendix (A.7) provides details for accessing the GitHub repository where the latest annotated Mathematica code notebooks supporting the analytical analysis of open string evolution presented here, can be found. The author believes it is important to make the Mathematica notebooks available for reference purposes and in the spirit of open collaboration.

⁹Historically, the drag force calculation was the first application of AdS/CFT to understand the behaviour of a probe heavy quark in the quark-gluon plasma (see [22, 35]).

Part I

Theory

2 The Gauge/String Duality

As recognised by 't Hooft [18], understanding gauge theories with an $SU(N_c)$ gauge group in the large N_c limit perhaps offers the best course to illuminating the strong coupling behaviour of QCD. In the late 1990's it was suspected that string theory could describe the large N_c limit [55]. Maldacena [21] first made the suggestion that a $(d-1)$ -dimensional, conformally invariant field theory in the limit of large N_c corresponds to string theory and supergravity on anti-de Sitter spacetime in d dimensions times by a d -dimensional spherical compact manifold ($\text{AdS} \times S$). This idea, based on the holographic principle¹⁰ and formally known as the AdS/CFT correspondence, was developed in the months that followed by [24–27], to name a few. The AdS/CFT correspondence is an example of gauge/string dualities which have subsequently been developed into a powerful tool in understanding strongly-coupled systems¹¹.

2.1 Anti-de Sitter Spacetime as a limit of D3-brane Geometry

The solution of low energy, type IIB string theory containing D3-branes prompted the formulation of the gauge/string dualities. Solving the supergravity equations of motion yields the spacetime metric sourced by N_c Dp-branes [59–61]. Specifically, the spacetime for the extremal D3-brane¹² is

$$ds^2 = H^{-1/2} (-dt^2 + d\vec{x}^2) + H^{1/2} (dr^2 + r^2 d\Omega_5^2), \quad (2.1)$$

where the D3-brane is extended along the spatial coordinates $\vec{x} = (x_1, x_2, x_3)$; $H(r) = 1 + l^4/r^4$ is known as the *warping factor*¹³; and the second term metric describes the y -directions transverse to the D3-brane written in spherical coordinates (where $r^2 = y_1^2 + y_2^2 + \dots + y_6^2$ is the radial coordinate). The parameter l is interpreted as the characteristic length scale of the range of the N_c D3-branes' gravitational effects [14]. In the limit $r \gg l$, $H \simeq 1$ and the metric Eq.(2.1) reduces to Minkowski spacetime¹⁴. In the limit $r \ll l$, $H \simeq l^4/r^4$ (which corresponds to a series expansion around $r/l = 0$ to leading order). Hence, in this limit the metric Eq.(2.1) becomes

$$ds^2 = ds_{\text{AdS}_5}^2 + l^2 d\Omega_5^2, \quad \text{where} \quad ds_{\text{AdS}_5}^2 = \frac{r^2}{l^2} (-dt^2 + d\vec{x}^2) + \frac{l^2}{r^2} dr^2. \quad (2.2)$$

Now l is identified as the radius of curvature of AdS_d and S^d (see table (1), page 6); $ds_{\text{AdS}_5}^2$ is the metric of five-dimensional anti-de Sitter spacetime^{15,16}; and $d\Omega_5^2$ is the metric on S^5 with unit radius. Therefore, the spacetime sourced from a stack of D3-branes corresponds to ten-dimensional Minkowski spacetime far away from the branes (see blue patch, figure (1)), while a *throat* geometry of the form $\text{AdS}_5 \times S^5$ becomes apparent close to the branes (see red patch, figure (1)).

Generalising to non-zero finite temperature T systems by exciting the degrees of freedom on the D3-brane, adapts the anti-de Sitter spacetime part of the metric. Specifically, Eq.(2.2) becomes

$$ds^2 = ds_{\text{AdS}_5\text{-Sch}}^2 + l^2 d\Omega_5^2, \quad \text{where} \quad ds_{\text{AdS}_5\text{-Sch}}^2 = \frac{r^2}{l^2} (-h dt^2 + d\vec{x}^2) + \frac{l^2}{r^2 h} dr^2, \quad (2.3)$$

¹⁰*Holographic* as proposed by 't Hooft, Susskind and Thorn in [56–58] respectively. In this sense, a holographic theory encodes a theory in d dimensions by a theory in $(d-1)$ dimensions.

¹¹A duality between two theories describes a situation where one theory is in the strong coupling limit, while the other theory is in the weak coupling limit [20]. In order to study a strongly-coupled gauge theory, the equivalent weakly-coupled gravitational string theory (i.e. a theory where the curvature of the spacetime is small) can instead be used.

¹²Only the ground state of the N_c D3-branes is being considered.

¹³The definition of the *warping factor* is independent of the dimensions of the theory.

¹⁴A small correction proportional to l^4/r^4 is present.

¹⁵The defining characteristic of AdS is a spacetime described by a constant negative curvature.

¹⁶The five-dimensional anti-de Sitter spacetime metric Eq.(2.2) represents a Poincaré chart of AdS_5 spacetime. There is an alternative formulation of anti-de Sitter spacetime in terms of global coordinates which provides a global coordinate chart (see, for example, [62]).

where $h(r) = 1 - r_H^4/r^4$ is known as the *blackening factor*. The first term of the metric in Eq.(2.3) describes an AdS_5 spacetime with a Schwarzschild black hole horizon at $r = r_H$ ^{17,18}.

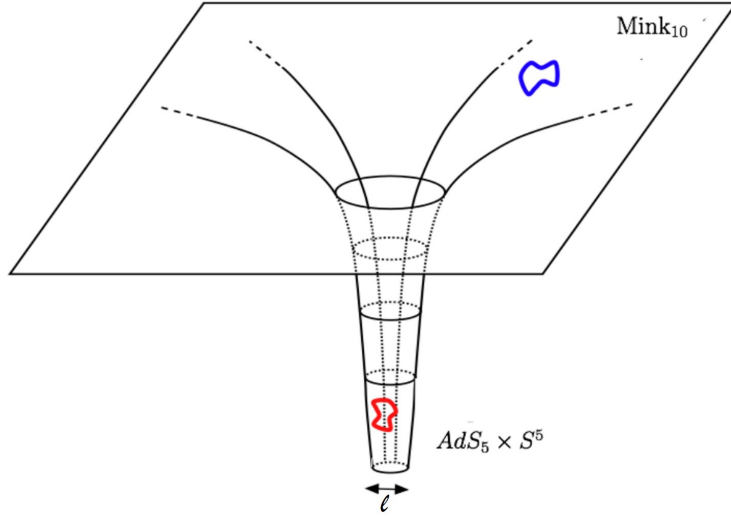


Figure 1: The spacetime around N_c D3-branes in type IIB theory, where l is the radius of curvature of AdS_5 and S^5 (adapted from [14, 63]). See page 4 for details.

A stack of N_c D3-branes can be described by (i) closed strings propagating in a curved spacetime geometry, which – in the low energy limit – becomes closed IIB string theory in $AdS_5 \times S^5$ (as discussed above); but also (ii) open strings attached to a hyper-plane in flat spacetime, where the low-energy limit is given by $\mathcal{N} = 4$, $SU(N_c)$ supersymmetric Yang-Mills theory [14, 63]. The hypothesis that the two descriptions are equivalent was the first example of the AdS/CFT conjecture.

2.2 The AdS/CFT Conjecture

The best example of a gauge/string duality remains the equivalence between type IIB string theory in an $AdS_5 \times S^5$ background to $\mathcal{N} = 4$, $SU(N_c)$ SYM theory on the four-dimensional Minkowski spacetime boundary of AdS_5 . As has been seen in subsection (2.1), if the above duality is considered at finite temperature, the addition of a black hole in the anti-de Sitter spacetime is necessary. The spacetime is then referred to as the anti-de Sitter-Schwarzschild spacetime (or AdS-Schwarzschild).

The AdS/CFT correspondence claims that the partition functions of the gauge and gravitational theories are equivalent, i.e. $Z_{\text{gauge}} = Z_{\text{AdS}}$ [20]. In doing so the conjecture specifies a *dictionary* between two physical theories which appear to be very different (these relations are summarised in the reference table (1)). In practice, the strong/weak coupling nature of the duality means that it is difficult to explicitly test the validity of the conjecture¹⁹. There are, however, several contiguous *tests* – coupling-independent properties of these theories that can be compared to investigate the duality. Specifically for $AdS_5 \times S^5/\mathcal{N} = 4$ supersymmetric Yang-Mills, *tests* include (i) comparing the global symmetries of the theories; (ii) matching the coupling-independent correlation functions (these are normally protected from quantum corrections and related to anomalies); (iii) comparing the spectrum of chiral operators; and (iv) examining the qualitative behaviour of the theory deformed by chiral operators²⁰ [27].

¹⁷The Schwarzschild black hole is the solution to the Einstein equation with no matter fields or cosmological constant.

¹⁸The radial position of the black-brane horizon r_H is proportional to the temperature T (see table (1), page 6).

¹⁹With contemporary knowledge, perturbative computations in λ can mostly only be achieved in the field theory, while in the string theory only perturbative calculations in $1/\lambda$ are possible. Therefore, comparing the correlation functions of these theories is in principle not realisable [27].

²⁰Qualitative tests include the existence of confinement in finite temperature gauge theories [64], and examining how the theory behaves on its moduli space [65–67].

AdS_d	$(d-1)\text{-dimensional Gauge Theory}$	Description
l	$\sqrt{\alpha'} \lambda^{1/4}$	Radius of curvature of AdS_d and S^d
ℓ_s	$\sqrt{\alpha'} \equiv \lambda^{-1/4} l$	Fundamental string length scale
T_0	$1/2\pi\alpha'$	String tension
$(l/\ell_s)^4$	λ	't Hooft coupling ²¹
r_H	$4\pi l^2 T/(d-1)$	Radial position of the black hole horizon
$(d-1)r_H/4\pi l^2$	$T \equiv 1/\beta$	Temperature of the gauge theory ²²
$r_c \equiv (r_s + \ell_0)$	$2\pi\alpha'(M_{\text{rest}} + \Delta m)$	Minimal radius of D7-brane ²³
$T_0 r_H$	$\Delta m(T)$	Thermal rest mass shift
$T_0 (r_c - r_H)$	$M_{\text{rest}}(T)$	Static thermal mass of external particle ²⁴

Table 1: The AdS/CFT dictionary - translating between quantities in the bulk and boundary theories (adapted from Herzog *et al.* [35])

The main advantage of the AdS/CFT correspondence is that otherwise intractable problems are able to be solved by their mapping onto the equivalent dual. Applications of the correspondence include gluon scattering amplitudes calculations in strongly-coupled $\mathcal{N} = 4$ supersymmetric Yang-Mills [69]; and the study of holographic superconductivity and critical phenomena [70–72]²⁵.

²⁰The 't Hooft coupling [18] is specifically defined in the phenomenologically relevant $\text{AdS}_5/\mathcal{N} = 4$ SYM case. In this case: $\lambda \equiv g_{\text{YM}}^2 N_c$, where N_c is the number of colours and the Yang-Mills coupling is related to the string coupling by: $g_{\text{YM}} = 2\sqrt{\pi} g_s$. However, this dissertation follows [42] in using the same terminology to refer to $(l/\ell_s)^4$ for general d dimensions.

²¹This is equivalent to the Hawking temperature of the black hole.

²²A UV cut-off surface imposed near the boundary in order to consider external particles of finite mass in the gauge theory.

²³In the $\text{AdS}_5/\mathcal{N} = 4$ SYM case, this is the free energy of a quark at rest in $\mathcal{N} = 4$ SYM plasma. In the limit of zero temperature it is equal to the QCD Lagrangian quark mass, m_q [68].

²⁵See [20] for a extensive review on systems with phase transitions in AdS/CFT, and [73] for an introduction to holographic methods for condensed matter physics.

3 Brownian Motion: the Dynamics of Langevin's Model

Discovered by Robert Brown in 1827 [53] the ceaseless and irregular motion which small pollen particles undergo when suspended in water, became known as Brownian motion. Brown postulated that this movement had a physical rather than biological origin. In 1905 Albert Einstein [74]²⁶ combined statistical mechanics and the diffusion equation, to arrive at a theoretical explanation of the phenomenon. His famous formula for the particle's mean-squared displacement, $\langle s^2(t) \rangle$, provided an observable for experimental physicists to measure. Independently, Marian Smoluchowski [75]²⁷ derived a similar result based on combinatorics and kinetic theory's mean-free-path approximation [76].

In a mathematical context, Louis Bachelier wrote his 1900 doctoral thesis on modelling prices on the Paris stock exchange as the limit of a random walk [77]²⁸. Neither Einstein nor Bachelier rigorously classified Brownian motion as a stochastic process. This was taken up by the American mathematician, Norbert Wiener, who ultimately proved the existence of Brownian motion by defining it as a stochastic process in 1923 [78]. Wiener's output includes a series of papers starting in 1918 giving the mathematical definition and properties of the physical process of Brownian motion abstracted as a stochastic process. Hence, Wiener processes (essentially the same concept as Brownian motion but emphasising the mathematical aspects) developed separately to the school of thought emphasising the physical aspects.

Turning back towards the explanations of physicists, Einstein and Smoluchowski failed to take into account the inertia of the particle undergoing Brownian motion. Applying Newtonian dynamics to a Brownian particle, Paul Langevin [79]²⁹ arrived at a useful phenomenological model in 1908.

3.1 The Non-retarded Langevin Model

Consider the following: a non-relativistic particle of mass m , undergoing Brownian motion in one spatial dimension, can be described by the Langevin equation

$$\begin{aligned} \dot{p}(t) &= -\gamma_0 p(t) + F(t), \\ \Rightarrow m \dot{v}(t) &= -m \gamma_0 v(t) + F(t), \end{aligned} \tag{3.1}$$

where $\dot{p} \equiv dp/dt$, γ_0 is a constant known as the friction coefficient, and v is the velocity of the particle. Eq.(3.1) is a stochastic differential equation and can be thought of as consisting of two parts: i). a systematic term $-m\gamma_0 v$ corresponding to the friction force, and ii). a fluctuating part $F(t)$ corresponding to a random force [80]. It is worthwhile to note that although it is simpler to understand the Langevin equation in terms of a friction force and a random force – on a microscopic scale both forces are caused by the particle's collision with the constituent modules of the immersive fluid [42].

Concerning the statistical properties of $F(t)$, three assumptions are made. First, the average value of the random force at time t , over a particle ensemble with the same initial velocity, vanishes

$$\langle F(t) \rangle = 0, \tag{3.2}$$

where an ensemble is defined as a large number of similar, but independent particles. Second, the autocorrelation of the random force is related to a constant, κ_0 , which measures the fluctuation strength

²⁶Original publication: *Über die von der molekularkinetischen Theorie der Wärme geforderte Bewegung von in ruhenden Flüssigkeiten suspendierten Teilchen*, Annalen der physik 322.8 (1905): 549-560. Translated from German.

²⁷Original publication: *Zarys kinetycznej teoriji ruchów browna i roztworów metnych*, Rozprawy i Sprawozdania z Posiedzen Wydziału Matematyczno-Przyrodniczego Akademii Umiejetnosci 3 (1906): 257-282. Reprinted in German: *Zur kinetischen theorie der brownischen molekularbewegung und der suspensionen*, Annalen der physik 326.14 (1906): 756-780. Translated from German.

²⁸Original publication: *Théorie de la spéculation*, Annales scientifiques de l'École normale supérieure. Vol. 17. (1900). Translated from French.

²⁹Original publication: *Sur la théorie du mouvement brownien*, Compt. Rendus 146 (1908): 530-533. Translated from French.

$$\langle F(t) F(t') \rangle = \kappa_0 \delta(t - t'), \quad (3.3)$$

where $\delta(x)$ is the Dirac delta function. This assumption implies

$$\int_{-\infty}^{\infty} \langle F(t) F(t') \rangle dt' = \kappa_0. \quad (3.4)$$

Lastly, $F(t)$ is assumed to be a Gaussian process³⁰.

To find the solutions of Eq.(3.1) – a first order linearly separable differential equation – the variables are separated, each side is multiplied with respect to $e^{\gamma_0 t}$, and integrated between initial time t_0 and t

$$\begin{aligned} m \dot{v}(t) e^{\gamma_0 t} + m \gamma_0 v(t) e^{\gamma_0 t} &= F(t) e^{\gamma_0 t} \\ \Rightarrow \int_{t_0}^t \dot{v}(t') e^{\gamma_0 t'} dt' + \int_{t_0}^t \gamma_0 v(t') e^{\gamma_0 t'} dt' &= \frac{1}{m} \int_{t_0}^t F(t') e^{\gamma_0 t'} dt' \\ \Rightarrow \int_{t_0}^t \dot{v}(t') e^{\gamma_0 t'} dt' + \left[v(t') e^{\gamma_0 t'} \right]_{t_0}^t - \int_{t_0}^t \dot{v}(t') e^{\gamma_0 t'} dt' &= \frac{1}{m} \int_{t_0}^t F(t') e^{\gamma_0 t'} dt' \\ \Rightarrow v(t) &= v_0 e^{-\gamma_0 t} + \frac{1}{m} \int_{t_0}^t F(t') e^{-\gamma_0 (t-t')} dt', \end{aligned} \quad (3.5)$$

where the initial velocity of the Brownian particle is denoted by $v(t_0) = v_0$, $\gamma_0 \in \mathbb{R}^+$ and it is assumed that $t \geq 0$. Unless otherwise stated, the system is thought of as having an initial time $t_0 = 0$, and being in equilibrium at $t = \infty$. As time progresses the velocity of the Brownian particle depends on the exponential decay of the initial velocity (the first term in Eq.(3.5)) and the extra velocity caused by the random force (the second term in Eq.(3.5)).

Since, on average, the random force vanishes (Eq.(3.2)) the average of the velocity (Eq.(3.5)) is

$$\langle v(t) \rangle = v_0 e^{-\gamma_0 t}, \quad t \geq 0. \quad (3.6)$$

Due to friction, the mean velocity decreases exponentially. Using Eq.(3.5), the autocorrelation function of the velocity is given by

$$\langle v(t)v(t') \rangle = v_0^2 e^{-\gamma_0 (t+t')} + \frac{1}{m^2} \int_{t_0}^t dt'' \int_{t_0}^{t'} dt''' \langle F(t'') F(t''') \rangle e^{-\gamma_0 (t'-t''')} e^{-\gamma_0 (t-t'')}, \quad (3.7)$$

where the two cross-terms which appeared when multiplying $v(t)v(t')$ are both first order in the noise and, as such, disappear when averaging over the noise. In the limit $t = t'$, Eq.(3.7) reduces to

$$\langle v^2(t) \rangle = v_0^2 e^{-2\gamma_0 t} + \frac{1}{m^2} \int_{t_0}^t dt' \int_{t_0}^t dt'' \langle F(t') F(t'') \rangle e^{-\gamma_0 (t-t')} e^{-\gamma_0 (t-t'')}. \quad (3.8)$$

Using the assumption Eq.(3.3), the mean-squared velocity becomes

³⁰The central limit theorem can be employed to justify this assumption. The random force $F(t)$ is thought of as resulting from the superposition of many identically distributed random functions, since the Brownian particle has undergone multiple collisions [81].

$$\begin{aligned}
\langle v^2(t) \rangle &= v_0^2 e^{-2\gamma_0 t} + \frac{\kappa_0}{m^2} \int_{t_0}^t dt' e^{-2\gamma_0(t-t')} \\
&= v_0^2 e^{-2\gamma_0 t} + \frac{\kappa_0}{m^2} e^{-2\gamma_0 t} \left(\frac{1}{2\gamma_0} e^{2\gamma_0 t'} \right) \Big|_{t'=t_0}^{t'=t} \\
&= v_0^2 e^{-2\gamma_0 t} + \frac{\kappa_0}{2m^2\gamma_0} (1 - e^{-2\gamma_0 t}).
\end{aligned} \tag{3.9}$$

Taking the limit as $t \rightarrow \infty$, the value of the mean-squared velocity at equilibrium is

$$\lim_{t \rightarrow \infty} \langle v^2(t) \rangle = \frac{\kappa_0}{2m^2\gamma_0}. \tag{3.10}$$

Assuming the fluid is in thermodynamic equilibrium at temperature T , the average energy of the particle takes on its equipartition value^{31,32} $\langle E \rangle = T/2$ [81]. Since $\langle E(t) \rangle := m\langle v^2(t) \rangle/2$, Eq.(3.10) becomes

$$\kappa_0 = 2\gamma_0 m T, \tag{3.11}$$

which describes the relationship between the magnitude of the random force κ_0 and the friction coefficient γ_0 . Using assumption Eq.(3.4), Eq.(3.11) can be rewritten into the form

$$\gamma_0 = \frac{1}{2mT} \int_{-\infty}^{\infty} \langle F(t) F(t') \rangle dt'. \tag{3.12}$$

This equation is recognised as the second fluctuation-dissipation theorem [82]. The theorem states that the random fluctuations of the Brownian particle have the same origin as the dissipative frictional force acting on the Brownian particle as it moves in the medium.

In order to calculate the position of the Brownian particle, $x(t) := v(t)t$, Eq.(3.5) can be integrated between the initial time t_0 and t

$$\begin{aligned}
\int_{t_0}^t v(t') dt' &= \int_{t_0}^t v_0 e^{-\gamma_0 t'} dt' + \frac{1}{m} \int_{t_0}^t \int_{t_0}^{t''} F(t') e^{-\gamma_0(t''-t')} dt' dt'' \\
\Rightarrow \int_{t_0}^t v(t') dt' &= \int_{t_0}^t v_0 e^{-\gamma_0 t'} dt' + \frac{1}{m} \int_{t_0}^t \int_{t'}^t F(t') e^{-\gamma_0(t''-t')} dt'' dt' \\
\Rightarrow v(t)t - v_0 t_0 &= -\frac{v_0}{\gamma_0} (e^{-\gamma_0 t}) \Big|_{t'=t_0}^{t'=t} + \frac{1}{m} \int_{t_0}^t F(t') \left(-\frac{1}{\gamma_0} e^{-\gamma_0(t''-t')} \right) \Big|_{t''=t'}^{t''=t} dt' \\
\Rightarrow x(t) &= x_0 + \frac{v_0}{\gamma_0} (1 - e^{-\gamma_0 t}) + \frac{1}{m} \int_{t_0}^t F(t') \frac{1 - e^{-\gamma_0(t-t')}}{\gamma_0} dt',
\end{aligned} \tag{3.13}$$

where, in the second line, the order of integration of the third term has been changed.

The average of the displacement (remembering Eq.(3.2)) is

$$\langle x(t) \rangle = x_0 + \frac{v_0}{\gamma_0} (1 - e^{-\gamma_0 t}). \tag{3.14}$$

³¹The equipartition theorem of classical statistical mechanics relates the average energy of a system to its temperature.

³²The Boltzmann constant is taken to be $k_B = 1$.

The displacement $s(t) := x(t) - x_0$, is easily read off from Eq.(3.13)

$$s(t) = \frac{v_0}{\gamma_0} (1 - e^{-\gamma_0 t}) + \frac{1}{m} \int_{t_0}^t F(t') \frac{1 - e^{\gamma_0(t-t')}}{\gamma_0} dt'. \quad (3.15)$$

In order to calculate the particle's mean-squared displacement, $\langle s^2(t) \rangle$, Eq.(3.15) can be squared and averaged,

$$\begin{aligned} \langle s^2(t) \rangle &= \frac{v_0^2}{\gamma_0^2} (1 - e^{-\gamma_0 t})^2 + \frac{1}{m^2 \gamma_0^2} \int_{t_0}^t dt' \int_{t_0}^t dt'' \langle F(t') F(t'') \rangle (1 - e^{\gamma_0(t-t')}) (1 - e^{\gamma_0(t-t'')}) \\ &= \frac{v_0^2}{\gamma_0^2} (1 - 2e^{-\gamma_0 t} + e^{-2\gamma_0 t}) + \frac{\kappa_0}{m^2 \gamma_0^2} \int_{t_0}^t dt' (1 - e^{\gamma_0(t-t')})^2 \\ &= \frac{v_0^2}{\gamma_0^2} (1 - 2e^{-\gamma_0 t} + e^{-2\gamma_0 t}) + \frac{\kappa_0}{m^2 \gamma_0^2} \left[t - \frac{2}{\gamma_0} (1 - e^{-\gamma_0 t}) + \frac{1}{2\gamma_0} (1 - e^{-2\gamma_0 t}) \right] \\ &= \frac{v_0^2}{\gamma_0^2} (1 - 2e^{-\gamma_0 t} + e^{-2\gamma_0 t}) + \frac{\kappa_0}{2m^2 \gamma_0^3} (2\gamma_0 t - 3 + 4e^{-\gamma_0 t} - e^{-2\gamma_0 t}). \end{aligned} \quad (3.16)$$

Note that, in the second line, the two cross-terms vanish and the assumption Eq.(3.3) has been used.

Further, a second average of $\langle s^2(t) \rangle$ over all possible initial velocities needs to be taken. This yields,

$$\begin{aligned} \langle s^2(t) \rangle &= \frac{\langle v_0^2 \rangle}{\gamma_0^2} (1 - 2e^{-\gamma_0 t} + e^{-2\gamma_0 t}) + \frac{\kappa_0}{2m^2 \gamma_0^3} (2\gamma_0 t - 3 + 4e^{-\gamma_0 t} - e^{-2\gamma_0 t}) \\ &= \frac{T}{m} \frac{1}{\gamma_0^2} (1 - 2e^{-\gamma_0 t} + e^{-2\gamma_0 t}) + \frac{T}{m} \frac{1}{\gamma_0^2} (2\gamma_0 t - 3 + 4e^{-\gamma_0 t} - e^{-2\gamma_0 t}) \\ &= 2 \frac{T}{m} \frac{1}{\gamma_0^2} (\gamma_0 t - 1 + e^{-\gamma_0 t}), \end{aligned} \quad (3.17)$$

where the relation for κ_0 (Eq.(3.11)), and the equipartition of energy ($\langle v_0^2 \rangle = T/m$) is used in the second line.

The Einstein-Sutherland relation defines the diffusion coefficient

$$D := \frac{T}{\gamma_0 m}. \quad (3.18)$$

Hence, Eq.(3.17) becomes

$$\langle s^2(t) \rangle = \frac{2D}{\gamma_0} (\gamma_0 t - 1 + e^{-\gamma_0 t}). \quad (3.19)$$

This result was first derived in 1917 by Dutch physicist Leonard Ornstein [83]. The early and late time limits of the mean-squared displacement $\langle s^2(t) \rangle$ should be examined.

(i) In the limit of early times ($t \ll \frac{1}{\gamma_0}$): a Taylor expansion of $e^{-\gamma_0 t}$ can be performed.

$$\therefore \langle s^2(t) \rangle \approx \frac{2D}{\gamma_0} \left(\gamma_0 t - 1 + \left(1 - \gamma_0 t + \frac{\gamma_0^2 t^2}{2} \right) \right) = D \gamma_0 t^2 = \frac{T}{m} t^2, \quad (3.20)$$

where the last equality comes from using the Einstein-Sutherland relation Eq.(3.18). In this limit, known as the ballistic regime, the Brownian particle's behaviour is proportional to time, $s(t) \sim t$. This

behaviour is expected since the initial behaviour of the Brownian particle – before it is bombarded by a substantial number of fluid particles – is inertial (with a velocity determined by the equipartition of energy $v(t) = \sqrt{T/m}$) [42].

(ii) In the limit of late times ($t \gg \frac{1}{\gamma_0}$): $e^{-\gamma_0 t} \rightarrow 0$ as $t \rightarrow \infty$, and $\gamma_0 t$ becomes the dominant term.

$$\therefore \langle s^2(t) \rangle \approx 2Dt. \quad (3.21)$$

Eq.(3.21) is the famous equation found by Einstein in his 1905 paper [74]. In this limit, referred to as the diffusive regime, $s(t) \sim \sqrt{t}$ and the particle experiences a random walk. The Brownian particle deviates from its initial course due to numerous collisions with the constituent fluid particles that cause the Brownian particle to ‘forget’ its early time behaviour [42].

The cross-over time³³ between the diffusive regime and the ballistic regime is denoted by

$$t_{\text{relax}} \sim \frac{1}{\gamma_0}, \quad (3.22)$$

which represents the time it takes for a Brownian particle that had some initial velocity at $t = t_0$ to thermalize in the medium.

3.2 The Generalised Langevin Model

The Langevin model can be generalised to include retardation effects. The retarded Langevin equation³⁴ is given by [82, 84]

$$\dot{p}(t) = - \int_{-\infty}^t dt' \gamma(t-t') p(t') + F(t) + K(t), \quad (3.23)$$

where the memory kernel $\gamma(t-t')$ allows the friction term to depend on the past trajectory of the Brownian particle, and $K(t)$ is an external force which acts on the system. The system is taken to be in equilibrium in the limit $t_0 \rightarrow -\infty$. The non-retarded Langevin Equation Eq.(3.1) only holds if the Brownian particle is taken to have infinite mass with respect to the constituent fluid particles. The generalisation of the Langevin equation to Eq.(3.23) fixes two physical problems, (i) the friction is no longer considered to be instantaneous, (ii) a correlation can exist between random forces at different times.

The random force in Eq.(3.23) is taken to satisfy

$$\langle F(t) \rangle = 0 \quad \text{and} \quad \langle F(t) F(t') \rangle = \kappa(t-t'), \quad (3.24)$$

where $\kappa(t)$ is an unspecified function. As in the non-retarded case, $F(t)$ is assumed to be a Gaussian process.

The retarded Langevin equation is Fourier transformed³⁵ in order to analyse its behaviour. The Fourier transform has the following useful properties:

- (i) linearity: $\mathcal{F}[c_1 g(t) + c_2 h(t)] = c_1 G(\omega) + c_2 H(\omega)$,
- (ii) convolution: $\mathcal{F}[g(t) \otimes h(t)] = \mathcal{F}[\int_{-\infty}^{\infty} g(\tau) h(t-\tau) d\tau] = G(\omega) H(\omega)$,
- (iii) derivative property: $\mathcal{F}[\dot{g}(t)] = -i\omega G(\omega)$.

³³In this dissertation, the cross-over time is interchangeably referred to as the relaxation time.

³⁴The retarded Langevin Equation is also known as the generalised Langevin Equation.

³⁵The Fourier and Inverse Fourier Transform are defined here as

$$G(\omega) := \mathcal{F}[g(t)] = \int_{-\infty}^{\infty} g(t) e^{i\omega t} dt \quad \text{and} \quad g(t) := \mathcal{F}^{-1}[G(\omega)] = \int_{-\infty}^{\infty} G(\omega) e^{-i\omega t} dt$$

where $\omega = -2\pi f$.

Fourier transforming both sides of Eq.(3.23), and using the linearity and derivative properties gives

$$\begin{aligned}\mathcal{F}\left[\dot{p}(t) + \int_{-\infty}^t dt' \gamma(t-t') p(t')\right] &= \mathcal{F}\left[F(t) + K(t)\right] \\ \Rightarrow -i\omega p(\omega) + \mathcal{F}\left[\int_{-\infty}^t dt' \gamma(t-t') p(t')\right] &= F(\omega) + K(\omega).\end{aligned}\tag{3.25}$$

The convolution property would be useful in calculating the second term in Eq.(3.25). However, the asymmetric bounds of this integral ($t' \in [-\infty, t]$) are inconvenient. Hence, the memory kernel's bounds are redefined by introducing the causal memory kernel

$$\tilde{\gamma}(t) = \Theta(t) \gamma(t),\tag{3.26}$$

where $\Theta(t)$ is the Heavy-side function. Notice that while $\gamma(t-t')$ is defined only for $t > 0$, $\tilde{\gamma}(t-t')$ is defined for all t .

Rewriting Eq.(3.25) in terms of the causal memory kernel yields

$$\begin{aligned}\Rightarrow -i\omega p(\omega) + \mathcal{F}\left[\int_{-\infty}^{\infty} dt' \tilde{\gamma}(t-t') p(t')\right] &= F(\omega) + K(\omega) \\ \Rightarrow -i\omega p(\omega) + p(\omega) \tilde{\gamma}(\omega) &= F(\omega) + K(\omega),\end{aligned}\tag{3.27}$$

where, in the second line, the symmetric bounds of the integral ensured that the convolution property can be applied. Note that in Eq.(3.27)

$$\tilde{\gamma}(\omega) = \int_{-\infty}^{\infty} dt \tilde{\gamma}(t) e^{i\omega t} = \int_{-\infty}^{\infty} dt \Theta(t) \gamma(t) e^{i\omega t} = \int_0^{\infty} dt \gamma(t) e^{i\omega t} := \gamma[\omega],\tag{3.28}$$

is actually the Fourier-Laplace transform of $\gamma(t)$, while

$$p(\omega) := \int_{-\infty}^{\infty} dt p(t) e^{i\omega t},\tag{3.29}$$

$F(\omega)$ and $K(\omega)$ are the standard Fourier transforms of $p(t)$, $F(t)$ and $K(t)$ respectively.

By rearranging Eq.(3.27) into a simpler form

$$p(\omega) = \frac{F(\omega) + K(\omega)}{\gamma[\omega] - i\omega},\tag{3.30}$$

it is now easy to take the statistical average. Remembering the assumptions regarding the random force (Eq.(3.24)), yields

$$\langle p(\omega) \rangle = \mu(\omega) K(\omega), \quad \text{where} \quad \mu(\omega) := \frac{1}{\gamma[\omega] - i\omega}.\tag{3.31}$$

The quantity $\mu(\omega)$ is known as the admittance, and describes the system's response to an external perturbation. Measuring the response $\langle p(\omega) \rangle$ to an external force on the system $K(\omega)$, the admittance $\mu(\omega)$ can be calculated and hence $\gamma[w]$ determined.

The first fluctuation-dissipation theorem relates the admittance to the autocorrelation of the equilibrium velocity [81, 82]. Following Eq.(3.7) the autocorrelation function of the equilibrium velocity for the retarded Langevin equation Eq.(3.23) is

$$\begin{aligned}
\langle v(t)v(0) \rangle &= \frac{1}{m^2} \int_{-\infty}^t dt' \int_{-\infty}^0 dt'' \langle F(t') F(t'') \rangle e^{\gamma t''} e^{-\gamma(t-t')} \\
&= \frac{\kappa_0}{m^2} \int_{-\infty}^t dt' \int_{-\infty}^0 dt'' \delta(t' - t'') e^{\gamma t''} e^{-\gamma(t-t')} \\
&= \frac{T}{m} e^{-\gamma t} [1 + \Theta(-t) (e^{2\gamma t} - 1)] \\
&= \frac{T}{m} e^{-\gamma |t|},
\end{aligned} \tag{3.32}$$

where $|t|$ is the absolute value of t ; the random force correlation function is chosen, for simplicity, to have the form $\kappa(t - t') = \kappa_0 \delta(t - t')$; and Eq.(3.11) has been used in the third line. The Fourier-Laplace transform of Eq.(3.32) is

$$\begin{aligned}
\int_0^\infty \langle v(t)v(0) \rangle e^{i\omega t} dt &= \frac{T}{m} \frac{1}{\gamma[\omega] - i\omega} \\
\Rightarrow \mu(\omega) &= \frac{m}{T} \int_0^\infty \langle v(t)v(0) \rangle e^{i\omega t} dt,
\end{aligned} \tag{3.33}$$

where the definition of the admittance is recognised. Eq.(3.33) is known as the first fluctuation-dissipation theorem [82].

The power spectrum

$$I_{\mathcal{O}}(\omega) = \int_{-\infty}^\infty dt \langle \mathcal{O}(t_0) \mathcal{O}(t_0 + t) \rangle e^{i\omega t}, \tag{3.34}$$

is defined for a quantity $\mathcal{O}(t)$. The Wiener-Khintchine theorem³⁶ states that a stationary random process' autocorrelation function has a spectral decomposition described by the process' power spectrum. The theorem allows one to compare the autocorrelation function and the power spectrum

$$\langle \mathcal{O}(\omega) \mathcal{O}(\omega') \rangle = 2\pi \delta(\omega + \omega') I_{\mathcal{O}}(\omega), \tag{3.35}$$

of a quantity $\mathcal{O}(t)$.

As previously mentioned, $\gamma(t)$ and $\kappa(t)$ are related to each other by the second fluctuation-dissipation theorem. However they can be individually determined by considering two cases where different external forces are applied on the system:

- (i) the external force is periodic with frequency ω (i.e. $K(t) = K_0 e^{-i\omega t}$), and Eq.(3.31) becomes

$$\langle p(t) \rangle = \mu(\omega) K_0 e^{-i\omega t}. \tag{3.36}$$

The memory kernel of the system $\gamma(t)$ can be determined by measuring the response $\langle p(t) \rangle$ to $K(t)$.

- (ii) the external force $K(t)$ is absent, and Eq.(3.30) becomes

$$p(\omega) = \frac{F(\omega)}{\gamma[\omega] - i\omega}. \tag{3.37}$$

³⁶The Wiener-Khintchine theorem was proven for a deterministic function by Norbert Wiener in 1930 [85].

In order to determine $\gamma(t)$ and $\kappa(t)$ individually, $p(\omega)$ should first be squared and averaged to find the relation between the power spectrum of p ($I_p(\omega)$) and the power spectrum of F ($I_F(\omega)$). Explicitly,

$$\begin{aligned}\langle p(\omega) p(\omega') \rangle &= \frac{\langle F(\omega) F(\omega') \rangle}{|\gamma[\omega] - i\omega|^2} \\ \Rightarrow 2\pi \delta(\omega + \omega') I_p(\omega) &= \frac{2\pi \delta(\omega + \omega') I_F(\omega)}{|\gamma[\omega] - i\omega|^2} \\ \Rightarrow I_p(\omega) &= \frac{I_F(\omega)}{|\gamma[\omega] - i\omega|^2},\end{aligned}\tag{3.38}$$

where, in the second line, the Wiener-Khintchine theorem is applied to both sides. The measured response's autocorrelation $\langle p(\omega) p(\omega') \rangle$ defines the power spectrum $I_p(\omega)$ through Eq.(3.35). Since $\gamma(t)$ and $I_p(\omega)$ are known, $I_F(\omega)$ can be determined from Eq.(3.38). Using $I_F(t)$ the function $\kappa(t)$ is then calculated from Eq.(3.24) and Eq.(3.35), i.e.

$$I_F(t) = \frac{\kappa(t - t')}{2\pi \delta(t + t')}.\tag{3.39}$$

For the generalised Langevin model, the relaxation time Eq.(3.22) becomes

$$t_{\text{relax}} = \frac{1}{\int_0^\infty dt \gamma(t)} = \frac{1}{\gamma[\omega = 0]} = \mu(\omega = 0),\tag{3.40}$$

where Eq.(3.28) and Eq.(3.31) have been used in the above simplification.

In order to gain an intuition regarding the relaxation time for the generalised Langevin model, consider an example where the memory kernel $\gamma(t)$ is sharply peaked around $t = 0$, i.e. the friction is approximated as being instantaneous. The retarded effect of the friction term in Eq.(3.23) is ignored, and the integral becomes

$$\int_0^\infty dt' \gamma(t - t') p(t') \approx \int_0^\infty dt' \gamma(t') p(t) = \frac{1}{t_{\text{relax}}} p(t),\tag{3.41}$$

where Eq.(3.40) is used in the final equality. Inserting Eq.(3.41) into the generalised Langevin equation Eq.(3.23), returns the non-retarded Langevin equation Eq.(3.1). Hence the interpretation of t_{relax} remains the same as for the non-retarded Langevin model: it is the time it takes for the Brownian particle to thermalize in the medium [42].

Another relevant time scale, the correlation (or microscopic) time, t_c , is defined. The correlation time is considered to be the width of the random force correlator function. Specifically,

$$t_c = \int_0^\infty dt \frac{\kappa(t)}{\kappa(0)}.\tag{3.42}$$

The quantity t_c measures the time duration of a single scattering process, i.e. it indicates how long the random force is correlated for. In most cases $t_{\text{relax}} \gg t_c$, however this does not necessarily hold for Brownian motion dual to AdS black holes.

On a final note for this subsection, the Langevin Model can also be generalised to d spatial dimensions. In Eq.(3.1), the momentum $p(t)$ and random force $F(t)$ become d -component vectors, while the assumptions Eq.(3.2) and Eq.(3.3) generalise to

$$\langle F_i(t) \rangle = 0 \quad \text{and} \quad \langle F_i(t) F_j(t') \rangle = \kappa_0 \delta_{ij} \delta(t - t'),\tag{3.43}$$

where $i, j = (1, 2, \dots, n)$. The fluctuation-dissipation theorem is independent of d ; as such κ_0 is still given by Eq.(3.11). The mean-squared displacement behaves like $\langle s^2(t) \rangle \approx 2 d D t$ in the late time limit ($t \gg \frac{1}{\gamma_0}$), where the diffusion coefficient D is still given by the Einstein-Sutherland relation Eq.(3.18).

This concludes a brief foray into some of the salient theory about Brownian motion³⁷. It is this motion which is responsible for the dissipative nature of a system and its approach to thermal equilibrium. Any particle suspended in a finite temperature fluid undergoes Brownian motion and as such a probe quark immersed in a thermal plasma behaves the same way. The AdS/CFT correspondence can be used to study the Brownian behaviour a probe quark exhibits while interacting with the strongly-coupled thermal plasma by modelling the external quark as a test string in the bulk theory. This is done in sections (4) and (6) for the heavy quark case, and section (5) for the light quark case.

³⁷For more detailed reading on the topic see [80, 86] who provide insightful early reviews, while [81, 87, 88] can be useful in understanding some of the more modern developments in the field.

Part II

Calculations in the Bulk

4 Analysing Heavy Quark Brownian Motion

In the previous section the theory of Brownian motion (specifically the Langevin model) was reviewed. An external test quark in a thermal plasma is governed by these equations. In the AdS/CFT context, this is the gauge theory – or boundary – side. The following three sections focus on the gravitational – or bulk – side, in which a probe string is set up in an anti-de Sitter black hole background³⁸ and the transverse fluctuations on this string (resulting from its proximity to the Schwarzschild black hole) are examined. The AdS/CFT correspondence is used to equate the two descriptions. Section (4) begins this incursion into the bulk theory by modelling an on-mass-shell quark of large finite mass, identified by particle physicists as an on-mass-shell heavy quark, as an open probe string stretched between the boundary and a Schwarzschild black hole in AdS spacetime³⁹. The presence of the black hole results in thermal fluctuations in the transverse X^I directions on the string. The resultant random movement of the string's endpoint on the boundary corresponds to the heavy quark undergoing Brownian motion. This set-up is depicted in figure (2).

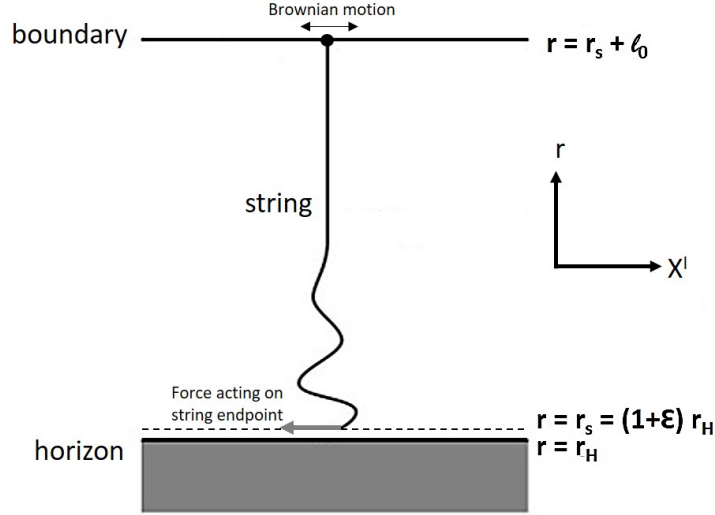


Figure 2: A fundamental open string of length ℓ_0 used as a probe in an AdS black hole background. The string starts at the boundary of the anti-de Sitter spacetime and hangs down to a *stretched horizon* ($r_s = (1 + \epsilon) r_H$ where $0 < \epsilon \ll 1$) placed just above the Schwarzschild black hole horizon. This figure is adapted from [42].

The stretched horizon depicted in figure (2) is introduced to regulate an infrared divergence. Similarly, a UV cut-off is imposed near the boundary to ensure the mass of the probe particle is finite⁴⁰. Dirichlet boundary conditions will be imposed on the fixed string endpoint attached to the stretched horizon, while Neumann boundary conditions will be imposed at the boundary.

4.1 Polyakov String Equations of Motion

The Brink-Di Vecchia-Howe-Deser-Zumino action [89, 90] – or Polyakov Action [91] for short – describes the leading order dynamics of the fundamental probe string and is given by

$$S_P := \frac{1}{4\pi\alpha'} \int_{\mathcal{M}} d^2\sigma \mathcal{L}_P = -\frac{1}{4\pi\alpha'} \int d^2\sigma \sqrt{-\det(\gamma_{ab})} \gamma^{ab} g_{ab}, \quad (4.1)$$

³⁸As discussed in section (2), the bulk theory is in $\text{AdS}_d \times S^d$. However, the physics on the compact S^d space corresponds to a set of scalar and fermion fields rotated among each other in $\mathcal{N} = 4$ SYM. In this dissertation, the rotational supersymmetric Yang-Mills charges are ignored. The calculations can be considered to take place in AdS_d and at a point on S^d .

³⁹Throughout this dissertation the test strings considered are in the probe approximation, i.e. the string's backreaction on the background is taken to be negligible. Further, it is assumed that no B -field is present in the background.

⁴⁰Following how this terminology used in [42], the terms *infrared* (IR) and *ultraviolet* (UV) are understood to be with respect to the boundary energy. In the bulk theory infrared means near the horizon, while ultraviolet means near the boundary.

where the slope parameter α' is related to the string tension T_0 [92]; \mathcal{L}_P is the Lagrangian density; the worldsheet parameter space is denoted by \mathcal{M} (with coordinates $(t, \sigma) \in [0, t_f] \times [0, \sigma_f] = \mathcal{M}$) and the spacetime by \mathcal{N} . The induced worldsheet metric is given by

$$g_{ab} := \partial_a X^\mu \partial_b X^\nu G_{\mu\nu}, \quad (4.2)$$

$G_{\mu\nu}$ is the spacetime metric, and γ_{ab} is an auxiliary worldsheet metric. From here onwards, the determinant of γ_{ab} will simply be denoted by γ . Notice that a gauge choice has been made: the static gauge is used. The reparameterization offered by the static gauge separates the time and space coordinates [92], identifying the τ parameter with the time coordinate, $\tau = t$.

The string worldsheet is embedded into the target spacetime by the mapping functions $X^\mu : \mathcal{M} \rightarrow \mathcal{N}; (t, \sigma) \rightarrow X^\mu(t, \sigma)$. The canonical conjugate momentum densities $\Pi_\mu^a(t, \sigma)$ are easily determined once the functional derivative of the Polyakov Action with respect to the derivatives of these embedding functions has been calculated⁴¹. Specifically,

$$\delta_{(\partial_a X^\mu)} S_P := \int_{\mathcal{M}} d^2\sigma \frac{\delta S_P}{\delta(\partial_a X^\mu(t, \sigma))} \delta(\partial_a X^\mu(t, \sigma)). \quad (4.3)$$

Using the definition of the Polyakov Action Eq.(4.1),

$$\begin{aligned} \delta_{(\partial_a X^\mu)} S_P &= -\frac{1}{2\pi\alpha'} \int_{\mathcal{M}} d^2\sigma \sqrt{-\gamma} \gamma^{ab} G_{\mu\nu} \delta(\partial_a X^\mu) \partial_b X^\nu \\ &= \int_{\mathcal{M}} d^2\sigma \delta(\partial_a X^\mu) \left(-\frac{1}{2\pi\alpha'} \sqrt{-\gamma} \gamma^{ab} G_{\mu\nu} \partial_b X^\nu \right), \end{aligned} \quad (4.4)$$

where the factor of two arises from symmetry (the variation of $\partial_a X^\mu$ and $\partial_b X^\nu$ gives the same the result). Hence the canonical momentum densities, defined as the variation of the action with respect to the derivatives of the embedding functions, is given by

$$\Pi_\mu^a(t, \sigma) := \frac{\delta S_P}{\delta(\partial_a X^\mu(t, \sigma))} = -\frac{1}{2\pi\alpha'} \sqrt{-\gamma} \gamma^{ab} G_{\mu\nu} \partial_b X^\nu. \quad (4.5)$$

The energy-momentum tensor T_{ab} can be defined by the variation of the Polyakov Action with respect to the auxiliary worldsheet metric [93],

$$T_{ab} := -4\pi \frac{1}{\sqrt{-\gamma}} \frac{\delta S_P}{\delta \gamma^{ab}}. \quad (4.6)$$

Before calculating T_{ab} , note that determining the functional derivative of the auxiliary worldsheet metric gives the two useful relations⁴²

$$\delta(\det(\gamma_{ab})) \equiv \delta\gamma = \gamma(\gamma^{ab} \delta\gamma_{ab}) = \gamma(\gamma_{ab} \delta\gamma^{ab}),$$

and

$$\delta(\sqrt{-\gamma}) = -\frac{1}{2\sqrt{-\gamma}} \delta\gamma = -\frac{\gamma}{2\sqrt{-\gamma}} (\gamma_{ab} \delta\gamma^{ab}) = -\frac{1}{2} \sqrt{-\gamma} \gamma_{ab} \delta\gamma^{ab}.$$

⁴¹The functional derivative (sometimes referred to as the variational or Fréchet derivative) compares the change in a functional to the change in a function that the functional depends on. The functional derivative of functional J with respect to function f (evaluated at point x) is defined as

$$\delta_f J = \int_a^b \frac{\delta J}{\delta f(x)} \delta f(x) dx.$$

⁴²To prove the first relation make use of the matrix property $\delta(\det(A)) = \det(A) \text{Tr}(A^{-1} \delta A)$, where A is an $n \times n$ matrix.

From the definition of the Polyakov Action Eq.(4.1) and the relation for $\delta(\sqrt{-\gamma})$, the functional derivative of the action with respect to the auxiliary worldsheet metric can be simplified to

$$\begin{aligned}
\delta_\gamma S_P &= -\frac{1}{4\pi\alpha'} \int_{\mathcal{M}} d^2\sigma \left(\delta(\sqrt{-\gamma}) \gamma^{ab} G_{\mu\nu} \partial_a X^\mu \partial_b X^\nu + \sqrt{-\gamma} \delta\gamma^{ab} G_{\mu\nu} \partial_a X^\mu \partial_b X^\nu \right) \\
&= -\frac{1}{4\pi\alpha'} \int_{\mathcal{M}} d^2\sigma \sqrt{-\gamma} \delta\gamma^{ab} G_{\mu\nu} \left[-\frac{1}{2} \gamma_{ab} \left(\gamma^{cd} \partial_c X^\mu \partial_d X^\nu \right) + \partial_a X^\mu \partial_b X^\nu \right] \\
&\equiv \int_{\mathcal{M}} d^2\sigma \delta\gamma^{ab} \frac{\delta S_P}{\delta\gamma^{ab}},
\end{aligned} \tag{4.7}$$

where the final line is simply the definition of the functional derivative. Hence, the energy-momentum tensor T_{ab} (Eq.(4.6)), becomes

$$\begin{aligned}
T_{ab} &= -4\pi \frac{1}{\sqrt{-\gamma}} \left[-\frac{1}{4\pi\alpha'} \sqrt{-\gamma} G_{\mu\nu} \left(-\frac{1}{2} \gamma_{ab} \gamma^{cd} \partial_c X^\mu \partial_d X^\nu + \partial_a X^\mu \partial_b X^\nu \right) \right] \\
&= \frac{1}{\alpha'} \left(-\frac{1}{2} \gamma_{ab} \gamma^{cd} G_{\mu\nu} \partial_c X^\mu \partial_d X^\nu + G_{\mu\nu} \partial_a X^\mu \partial_b X^\nu \right) \\
&= \frac{1}{\alpha'} \left(-\frac{1}{2} \gamma_{ab} \gamma^{cd} g_{cd} + g_{ab} \right),
\end{aligned} \tag{4.8}$$

where the definition of the induced worldsheet metric (Eq.(4.2)) is used in the last line. Requiring by the principle of least action that the energy-momentum tensor vanishes, implies

$$g_{ab} = \frac{1}{2} \gamma_{ab} \gamma^{cd} g_{cd}. \tag{4.9}$$

Eq.(4.9) sets the auxiliary metric γ_{ab} proportional to the induced metric g_{ab} at every point of the worldsheet. If the proportionality constant is defined to be positive (the notions of *timelike* and *spacelike* vectors defined by γ_{ab} and g_{ab} should agree); the metrics are said to be conformal to each other. This proportionality constant is denoted by f^2 . Writing,

$$\begin{aligned}
\gamma_{ab} &= f^2 g_{ab} \\
\Rightarrow \det(\gamma_{ab}) &= f^4 \det(g_{ab}) \\
\Rightarrow (-\gamma)^{-\frac{1}{2}} &= \frac{1}{f^2} (-g)^{-\frac{1}{2}} \\
\Rightarrow (-\gamma)^{-\frac{1}{2}} \gamma_{ab} &= \frac{1}{f^2} (-g)^{-\frac{1}{2}} f^2 g_{ab} \\
\Rightarrow \frac{\gamma_{ab}}{\sqrt{-\gamma}} &= \frac{g_{ab}}{\sqrt{-g}},
\end{aligned} \tag{4.10}$$

a constraint equation is obtained. From Eq.(4.10) it is evident that the Polyakov action has an additional symmetry to the Nambu-Goto string action (an action defined in terms of the induced metric g_{ab}) [94, 95], since the auxiliary worldsheet metric can be rescaled arbitrarily. Indeed, the Polyakov action is locally scale invariant on the string worldsheet. This is known as conformal/Weyl invariance: under a local change of scale all angles are kept fixed on the worldsheet, while the length of the lines may change.

Due to this additional symmetry, another gauge choice presents itself. Choosing the conformal gauge $\gamma^{ab} = \eta^{ab}$ (which restricts the choice of worldsheet to one with vanishing Euler characteristic), the constraint Eq.(4.10) simplifies to

$$\eta^{ab} = \frac{g_{ab}}{\sqrt{-g}}, \quad (4.11)$$

since $\eta^{ab} = \eta_{ab}$, and $\eta = \det(\eta_{ab}) = -1$. Hence, with this choice of gauge restricting the auxiliary metric γ_{ab} , the induced worksheet metric g_{ab} becomes conformally flat. In the conformal gauge, the energy-momentum tensor Eq.(4.8) becomes

$$T_{ab} = \frac{1}{\alpha'} G_{\mu\nu} \left(-\frac{1}{2} \eta_{ab} \eta^{cd} \partial_c X^\mu \partial_d X^\nu + \partial_a X^\mu \partial_b X^\nu \right). \quad (4.12)$$

The worldsheet parameter space coordinate system can be changed to light-cone coordinates, where the light-cone coordinates are defined as

$$\sigma^\pm = \frac{1}{\sqrt{2}}(\tau \pm \sigma) \quad \text{and} \quad \partial_\pm = \frac{1}{2}(\partial_\tau \pm \partial_\sigma). \quad (4.13)$$

The energy-momentum tensor can be written in terms of light-cone coordinates. This is easily done after explicitly writing out the components of T_{ab} (Eq.(4.12)),

$$\begin{aligned} T_{\tau\tau} &= T_{\sigma\sigma} = \frac{1}{2\alpha'} G_{\mu\nu} (\dot{X}^\mu \dot{X}^\nu + X'^\mu X'^\nu), \quad \text{and} \\ T_{\tau\sigma} &= T_{\sigma\tau} = \frac{1}{\alpha'} G_{\mu\nu} \dot{X}^\mu X'^\nu, \end{aligned} \quad (4.14)$$

where $\dot{X}^\mu = \partial_\tau X^\mu$ and $X'^\mu = \partial_\sigma X^\mu$. Further, $X'^\mu \dot{X}^\nu = \dot{X}^\mu X'^\nu$ since $G_{\mu\nu}$ is a diagonal matrix. In light-cone coordinates the components of the energy-momentum tensor are

$$T_{++} = \frac{1}{2}(T_{\tau\tau} + T_{\sigma\sigma}) \quad \text{and} \quad T_{--} = \frac{1}{2}(T_{\tau\tau} - T_{\sigma\sigma}), \quad (4.15)$$

which is easily proven from Eq.(4.12) using the definition Eq.(4.13) and the light-cone metric (where $\eta_{+-} = \eta_{-+} = -1$, $\eta_{++} = \eta_{--} = 0$). Inserting Eq.(4.14) into Eq.(4.15), yields

$$\begin{aligned} T_{++} &= \frac{1}{2} \frac{1}{\alpha'} G_{\mu\nu} \left[\frac{1}{2} (\partial_\tau X^\mu \partial_\tau X^\nu + \partial_\sigma X^\mu \partial_\sigma X^\nu) + \partial_\tau X^\mu \partial_\sigma X^\nu \right] \\ &= \frac{1}{\alpha'} G_{\mu\nu} \left[\left(\frac{1}{2} (\partial_\tau + \partial_\sigma) X^\mu \right) \left(\frac{1}{2} (\partial_\tau + \partial_\sigma) X^\nu \right) \right] \\ &= \frac{1}{\alpha'} G_{\mu\nu} \partial_+ X^\mu \partial_+ X^\nu, \end{aligned} \quad (4.16)$$

and

$$\begin{aligned} T_{--} &= \frac{1}{2} \frac{1}{\alpha'} G_{\mu\nu} \left[\frac{1}{2} (\partial_\tau X^\mu \partial_\tau X^\nu + \partial_\sigma X^\mu \partial_\sigma X^\nu) - \partial_\tau X^\mu \partial_\sigma X^\nu \right] \\ &= \frac{1}{\alpha'} G_{\mu\nu} \left[\left(\frac{1}{2} (\partial_\tau - \partial_\sigma) X^\mu \right) \left(\frac{1}{2} (\partial_\tau - \partial_\sigma) X^\nu \right) \right] \\ &= \frac{1}{\alpha'} G_{\mu\nu} \partial_- X^\mu \partial_- X^\nu. \end{aligned} \quad (4.17)$$

As previously mentioned, due to energy conservation, the energy-momentum tensor vanishes: $T_{ab} = 0$. In light-cone coordinates $T_{++} = T_{--} = 0$. Hence, Eqs.(4.16, 4.17) become

$$G_{\mu\nu} \partial_\pm X^\mu \partial_\pm X^\nu = 0, \quad (4.18)$$

which are known as the Virasoro constraint equations.

Finally, varying the Polyakov Action with respect to the string worldsheet coordinates and setting this functional variation to zero, yields the string equations of motion in the static gauge

$$0 = \partial_a \Pi_\mu^a - \Gamma_{\mu\nu}^\alpha \partial_a X^\nu \Pi_\alpha^a =: \nabla_a \Pi_\mu^a, \quad (4.19)$$

where the Christoffel symbols are defined as

$$\Gamma_{\mu\nu}^\alpha := \frac{1}{2} G^{\alpha\gamma} (\partial_\mu G_{\nu\gamma} + \partial_\nu G_{\mu\gamma} - \partial_\gamma G_{\mu\nu}). \quad (4.20)$$

The details of this derivation are given in appendix (A.1). The boundary conditions chosen in order to satisfy Eq.(4.19) are

$$\delta X^\mu \Pi_\mu^a \Big|_{\sigma=0}^{\sigma=\sigma_f} = 0. \quad (4.21)$$

This becomes a Dirichlet boundary condition at the stretched horizon ($r = r_s$)⁴³

$$\delta X^\mu(t, 0) = 0, \quad (4.22)$$

and a Neumann boundary condition at the boundary endpoint⁴⁴

$$\Pi_\mu^a(t, \sigma_f) = 0. \quad (4.23)$$

Eq.(4.19) is the equations of motion describing the leading order string behaviour. Considering additional behaviour, small transverse fluctuations for example, would result in supplementary equations of motion for X^I (where I denote the transverse directions). This is precisely the focus of subsection (4.3).

The general, leading order solution to the string equations of motion is found by solving Eqs.(4.18, 4.19) with respect to the boundary conditions Eqs.(4.22, 4.23) and the relevant initial conditions. The metric $G_{\mu\nu}$, the initial conditions, and hence the string solution will depend on the geometry of the spacetime the test string is set up in. For example, in $\mathbb{R}^{1,1}$ the string's worldsheet parameter space \mathcal{M} (with coordinates $(t, \sigma) \in [0, t_f] \times [0, \sigma_f] = \mathcal{M}$) is embedded into the target spacetime $\mathcal{N} = \mathbb{R}^{1,1}$ by the function

$$X_{\text{Mink}}^\mu(t, \sigma) = (t, x(t, \sigma))^\mu, \quad (4.24)$$

where $x(t, \sigma)$ still needs to be determined. This is the aim of the following two subsections, where the general solutions for the test string in an $\mathbb{R}^{1,1}$ and an AdS_3 -Schwarzschild background respectively are found⁴⁵.

4.2 Leading Order String Behaviour

4.2.1 Test Strings in $\mathbb{R}^{1,1}$

The embedding functions⁴⁶, X_{Mink}^μ , given in Eq.(4.24) are found by solving the Virasoro constraints and string equations of motion in $\mathbb{R}^{1,1}$. For simplicity, a square parameter space is chosen i.e. $t_f = \sigma_f$. Working in the static gauge, a Dirichlet Boundary condition at $\sigma = 0$ is imposed (corresponding to the fixed initial position of the string endpoint)

⁴³The stretched horizon is defined by $r_s = (1 + \epsilon) r_H$ where $0 < \epsilon \ll 1$. In the limit $\epsilon \rightarrow 0$ implementing a Neumann boundary condition here instead of a Dirichlet condition would be equivalent. This is done by de Boer *et al.* [42].

⁴⁴From the bulk perspective, this endpoint terminates on a space filling flavour D7-brane which is introduced in order to ensure the test quarks in the field theory have a finite mass [54].

⁴⁵A note to the reader: a more interesting embedding occurs when studying the off-mass-shell light quark, since the parameter space is divided into two separate regions. This will be explored in detail in subsection (5.1).

⁴⁶Referred to interchangeably throughout this dissertation as the leading order solution to the string equations of motion.

$$x(t, 0) = x_0 \in \mathbb{R}, \quad (4.25)$$

and a Neumann Boundary condition at $\sigma = \sigma_f$ is imposed (enforcing zero flux through the other string endpoint)

$$\partial_\sigma x(t, \sigma)|_{\sigma=\sigma_f} = 0. \quad (4.26)$$

For initial conditions, take the string to be static at $t = 0$,

$$\partial_t x(t, \sigma)|_{t=0} = 0, \quad (4.27)$$

and stretched between x_0 and $x_0 + \ell_0$ in the x spatial direction,

$$x(0, \sigma) = x_0 + \frac{\sigma}{\sigma_f} \ell_0, \quad \ell_0 \in \mathbb{R}^+. \quad (4.28)$$

The total energy and momentum of the string are given by

$$E = - \int d\sigma \Pi_t^\tau \quad \text{and} \quad p = \int d\sigma \Pi_x^\tau, \quad (4.29)$$

where Π_μ^a are the canonical momentum densities defined in Eq.(4.5) [92]. In flat space the total energy of the static string⁴⁷ – which would be equal to the mass of a heavy test quark in the boundary theory⁴⁸ – is given by

$$\begin{aligned} E &= -\frac{1}{2\pi\alpha'} \int_0^{\sigma_f} d\sigma \eta^{\tau b} \eta_{t\nu} \partial_b X^\nu \\ &= -\frac{1}{2\pi\alpha'} \int_0^{\ell_0} d\sigma \partial_\tau X^t \\ &= -\frac{\ell_0}{2\pi\alpha'}. \end{aligned} \quad (4.30)$$

In the second line it has been recognised that $\sigma_f = \ell_0$ (which follows from the Virasoro constraints in flat space [52]); and the last line follows due to the static gauge choice ($\tau = t$), and $X^0 = t$ (Eq.(4.24)). Therefore,

$$E^2 \equiv m_q^2 = \frac{\ell_0^2}{4\pi^2\alpha'^2}, \quad (4.31)$$

where $E^2 = m^2$ since the string is initially static – i.e. the total momentum vanishes. The length of the string and the magnitude of the quark's mass are directly proportional. This same relationship holds for a test string in an AdS-Schwarzschild background, and indeed Eq.(4.31) remains true. For proof of this see appendix (A.3).

Since the leading order dynamics are that of a static string, the initial condition Eq.(4.28) holds for all $t \in \mathbb{R}^+$. Hence, the embedding functions X_{Mink}^μ are somewhat trivially⁴⁹ given by

$$X_{\text{Mink}}^\mu(t, \sigma) = (t, x_0 + \sigma)^\mu, \quad (4.32)$$

with coordinates $(t, \sigma) \in [0, \sigma_f] \times [0, \sigma_f] = \mathcal{M}$.

⁴⁷Static in terms of the string's configuration, not in terms of gauge choice.

⁴⁸Supposing for a moment that the gauge/string duality postulated the existence of such a boundary theory to $\mathbb{R}^{1,1}$ spacetime.

⁴⁹As (t, σ) sweep out a square region of parameter space $(t, \sigma) \in [0, \sigma_f] \times [0, \sigma_f] = \mathcal{M}$, the embedding functions map out a rectangular region (square if $x_0 = 0$) of target spacetime.

4.2.2 Test Strings in AdS₃-Schwarzschild

Consider a test string in AdS₃-Schwarzschild set up as in figure (2), page 16. Examining the leading order behaviour of the string (no transverse fluctuations are present), the equations of motion with respect to the boundary and initial conditions can be solved in order to find the embedding functions $X_{\text{AdS}_3\text{-Sch}}^\mu(t, \sigma)$. The AdS_d-Schwarzschild metric in d dimensions is given by⁵⁰

$$ds_d^2 = \frac{r^2}{l^2} \left(-h(r; d) dt^2 + d\vec{X}_I^2 \right) + \frac{l^2}{r^2} \frac{dr^2}{h(r; d)}, \quad (4.33)$$

where $t \in [0, \infty)$ is the temporal coordinate, $r \in [0, \infty)$ is the radial coordinate, and the transverse spatial directions are denoted by $\vec{X}_I = (X^2, X^3, \dots, X^{(d-1)}) \in \mathbb{R}^{d-2}$. Further, $l \in \mathbb{R}^+$ is the curvature radius of AdS_d and S^d , and the blackening factor of the Schwarzschild black hole situated at the horizon, $h(r; d)$, is given by

$$h(r; d) := 1 - \left(\frac{r_H}{r} \right)^{d-1}. \quad (4.34)$$

The function $h(r; d) \in [0, 1]$, where $h(r; d) = 0$ at the stretched horizon and $h(r; d) = 1$ at the AdS-Schwarzschild boundary. The radial position of the black-brane horizon is denoted by $r_H \in \mathbb{R}^+$. The Hawking temperature of the black-brane in AdS_d-Schwarzschild – corresponding to the temperature of the thermal plasma in the boundary theory – is

$$T \equiv \frac{1}{\beta} = \frac{(d-1)r_H}{4\pi l^2}. \quad (4.35)$$

In order to consider whether r is a good radial coordinate to use to find the embedding functions, the causal structure of the spacetime is briefly explored using probe light rays approaching the horizon ($r = r_H$). Considering a null geodesic ($ds_d^2 = 0$) along the radial direction ($\vec{X}_I = 0$), the AdS_d-Schwarzschild metric Eq.(4.33) becomes

$$\frac{dt}{dr} = \pm \left(\frac{r^2}{l^2} h(r; d) \right)^{-1}, \quad (4.36)$$

i.e. as a probe light ray approaches the black hole event horizon ($r = r_H$), $dt/dr \rightarrow \pm\infty$ ⁵¹. There appears to be singular behaviour at $r = r_H$ (as the event horizon is approached, movement in the radial direction with respect to the coordinate time t becomes less and less successful), but it's actually highly dependent on the chosen coordinate system. For instance, the singular behaviour can be assuaged if the time coordinate is replaced with a coordinate which moves *appropriately slowly* along the null geodesic. Defining $t := \pm r_*$ along this null geodesic, Eq.(4.36) can be integrated with respect to r to yield

$$r_*(d) = l^2 \int dr \frac{1}{r^2 h(r; d)}, \quad (4.37)$$

where r_* is known as the tortoise coordinate [96]. Using Eq.(4.34) to solve the integral⁵² yields

$$r_*(d) = -\frac{l^2}{r} {}_2F_1 \left(1, \frac{1}{d-1}; \frac{d}{d-1}; \left(\frac{r_H}{r} \right)^{d-1} \right), \quad (4.38)$$

where ${}_2F_1$ is the Gaussian hypergeometric function⁵³. Using the tortoise coordinate r_* as the new radial coordinate presents an advantage – the horizon can be approached at the relevant rate (dt/dr_* remains

⁵⁰As mentioned in section (2), the anti-de Sitter-Schwarzschild spacetime metric Eq.(4.33) represents a Poincaré chart of AdS_d spacetime. The global AdS-Schwarzschild spacetime yields two black hole solutions at the same temperature: a black hole with a specific heat which is negative, and a black hole in thermal equilibrium exhibiting Hawking radiation. In order to access both solutions, global AdS-Schwarzschild geometry with a compact spatial boundary would need to be considered [42] – which is beyond the current scope of this work.

⁵¹Think of a series of light-cones drawn from each point along the trajectory of the light ray approaching the horizon – as the light ray approaches $r = r_H$, the light-cones *close up* [96].

⁵²The integral Eq.(4.37) was solved using Mathematica [97], and specifically an integration package called Rubi [98].

⁵³See footnote 66, page 34, for the definition of the Gaussian hypergeometric function.

finite)⁵⁴. Hence, to proceed in solving the string equations of motion, the coordinate set (t, r_*) is chosen since it allows the correct boundary conditions for the fluctuations at the black hole horizon to be specified. The tortoise coordinate, however, can only be inverted for $d = 3$. Therefore it is only trivial to solve the string equations of motion to find the embedding functions of the test string in AdS₃-Schwarzschild. For $d = 3$, Eq.(4.38) becomes

$$r_*(3) = \frac{1}{2} \frac{l^2}{r_H} \ln \left(\frac{r - r_H}{r + r_H} \right) = \frac{l^2}{r_H} \coth^{-1} \left(-\frac{r}{r_H} \right), \quad (4.39)$$

which can be easily inverted to find r in terms of $r_*(3)$:

$$r = -r_H \coth \left(\frac{r_H r_*}{l^2} \right), \quad (4.40)$$

where $r_*(3)$ is given by r_* for concision. In $d = 3$ dimensions, the metric Eq.(4.33) is given by⁵⁵

$$\begin{aligned} ds_3^2 &:= \frac{r^2}{l^2} \left(-h(r) dt^2 + dx^2 \right) + \frac{l^2}{r^2} \frac{dr^2}{h(r)}, \quad \text{where} \quad h(r) = \frac{r^2 - r_H^2}{r^2} \\ &= -\frac{r^2 - r_H^2}{l^2} dt^2 + \frac{l^2}{r^2 - r_H^2} dr^2 + \frac{r^2}{l^2} dx^2. \end{aligned} \quad (4.41)$$

This, incidentally, is also the metric for the non-rotating BTZ black hole [99]. The AdS₃-Schwarzschild metric Eq.(4.41) can be written in terms of the coordinate set (t, r_*) using Eq.(4.40) and its differential,

$$dr = \frac{r_H^2}{l^2} \operatorname{csch}^2 \left(\frac{r_H r_*}{l^2} \right) dr_*. \quad (4.42)$$

Inserting Eqs.(4.40, 4.42) into the metric Eq.(4.41)⁵⁶, yields

$$\begin{aligned} ds_3^2 &:= -\frac{r_H^2 \coth^2 \left(\frac{r_H r_*}{l^2} \right) - r_H^2}{l^2} dt^2 + \frac{l^2}{r_H^2 \coth^2 \left(\frac{r_H r_*}{l^2} \right) - r_H^2} \frac{r_H^4}{l^4} \operatorname{csch}^4 \left(\frac{r_H r_*}{l^2} \right) dr_*^2 + \frac{r_H^2}{l^2} \coth^2 \left(\frac{r_H r_*}{l^2} \right) dx^2 \\ &= \frac{r_H^2}{l^2} \operatorname{csch}^2 \left(\frac{r_H r_*}{l^2} \right) (-dt^2 + dr_*^2) + \frac{r_H^2}{l^2} \coth^2 \left(\frac{r_H r_*}{l^2} \right) dx^2. \end{aligned} \quad (4.43)$$

From Eq.(4.43), notice that the AdS₃-Schwarzschild metric in the (t, r_*) coordinate system is conformally flat, i.e. the chosen coordinates (t, r_*) are a set of isothermal coordinates.

As discussed previously, to regulate an infrared divergence at the horizon, the stretched horizon $r_s = (1 + \epsilon) r_H$ (where $0 < \epsilon \ll 1$) is introduced. At the stretched horizon, a Dirichlet boundary condition (comparable to Eq.(4.22)) for the test string in AdS₃-Schwarzschild is implemented

$$X_{\text{AdS}_3\text{-Sch}}^r(t, 0) = r_s, \quad (4.44)$$

while a Neumann boundary condition (comparable to Eq.(4.23)) is implemented at the boundary endpoint

$$\partial_\sigma X_{\text{AdS}_3\text{-Sch}}^r(t, \sigma) \Big|_{\sigma=\sigma_f} = 0. \quad (4.45)$$

The boundary conditions Eq.(4.44) and Eq.(4.45) are rewritten in terms of the coordinate set (t, r_*) . The Dirichlet condition Eq.(4.44) becomes

⁵⁴The cost of this coordinate replacement is that the horizon surface is pushed to infinity, i.e. at $r_* = \infty$ [96].

⁵⁵In AdS₃-Schwarzschild there is only one transverse direction, referred to as x .

⁵⁶Mathematica is used to help simplify the trigonometry. This computation (and others in this section) are explicitly shown in Mathematica Notebook [b] (`BrownianMotion.nb`). For access, see appendix (A.7).

$$X_{\text{AdS}_3\text{-Sch}}^{r_*}(t, 0) = r_{s*}, \quad (4.46)$$

where r_{s*} is defined using Eq.(4.39),

$$r_{s*} = \frac{l^2}{r_H} \coth^{-1} \left(-\frac{r_s}{r_H} \right), \quad (4.47)$$

and the Neumann condition Eq.(4.45) becomes

$$\begin{aligned} 0 &= \frac{r_H^2}{l^2} \text{csch}^2 \left(\frac{r_H}{l^2} X_{\text{AdS}_3\text{-Sch}}^{r_*}(t, \sigma) \right) \partial_\sigma X_{\text{AdS}_3\text{-Sch}}^{r_*}(t, \sigma) \Big|_{\sigma=\sigma_f} \\ &= \partial_\sigma X_{\text{AdS}_3\text{-Sch}}^{r_*}(t, \sigma) \Big|_{\sigma=\sigma_f}, \end{aligned} \quad (4.48)$$

where Eq.(4.42) is used in the first line, and the last line follows since $\text{csch}(x) \neq 0, \forall x \in \mathbb{R}$. The boundary conditions in the conformally flat description of AdS₃-Schwarzschild (Eqs.(4.46, 4.48)) are respectively analogous to the boundary conditions for the test string in \mathbb{R}^{1+1} , Eqs.(4.25, 4.26). Hence, the embedding functions for the test string in the conformally flat description of AdS₃-Schwarzschild are the direct analogue of Eq.(4.32). In (t, r_*) coordinates, the embedding functions are

$$X_{\text{AdS}_3\text{-Sch}}^\mu(t, \sigma) = (t, r_{s*} + \sigma, 0)^\mu, \quad (4.49)$$

with coordinates $(t, \sigma) \in [0, \sigma_f] \times [0, \sigma_f] = \mathcal{M}$. Using the inverse tortoise transformation Eq.(4.40), the embedding functions Eq.(4.49) can be written in terms of the original (t, r) coordinates

$$X_{\text{AdS}_3\text{-Sch}}^\mu(t, \sigma) = \left(t, -r_H \coth \left(\frac{r_H}{l^2} (r_{s*} + \sigma) \right) + \sigma, 0 \right)^\mu, \quad (4.50)$$

where the position of the fixed string endpoint attached to the stretched horizon r_{s*} is given by Eq.(4.47) and the length of the string in tortoise coordinates is given by

$$\sigma_f = \frac{l^2}{r_H} \coth^{-1} \left(-\frac{r_s + \ell_0}{r_H} \right) - r_{s*}. \quad (4.51)$$

Making the identification

$$r = -r_H \coth \left(\frac{r_H (r_{s*} + \sigma)}{l^2} \right), \quad (4.52)$$

leads to agreement between Eq.(4.50), and the stretched string of de Boer *et al.*'s [42, 46] calculations. Finally, notice that comparing Eq.(4.40) with Eq.(4.52), yields $r_* \equiv r_{s*} + \sigma$.

4.3 Fluctuating Test String Dynamics

In this subsection transverse fluctuations of the test string in AdS₃-Schwarzschild are studied⁵⁷, in order to explore (using the *AdS/CFT* correspondence) the heavy quark's Brownian motion induced by the thermal noise in the plasma. The fluctuations are chosen to be small so as to not affect the leading order radial solution (discovered in subsection (4.2.2)). de Boer *et al.* [42] outlays a semiclassical treatment of the test string's transverse motion in AdS₃-Schwarzschild by quantizing these transverse fluctuations and relating the behaviour of the modes on the string to the dynamics of the boundary endpoint.

The following subsection (4.3.1) derives the equations of motion for small transverse fluctuations on the test string in AdS_d-Schwarzschild. Following the method first laid out in [42], subsection (4.3.2) solves these equations of motion to find the general solution, and from there the mean-squared displacement of the test string's boundary endpoint, $s^2(t)$.

⁵⁷Later, in subsection (4.4), this will be generalised to AdS_d-Schwarzschild.

4.3.1 Nambu-Goto String Equations of Motion for Transverse Fluctuations

The standard Nambu-Goto action⁵⁸ can be used to describe the dynamics of the transverse fluctuations on the test string

$$S_{NG} := \frac{1}{2\pi\alpha'} \int_{\mathcal{M}} d^2\sigma \mathcal{L}_{NG} = -\frac{1}{2\pi\alpha'} \int_{\mathcal{M}} d^2\sigma \sqrt{-g}, \quad (4.53)$$

where \mathcal{L}_{NG} is the Lagrangian density, $g := \det(g_{ab})$ and the induced worldsheet metric g_{ab} is given by Eq.(4.2).

Take the embedding functions (given in AdS₃-Schwarzschild by Eq.(4.50)) to be the leading order static string solution in a (1+1)-dimensional subspace of spacetime spanned by the temporal and radial directions (t, r) , denoted by $X_0^\mu(t, \sigma)$ (where $X_0^\mu : [0, t_f] \times [0, \sigma_f] \rightarrow \mathbb{R}^{d-1,1}$; $(t, \sigma) \rightarrow X_0^\mu(t, \sigma)$). Consider the addition of transverse fluctuations X^I (where $I \in (2, 3, \dots, d-1)$) to $X_0^\mu(t, \sigma)$. The effective action for the transverse fluctuations appears as a correction to the leading order Nambu-Goto action. It follows that to find the effective action for the transverse fluctuations (and from this the equations of motion) the Nambu-Goto action needs to be expanded about $X_0^\mu(t, \sigma)$, in terms of X^I ,

$$S_{NG} = \frac{1}{2\pi\alpha'} \int_{\mathcal{M}} d^2\sigma \mathcal{L}_{NG} \Big|_{X_0^\mu} + S_{NG}^{(2)} + S_{NG}^{(4)} + \mathcal{O}\left(S_{NG}^{(6)}\right), \quad (4.54)$$

where

$$S_{NG}^{(2)} := \frac{1}{2\pi\alpha'} \int_{\mathcal{M}} d^2\sigma \mathcal{L}_{NG}^{(2)} \quad \text{and} \quad S_{NG}^{(4)} := \frac{1}{2\pi\alpha'} \int_{\mathcal{M}} d^2\sigma \mathcal{L}_{NG}^{(4)}. \quad (4.55)$$

In order to explicitly calculate the expansion in Eq.(4.54), the determinant of the induced worldsheet metric is needed. This is derived in appendix (A.3) and is given below

$$g := \det(g_{ab}) = G_{rr} G_{tt} \left(r'^2 + \frac{r'^2}{G_{tt}} G_{II} \dot{X}_I^2 + \frac{1}{G_{rr}} G_{II} X_I'^2 \right), \quad (4.56)$$

where $\dot{X} = \partial_\tau X$ and $X' = \partial_\sigma X$; I indexes over the transverse directions $X_I = (X^2, X^3, \dots, X^{(d-1)})$; and the AdS_d-Schwarzschild spacetime metric $G_{\mu\nu}$ is the given explicitly by Eq.(A.32). Using Eq.(4.56) the Nambu-Goto action Eq.(4.53) becomes

$$\begin{aligned} S_{NG} &= -\frac{1}{2\pi\alpha'} \int_{\mathcal{M}} d^2\sigma (-r'^2 G_{rr} G_{tt})^{\frac{1}{2}} \sqrt{1 + \frac{1}{G_{tt}} G_{II} \dot{X}_I^2 + \frac{1}{r'^2 G_{rr}} G_{II} X_I'^2} \\ &= -\frac{1}{2\pi\alpha'} \int_{\mathcal{M}} d^2\sigma (-r'^2 G_{rr} G_{tt})^{\frac{1}{2}} \left[1 + \frac{1}{2} \left(\frac{G_{II}}{G_{tt}} \dot{X}_I^2 + \frac{G_{II}}{r'^2 G_{rr}} X_I'^2 \right) - \frac{1}{8} \left(\frac{G_{II}}{G_{tt}} \dot{X}_I^2 + \frac{G_{II}}{r'^2 G_{rr}} X_I'^2 \right)^2 \right] \Big|_{X_0^\mu} \\ &= -\frac{1}{2\pi\alpha'} \int_{\mathcal{M}} d^2\sigma \sqrt{-g} \Big|_{X_0^\mu} - \frac{1}{4\pi\alpha'} \int_{\mathcal{M}} d^2\sigma \sqrt{-g} \Big|_{X_0^\mu} \left(\frac{G_{II}}{G_{tt}} \dot{X}_I^2 + \frac{G_{II}}{r'^2 G_{rr}} X_I'^2 \right) \Big|_{X_0^\mu} \\ &\quad + \frac{1}{16\pi\alpha'} \int_{\mathcal{M}} d^2\sigma \sqrt{-g} \Big|_{X_0^\mu} \left(\frac{G_{II}}{G_{tt}} \dot{X}_I^2 + \frac{G_{II}}{r'^2 G_{rr}} X_I'^2 \right)^2 \Big|_{X_0^\mu}, \end{aligned} \quad (4.57)$$

where a Taylor expansion up to quadratic order (i.e. $(1+x)^{1/2} \approx 1 + \frac{x}{2} - \frac{x^2}{8}$) was performed in the second line. In the following line it is noticed from Eq.(4.56) that to leading order the determinant of the induced worldsheet metric is simply given by

$$g \Big|_{X_0^\mu} = r'^2 G_{rr} G_{tt}. \quad (4.58)$$

⁵⁸Using Eq.(4.10) the equivalence between the Polyakov action Eq.(4.1) and the Nambu-Goto action Eq.(4.53) is apparent.

The quadratic correction in the expansion of the Nambu-Goto action (defined in Eq.(4.55)) is the effective action for the transverse fluctuations. Matching terms between Eq.(4.54) and Eq.(4.57), the quadratic correction is given by

$$\begin{aligned}
S_{NG}^{(2)} &= -\frac{1}{4\pi\alpha'} \int_{\mathcal{M}} d^2\sigma \sqrt{-g} \Big|_{X_0^\mu} \left(\frac{G_{II}}{G_{tt}} \dot{X}_I^2 + \frac{G_{II}}{r'^2 G_{rr}} X_I'^2 \right) \Big|_{X_0^\mu} \\
&= -\frac{1}{4\pi\alpha'} \int_{\mathcal{M}} d^2\sigma \sqrt{-g} \Big|_{X_0^\mu} \left(\frac{G_{II}}{G_{tt}} \partial_t X^I \partial_t X^I + \frac{G_{II}}{r'^2 G_{rr}} \partial_\sigma X^I \partial_\sigma X^I \right) \Big|_{X_0^\mu} \\
&= -\frac{1}{4\pi\alpha'} \int_{\mathcal{M}} d^2\sigma \left(\frac{\sqrt{-g}}{g_{ab}} G_{IJ} \right) \Big|_{X_0^\mu} \partial_a X^I \partial_a X^J,
\end{aligned} \tag{4.59}$$

where a, b indexes over the static gauge worldsheet coordinates (t, σ) , the spacetime metric (Eq.(A.32)) is recognised as a diagonal matrix, and to leading order the induced worldsheet metric (see appendix (A.3)) is given by

$$g_{ab} \Big|_{X_0^\mu} = \begin{bmatrix} G_{tt} + G_{II} \dot{X}^2 & G_{II} \dot{X}_I X_I' \\ G_{II} X_I' \dot{X}_I & r'^2 G_{rr} + G_{II} X_I'^2 \end{bmatrix} \Big|_{X_0^\mu} = \begin{bmatrix} G_{tt} & 0 \\ 0 & r'^2 G_{rr} \end{bmatrix}. \tag{4.60}$$

Hence, the effective action for the transverse fluctuations $S_{NG}^{(2)}$ is given by

$$\begin{aligned}
S_{NG}^{(2)} &= -\frac{1}{4\pi\alpha'} \int_{\mathcal{M}} d^2\sigma (\sqrt{-g} g^{ab} G_{IJ}) \Big|_{X_0^\mu} \partial_a X^I \partial_b X^J \\
&\equiv \frac{1}{4\pi\alpha'} \int_{\mathcal{M}} d^2\sigma \frac{\partial^2 \mathcal{L}_{NG}}{\partial(\partial_a X^I) \partial(\partial_b X^J)} \Big|_{X_0^\mu} \partial_a X^I \partial_b X^J,
\end{aligned} \tag{4.61}$$

where I, J index over the transverse directions $(2, 3, \dots, d-1)$. Comparing Eq.(4.61) with Eq.(4.1), notice that if the auxiliary worldsheet metric is chosen to be the leading order induced worldsheet metric ($\gamma_{ab} = g_{ab} \Big|_{X_0^\mu}$) the action for transverse fluctuations Eq.(4.61) can be understood as an effective Polyakov Action. It remains to be proven whether or not the quartic term $S_{NG}^{(4)}$ is significant and contributes to the effective action of the transverse fluctuations. The quartic term $S_{NG}^{(4)}$ (defined in Eq.(4.55)) is given by

$$S_{NG}^{(4)} = \frac{1}{16\pi\alpha'} \int_{\mathcal{M}} d^2\sigma \left((\sqrt{-g} g^{ab} G_{IJ}) \Big|_{X_0^\mu} \partial_a X^I \partial_b X^J \right)^2. \tag{4.62}$$

Comparing the quadratic action term Eq.(4.61) with the quartic action term Eq.(4.62), yields

$$S_{NG}^{(2)} = -\frac{1}{\sqrt{\pi\alpha'}} \left(S_{NG}^{(4)} \right)^{\frac{1}{2}}. \tag{4.63}$$

Hence the quartic correction term $S_{NG}^{(4)}$ will significantly contribute to the effective action for the transverse fluctuations when the test string is within a distance of $\sqrt{\alpha'}$ from the black-brane horizon. Therefore the quadratic action $S_{NG}^{(2)}$ (Eq.(4.61)) can be considered to solely contribute to the effective action for the transverse fluctuations, as long as the fluctuations are small and the test string is in the region further than $\sqrt{\alpha'}$ away from the black-brane horizon, where

$$\sqrt{\alpha'} = \lambda^{-1/4} l, \tag{4.64}$$

in AdS_d -Schwarzschild. Eq.(4.64) defines the fundamental string length scale $\sqrt{\alpha'}$ in terms of the radius of curvature of AdS_d spacetime l and the 't Hooft coupling λ .

The canonical momentum densities conjugate to the transverse coordinates X^I are defined as

$$\Pi_I^a := \frac{\delta \mathcal{S}_{NG}^{(2)}}{\delta(\partial_a X^I)} = -\frac{1}{2\pi\alpha'} (\sqrt{-g} g^{ab} G_{IJ})|_{X_0^\mu} \partial_b X^J, \quad (4.65)$$

where the factor of two arises from symmetry (the variation of $\partial_a X^I$ and $\partial_b X^J$ gives the same the result).

Varying the effective action for the transverse fluctuations $\mathcal{S}_{NG}^{(2)}$ with respect to the transverse string worldsheet coordinates X^I and setting this functional variation to zero, yields the equations of motion

$$0 = \partial_a \Pi_I^a = \nabla_a \Pi_I^a. \quad (4.66)$$

These equations of motion are analogous to Eq.(4.19); but in Eq.(4.66) the Christoffel symbols (defined in Eq.(4.20)) are identically zero ($\Gamma_{IJ}^\alpha = 0$) due to the symmetry between each of the transverse directions. The details of this derivation are given in appendix (A.4). The chosen boundary conditions (analogous to Eq.(4.21)) are

$$\Pi_I^a \delta X^I \Big|_{\sigma=0}^{\sigma=\sigma_f} = 0, \quad (4.67)$$

which ensures the correct boundary terms vanish in the derivation of the string equations of motion for the transverse fluctuations (Eq.(4.66)).

4.3.2 Calculating the Heavy Quark's Mean-Squared Displacement $s^2(t)$ in AdS₃-Schwarzschild

The leading order static solution to the string equations of motion is given by Eq.(4.50) in AdS₃-Schwarzschild. Following subsection (4.3.1), this solution is renamed $X_0^\mu(t, \sigma)$. Adding non-zero fluctuations in the transverse x -direction, the test string solution becomes

$$X_{\text{AdS}_3\text{-Sch}}^\mu(t, \sigma) = X_0^\mu(t, \sigma) + (0, 0, X(t, \sigma))^\mu = \left(t, -r_H \coth\left(\frac{r_H}{l^2}(r_{s*} + \sigma)\right), X(t, \sigma)\right)^\mu. \quad (4.68)$$

In AdS₃-Schwarzschild, the equations of motion for the transverse fluctuations, Eq.(4.66), become

$$\begin{aligned} 0 &= \partial_a \left(-\frac{1}{2\pi\alpha'} (\sqrt{-g} g^{ab} G_{IJ})|_{X_0^\mu} \partial_b X^J \right) \\ &= \partial_a \left(\left(\sqrt{-g} g^{ab} \frac{r^2}{l^2} \right) \Big|_{X_0^\mu} \partial_b X(t, \sigma) \right), \end{aligned} \quad (4.69)$$

where the definition transverse momentum densities Eq.(4.65) are used in the first line, and the spacetime metric Eq.(A.32) in the second line. To leading order the induced worldsheet metric is given by Eq.(4.60). For $d = 3$, this metric simplifies to

$$g_{ab}|_{X_0^\mu} := \begin{bmatrix} g_{tt} & g_{t\sigma} \\ g_{\sigma t} & g_{\sigma\sigma} \end{bmatrix} \Big|_{X_0^\mu} = \begin{bmatrix} G_{tt} & 0 \\ 0 & r'^2 G_{rr} \end{bmatrix} = \begin{bmatrix} \left(-\frac{r^2 - r_H^2}{l^2}\right) & 0 \\ 0 & r'^2 \left(\frac{l^2}{r^2 - r_H^2}\right) \end{bmatrix}, \quad (4.70)$$

where Eq.(4.41) is used, and $r' = \partial_\sigma r$. Hence, its inverse is given by

$$g^{ab}|_{X_0^\mu} := \begin{bmatrix} g^{tt} & g^{t\sigma} \\ g^{\sigma t} & g^{\sigma\sigma} \end{bmatrix} \Big|_{X_0^\mu} = \frac{1}{\det(g_{ab}|_{X_0^\mu})} \begin{bmatrix} r'^2 G_{rr} & 0 \\ 0 & G_{tt} \end{bmatrix} = \begin{bmatrix} \left(-\frac{l^2}{r^2 - r_H^2}\right) & 0 \\ 0 & \frac{1}{r'^2} \left(\frac{r^2 - r_H^2}{l^2}\right) \end{bmatrix}, \quad (4.71)$$

where $\det(g_{ab}|_{X_0^\mu})$ is given in Eq.(4.58). The indices in Eq.(4.69) can be expanded

$$\begin{aligned}
0 &= \partial_\sigma \left(\left(\sqrt{-g} g^{\sigma\sigma} \frac{r^2}{l^2} \right) \Big|_{X_0^\mu} \partial_\sigma X(t, \sigma) \right) + \partial_t \left(\left(\sqrt{-g} g^{tt} \frac{r^2}{l^2} \right) \Big|_{X_0^\mu} \partial_t X(t, \sigma) \right) \\
&= \partial_\sigma \left(r' \left[\frac{1}{r'^2} \left(\frac{r^2 - r_H^2}{l^2} \right) \right] \frac{r^2}{l^2} \partial_\sigma X(t, \sigma) \right) + \partial_t \left(r' \left(-\frac{l^2}{r^2 - r_H^2} \right) \frac{r^2}{l^2} \partial_t X(t, \sigma) \right) \\
&= -\partial_t^2 X(t, \sigma) + \frac{r^2 - r_H^2}{l^4 r^2} \frac{1}{\partial_\sigma r} \partial_\sigma \left(\frac{1}{\partial_\sigma r} r^2 (r^2 - r_H^2) \partial_\sigma X(t, \sigma) \right),
\end{aligned} \tag{4.72}$$

where Eqs.(4.58, 4.71) are used in the second line. The transverse equations of motion can be fully converted into spacetime variables (t, r) . The derivative operator ∂_σ first needs to be converted into ∂_r using Eq.(4.52). The differential of Eq.(4.52) is

$$\begin{aligned}
dr &= \frac{r_H^2}{l^2} \operatorname{csch}^2 \left(\frac{r_H (r_{s*} + \sigma)}{l^2} \right) d\sigma \\
\Rightarrow \partial_\sigma &= \frac{r_H^2}{l^2} \operatorname{csch}^2 \left(\frac{r_H (r_{s*} + \sigma)}{l^2} \right) \partial_r \\
\Rightarrow \partial_\sigma &= -\frac{r_H^2}{l^2} \left(1 - \coth^2 \left(\frac{r_H (r_{s*} + \sigma)}{l^2} \right) \right) \partial_r \\
\Rightarrow \partial_\sigma &= \frac{r^2 - r_H^2}{l^2} \partial_r.
\end{aligned} \tag{4.73}$$

Using Eq.(4.73), the transverse equations of motion Eq.(4.72) become

$$0 = -\partial_t^2 X(t, r) + \frac{r^2 - r_H^2}{l^4 r^2} \partial_r (r^2 (r^2 - r_H^2) \partial_r X(t, r)). \tag{4.74}$$

Further, the transverse equations of motion can be completely written in terms of worldsheet parameter coordinates (t, σ) using Eqs.(4.52, 4.73), which yields

$$0 = -\partial_t^2 X(t, \sigma) + \frac{1}{\coth^2 \left(\frac{r_H}{l^2} (r_{s*} + \sigma) \right)} \partial_\sigma \left(\coth^2 \left(\frac{r_H}{l^2} (r_{s*} + \sigma) \right) \partial_\sigma X(t, \sigma) \right). \tag{4.75}$$

To proceed in solving the linear and homogeneous partial differential equation Eq.(4.74) – or Eq.(4.75) in (t, σ) coordinates – the method laid out in de Boer *et al.* [42] is followed. Explicitly, consider a mode expansion in X ,

$$X(t, r) = f_\omega(r) e^{-i\omega t}, \tag{4.76}$$

where $X(t, r)$ is a separable eigenmode solution to Eq.(4.74) which oscillates in time with a well-defined angular frequency $\omega \in \mathbb{R}^+$. Inserting Eq.(4.76) into Eq.(4.74), it can be seen that $f_\omega(r)$ satisfies the ordinary differential equation

$$\begin{aligned}
0 &= -\partial_t^2 (f_\omega(r) e^{-i\omega t}) + \frac{r^2 - r_H^2}{l^4 r^2} \partial_r (r^2 (r^2 - r_H^2) \partial_r (f_\omega(r) e^{-i\omega t})) \\
&= \omega^2 f_\omega(r) + \frac{r^2 - r_H^2}{l^4 r^2} \partial_r (r^2 (r^2 - r_H^2) \partial_r f_\omega(r)).
\end{aligned} \tag{4.77}$$

Defining the dimensionless quantity

$$\nu := \frac{l^2 \omega}{r_H}, \tag{4.78}$$

the ordinary differential equation (Eq.(4.77)) can be rewritten as

$$\left(\nu^2 + \frac{r_H^2 (r^2 - r_H^2)}{l^8 r^2} \partial_r (r^2 (r^2 - r_H^2) \partial_r) \right) f_\omega(r) = 0. \quad (4.79)$$

This second order ODE has two linearly independent solutions⁵⁹

$$f_\omega^{(\pm)}(r) = \frac{1}{1 \pm i\nu} \frac{r \pm ir_H \nu}{r} \left(\frac{r - r_H}{r + r_H} \right)^{\pm i\nu/2}. \quad (4.80)$$

In solving Eq.(4.79) the initial condition near the horizon is chosen to be

$$f_\omega^{(\pm)}(r) \rightarrow \left(\frac{r - r_H}{r + r_H} \right)^{\pm i\nu/2} \quad \text{as} \quad r \rightarrow r_H, \quad (4.81)$$

i.e. the normalization at the black-brane horizon ($r = r_H$) is taken to be $\frac{1}{1 \pm i\nu} \frac{r \pm ir_H \nu}{r} = 1$. For convenience, the solutions Eq.(4.80) can be partially rewritten in terms of the tortoise coordinate r_* . Rearranging Eq.(4.52) yields

$$\begin{aligned} r_{s*} + \sigma &= \frac{l^2}{r_H} \coth^{-1} \left(-\frac{r}{r_H} \right) \\ \Rightarrow r_{s*} + \sigma &= \frac{l^2}{2r_H} \ln \left(\frac{r - r_H}{r + r_H} \right) \\ \Rightarrow \pm i\omega (r_{s*} + \sigma) &= \ln \left(\frac{r - r_H}{r + r_H} \right)^{\pm i\nu/2} \\ \Rightarrow e^{\pm i\omega (r_{s*} + \sigma)} &= \left(\frac{r - r_H}{r + r_H} \right)^{\pm i\nu/2}, \end{aligned} \quad (4.82)$$

where the definition for ν , Eq.(4.78), is used in the third line. Inputting Eq.(4.82) into Eq.(4.80) gives

$$f_\omega^{(\pm)}(r) = \frac{1}{1 \pm i\nu} \frac{r \pm ir_H \nu}{r} e^{\pm i\omega (r_{s*} + \sigma)}, \quad (4.83)$$

where the initial condition near the horizon Eq.(4.81) becomes

$$f_\omega^{(\pm)}(r) \rightarrow e^{\pm i\omega (r_{s*} + \sigma)} \quad \text{as} \quad r \rightarrow r_H. \quad (4.84)$$

From Eq.(4.84) it is apparent that $f_\omega^{(\pm)}(r)$ denotes out-going (+) and in-falling (−) basis modes⁶⁰. The general solution to the ODE, $f_\omega(r)$, is a linear combination of these modes

$$f_\omega(r) = f_\omega^{(+)}(r) + B_\omega f_\omega^{(-)}(r), \quad (4.85)$$

where the constant B_ω measures the difference in phase between the (+) and (−) modes, and is yet to be determined. Imposing a Neumann boundary condition in the radial direction at the boundary endpoint,

$$\begin{aligned} 0 &= \partial_r f_\omega(r) \Big|_{r=r_s+\ell_o} \\ &= \partial_r \left(\frac{1}{1 + i\nu} \frac{r + ir_H \nu}{r} \left(\frac{r - r_H}{r + r_H} \right)^{i\nu/2} + B_\omega \frac{1}{1 - i\nu} \frac{r - ir_H \nu}{r} \left(\frac{r - r_H}{r + r_H} \right)^{-i\nu/2} \right) \Big|_{r=r_s+\ell_o}, \end{aligned} \quad (4.86)$$

⁵⁹This is consistent with Eq.(2.36) in de Boer *et al.*'s paper [42].

⁶⁰The mode $f_\omega^+(r)$ is outgoing at the horizon; while $f_\omega^-(r)$ is a mode which is reflected at the boundary and – after experiencing a phase shift – falls back towards the horizon.

enables B_ω to be fixed. Note that Eqs.(4.80, 4.85) have been used in the second line. Hence, Eq.(4.86) is solved⁶¹ to find B_ω :

$$\begin{aligned} B_\omega &= \left(\frac{i + \nu}{-i + \nu} \right) \left(\frac{r\nu - ir_H}{r\nu + ir_H} \right) \left(\frac{r - r_H}{r + r_H} \right)^{i\nu} \Big|_{r=r_s+\ell_o} \\ &= \left(\frac{1 - i\nu}{1 + i\nu} \right) \left(\frac{1 + i\tilde{r}_0\nu}{1 - i\tilde{r}_0\nu} \right) \left(\frac{\tilde{r}_0 - 1}{\tilde{r}_0 + 1} \right)^{i\nu}, \end{aligned} \quad (4.87)$$

where the dimensionless quantity

$$\tilde{r}_0 := \frac{r_s + \ell_0}{r_H}, \quad (4.88)$$

has been defined in the second line. The coefficient B_ω can be partially rewritten in terms of the tortoise coordinate r_* . To this end Eq.(4.51) is rearranged,

$$\begin{aligned} r_{s*} + \sigma_f &= \frac{l^2}{r_H} \coth^{-1} \left(-\frac{r_s + \ell_0}{r_H} \right) \\ \Rightarrow r_{s*} + \sigma_f &= \frac{l^2}{2r_H} \ln \left(\frac{(r_s + \ell_0) - r_H}{(r_s + \ell_0) + r_H} \right) \\ \Rightarrow i2\omega(r_{s*} + \sigma_f) &= \ln \left(\frac{(r_s + \ell_0) - r_H}{(r_s + \ell_0) + r_H} \right)^{i\nu} \\ \Rightarrow e^{i2\omega(r_{s*} + \sigma_f)} &= \left(\frac{\tilde{r}_0 - 1}{\tilde{r}_0 + 1} \right)^{i\nu}, \end{aligned} \quad (4.89)$$

where the definition for ν , Eq.(4.78), is used in the third line; and used Eq.(4.88) in the final line. Inputting Eq.(4.89) into Eq.(4.87), yields

$$B_\omega = \left(\frac{1 - i\nu}{1 + i\nu} \right) \left(\frac{1 + i\tilde{r}_0\nu}{1 - i\tilde{r}_0\nu} \right) e^{i2\omega(r_{s*} + \sigma_f)}. \quad (4.90)$$

The Eqs.(4.83, 4.85, 4.90) determine $f_\omega(r)$ completely. The linear superposition of $f_\omega(r)$ for all frequencies $\omega \in \mathbb{R}^+$, yields the general solution for $X(t, r)$,

$$X(t, r) := \int_0^\infty \frac{d\omega}{2\pi} A_\omega [f_\omega(r) e^{-i\omega t} a_\omega + f_\omega^*(r) e^{i\omega t} a_\omega^*], \quad (4.91)$$

where the mode expansion Eq.(4.76) is used, and (a_ω, a_ω^*) are Fourier coefficients. The constant A_ω is fixed by demanding the normalization of the appropriate basis.

To quantize the theory, the scalar field $X(t, \sigma)$ and its canonically conjugate momentum $P^t(t, \sigma)$ are promoted to operators and suitable commutation relations are imposed. From Eq.(4.91), the position operator is given by

$$\hat{X}(t, \sigma) := \int_0^\infty \frac{d\omega}{2\pi} A_\omega [f_\omega(\sigma) e^{-i\omega t} \hat{a}_\omega + f_\omega^*(\sigma) e^{i\omega t} \hat{a}_\omega^\dagger], \quad (4.92)$$

and from Eq.(4.65) the conjugate momentum operator is given by

⁶¹Mathematica is used (see Mathematica Notebook [b]: `BrownianMotion.nb`).

$$\begin{aligned}
\hat{P}^t(t, \sigma) &:= -\frac{1}{2\pi\alpha'} (\sqrt{-g} g^{tt} G_{II})|_{X_0^\mu} \partial_t \hat{X}(t, \sigma) \\
&= -\frac{1}{2\pi\alpha'} (\sqrt{-g} g^{tt} G_{II})|_{X_0^\mu} \int_0^\infty \frac{d\omega}{2\pi} (-i\omega) A_\omega [f_\omega(\sigma) e^{-i\omega t} \hat{a}_\omega - f_\omega^*(\sigma) e^{i\omega t} \hat{a}_\omega^*] \\
&= -\frac{1}{2\pi\alpha'} \left(\frac{r_H^2}{l^2} \operatorname{csch}^2 \left(\frac{r_H (r_{s*} + \sigma)}{l^2} \right) \right) \left(-\frac{l^2}{r_H^2} \sinh^2 \left(\frac{r_H (r_{s*} + \sigma)}{l^2} \right) \right) \left(\frac{r_H^2}{l^2} \coth^2 \left(\frac{r_H (r_{s*} + \sigma)}{l^2} \right) \right) \\
&\quad \times \int_0^\infty \frac{d\omega}{2\pi} (-i\omega) A_\omega [f_\omega(\sigma) e^{-i\omega t} \hat{a}_\omega - f_\omega^*(\sigma) e^{i\omega t} \hat{a}_\omega^\dagger] \\
&= -\frac{i}{2\pi\alpha'} \frac{r_H^2}{l^2} \coth^2 \left(\frac{r_H (r_{s*} + \sigma)}{l^2} \right) \int_0^\infty \frac{d\omega}{2\pi} \omega A_\omega [f_\omega(\sigma) e^{-i\omega t} \hat{a}_\omega - f_\omega^*(\sigma) e^{i\omega t} \hat{a}_\omega^\dagger] \\
&= -\frac{i}{2\pi\alpha'} \frac{r^2}{l^2} \int_0^\infty \frac{d\omega}{2\pi} \omega A_\omega [f_\omega(\sigma) e^{-i\omega t} \hat{a}_\omega - f_\omega^*(\sigma) e^{i\omega t} \hat{a}_\omega^\dagger] ,
\end{aligned} \tag{4.93}$$

where Eq.(4.92) is used in the second line, $r_* \equiv r_{s*} + \sigma$ is used in the fourth line, and the identification Eq.(4.52) in the final line. The metric entries in the third line follow from using the identification Eq.(4.52) to convert the spacetime metric as well as the induced metric, its determinant and its inverse into (t, r_*) coordinates. From the spacetime metric Eq.(A.32),

$$G_{II} = G_{II}|_{X_0^\mu} = \frac{r_H^2}{l^2} \coth^2 \left(\frac{r_H (r_{s*} + \sigma)}{l^2} \right) , \tag{4.94}$$

while the induced metric, its determinant and its inverse (Eqs.(4.70, 4.58, 4.71)) are given by

$$g_{ab} \equiv g_{ab}|_{X_0^\mu} = \begin{bmatrix} G_{tt} & 0 \\ 0 & r'^2 G_{rr} \end{bmatrix} = \begin{bmatrix} -\frac{r_H^2}{l^2} \operatorname{csch}^2 \left(\frac{r_H (r_{s*} + \sigma)}{l^2} \right) & 0 \\ 0 & \frac{r_H^2}{l^2} \operatorname{csch}^2 \left(\frac{r_H (r_{s*} + \sigma)}{l^2} \right) \end{bmatrix} , \tag{4.95}$$

$$g := \det(g_{ab}) \equiv \det(g_{ab}|_{X_0^\mu}) = -\frac{r_H^4}{l^4} \operatorname{csch}^4 \left(\frac{r_H (r_{s*} + \sigma)}{l^2} \right) , \tag{4.96}$$

$$g^{ab} \equiv g^{ab}|_{X_0^\mu} = \frac{1}{\det(g_{ab}|_{X_0^\mu})} \begin{bmatrix} r'^2 G_{rr} & 0 \\ 0 & G_{tt} \end{bmatrix} = \begin{bmatrix} -\frac{l^2}{r_H^2} \sinh^2 \left(\frac{r_H (r_{s*} + \sigma)}{l^2} \right) & 0 \\ 0 & \frac{l^2}{r_H^2} \sinh^2 \left(\frac{r_H (r_{s*} + \sigma)}{l^2} \right) \end{bmatrix} , \tag{4.97}$$

in the preferred isothermal set of coordinates (t, r_*) . In order to fix the normalization constant A_ω canonical commutation relations between $\hat{X}(t, \sigma)$ and $\hat{P}^t(t, \sigma)$ are enforced:

$$\begin{aligned}
\left[\hat{X}(t, \sigma), n_t \hat{P}^t(t, \sigma') \right]_\Sigma &= i \delta(\sigma, \sigma') = i \frac{\delta(\sigma - \sigma')}{\sqrt{\tilde{g}}|\Sigma} , \\
\left[\hat{X}(t, \sigma), \hat{X}(t, \sigma') \right]_\Sigma &= 0 = \left[n_t \hat{P}^t(t, \sigma), n_t \hat{P}^t(t, \sigma') \right]_\Sigma ,
\end{aligned} \tag{4.98}$$

where Σ is a Cauchy hypersurface in the $x^\mu = (t, r)^\mu$ part of spacetime that is chosen to be a constant time surface⁶², \tilde{g} is the induced metric on Σ , and n_μ is the future pointing normal to Σ (where $n_\mu = \delta_{\mu t} / \sqrt{-\tilde{g}_{tt}}$).

⁶²Giving initial conditions on this hypersurface determines the future (and past) evolution uniquely.

Additionally, canonical creation and annihilation commutation relations on the Fourier coefficient operators ($\hat{a}_\omega, \hat{a}_\omega^\dagger$) are enforced:

$$\begin{aligned} [\hat{a}_\omega, \hat{a}_{\omega'}^\dagger]_\Sigma &= 2\pi\delta(\omega - \omega'), \\ [\hat{a}_\omega, \hat{a}_{\omega'}]_\Sigma &= 0 = [\hat{a}_\omega^\dagger, \hat{a}_{\omega'}^\dagger]_\Sigma. \end{aligned} \quad (4.99)$$

Demanding consistency between the sets of commutation relations Eq.(4.98) and Eq.(4.99), requires the normalization constant to be defined as

$$A_\omega := \frac{l}{r_H} \sqrt{\frac{\pi\alpha'}{\omega}} = \frac{\beta}{2\sqrt{\pi\omega}\lambda^{1/4}}, \quad (4.100)$$

where the second equality follows from using the definition of the AdS radius of curvature l (Eq.(4.64)), and the relation $l = \beta r_H^2/2\pi$ from Eq.(4.35). The derivation of Eq.(4.100) is the subject of appendix (A.5).

With the constants B_ω and A_ω (Eqs.(4.90, 4.100) respectively) found, the general solution for transverse equations of motion (Eq.(4.91)) is completely determined. The displacement of the boundary endpoint as the test string undergoes these transverse fluctuations can now be calculated. The position of the endpoint of the test string on the boundary is defined by the operator

$$\hat{X}_{\text{end}}(t) := \hat{X}(t, \sigma_f). \quad (4.101)$$

At the Hawking temperature, the transverse fluctuations on the string are excited. Assume – as was done by de Boer *et al.* [42] – that these excitations are purely thermal and are therefore described by the Bose-Einstein distribution

$$\langle \hat{a}_\omega^\dagger \hat{a}_{\omega'} \rangle = \frac{2\pi\delta(\omega - \omega')}{e^{\beta\omega} - 1}. \quad (4.102)$$

The Bose-Einstein distribution applies when (i) quantum effects are important, (ii) particles are indistinguishable, and (iii) are bosons (particles which do not obey the Pauli exclusion principle). The string boundary endpoint's mean-squared transverse displacement, $s^2(t)$, is defined as⁶³

$$s^2(t) := \langle (\hat{X}_{\text{end}}(t) - \hat{X}_{\text{end}}(0))^2 \rangle = \langle \hat{X}_{\text{end}}^2(t) \rangle + \langle \hat{X}_{\text{end}}^2(0) \rangle - 2\langle \hat{X}_{\text{end}}(t) \hat{X}_{\text{end}}(0) \rangle. \quad (4.103)$$

In order to determine $s^2(t)$, begin by calculating the expectation value of the position of the boundary endpoint at two different times. Using Eq.(4.92),

$$\begin{aligned} &\langle \hat{X}_{\text{end}}(t_1) \hat{X}_{\text{end}}(t_2) \rangle \\ &= \langle \int_0^\infty \frac{d\omega d\omega'}{(2\pi)^2} \frac{\beta^2}{4\pi\sqrt{\omega\omega'}\sqrt{\lambda}} [f_\omega(\sigma_f)e^{-i\omega t_1}\hat{a}_\omega + f_\omega^*(\sigma_f)e^{i\omega t_1}\hat{a}_\omega^\dagger] [f_{\omega'}(\sigma_f)e^{-i\omega' t_2}\hat{a}_{\omega'} + f_{\omega'}^*(\sigma_f)e^{i\omega' t_2}\hat{a}_{\omega'}^\dagger] \rangle \\ &= \frac{\beta^2}{4\pi\sqrt{\lambda}} \int_0^\infty \frac{d\omega d\omega'}{(2\pi)^2} \frac{1}{\sqrt{\omega\omega'}} \left[f_\omega(\sigma_f)f_{\omega'}^*(\sigma_f)e^{-i\omega t_1+i\omega' t_2} \langle \hat{a}_\omega \hat{a}_{\omega'}^\dagger \rangle + f_\omega^*(\sigma_f)f_{\omega'}(\sigma_f)e^{i\omega t_1-i\omega' t_2} \langle \hat{a}_\omega^\dagger \hat{a}_{\omega'} \rangle \right] \\ &= \frac{\beta^2}{4\pi\sqrt{\lambda}} \int_0^\infty \frac{d\omega d\omega'}{2\pi} \frac{1}{\sqrt{\omega\omega'}} \left[\delta(\omega' - \omega)f_\omega(\sigma_f)f_{\omega'}^*(\sigma_f)\frac{e^{-i\omega t_1+i\omega' t_2}}{e^{\beta\omega'} - 1} + \delta(\omega - \omega')f_\omega^*(\sigma_f)f_{\omega'}(\sigma_f)\frac{e^{i\omega t_1-i\omega' t_2}}{e^{\beta\omega} - 1} \right] \\ &= \frac{\beta^2}{4\pi\sqrt{\lambda}} \int_0^\infty \frac{d\omega}{2\pi} \frac{1}{\omega} \frac{1}{e^{\beta\omega} - 1} \left[f_\omega(\sigma_f)f_\omega^*(\sigma_f)e^{-i\omega(t_1-t_2)} + f_\omega^*(\sigma_f)f_\omega(\sigma_f)e^{i\omega(t_1-t_2)} \right], \end{aligned} \quad (4.104)$$

⁶³The mean-squared transverse displacement, $s^2(t)$, is a gauge and coordinate independent quantity, i.e. it doesn't matter which coordinate system $s^2(t)$ is calculated in. Note that the position of the horizon is still dependent on the choice of coordinates (as discussed in subsection (5.1.3) when motivating for the use of (t, r_*) coordinates).

where $:\hat{a}_\omega^\dagger \hat{a}_{\omega'}: = :\hat{a}_\omega^\dagger \hat{a}_\omega^\dagger: = \hat{a}_\omega^\dagger \hat{a}_{\omega'}$ is the normal ordering operator, and the definition of the Bose-Einstein distribution (Eq.(4.102)) is used in the third equality. The final line follows from the property of the Dirac delta function $\int_0^\infty dk e^{-kx} \delta(k-a) = e^{-ax}$. Using the complex conjugate property $\text{Re}(z) = (z + \bar{z})/2$, Eq.(4.104) simplifies to

$$\langle :\hat{X}_{\text{end}}(t_1) \hat{X}_{\text{end}}(t_2): \rangle = \frac{\beta^2}{4\pi^2 \sqrt{\lambda}} \int_0^\infty \frac{d\omega}{\omega} \frac{1}{e^{\beta\omega} - 1} \text{Re} \left(f_\omega(\sigma_f) f_\omega^*(\sigma_f) e^{-i\omega(t_1-t_2)} \right). \quad (4.105)$$

The normal ordering operator is necessary to remove the logarithmic ultraviolet divergences. Had it not been used, extra terms would arise in the calculation of Eq.(4.104). Specifically,

$$\begin{aligned} & \langle \hat{X}_{\text{end}}(t_1) \hat{X}_{\text{end}}(t_2) \rangle \\ &= \left\langle \int_0^\infty \frac{d\omega d\omega'}{(2\pi)^2} \frac{\beta^2}{4\pi \sqrt{\omega\omega'} \sqrt{\lambda}} [f_\omega(\sigma_f) e^{-i\omega t_1} \hat{a}_\omega + f_\omega^*(\sigma_f) e^{i\omega t_1} \hat{a}_\omega^\dagger] [f_{\omega'}(\sigma_f) e^{-i\omega' t_2} \hat{a}_{\omega'} + f_{\omega'}^*(\sigma_f) e^{i\omega' t_2} \hat{a}_{\omega'}^\dagger] \right\rangle \\ &= \frac{\beta^2}{4\pi \sqrt{\lambda}} \int_0^\infty \frac{d\omega d\omega'}{(2\pi)^2} \frac{1}{\sqrt{\omega\omega'}} \left[f_\omega(\sigma_f) f_{\omega'}^*(\sigma_f) e^{-i\omega t_1 + i\omega' t_2} \left(\langle \hat{a}_\omega^\dagger, \hat{a}_\omega \rangle + 2\pi \delta(\omega - \omega') \right) \right. \\ &\quad \left. + f_\omega^*(\sigma_f) f_{\omega'}(\sigma_f) e^{i\omega t_1 - i\omega' t_2} \langle \hat{a}_\omega^\dagger \hat{a}_{\omega'} \rangle \right] \\ &= \frac{\beta^2}{4\pi \sqrt{\lambda}} \int_0^\infty \frac{d\omega d\omega'}{2\pi} \frac{1}{\sqrt{\omega\omega'}} \left[\delta(\omega' - \omega) f_\omega(\sigma_f) f_{\omega'}^*(\sigma_f) \frac{e^{-i\omega t_1 + i\omega' t_2}}{e^{\beta\omega'} - 1} + \delta(\omega - \omega') f_\omega(\sigma_f) f_{\omega'}^*(\sigma_f) e^{-i\omega t_1 + i\omega' t_2} \right. \\ &\quad \left. + \delta(\omega - \omega') f_\omega^*(\sigma_f) f_{\omega'}(\sigma_f) \frac{e^{i\omega t_1 - i\omega' t_2}}{e^{\beta\omega} - 1} \right] \\ &= \frac{\beta^2}{4\pi \sqrt{\lambda}} \int_0^\infty \frac{d\omega}{2\pi} \frac{1}{\omega} \left[f_\omega(\sigma_f) f_\omega^*(\sigma_f) e^{-i\omega(t_1-t_2)} \left(\frac{1}{e^{\beta\omega} - 1} + 1 \right) + f_\omega^*(\sigma_f) f_\omega(\sigma_f) \frac{e^{i\omega(t_1-t_2)}}{e^{\beta\omega} - 1} \right] \\ &= \frac{\beta^2}{4\pi^2 \sqrt{\lambda}} \int_0^\infty \frac{d\omega}{\omega} \left[\frac{1}{e^{\beta\omega} - 1} \text{Re} \left(f_\omega(\sigma_f) f_\omega^*(\sigma_f) e^{-i\omega(t_1-t_2)} \right) + \frac{1}{2} f_\omega(\sigma_f) f_\omega^*(\sigma_f) e^{-i\omega(t_1-t_2)} \right], \end{aligned} \quad (4.106)$$

where the relation $\langle \hat{a}_\omega \hat{a}_{\omega'}^\dagger \rangle = \langle \hat{a}_\omega^\dagger, \hat{a}_\omega \rangle + 2\pi \delta(\omega - \omega')$ results from the commutation relation Eq.(4.99). Following [42], the term $\frac{1}{2} f_\omega(\sigma_f) f_\omega^*(\sigma_f) e^{-i\omega(t_1-t_2)}$ is interpreted as a logarithmic UV divergence. Since this divergence stems from the zero-point energy and exists at zero temperature, it can be regularised by instituting normal ordering of the oscillators $a_\omega, \hat{a}_\omega^\dagger$ (as was done in Eq.(4.104)). At specific times, the regularized correlator (Eq.(4.104)) becomes

$$\langle :\hat{X}_{\text{end}}(t) \hat{X}_{\text{end}}(0): \rangle = \frac{\beta^2}{4\pi^2 \sqrt{\lambda}} \int_0^\infty \frac{d\omega}{\omega} \frac{1}{e^{\beta\omega} - 1} \text{Re} \left(f_\omega(\sigma_f) f_\omega^*(\sigma_f) e^{-i\omega t} \right), \quad (4.107)$$

$$\langle :\hat{X}_{\text{end}}(0) \hat{X}_{\text{end}}(0): \rangle = \langle :\hat{X}_{\text{end}}(t) \hat{X}_{\text{end}}(t): \rangle = \frac{\beta^2}{4\pi^2 \sqrt{\lambda}} \int_0^\infty \frac{d\omega}{\omega} \frac{1}{e^{\beta\omega} - 1} \text{Re} \left(f_\omega(\sigma_f) f_\omega^*(\sigma_f) \right). \quad (4.108)$$

Inputting Eqs.(4.107, 4.108) into Eq.(4.103), the string boundary endpoint's mean-squared transverse displacement can be calculated

$$\begin{aligned} s^2(t) &= \frac{\beta^2}{4\pi^2 \sqrt{\lambda}} \int_0^\infty \frac{d\omega}{\omega} \frac{1}{e^{\beta\omega} - 1} \text{Re} \left(2f_\omega(\sigma_f) f_\omega^*(\sigma_f) - 2f_\omega(\sigma_f) f_\omega^*(\sigma_f) e^{-i\omega t} \right) \\ &= \frac{\beta^2}{4\pi^2 \sqrt{\lambda}} \int_0^\infty \frac{d\omega}{\omega} \frac{1}{e^{\beta\omega} - 1} [f_\omega(\sigma_f) f_\omega^*(\sigma_f) + f_\omega^*(\sigma_f) f_\omega(\sigma_f) - f_\omega(\sigma_f) f_\omega^*(\sigma_f) e^{-i\omega t} - f_\omega^*(\sigma_f) f_\omega(\sigma_f) e^{i\omega t}] \\ &= \frac{\beta^2}{4\pi^2 \sqrt{\lambda}} \int_0^\infty \frac{d\omega}{\omega} \frac{1}{e^{\beta\omega} - 1} [f_\omega(\sigma_f) f_\omega^*(\sigma_f) (2 - e^{-i\omega t} - e^{i\omega t})], \end{aligned} \quad (4.109)$$

where in the second line the complex conjugate property $\text{Re}(z) = (z + \bar{z})/2$ is again used.

4.3.3 The Limiting Cases of $s^2(t)$

In this subsection the behaviour of $s^2(t)$, Eq.(4.109), in the asymptotic early and late time limits is considered. Inputting⁶⁴ Eqs.(4.83, 4.85, 4.90) to calculate $f_\omega(\sigma_f)f_\omega^*(\sigma_f)$, yields

$$\begin{aligned} s^2(t) &= \frac{4\beta^2}{\pi^2\sqrt{\lambda}} \int_0^\infty \frac{d\omega}{\omega} \frac{1+\nu^2}{1+\tilde{r}_0^2\nu^2} \frac{\sin^2 \frac{\omega t}{2}}{e^{\beta\omega} - 1} \\ &= \frac{4\beta^2}{\pi^2\sqrt{\lambda}} \int_0^\infty \frac{d\nu}{\nu} \frac{1+\nu^2}{1+\tilde{r}_0^2\nu^2} \frac{\sin^2 \frac{\pi t \nu}{\beta}}{e^{2\pi\nu} - 1}, \end{aligned} \quad (4.110)$$

where the change of variables was performed using Eqs.(4.35, 4.78) in the last line. The integral in Eq.(4.110) is tricky to analytically evaluate. Following the insights of de Boer *et al.* [42], the integral can be broken into two parts,

$$\begin{aligned} s^2(t) &= \frac{4\beta^2}{\pi^2\sqrt{\lambda}} \left[4 \frac{\tilde{r}_0^2 - 1}{\tilde{r}_0^2} \left(\int_0^\infty \frac{d\nu}{\nu} \frac{1}{1+\tilde{r}_0^2\nu^2} \frac{\sin^2 \frac{\pi \nu t}{\beta}}{e^{2\pi\nu} - 1} \right) + 4 \frac{1}{\tilde{r}_0^2} \left(\int_0^\infty \frac{d\nu}{\nu} \frac{\sin^2 \frac{\pi \nu t}{\beta}}{e^{2\pi\nu} - 1} \right) \right] \\ &= \frac{\beta^2}{\pi^2\sqrt{\lambda}} \left[\frac{\tilde{r}_0^2 - 1}{\tilde{r}_0^2} I_1 + \frac{1}{\tilde{r}_0^2} I_2 \right], \end{aligned} \quad (4.111)$$

where the integrals I_1 and I_2 have been defined as,

$$I_1 := 4 \int_0^\infty \frac{d\nu}{\nu} \frac{1}{1+\tilde{r}_0^2\nu^2} \frac{\sin^2 \frac{\pi \nu t}{\beta}}{e^{2\pi\nu} - 1} = 4 \int_0^\infty \frac{dx}{x} \frac{1}{1+a^2x^2} \frac{\sin^2 \frac{kx}{2}}{e^x - 1}, \quad (4.112)$$

and

$$I_2 := 4 \int_0^\infty \frac{d\nu}{\nu} \frac{\sin^2 \frac{\pi \nu t}{\beta}}{e^{2\pi\nu} - 1} = 4 \int_0^\infty \frac{dx}{x} \frac{\sin^2 \frac{kx}{2}}{e^x - 1}. \quad (4.113)$$

The change of variables in Eqs.(4.112, 4.113) is made by defining the new variables

$$x := 2\pi\nu, \quad a := \frac{\tilde{r}_0}{2\pi}, \quad k := \frac{t}{\beta}. \quad (4.114)$$

The integral I_1 is solved by deforming the contour on the complex x plane. The solution is given by [42],

$$\begin{aligned} I_1 &= \frac{1}{2} \left(\psi \left(1 + \frac{1}{2\pi a} \right) + \psi \left(1 - \frac{1}{2\pi a} \right) \right) + \frac{1}{2} \left(e^{\frac{k}{a}} \text{Ei} \left(-\frac{k}{a} \right) + e^{-\frac{k}{a}} \text{Ei} \left(\frac{k}{a} \right) \right) - \frac{\pi}{2} \left(1 - e^{-\frac{|k|}{a}} \right) \cot \left(\frac{1}{2a} \right) \\ &\quad + \frac{e^{-2\pi|k|}}{2} \left(\frac{{}_2F_1 \left(1, 1 + \frac{1}{2\pi a}; 2 + \frac{1}{2\pi a}; e^{-2\pi|k|} \right)}{\frac{1}{2\pi a} + 1} + \frac{{}_2F_1 \left(1, 1 - \frac{1}{2\pi a}; 2 - \frac{1}{2\pi a}; e^{-2\pi|k|} \right)}{1 - \frac{1}{2\pi a}} \right) \\ &\quad + \ln \left(\frac{2a \sinh(\pi k)}{k} \right), \end{aligned} \quad (4.115)$$

where $\text{Ei}(z)$ is the exponential integral⁶⁵; ${}_2F_1(a, b; c; z)$ is the Gaussian hypergeometric function⁶⁶; and $\psi(z)$ is the digamma function⁶⁷.

⁶⁴Mathematica is used to simplify the algebra (see Mathematica Notebook [b]: **BrownianMotion.nb**).

⁶⁵For real, non-zero values of z , the exponential integral is defined as $\text{Ei}(z) = -\int_{-z}^\infty dt (e^{-t}/t)$.

⁶⁶The hypergeometric function is a special function defined for $|z| < 1$ by the hypergeometric series, ${}_2F_1(a, b; c; z) = \sum_{k=0}^\infty \frac{(a)_k (b)_k}{(c)_k} \frac{z^k}{k!}$.

⁶⁷The digamma function is defined in terms of derivatives of the gamma function: $\psi(z) := \frac{1}{\Gamma(z)} \frac{d\Gamma(z)}{dz}$. The function is meromorphic, and defined on the complex numbers \mathbb{C} .

The integral I_2 can be solved analytically,

$$\begin{aligned}
I_2 &= 4 \int_0^\infty \frac{dx}{x} e^{-x} \frac{1}{1-e^{-x}} \sin^2\left(\frac{kx}{2}\right) \\
&= 4 \sum_{n=1}^\infty \int_0^\infty \frac{dx}{x} \sin^2\left(\frac{kx}{2}\right) e^{-nx} \\
&= \sum_{n=1}^\infty \ln\left(1 + \frac{k^2}{n^2}\right) \\
&= \ln\left(\prod_{n=1}^\infty \left(1 + \frac{k^2}{n^2}\right)\right) \\
&= \ln\left(\frac{\sinh(\pi k)}{\pi k}\right),
\end{aligned} \tag{4.116}$$

where, in the second line, the geometric series $1/(1-x) = \sum_{n=0}^\infty x^n$ is used; and in the fourth line the integral was performed using Mathematica [97]. In the final line, Mathematica was again used.

From Eq.(4.116) it appears that $\beta = t/k$ naturally defines a cross-over time scale between the dynamics of early and late times⁶⁸. The integrals I_1 and I_2 can be examined in the limits $(t \ll \beta)$ and $(t \gg \beta)$ to yield the early and late time behaviour respectively. Since the probe particle in the boundary theory is an on-mass-shell heavy quark, the assumption $\tilde{r}_0 \gg 1$ (equivalently $a \gg 1$) can be made. This is essentially the statement that the large mass of the external particle translates to the distance in the radial direction between the test string's boundary endpoint and the stretched horizon being large⁶⁹.

(I) Asymptotic Early Time Dynamics

In the early time limit $t \ll \beta$ (equivalently $k \ll 1 \ll a$), the integrals I_1 and I_2 can be simplified. Defining a temporary variable $f := 1/a$, and series expanding the solution to I_1 (Eq.(4.115)) around $f = 0$ yields

$$\begin{aligned}
I_1 &= \left(-\ln(1 - e^{-2k\pi}) + \ln(f) + \ln\left(\frac{2\sinh(k\pi)}{f}\right) - k\pi\right) + \frac{1}{2}k^2\pi f + \mathcal{O}(f^2) \\
&= \frac{k^2\pi}{2a} + \mathcal{O}\left(\frac{1}{a^2}\right),
\end{aligned} \tag{4.117}$$

where, in the second line, the expression is rewritten in terms of the variable a and appropriately truncated at leading order. For the I_2 integral, notice there is no a -dependence – hence a series expansion in $1/a$ yields $I_2 = \mathcal{O}(a^0)$. Therefore, in the early time limit, $s^2(t)$ (Eq.(4.111)) becomes

$$s^2(t)|_{(t \ll \beta)} \frac{\beta^2}{\pi^2 \sqrt{\lambda}} \left[\frac{\tilde{r}_0^2 - 1}{\tilde{r}_0^2} \left(\frac{\pi^2 t^2}{\beta^2 \tilde{r}_0} + \mathcal{O}\left(\frac{1}{\tilde{r}_0^2}\right) \right) + \frac{1}{\tilde{r}_0^2} \mathcal{O}(\tilde{r}_0)^0 \right] = \frac{t^2}{\tilde{r}_0 \sqrt{\lambda}} + \mathcal{O}\left(\frac{1}{\tilde{r}_0^2}\right), \tag{4.118}$$

where the variables have been changed using Eq.(4.114). In terms of the relevant field theoretic quantities, Eq.(4.118) can be converted using Eq.(A.43). Specifically, $s^2(t) = (T t^2)/m_q$, where m_q is the mass of the probe quark and T is the temperature of the thermal plasma. Since $s^2(t) \sim t^2$, the early time dynamics exhibit ballistic behaviour (see Eq.(3.20))⁷⁰.

⁶⁸More specifically, the cross-over time (defined in Eq.(3.42)) is given by $t_c \sim \beta \tilde{r}_0 \sim (\alpha' m_q)/(l^2 T^2)$, where Eqs.(4.64, A.43) have been used in the second approximation.

⁶⁹The assumption $\tilde{r}_0 \rightarrow \infty$ would correspond to an infinitely massive quark, such as the probe particle considered in section (6).

⁷⁰The result for $s^2(t)$ in the early time limit given in Eq.(4.118) agrees exactly with de Boer *et al.* [42], Eq.(3.6) (after recognising $\tilde{r}_0 = \rho_c$, and making use of Eq.(4.64)).

(II) Asymptotic Late Time Dynamics

At asymptotically late times, $t \gg \beta$ (equivalently $k \gg a \gg 1$), the integrals I_1 and I_2 have the same behaviour. To prove this, take the integral I_1 (Eq.(4.112)) and make the change of variables $x := \frac{x'}{k}$,

$$I_1 = 4 \int_0^\infty \frac{dx'}{x'} \frac{1}{1 + \frac{a^2 x'}{k^2}} \frac{\sin^2 \frac{x'}{2}}{e^{\frac{x'}{k}} - 1} \xrightarrow{(\beta \ll t)} 4 \int_0^\infty \frac{dx'}{x'} \frac{\sin^2 \frac{x'}{2}}{e^{\frac{x'}{k}} - 1} \equiv I_2, \quad (4.119)$$

where it is noticed that the term $\frac{a^2 x'}{k^2} \ll 1$ can be neglected in the late time limit. Expanding the solution to I_2 (Eq.(4.116)), yields

$$\begin{aligned} I_1|_{\beta \ll t} &\equiv I_2 = \ln(\sinh \pi k) - \ln(\pi k) \\ &= \ln\left(\frac{e^{\pi k}}{2} - \frac{e^{-\pi k}}{2}\right) - \ln(\pi k) \\ &= \ln(e^{\pi k}) - \ln(2) - \ln(\pi k) \\ &= \pi k + \mathcal{O}(\ln k), \end{aligned} \quad (4.120)$$

where the second line follows from trigonometric identity $\sinh(x) = (e^x - e^{-x})/2$, and in the fourth line the term $e^{-\pi k}/2 \rightarrow 0$ since $k \gg 1$ at late times.

Therefore, in the late time limit, $s^2(t)$ (Eq.(4.111)) becomes

$$s^2(t)|_{(t \ll \beta)} \frac{\beta^2}{\pi^2 \sqrt{\lambda}} \left[\frac{\tilde{r}_0^2 - 1}{\tilde{r}_0^2} \left(\frac{\pi t}{\beta} + \mathcal{O}\left(\ln \frac{t}{\beta}\right) \right) + \frac{1}{\tilde{r}_0^2} \left(\frac{\pi t}{\beta} + \mathcal{O}\left(\ln \frac{t}{\beta}\right) \right) \right] = \frac{\beta t}{\pi \sqrt{\lambda}} + \mathcal{O}\left(\ln \frac{t}{\beta}\right), \quad (4.121)$$

where the variables have been changed using Eq.(4.114). Since $s^2(t) \sim t$, the late time dynamics exhibit diffusive behaviour⁷¹. Concretely, at late times $s^2(t) = 2 D t$, where D is the diffusion coefficient (Eq.(3.21)). Comparing this to Eq.(4.121), the diffusion coefficient in AdS₃-Schwarzschild is extricated,

$$D_{\text{HQ}}^{\text{AdS}_3} = \frac{\beta}{2 \pi \sqrt{\lambda}}. \quad (4.122)$$

4.4 Generalising to AdS_d-Schwarzschild

For the off-mass-shell light quark case – as will be seen in subsection (5.3) – generalising the diffusion coefficient to AdS_d-Schwarzschild⁷² relies on the observation that the behaviour of an arbitrary virtuality light quark at asymptotically late times is encoded in the small virtuality light quark case. Since $s^2(t)$ in the latter case can easily be calculated for any dimensions $d \geq 3$ in AdS_d-Schwarzschild, the diffusion coefficient $D_{\text{LQ}}^{\text{AdS}_d}$ can be determined. Unfortunately, this method can not be applied to the on-mass-shell heavy quark case⁷³. The avenue left is to determine, in AdS_d-Schwarzschild, the friction coefficient of the medium plasma and relate this – via the Einstein-Sutherland equation (Eq.(3.18)) – to the diffusion coefficient. This is precisely what is done in section (6), where the friction coefficient in AdS_d-Schwarzschild is found by first calculating the drag force on an infinitely massive, heavy quark moving through the thermal plasma with a constant velocity⁷⁴ in the bulk theory. As will be seen, the diffusion coefficient extracted from this method⁷⁵, agrees exactly with the the diffusion coefficient given in Eq.(4.122) for $d = 3$.

⁷¹The result for $s^2(t)$ in the late time limit given in Eq.(4.121) agrees exactly with de Boer *et al.* [42], Eq.(3.6) (where Eqs.(4.35, 4.64) have been used to show the equivalence).

⁷²Remember that a general d dimensions in the bulk theory corresponds to a $(d-1)$ -dimensional thermal plasma in the boundary theory.

⁷³To talk about the small virtuality/small mass limit of a massive, heavy probe quark, would be nonsensical.

⁷⁴Implies that the probe quark is under the influence of an external force.

⁷⁵These calculations predominantly follow the work of [22, 35].

5 Analysing Light Quark Brownian Motion

A light quark probe in a thermal medium on the boundary starts at $t = 0$ as an off-mass-shell particle, radiates energy as it travels through the thermal medium and finally stops radiating as it becomes an on-mass-shell particle. Dual to this light quark in the boundary theory, a test string in the bulk can be thought of as half the *yo-yo string* in $\mathbb{R}^{1,1}$. The latter is a string which, at a time $t = 0$, stretches a length of $2L$ along the x-axis; as time progresses the string shrinks till, at a time $t = L$, it is a point; then it begins to expand again and the process repeats. The yo-yo solution is a well-studied classical solution of the open string [100]. There is plenty of recent work [15, 101–105] modelling gluons and light quarks as half the initial yo-yo string contracting to a point after a time t , in order to calculate energy loss (see also [52, 106] for other works using this string set-up). This idea of a *falling string* is precisely what is used in order to study the off-mass-shell light quark in this dissertation. Such a string set-up is referred to, following the convention of [52], as the *Limp Noodle*.

If the test string is placed in an AdS-Schwarzschild background, the presence of the black hole results in thermal fluctuations in the transverse X^I directions on the string. The resultant random movement of the string endpoint on the boundary corresponds to the light quark undergoing Brownian motion. This set-up is depicted in figure (3).

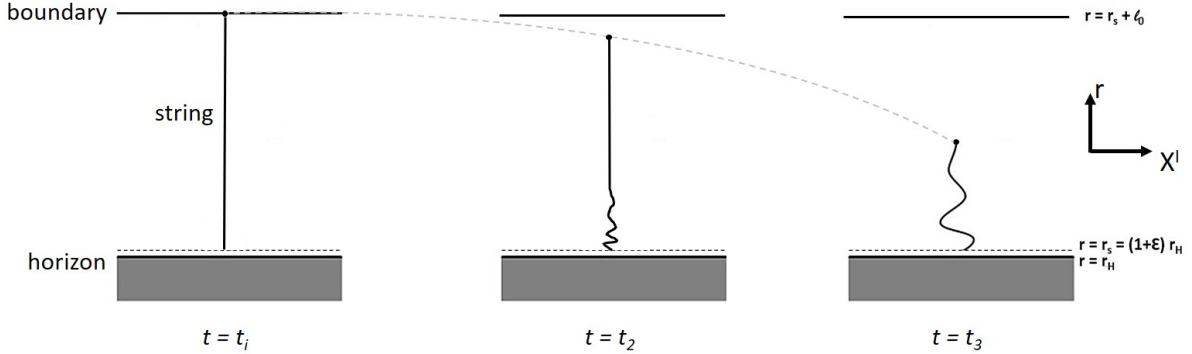


Figure 3: A fundamental falling open string of length ℓ_0 used as a probe in an AdS black hole background. Initially, at $t = t_i$, the string starts at the boundary of the anti-de Sitter spacetime and hangs down to a *stretched horizon* ($r_s = (1 + \epsilon) r_H$ where $0 < \epsilon \ll 1$) placed just above the Schwarzschild black hole horizon. As time evolves $t_i < t_2 < t_3$, the string endpoint at the boundary is released and the string collapses. Its trajectory as it falls (grey, dashed line) is predicted by [15, 101–105].

The initial static set-up of the Limp Noodle (where one of its endpoints are held fixed at the boundary) is equivalent to the leading order static stretched string for the heavy quark, described in subsection (4.2). This changes once the boundary endpoint of the string is released, and the endpoint starts to fall at the local speed of light. Information, however, is also restricted to travel at the local speed of light. Hence, all parts of the string below the falling boundary endpoint can not *know* whether the boundary endpoint has remained fixed (as in the case of the heavy quark's test string) or been released to fall until the endpoint crashes through it. Intuitively, it is therefore expected that all parts of the string except the falling boundary endpoint are described by a solution (embedding functions) identical to Eq.(4.32) in $\mathbb{R}^{1,1}$ and Eq.(4.50) in AdS₃-Schwarzschild, while the stretched endpoint falls at the local speed of light. This will be confirmed in the following subsection.

5.1 Leading Order String Behaviour

The basics of string theory discussed in subsection (4.1) – leading to the Virasoro constraints (Eq.(4.18)) and the string equations of motion (Eq.(4.19)) – hold for the light quark's test string (Limp Noodle). In order to solve Eqs.(4.18, 4.19) (with respect to the boundary conditions Eqs.(4.22, 4.23) and the relevant initial conditions) to yield the embedding functions requires the correct partitioning of the worldsheet parameter space. This partitioning was trivial in the heavy quark's test string case, since its leading order behaviour is static for all t . It is however more complicated in the Limp Noodle case, considering that the boundary

string endpoint is allowed to fall at the local speed of light for $t > 0$. A method in which to partition the worldsheet in order to find the solution to the string equations of motion was given by Itzhak Bars in 1994 [107], and expounded upon a year later, in 1995, by himself and a collaborator Jürgen Schulze [108]. The Bars *et al.* method is summarised in the following subsection.

5.1.1 Parameterising the Limp Noodle: The Bars *et al.* method

The Bars *et al.* method can be used to solve the classical motion of a relativistic string in any $(1+1)$ -dimensional spacetime. Originally, the method was used by Bars *et al.* to study the motion of folded strings in curved spacetime. However the Limp Noodle can be interpreted as half a folded (or yo-yo) string. The application of the Bars *et al.* method to parameterise the Limp Noodle and find the general solution to the string equations of motion was first proposed by Moerman *et al.* in [52]. The Bars *et al.* method can be broken into the following steps:

- (i) Define lattice-like patches on the worldsheet using the light-cone coordinates.

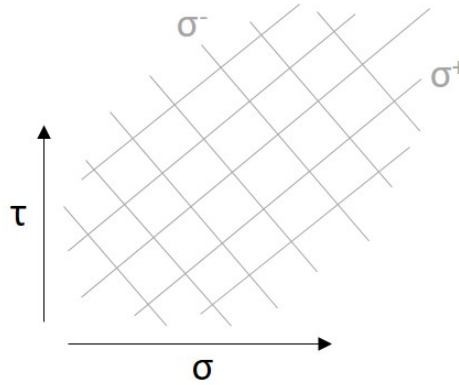


Figure 4: Lattice structure imposed on the worldsheet parameter space using the light-cone coordinates σ^+ and σ^- . This structure is used in the Bars *et al.* method [107, 108] in order to determine the general solution for a moving open string on a manifold.

- (ii) Naive solutions to the string equations of motion come in four classes, referred to as: A , B , C , and D . They can be defined only on patches of the worldsheet, since the full solution needs to satisfy two conditions: (a) string solutions must be periodic in σ , and (b) the global time coordinate must be an increasing function of τ and σ (in order to exclude anti-strings from appearing in the same solutions as strings). In the static gauge the latter condition is trivially satisfied. Hence to build the general solution from the solution classes A , B , C , D , assign the pattern of solutions to ensure forward propagation and impose periodicity at a fixed value of τ .
- (iii) Complete solutions are obtained by matching boundary conditions at the boundary of the patches.
- (iv) Define a transfer operation matrix to determine future evolution. The propagation of the solution into the future is performed by using this matrix to matching the boundary conditions while increasing τ .

The leading order dynamics of the Limp Noodle are constrained to the $(1+1)$ -dimensional subspace of AdS_d -Schwarzschild described by the set of coordinates (x^0, x^1) , where x^0 denotes the temporal direction and x^1 denotes the radial direction. The metric of any $(1+1)$ -dimensional subspace (where one of these dimensions is the temporal dimension) can be transformed into a conformally flat metric [107, 108]. In order to perform this transformation the string field in the target spacetime is redefined by the coordinate reparametrization $x^\mu(\tau, \sigma) = x^\mu(y^{\mu'}(\tau, \sigma))$. This yields the new spacetime metric in terms of isothermal coordinates $y^{\mu'}(\tau, \sigma)$, which can be related to the old spacetime metric by

$$G_{\mu\nu}(x) = \frac{\partial y^{\mu'}}{\partial x^\mu} \frac{\partial y^{\nu'}}{\partial x^\nu} G_{\mu'\nu'}(y), \quad (5.1)$$

where the isothermal coordinates in the static gauge $y^{\mu'}(t, \sigma)$, are given by

$$y^{0'} = \frac{1}{\sqrt{2}}(x^0 + x^1) \quad \text{and} \quad y^{1'} = \frac{1}{\sqrt{2}}(x^0 - x^1). \quad (5.2)$$

In this isothermal coordinate frame the metric is conformally flat

$$ds^2 = G_{\mu'\nu'}(y) dy^{\mu'} dy^{\nu'}, \quad (5.3)$$

and the new spacetime metric is found by inverting Eq.(5.1)

$$G_{\mu'\nu'}(y) = \frac{\partial x^\mu}{\partial y^{\mu'}} \frac{\partial x^\nu}{\partial y^{\nu'}} G_{\mu\nu}(x) = \frac{\partial x^\mu}{\partial y^{\mu'}} \frac{\partial x^\nu}{\partial y^{\nu'}} G \eta_{\mu\nu}, \quad (5.4)$$

where the second equality follows from choosing the conformal gauge, and $G = G(y^0, y^1) \in \mathbb{R}^+$ is some non-zero coordinate dependent scalar function. The metric can be calculated component-wise

$$\begin{aligned} G_{0'0'}(y) &= G \left[-\frac{\partial x^0}{\partial y^{0'}} \frac{\partial x^0}{\partial y^{0'}} + \frac{\partial x^1}{\partial y^{0'}} \frac{\partial x^1}{\partial y^{0'}} \right] = G \left[-\left(\frac{1}{\sqrt{2}}\right) \left(\frac{1}{\sqrt{2}}\right) + \left(\frac{1}{\sqrt{2}}\right) \left(\frac{1}{\sqrt{2}}\right) \right] = 0, \\ G_{0'1'}(y) &= G \left[-\frac{\partial x^0}{\partial y^{0'}} \frac{\partial x^0}{\partial y^{1'}} + \frac{\partial x^1}{\partial y^{0'}} \frac{\partial x^1}{\partial y^{1'}} \right] = G \left[-\left(\frac{1}{\sqrt{2}}\right) \left(\frac{1}{\sqrt{2}}\right) + \left(\frac{1}{\sqrt{2}}\right) \left(-\frac{1}{\sqrt{2}}\right) \right] = -G, \\ G_{1'0'}(y) &= G \left[-\frac{\partial x^0}{\partial y^{1'}} \frac{\partial x^0}{\partial y^{0'}} + \frac{\partial x^1}{\partial y^{1'}} \frac{\partial x^1}{\partial y^{0'}} \right] = G \left[-\left(\frac{1}{\sqrt{2}}\right) \left(\frac{1}{\sqrt{2}}\right) + \left(-\frac{1}{\sqrt{2}}\right) \left(\frac{1}{\sqrt{2}}\right) \right] = -G, \\ G_{1'1'}(y) &= G \left[-\frac{\partial x^0}{\partial y^{1'}} \frac{\partial x^0}{\partial y^{1'}} + \frac{\partial x^1}{\partial y^{1'}} \frac{\partial x^1}{\partial y^{1'}} \right] = G \left[-\left(\frac{1}{\sqrt{2}}\right) \left(\frac{1}{\sqrt{2}}\right) + \left(-\frac{1}{\sqrt{2}}\right) \left(-\frac{1}{\sqrt{2}}\right) \right] = 0, \end{aligned} \quad (5.5)$$

where the definition of the isothermal coordinates Eq.(5.2) have been used. Hence $G_{\mu'\nu'}(y)$ has the explicit form

$$G_{\mu'\nu'}(y) = G \begin{bmatrix} 0 & -1 \\ -1 & 0 \end{bmatrix} = G \tilde{\eta}_{\mu'\nu'}, \quad (5.6)$$

where $\tilde{\eta}_{\mu\nu}$ is the light-cone metric, and $G := G(y^{0'}, y^{1'}) \in \mathbb{R}^+$ is defined as some non-zero coordinate dependent scalar function. Using Eq.(5.6), the metric Eq.(5.3) becomes

$$ds^2 = -G(dy^{0'} dy^{1'} + dy^{1'} dy^{0'}). \quad (5.7)$$

The string mapping functions $Y^{\mu'}(\sigma^+, \sigma^-)$ are given by

$$Y^{0'} = \frac{1}{\sqrt{2}}(X^0 + X^1) \quad \text{and} \quad Y^{1'} = \frac{1}{\sqrt{2}}(X^0 - X^1). \quad (5.8)$$

Note that since the coordinates are isothermal, $Y^0 = -Y_1$ and $Y^1 = -Y_0$. The canonically conjugate momentum densities Eq.(4.5) can be rewritten in terms of the isothermal embedding functions, $Y^{\mu'}$. In the conformal gauge, the canonical momentum densities are given by

$$\begin{aligned} \Pi_\mu^a(t, \sigma) &= -\frac{1}{2\pi\alpha'} \eta^{ab} G_{\mu\nu} \partial_b X^\nu \\ \Rightarrow \Pi_\mu^\pm(t, \sigma) &= \frac{1}{2\pi\alpha'} \tilde{\eta}^{\pm b} G \eta_{\mu\nu} \partial_b X^\nu \\ \Rightarrow \Pi_\mu^\pm(t, \sigma) &= \frac{1}{2\pi\alpha'} G \eta_{\mu\nu} \partial_\mp X^\nu, \end{aligned} \quad (5.9)$$

if the light-cone coordinate frame is chosen (where $\partial_{\mp} := \frac{\partial}{\partial \sigma^{\mp}}$). Specifically,

$$\Pi_0^{\pm}(t, \sigma) = -\frac{1}{2\pi\alpha'} G \partial_{\mp} X^0 \quad \text{and} \quad \Pi_1^{\pm}(t, \sigma) = \frac{1}{2\pi\alpha'} G \partial_{\mp} X^1. \quad (5.10)$$

Hence the conjugate momentum densities can be defined in terms of the string mapping functions $Y^{\mu'}(\sigma^+, \sigma^-)$

$$\begin{aligned} \Pi_0^{\pm}(t, \sigma) &:= \frac{1}{\sqrt{2}} \left(\Pi_0^{\pm} + \Pi_1^{\pm} \right) = -\frac{1}{\sqrt{2}} \frac{1}{2\pi\alpha'} G \partial_{\mp} (X^0 - X^1) \equiv -\frac{1}{2\pi\alpha'} G \partial_{\mp} Y^{1'}, \quad \text{and} \\ \Pi_1^{\pm}(t, \sigma) &:= \frac{1}{\sqrt{2}} \left(\Pi_0^{\pm} - \Pi_1^{\pm} \right) = -\frac{1}{\sqrt{2}} \frac{1}{2\pi\alpha'} G \partial_{\mp} (X^0 + X^1) \equiv -\frac{1}{2\pi\alpha'} G \partial_{\mp} Y^{0'}. \end{aligned} \quad (5.11)$$

Combining the components in Eq.(5.11), renaming the indices $\mu' = \mu$, and recognising the raising and lowering property of the isothermal coordinates, leaves

$$\Pi_{\mu}^{\pm}(t, \sigma) = \frac{1}{2\pi\alpha'} G \partial_{\mp} Y_{(1-\mu)}. \quad (5.12)$$

The Virasoro constraint equations and the string equations of motion, Eqs.(4.18, 4.19), can also be rewritten in terms the new string mapping functions $Y^{\mu'}(\sigma^+, \sigma^-)$:

$$\begin{aligned} (\partial_{\pm} Y^0) (\partial_{\pm} Y^1) &= 0, \\ \partial_+ (G \partial_- Y^1) + \partial_- (G \partial_+ Y^1) &= (\partial_0 G) [(\partial_+ Y^0) (\partial_- Y^1) + (\partial_+ Y^1) (\partial_- Y^0)], \\ \partial_+ (G \partial_- Y^0) + \partial_- (G \partial_+ Y^0) &= (\partial_1 G) [(\partial_+ Y^0) (\partial_- Y^1) + (\partial_+ Y^1) (\partial_- Y^0)], \end{aligned} \quad (5.13)$$

where $\partial_{\mu} := \frac{\partial}{\partial Y^{\mu}}$ for $\mu = (0, 1)$. Since, the derivation of Eq.(5.13) is somewhat tedious, it has been relegated to appendix (A.2).

There are four classes of solutions to the set of equations Eqs.(5.13). Videlicet,

$$\begin{aligned} A: \quad Y^0(\sigma^+, \sigma^-) &= Y_A^0(\sigma^+), \quad Y^1(\sigma^+, \sigma^-) = Y_A^1(\sigma^-) \\ B: \quad Y^0(\sigma^+, \sigma^-) &= Y_B^0(\sigma^-), \quad Y^1(\sigma^+, \sigma^-) = Y_B^1(\sigma^+) \\ C: \quad Y^0(\sigma^+, \sigma^-) &= Y_C^0 = c_1, \quad Y^1(\sigma^+, \sigma^-) = f_C(\alpha_C(\sigma^+) + \beta_C(\sigma^-); Y_C^0) \\ D: \quad Y^0(\sigma^+, \sigma^-) &= f_D(\alpha_D(\sigma^+) + \beta_D(\sigma^-); Y_D^0), \quad Y^1(\sigma^+, \sigma^-) = Y_D^1 = c_2, \end{aligned} \quad (5.14)$$

where $c_{1,2}$ are constants, and $Y_A^0(\sigma^+)$, $Y_A^1(\sigma^-)$, $Y_B^0(\sigma^-)$, $Y_B^1(\sigma^+)$, $\alpha_C(\sigma^+)$, $\beta_C(\sigma^-)$, $\alpha_D(\sigma^+)$, and $\beta_D(\sigma^-)$ are arbitrary functions [107, 108]. The string solutions A , B , C and D given in Eq.(5.14) may be verified by direct substitution into Eqs.(5.13). This is easy for classes A and B , since these classes exist for any metric. Taking the derivative with respect to the light-cone coordinates σ_{\pm} , yields

$$\begin{aligned} A: \quad \partial_- (Y_A^0(\sigma^+)) &= 0, \quad \partial_+ (Y_A^1(\sigma^-)) = 0 \\ B: \quad \partial_+ (Y_B^0(\sigma^-)) &= 0, \quad \partial_- (Y_B^1(\sigma^+)) = 0, \end{aligned} \quad (5.15)$$

which is used, together with the chain rule, to easily show that the A and B classes of string solutions satisfy the Virasoro constraints and the string equations of motion Eqs.(5.13). This is harder to prove for classes C and D . These classes are metric dependent solutions since the functions f_C and f_D are metric

dependent. These functions are calculated by inverting the following relations that depend on the target spacetime metric,

$$\begin{aligned}
C: \quad Y^0(\sigma^+, \sigma^-) &= Y_C^0, & \int_{f_C} ds G(Y_C^0, s) &= \alpha_C(\sigma^+) + \beta_C(\sigma^-) \\
D: \quad Y^1(\sigma^+, \sigma^-) &= Y_D^1, & \int_{f_D} ds G(s, Y_D^1) &= \alpha_D(\sigma^+) + \beta_D(\sigma^-).
\end{aligned} \tag{5.16}$$

Taking the derivatives of Eq.(5.16) with respect to the light-cone coordinates σ_{\pm} and making use of Eq.(5.14),

$$\begin{aligned}
C: \quad \partial_{\pm} Y^0(\sigma^+, \sigma^-) &= 0, & G \partial_{\pm} s|_{f_C} &= \partial_{\pm}(\alpha_C(\sigma^+) + \beta_C(\sigma^-)) \\
&\Rightarrow G \partial_{\pm} Y^1(\sigma^+, \sigma^-) &= \partial_{\pm}(\alpha_C(\sigma^+) + \beta_C(\sigma^-)) \\
D: \quad \partial_{\pm} Y^1(\sigma^+, \sigma^-) &= 0, & G \partial_{\pm} s|_{f_D} &= \partial_{\pm}(\alpha_D(\sigma^+) + \beta_D(\sigma^-)) \\
&\Rightarrow G \partial_{\pm} Y^0(\sigma^+, \sigma^-) &= \partial_{\pm}(\alpha_D(\sigma^+) + \beta_D(\sigma^-)).
\end{aligned} \tag{5.17}$$

Using Eq.(5.17), the C and D classes of string solutions can be easily proven to satisfy the Virasoro constraints and string equations of motion Eqs.(5.13) by direct substitution. For the C class, the Virasoro constraints and second equation of motion are trivially satisfied. It remains to be checked whether the first equation of motion is satisfied. To this end, Eq.(5.17) can be substituted into the first equation of motion in Eq.(5.13)

$$\begin{aligned}
0 &= \partial_+ (G \partial_- Y^1) + \partial_- (G \partial_+ Y^1) \\
&= \partial_+ \left(G \left(\frac{1}{G} \partial_- \beta_C(\sigma^-) \right) \right) + \partial_- \left(G \left(\frac{1}{G} \partial_+ \alpha_C(\sigma^+) \right) \right) \\
&= \partial_+ (\partial_- \beta_C(\sigma^-)) + \partial_- (\partial_+ \alpha_C(\sigma^+)) \\
&= 0.
\end{aligned} \tag{5.18}$$

Similarly for class D , the Virasoro constraints and the first equation of motion are trivially satisfied, while the second equation of motion is verified by substituting Eq.(5.17) into Eq.(5.13).

It is not immediately obvious that the classes of solutions presented in Eq.(5.14) form a complete set. Completeness was shown in Bars *et al.* [108] by using the curved spacetime approach based on G/H gauged WZW models. Note that the pattern of solutions defined on the patches of the worldsheet is metric independent and spacetime dimension independent [107]. Hence, in order to find the general string solution for the Limp Noodle in AdS_d -Schwarzschild, start by finding the pattern of solutions defined on the patches of the worldsheet for the Limp Noodle in flat space. This is done in the next subsection.

Prior to this, some intuition regarding the patch-parametrization of the Limp Noodle can be developed. At a fold in a string or a string endpoint, the determinant of the induced worldsheet metric g_{ab} (Eq.(4.2)) vanishes. Hence the string endpoint's trajectory in the target spacetime is a null geodesic (the point travels at the local speed of light). For classes C and D – by virtue of either Y^0 or Y^1 reducing to a constant over the patch of parameter space where the class is a solution – the induced worldsheet metric reduces to zero, $g_{ab} = 0$. From this it can be deduced that all points in C or D parameter space patches map to the trajectory of the string endpoint (or fold) in target spacetime. This is a many-to-one mapping: the string's endpoint in target spacetime is represented several times on the worldsheet [107]. The string (sans the endpoints) behaves like a massive state, hence it is expected that motion of the string is described by classes A and B – ever-present, metric independent solutions.

5.1.2 Test Strings in $\mathbb{R}^{1,1}$

In order to study the Limp Noodle in $\mathbb{R}^{1,1}$ the static gauge ansatz is chosen

$$X^\mu : [0, t_f] \times [0, \sigma_f] \rightarrow \mathbb{R}^{1,1}, \quad (5.19)$$

$$(t, \sigma) \rightarrow x^\mu(t, \sigma) = (t, x(t, \sigma))^\mu. \quad (5.20)$$

The initial test string set-up is the same as in the heavy quark case. Eqs.(4.25, 4.26) are chosen as the boundary conditions for the position of the fixed endpoint at the horizon and the boundary endpoint falling in the $x(t, \sigma)$ direction respectively. For initial conditions Eqs.(4.27, 4.28) are chosen i.e. at $t = 0$ the string is static and stretches between x_0 and $x_0 + \ell_0$. Set t_f to be the minimum time it takes for a string to shrink from its initial length ℓ_0 to a point x_0 .

In flat space the total energy of the string, which represents the mass of an initially off-mass-shell light quark, is given by Eq.(4.31)⁷⁶. The equation of motion for $x(t, \sigma)$ can be easily adapted from Eqs.(A.18, A.24), since the spacetime is \mathbb{R}^{1+1} (therefore $G = 1$ and $(\partial_0 G) = (\partial_1 G) = 0$). Hence, the non-trivial string equation of motion reduces to

$$\begin{aligned} \partial_+ \partial_- X^1 &= 0 \\ \Rightarrow \partial_+ \partial_- x(t, \sigma) &= 0 \quad \text{in} \quad \mathbb{R}^{1+1}, \end{aligned} \quad (5.21)$$

which is simply the wave equation. The general solution to Eq.(5.21) is a sum of continuous analytic functions of σ^+ and σ^- (i.e. *left and right movers*)

$$x(t, \sigma) = \frac{1}{2} (f_1(\sigma^+) + f_2(\sigma^-)). \quad (5.22)$$

Using the boundary condition Eq.(4.25) to redefine $f(z) := f_1(z) = 2x_0 - f_2(z)$, Eq.(5.22) becomes

$$\begin{aligned} x(t, \sigma) &= \frac{1}{2} (f(\sigma^+) + [2x_0 - f(\sigma^-)]) \\ &= x_0 + \frac{1}{2} (f(\sigma^+) - f(\sigma^-)). \end{aligned} \quad (5.23)$$

The Neumann boundary condition Eq.(4.26) becomes

$$\begin{aligned} 0 &= \partial_\sigma \left[x_0 + \frac{1}{2} (f(\sigma^+) - f(\sigma^-)) \right] \Big|_{\sigma=\sigma_f} \\ &= \frac{1}{2} [\partial_+ f(\sigma^+) + \partial_- f(\sigma^-)] \Big|_{\sigma=\sigma_f}, \end{aligned} \quad (5.24)$$

where the second line follows from the fact that $x_0 \in \mathbb{R}$ and the definition Eq.(4.13), since $\partial_\sigma f(\sigma^+) = (\partial_+ - \partial_-) f(\sigma^+) = \partial_+ f(\sigma^+)$. To simplify Eq.(5.24) let $z := t - \sigma_f$, then

$$\sigma^-|_{\sigma=\sigma_f} = t - \sigma_f = z \quad \text{and} \quad \sigma^+|_{\sigma=\sigma_f} = t + \sigma_f = z + 2\sigma_f. \quad (5.25)$$

⁷⁶The derivation of the total energy of the test string in an AdS-Schwarzschild background is given in appendix (A.3).

Using Eq.(5.25) and defining $F(z) := \frac{d}{dz}f(z)$, Eq.(5.24) becomes

$$\begin{aligned} 0 &= \frac{1}{2} [F(z + 2\sigma_f) + F(z)] \\ \Rightarrow F(z + 2\sigma_f) &= -F(z), \end{aligned} \quad (5.26)$$

which shows that $F(z)$ is anti-periodic with an interval of $2\sigma_f$. The Virasoro constraint equations Eq.(4.18) can also be rewritten in terms of $F(z)$

$$\begin{aligned} 0 &= \eta_{00} (\partial_{\pm} X^0) (\partial_{\pm} X^0) + \eta_{11} (\partial_{\pm} X^1) (\partial_{\pm} X^1) \\ &= -(\partial_{\pm} t) (\partial_{\pm} t) + (\partial_{\pm} x(t, \sigma)) (\partial_{\pm} x(t, \sigma)) \\ &= -(\partial_{\pm} t) (\partial_{\pm} t) + \left[\partial_{\pm} \left(x_0 + \frac{1}{2} (f(\sigma^+) - f(\sigma^-)) \right) \right]^2. \end{aligned} \quad (5.27)$$

The first line follows since the spacetime is \mathbb{R}^{1+1} , Eq.(5.20) was used in the second line, and Eq.(5.23) was used in the final line. Eq.(5.27) breaks up into two, (+) and (-), constraint equations. For the (+) equation, Eq.(5.27) becomes

$$\begin{aligned} 0 &= -\left(\frac{1}{2}\right) \left(\frac{1}{2}\right) + \left(\frac{1}{2} \partial_+ f(\sigma^+)\right)^2 \\ \Rightarrow -\frac{1}{4} + \frac{1}{4} F(\sigma^+)^2 &= 0 \\ \Rightarrow F(\sigma^+)^2 &= 1. \end{aligned} \quad (5.28)$$

Similarly, for the (-) equation $F(\sigma^-)^2 = 1$. Hence the Virasoro constraint equations become

$$F(\sigma^{\pm})^2 = 1, \quad (5.29)$$

which implies $F(\sigma^-)^2|_{\sigma=\sigma_f} = 1$ or equivalently $F(z)^2 = 1$. What remains to be determined is the sign of $F(z)$. This is given by the anti-periodicity condition Eq.(5.26) which results in

$$F(z) = (-1)^{\left\lfloor \frac{z+\sigma_f}{2\sigma_f} \right\rfloor}, \quad (5.30)$$

where $\lfloor x \rfloor$ is the floor operation which returns the largest integer less than or equal to x . The function $F(z)$, plotted in figure (5), is a step function. The definition of $F(z)$ as the derivative of $f(z)$ with respect to z , implies that $f(z)$ can be found through integrating Eq.(5.30). But $F(z)$ is a discrete function – performing this integration involves integrating each segment of $F(z)$ separately. Since it is already known that $F(z)$ is alternating (+1) or (-1) in each $2\sigma_f$ interval, and the integral of a constant is a straight monotonic function; all that remains to be determined is if the function $f(z)$ is monotonically increasing or decreasing on each interval. Hence $f(z)$ can be defined by

$$f(z) = (-1)^{\left\lfloor \frac{z+\sigma_f}{2\sigma_f} \right\rfloor} ([(z + \sigma_f) \bmod 2\sigma_f] - \sigma_f) + \sigma_f, \quad (5.31)$$

where $(-1)^{\left\lfloor \frac{z+\sigma_f}{2\sigma_f} \right\rfloor}$ defines the domain of each segment to be integrated, and $([(z + \sigma_f) \bmod 2\sigma_f] - \sigma_f)$ yields 0 if $z \in z_1 \sigma_f$ (where z_1 is an even integer) and $-\sigma_f$ if $z \in z_2 \sigma_f$ (where z_2 is an odd integer). The function $f(z)$ is a triangular wave function and is plotted in figure (5).

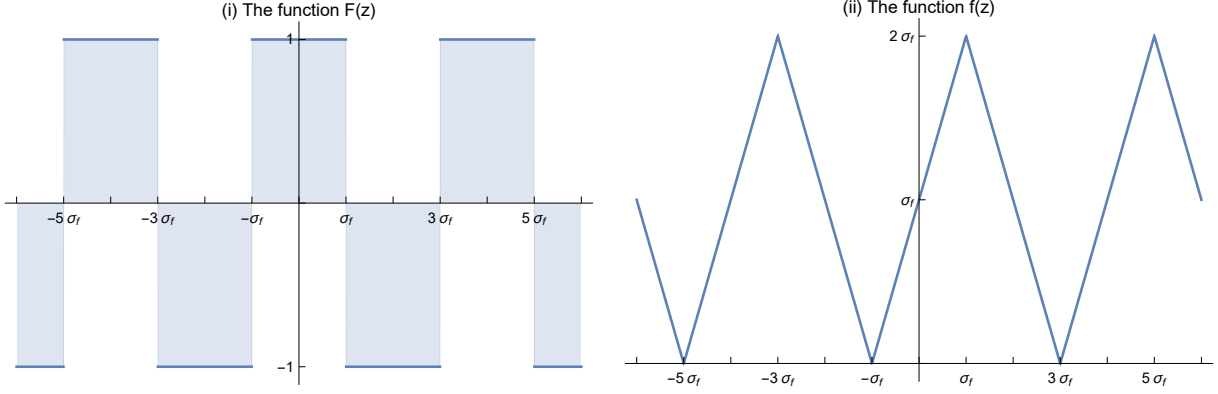


Figure 5: The functions (i) $F(z)$ and (ii) $f(z)$ over the range $[-6\sigma_f, 6\sigma_f]$, given by Eq.(5.30) and Eq.(5.31) respectively.

Now that a specific form of the function $f(z)$ has been obtained, $x(t, \sigma)$ (Eq.(5.23)) is completely known. For example, at $t = \sigma_f$, Eq.(5.23) becomes

$$x(\sigma_f, \sigma) = x_0 + \frac{1}{2} (f(\sigma_f + \sigma) - f(\sigma_f - \sigma)) = x_0, \quad (5.32)$$

where the second equality follows from using the definition Eq.(5.31). In studying the Limp Noodle, the primary interest is in the behaviour of the string as it shrinks from a length of ℓ_0 to a single point x_0 . From Eq.(5.32) this clearly is achieved in a $t = \sigma_f$ amount of time; hence the choice $t_f = \sigma_f$ is made. The worldsheet parameter space is therefore given by $\mathcal{M} = [0, \sigma_f] \times [0, \sigma_f]$, i.e. the parameter space is square.

Given the insight of [106–108] the parameter space \mathcal{M} can be minimally partitioned into two exclusive triangular regions

$$\begin{aligned} \mathcal{M}_1 &:= \{(t, \sigma) \in \mathcal{M} | \sigma \in [0, \sigma_f - t]\} \\ \mathcal{M}_2 &:= \{(t, \sigma) \in \mathcal{M} | \sigma \in (\sigma_f - t, \sigma_f]\}. \end{aligned} \quad (5.33)$$

In order to satisfy the boundary and initial conditions two classes of solutions exist, one in each of the two parameter space regions: the upper triangular region (\mathcal{M}_2) and the lower triangular region (\mathcal{M}_1). The embedding functions of the Limp Noodle in \mathbb{R}^{1+1} is therefore given by

$$X_{\text{Mink}}^\mu(t, \sigma) = \left(t, x_0 + \begin{cases} \sigma, & \text{if } (t, \sigma) \in \mathcal{M}_1 \\ \sigma_f - t, & \text{if } (t, \sigma) \in \mathcal{M}_2 \end{cases} \right)^\mu. \quad (5.34)$$

The Limp Noodle embedding functions satisfy the given boundary and initial conditions. The boundary conditions can be checked first: for $\sigma = 0$, $(t, \sigma) \in \mathcal{M}_1$ and the Dirichlet condition Eq.(4.25) is satisfied; while for $\sigma = \sigma_f$, $(t, \sigma) \in \mathcal{M}_2$ and the Neumann condition Eq.(4.26) is satisfied. The initial conditions are also fulfilled. For $t = 0$, $(t, \sigma) \in \mathcal{M}_1$ and the initial condition Eq.(4.27) is satisfied. Further the initial condition Eq.(4.28) is satisfied, since $\sigma_f = \ell_0$ is a requirement of the Virasoro constraints in flat space.

From Eq.(5.34), observe that the functions $X_{\text{Mink}}^\mu(t, \sigma)$ map the parameter space \mathcal{M}_1 region to an extended, space-like region in the target spacetime; while the parameter space \mathcal{M}_2 region is mapped to a null geodesic in the target spacetime. Null geodesics describe the trajectories of massless ‘point-like’ objects, and as such the worldsheet is considered to be wrapped up to a point along this geodesic. Hence, the string solution on \mathcal{M}_1 describes the entire string sans the falling endpoint, while the string solution on \mathcal{M}_2 describes the falling endpoint. This is evident from figure (6)⁷⁷.

⁷⁷Details regarding figures (6)-(8) can be found in Mathematica Notebook [a] (`MappingWorldSheetToTarget.nb`) – see appendix (A.7) for access.

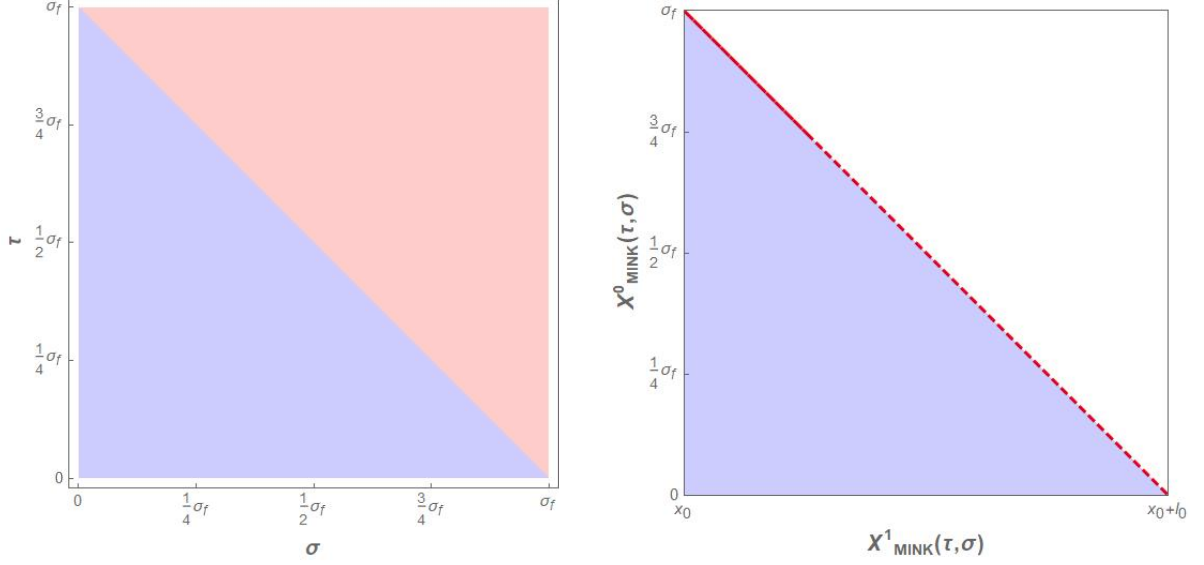


Figure 6: Left: The worldsheet parameter space, where \mathcal{M}_1 is the blue region and \mathcal{M}_2 is the red region (Eq.(5.33)). Right: The embedding functions $X^\mu_{\text{Mink}}(t, \sigma)$, Eq.(5.34), where \mathcal{M}_1 is mapped to a space-like region (blue region) and \mathcal{M}_2 is mapped to a null geodesic (red, dashed line) in the target spacetime.

$X^\mu_{\text{Mink}}(\mathcal{M}_2)$ lies on the boundary of $X^\mu_{\text{Mink}}(\mathcal{M}_1)$, and momentum flows between these two regions in the target spacetime. In order to continue to satisfy the Neumann boundary condition Eq.(4.26), momentum flows out of the \mathcal{M}_1 region at $\sigma = \sigma_f - t$, but immediately stops at \mathcal{M}_2 since any momentum flowing out of the string endpoint would change the physics in the boundary theory⁷⁸.

If Eq.(5.34) is converted into isothermal coordinates in terms of light-cone parameter space (σ^+, σ^-) , $Y^\mu_{\text{Mink}}(\sigma^+, \sigma^-)$ defined on the region \mathcal{M}_1 is a Bars *et al.* [107, 108] class A solution⁷⁹ and the solution defined on the region \mathcal{M}_2 is a class C solution, as expected. To see this, use the definition Eq.(5.8) to define the isothermal embedding functions on \mathcal{M}_1 ,

$$\begin{aligned}
Y^{0'} &= \frac{1}{\sqrt{2}} \left(t + (x_0 + \sigma) \right) \\
&= \frac{1}{\sqrt{2}} \left(\frac{1}{\sqrt{2}} (\sigma^+ + \sigma^-) + x_0 + \frac{1}{\sqrt{2}} (\sigma^+ - \sigma^-) \right) \\
&= \sigma^+ + \frac{1}{\sqrt{2}} x_0 =: Y^{0'}(\sigma^+) ,
\end{aligned} \tag{5.35}$$

where the definition of the light-cone coordinates (Eq.(4.13)) is used in the second line, and

$$\begin{aligned}
Y^{1'} &= \frac{1}{\sqrt{2}} \left(t - (x_0 + \sigma) \right) \\
&= \frac{1}{\sqrt{2}} \left(\frac{1}{\sqrt{2}} (\sigma^+ + \sigma^-) - x_0 - \frac{1}{\sqrt{2}} (\sigma^+ - \sigma^-) \right) \\
&= \sigma^- - \frac{1}{\sqrt{2}} x_0 =: Y^{1'}(\sigma^-) .
\end{aligned} \tag{5.36}$$

⁷⁸An infinite force is required to stop the flow of momentum abruptly at the $\mathcal{M}_1/\mathcal{M}_2$ divide, and yet the string has a finite energy density (since the string has a finite tension). This discrepancy stems from the fact that strings are fundamentally one-dimensional objects and are not made up of $d = 0$ constituent objects.

⁷⁹See subsection (5.1.1) for details.

Comparing Eqs.(5.35, 5.36) against the four classes of Bars *et al.* solutions (Eq.(5.14)), it is obvious that the isothermal embedding functions $Y_{\text{Mink}}^\mu(\sigma^+, \sigma^-)$ defined on the region \mathcal{M}_1 are a class *A* solution. This is depicted in figure (7).

The isothermal embedding functions on \mathcal{M}_2 are given by

$$\begin{aligned} Y^{0'} &= \frac{1}{\sqrt{2}} \left(t + (x_0 + \sigma_f - t) \right) \\ &= \frac{1}{\sqrt{2}} \left(\frac{1}{\sqrt{2}} (\sigma^+ + \sigma^-) + x_0 + \sigma_f - \frac{1}{\sqrt{2}} (\sigma^+ + \sigma^-) \right) \\ &= \frac{1}{\sqrt{2}} (x_0 + \sigma_f) =: Y_C^{0'}, \end{aligned} \quad (5.37)$$

and

$$\begin{aligned} Y^{1'} &= \frac{1}{\sqrt{2}} \left(t - (x_0 + \sigma_f - t) \right) \\ &= \frac{1}{\sqrt{2}} \left(\frac{1}{\sqrt{2}} (\sigma^+ + \sigma^-) - x_0 - \sigma_f + \frac{1}{\sqrt{2}} (\sigma^+ + \sigma^-) \right) \\ &= - (x_0 + \sigma_f - (\sigma^+ + \sigma^-)) =: Y^{1'}(\sigma^+, \sigma^-). \end{aligned} \quad (5.38)$$

Matching Eqs.(5.37, 5.38) with four classes of Bars *et al.* solutions (Eq.(5.14)) it is easily apparent that the embedding functions $Y_{\text{Mink}}^\mu(\sigma^+, \sigma^-)$ defined on the region \mathcal{M}_2 are a class *C* solution. Figure (7) displays this graphically.

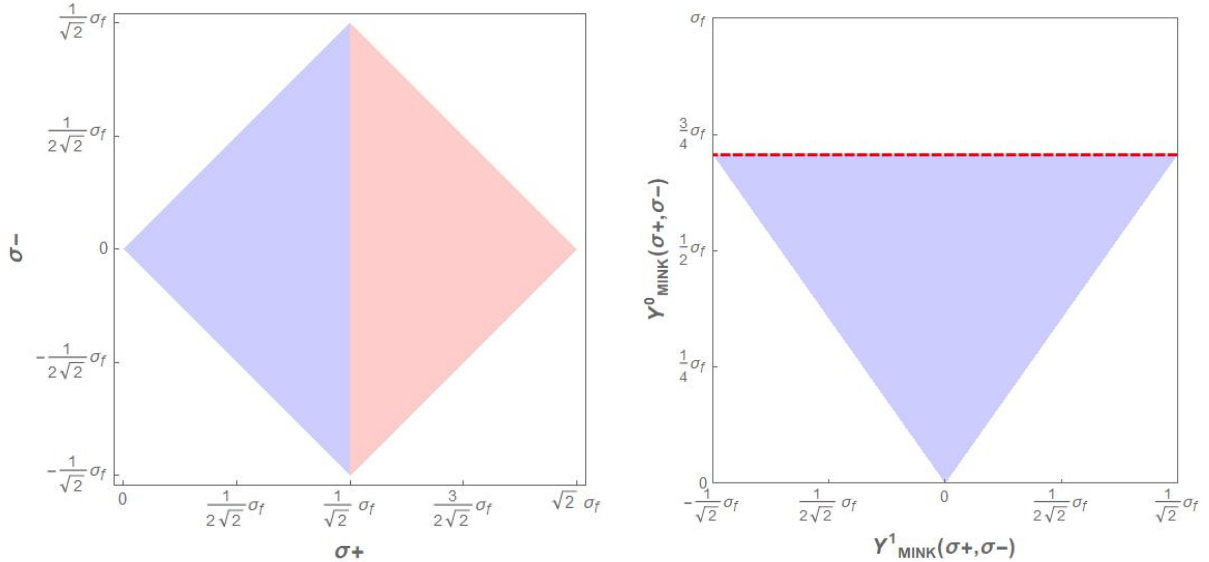


Figure 7: Left: The worldsheet parameter space in light-cone coordinates (σ^+, σ^-) , where \mathcal{M}_1 is the blue region and \mathcal{M}_2 is the red region. The parameter space regions \mathcal{M}_1 and \mathcal{M}_2 are plotted from Eq.(5.33) which is converted to (σ^+, σ^-) coordinates using Eq.(4.13). Right: The isothermal embedding functions $Y_{\text{Mink}}^\mu(\sigma^+, \sigma^-)$, Eqs.(5.35, 5.36, 5.37, 5.38), where \mathcal{M}_1 is mapped to a space-like region (blue region) and \mathcal{M}_2 is mapped to a null geodesic (red, dashed line) in the target spacetime.

5.1.3 Test Strings in AdS₃-Schwarzschild

In the previous subsection, the general embedding functions for the Limp Noodle in \mathbb{R}^{1+1} , Eq.(5.34), were discovered. From this the embedding functions for the Limp Noodle in AdS₃-Schwarzschild can be found using the same minimal partitioning of the parameter space and the determined pattern of solution classes on the patches of the parameter space.

In order to trivially write down the general solution for the Limp Noodle in AdS₃-Schwarzschild a set of isothermal coordinates is needed. As was shown in subsection (4.2.2), the tortoise coordinate r_* together with the temporal coordinate t forms such a set of coordinates in AdS_d-Schwarzschild.

The Dirichlet and Neumann conditions, Eqs.(4.44, 4.45), are chosen as boundary conditions for the Limp Noodle in AdS₃-Schwarzschild. The boundary conditions can be rewritten in terms of the isothermal (t, r_*) coordinate set. In subsection (4.2.2), it was noticed that these boundary conditions in the conformally flat description of AdS₃-Schwarzschild, Eqs.(4.46, 4.48), are respectively analogous to the boundary conditions for the Limp Noodle (and the heavy quark test string) in \mathbb{R}^{1+1} , Eqs.(4.25, 4.26). Hence, the embedding functions of the Limp Noodle in the conformally flat description of AdS₃-Schwarzschild are the direct analogue of Eq.(5.34). In (t, r_*) coordinates, the embedding functions are

$$X_{\text{AdS}_3\text{-Sch}}^\mu(t, \sigma) = \left(t, r_{s*} + \begin{cases} \sigma, & \text{if } (t, \sigma) \in \mathcal{M}_1 \\ \sigma_f - t, & \text{if } (t, \sigma) \in \mathcal{M}_2 \end{cases}, 0 \right)^\mu, \quad (5.39)$$

where the \mathcal{M}_1 and \mathcal{M}_2 parameter space regions are given by Eq.(5.33). Using the inverse tortoise transformation Eq.(4.40), the embedding functions for the AdS₃-Schwarzschild Limp Noodle (Eq.(5.39)) can be rewritten in (t, r) coordinates

$$X_{\text{AdS}_3\text{-Sch}}^\mu(t, \sigma) = \left(t, \begin{cases} -r_H \coth\left(\frac{r_H}{l^2}(r_{s*} + \sigma)\right), & \text{if } (t, \sigma) \in \mathcal{M}_1 \\ -r_H \coth\left(\frac{r_H}{l^2}(r_{s*} + \sigma_f - t)\right), & \text{if } (t, \sigma) \in \mathcal{M}_2 \end{cases}, 0 \right)^\mu, \quad (5.40)$$

where the position of the fixed string endpoint attached to the stretched horizon r_{s*} is given by Eq.(4.47) and the length of the string in tortoise coordinates is given by Eq.(4.51). Notice that the identification Eq.(4.52) still holds. The embedding functions are plotted in figure (8).

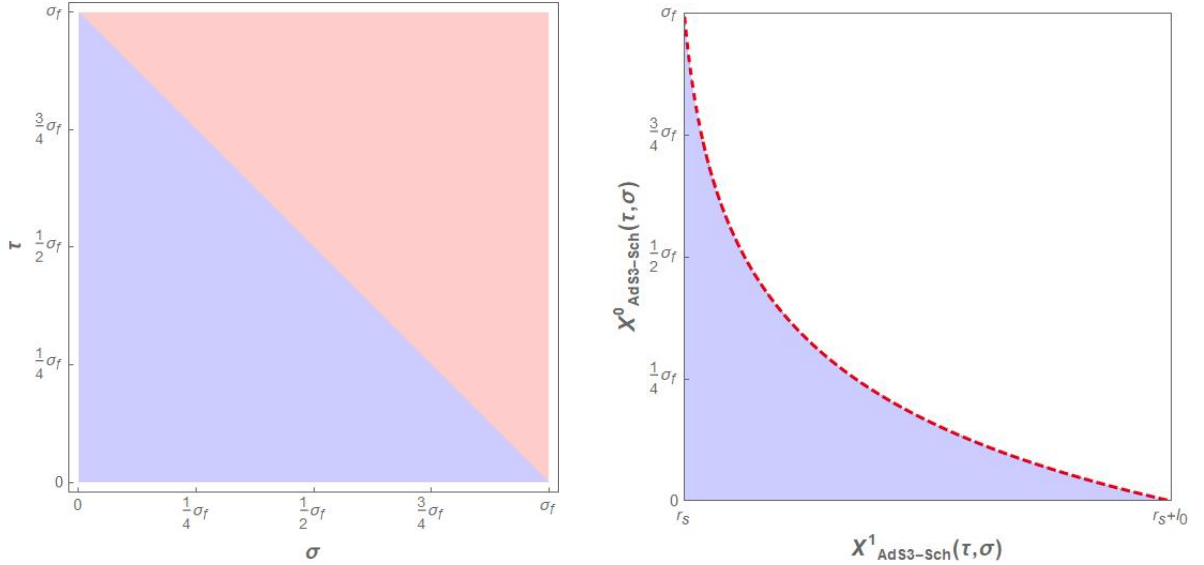


Figure 8: Left: The worldsheet parameter space, where \mathcal{M}_1 is the blue region and \mathcal{M}_2 is the red region (Eq.(5.33)). Right: The embedding functions $X_{\text{AdS}_3\text{-Sch}}^\mu(t, \sigma)$, Eq.(5.40), where \mathcal{M}_1 is mapped to a space-like region (blue region) and \mathcal{M}_2 is mapped to a null geodesic (red, dashed line) in the target spacetime.

5.2 Fluctuating Test String Dynamics

As discussed previously, the boundary endpoint of the Limp Noodle falls at the local speed of light – the same speed at which information propagates. Hence, any part of the string below the falling endpoint does not *know* if the string is stretched like an on-mass-shell quark or its endpoint is falling like an off-mass-shell quark. Therefore, the transverse fluctuations of all parts of the Limp Noodle except the falling endpoint are described by the same transverse equations of motion as those of the on-mass-shell heavy quark’s test string and its solution (discussed in subsections (4.3.1) and (4.3.2)).

The leading order solution to the string equations of motion – renamed $X_0^\mu(t, \sigma)$ – is given by Eq.(5.40) in AdS₃-Schwarzschild. Adding non-zero fluctuations in the transverse x -direction, the Limp Noodle solution becomes

$$X_{\text{AdS}_3\text{-Sch}}^\mu(t, \sigma) \Big|_{\mathcal{M}_1} = X_0^\mu(t, \sigma) + (0, 0, X(t, \sigma))^\mu = \left(t, -r_H \coth \left(\frac{r_H}{l^2} (r_{s*} + \sigma) \right), X(t, \sigma) \right)^\mu. \quad (5.41)$$

The transverse string equations of motion are supplied in Eq.(4.75); and its solution is given by Eq.(4.92) in AdS₃-Schwarzschild. Continuity of the string solution in spacetime means that it is unnecessary to find the explicit string solution on the \mathcal{M}_2 parameter space region which maps onto the falling string endpoint.

5.2.1 Calculating the Light Quark’s Mean-Squared Displacement $s^2(t)$ in AdS₃-Schwarzschild

Unlike in the case of the heavy quark’s test string where the boundary endpoint is fixed in the radial direction (subsection (4.3.2)); for the Limp Noodle the position of the boundary endpoint is falling at the local speed of light and is defined by the operator

$$\hat{X}_{\text{end}}(t) := \hat{X}(t, \sigma_f - t). \quad (5.42)$$

As in subsection (4.3.2), in order to determine $s^2(t)$ – the falling string endpoint’s mean-squared transverse displacement defined in Eq.(4.103) – begin by calculating the expectation value of the position of the free endpoint at two different times. Using Eq.(4.92),

$$\begin{aligned} & \langle : \hat{X}_{\text{end}}(t_1) \hat{X}_{\text{end}}(t_2) : \rangle \\ &= \langle : \int_0^\infty \frac{d\omega d\omega'}{(2\pi)^2} \frac{\beta^2}{4\pi\sqrt{\omega\omega'}\sqrt{\lambda}} [f_\omega(\sigma_f - t_1)e^{-i\omega t_1}\hat{a}_\omega + f_\omega^*(\sigma_f - t_1)e^{i\omega t_1}\hat{a}_\omega^\dagger] \\ & \quad \times [f_{\omega'}(\sigma_f - t_2)e^{-i\omega' t_2}\hat{a}_{\omega'} + f_{\omega'}^*(\sigma_f - t_2)e^{i\omega' t_2}\hat{a}_{\omega'}^\dagger] : \rangle \\ &= \frac{\beta^2}{4\pi\sqrt{\lambda}} \int_0^\infty \frac{d\omega d\omega'}{(2\pi)^2} \frac{1}{\sqrt{\omega\omega'}} \left[f_\omega(\sigma_f - t_1)f_{\omega'}^*(\sigma_f - t_2)e^{-i\omega t_1 + i\omega' t_2} \langle : \hat{a}_\omega \hat{a}_{\omega'}^\dagger : \rangle \right. \\ & \quad \left. + f_\omega^*(\sigma_f - t_1)f_{\omega'}(\sigma_f - t_2)e^{i\omega t_1 - i\omega' t_2} \langle : \hat{a}_\omega^\dagger \hat{a}_{\omega'} : \rangle \right] \\ &= \frac{\beta^2}{4\pi\sqrt{\lambda}} \int_0^\infty \frac{d\omega d\omega'}{2\pi} \frac{1}{\sqrt{\omega\omega'}} \left[\delta(\omega' - \omega) f_\omega(\sigma_f - t_1)f_{\omega'}^*(\sigma_f - t_2) \frac{e^{-i\omega t_1 + i\omega' t_2}}{e^{\beta\omega} - 1} \right. \\ & \quad \left. + \delta(\omega - \omega') f_\omega^*(\sigma_f - t_1)f_{\omega'}(\sigma_f - t_2) \frac{e^{i\omega t_1 - i\omega' t_2}}{e^{\beta\omega} - 1} \right] \\ &= \frac{\beta^2}{4\pi\sqrt{\lambda}} \int_0^\infty \frac{d\omega}{2\pi} \frac{1}{\omega} \frac{1}{e^{\beta\omega} - 1} \left[f_\omega(\sigma_f - t_1)f_\omega^*(\sigma_f - t_2)e^{-i\omega(t_1 - t_2)} + f_\omega^*(\sigma_f - t_1)f_\omega(\sigma_f - t_2)e^{i\omega(t_1 - t_2)} \right] \\ &= \frac{\beta^2}{4\pi^2\sqrt{\lambda}} \int_0^\infty \frac{d\omega}{\omega} \frac{1}{e^{\beta\omega} - 1} \text{Re} \left(f_\omega(\sigma_f - t_1)f_\omega^*(\sigma_f - t_2)e^{-i\omega(t_1 - t_2)} \right), \end{aligned} \quad (5.43)$$

where $:\hat{a}_\omega^\dagger \hat{a}_{\omega'}: = :\hat{a}_{\omega'} \hat{a}_\omega^\dagger: = \hat{a}_\omega^\dagger \hat{a}_{\omega'}$ is the normal ordering operator⁸⁰, and the definition of the Bose-Einstein distribution (Eq.(4.102)) is used in the third equality. The penultimate equality follows from the property of the Dirac delta function $\int_0^\infty dk e^{-kx} \delta(k-a) = e^{-ax}$; and in the final line the complex conjugate property $\text{Re}(z) = (z + \bar{z})/2$ is used. At specific times, the regularized correlator Eq.(5.43) becomes

$$\langle :\hat{X}_{\text{end}}(t) \hat{X}_{\text{end}}(0): \rangle = \frac{\beta^2}{4\pi^2 \sqrt{\lambda}} \int_0^\infty \frac{d\omega}{\omega} \frac{1}{e^{\beta\omega} - 1} \text{Re}(f_\omega(\sigma_f - t) f_\omega^*(\sigma_f) e^{-i\omega t}), \quad (5.44)$$

$$\langle :\hat{X}_{\text{end}}(0) \hat{X}_{\text{end}}(0): \rangle = \frac{\beta^2}{4\pi^2 \sqrt{\lambda}} \int_0^\infty \frac{d\omega}{\omega} \frac{1}{e^{\beta\omega} - 1} \text{Re}(f_\omega(\sigma_f) f_\omega^*(\sigma_f)), \quad (5.45)$$

$$\langle :\hat{X}_{\text{end}}(t) \hat{X}_{\text{end}}(t): \rangle = \frac{\beta^2}{4\pi^2 \sqrt{\lambda}} \int_0^\infty \frac{d\omega}{\omega} \frac{1}{e^{\beta\omega} - 1} \text{Re}(f_\omega(\sigma_f - t) f_\omega^*(\sigma_f - t)). \quad (5.46)$$

Inputting Eqs.(5.44, 5.45, 5.46) into the definition Eq.(4.103), the string falling endpoint's mean-squared transverse displacement can be calculated as

$$\begin{aligned} s^2(t) &= \frac{\beta^2}{4\pi^2 \sqrt{\lambda}} \int_0^\infty \frac{d\omega}{\omega} \frac{1}{e^{\beta\omega} - 1} \text{Re}(f_\omega(\sigma_f - t) f_\omega^*(\sigma_f - t) + f_\omega(\sigma_f) f_\omega^*(\sigma_f) - 2f_\omega(\sigma_f - t) f_\omega^*(\sigma_f) e^{-i\omega t}) \\ &= \frac{\beta^2}{4\pi^2 \sqrt{\lambda}} \int_0^\infty \frac{d\omega}{\omega} \frac{1}{e^{\beta\omega} - 1} [f_\omega(\sigma_f - t) f_\omega^*(\sigma_f - t) + f_\omega(\sigma_f) f_\omega^*(\sigma_f) - f_\omega(\sigma_f - t) f_\omega^*(\sigma_f) e^{-i\omega t} \\ &\quad - f_\omega^*(\sigma_f - t) f_\omega(\sigma_f) e^{i\omega t}] \\ &= \frac{\beta^2}{4\pi^2 \sqrt{\lambda}} \int_0^\infty \frac{d\omega}{\omega} \frac{1}{e^{\beta\omega} - 1} [(f_\omega(\sigma_f - t) - f_\omega(\sigma_f) e^{i\omega t}) (f_\omega^*(\sigma_f - t) - f_\omega^*(\sigma_f) e^{-i\omega t})] \\ &= \frac{\beta^2}{4\pi^2 \sqrt{\lambda}} \int_0^\infty \frac{d\omega}{\omega} \frac{1}{e^{\beta\omega} - 1} |f_\omega(\sigma_f - t) - f_\omega(\sigma_f) e^{i\omega t}|^2, \end{aligned} \quad (5.47)$$

where in the second line the complex conjugate property $\text{Re}(z) = (z + \bar{z})/2$ is again used, and in the final line another complex conjugate property $|z|^2 = z \bar{z}$ is used.

5.2.2 The Limiting Cases of $s^2(t)$

The mass (or *virtuality*) of the probe, off-mass-shell light quark⁸¹ in the boundary theory determines the length of the test string ℓ_0 in the bulk. Specifically⁸²,

$$\tilde{r}_0 r_H \equiv r_c := (r_s + \ell_0) \iff 2\pi \alpha' (M_{\text{rest}} + \Delta m), \quad (5.48)$$

where $M_{\text{rest}}(T)$ is the static thermal mass of external particle⁸³ and $\Delta m(T)$ is the thermal rest mass shift. In the boundary theory this corresponds to the virtuality of the probe light quark being much less than the temperature of the thermal plasma, i.e. $Q^2 \ll T^2$. Equivalently in the dual gravitational picture,

⁸⁰Normal ordering of the annihilation and creation operators $\hat{a}_\omega, \hat{a}_\omega^\dagger$ is used to remove logarithmic UV divergences.

⁸¹An off-mass-shell quark does not satisfy Einstein's energy and momentum relation $E^2 = (pc)^2 + (mc)^2$. In the case of the light quark it starts at $t = 0$ as an off-mass-shell particle (corresponding to the initial static string), radiates energy as it travels through the thermal medium (string contracts as the boundary endpoint falls at the local speed of light), and finally stops radiating as it becomes an on-mass-shell particle.

⁸²See table (1), page 6, for a comprehensive dictionary between quantities in the boundary theory and the bulk theory.

⁸³In the $\text{AdS}_5/\mathcal{N} = 4$ SYM case, this is the free energy of a quark at rest in $\mathcal{N} = 4$ SYM plasma. In the limit of zero temperature it is equal to the QCD Lagrangian quark mass, m_q [68].

$$Q^2 \ll T^2 \implies \frac{\lambda \ell_0^2}{4 \pi^2 l^4} \ll \frac{1}{\beta^2} \implies \frac{4\lambda}{(d-1)^2} \frac{\ell_0^2}{r_H^2} \ll 1 \implies \ell_0 \ll r_H, \quad (5.49)$$

for fixed λ . In the second equality, the Hawking temperature Eq.(4.35) and the definition of the quark mass (or *virtuality*) Eq.(4.31) is used; and in the third equality, Eq.(4.35) is used again. In the small virtuality limit, the minimum radius of the space filling D7-brane is small, i.e. $\tilde{r}_0 \rightarrow 1 + \epsilon$, where $0 < \epsilon \ll 1$ and \tilde{r}_0 is defined in Eq.(4.88). In juxtaposition, the large virtuality limit refers $\tilde{r}_0 \rightarrow \infty$.

In the current subsection the string falling endpoint's mean-squared transverse displacement, $s^2(t)$, is examined in a number of different limiting cases. Videlicet, the small virtuality case and the arbitrary virtuality case. In both of these cases, the asymptotically early time and the asymptotically late time limit is explored. For the arbitrary virtuality case, a further limit of small or large virtuality can be considered. It is expected that the large virtuality, early time limit will correspond exactly with the early time limit of the on-mass-shell heavy quark – since, at early times the light quark's test string is static (i.e. the boundary endpoint has not yet begun to fall).

5.2.2.1 Small Virtuality

In this subsection the behaviour of $s^2(t)$, Eq.(5.47), in the small virtuality limit is considered; and after obtaining a suitable expression for $s_{\text{small}}^2(t)$, the asymptotic early and late time dynamics are explored. The defining condition for the small virtuality limit is given in Eq.(5.49). This equation implies⁸⁴

$$\coth^2 \left(\frac{r_H (r_{s*} + \sigma)}{l^2} \right) \rightarrow 1, \quad \text{since } \ell_0 \ll r_H, \quad (5.50)$$

where $\sigma \in [0, \sigma_f]$. Using Eq.(5.50) the equations of motion in AdS₃-Schwarzschild, Eq.(4.75), simplifies to the wave equation

$$-\partial_t^2 X(t, \sigma) + \partial_\sigma^2 X(t, \sigma) = 0. \quad (5.51)$$

The plane wave solutions to Eq.(5.51) are the near-horizon solutions described in Eq.(4.84). Hence in the small virtuality limit the in-falling (+) and out-going (−) modes of the general solution $f_\omega(\sigma)$ are given by,

$$f_\omega^{(\pm)}(\sigma) = e^{\pm i\omega (r_{s*} + \sigma)}. \quad (5.52)$$

The general solution $f_\omega(\sigma)$ is a linear combination of the in-falling and out-going modes (defined in Eq.(4.85)). The coefficient B_ω is fixed in the same way as in subsection (4.3.2): by imposing a Neumann boundary condition at the falling string endpoint in the radial direction at $t = 0$,

$$\partial_\sigma f_\omega(\sigma)|_{\sigma=\sigma_f} = 0. \quad (5.53)$$

⁸⁴Explicitly, for the case $\sigma = \sigma_f$,

$$\coth^2 \left(\frac{r_H (r_{s*} + \sigma)}{l^2} \right) = \coth^2 \left(\frac{r_H (r_{s*} + \sigma_f)}{l^2} \right) = \coth^2 \left(\coth^{-1} \left(-\frac{r_s + \ell_0}{r_H} \right) \right) \approx \coth^2 \left(\coth^{-1} \left(-\frac{r_s}{r_H} \right) \right) \xrightarrow{(\epsilon \rightarrow 0)} 1$$

where the second equality follows from using the definition for σ_f , Eq.(4.51); the approximation follows since $\ell_0 \ll r_H$; and in taking the limit the definition of the stretched horizon $r_s = (1 + \epsilon) r_H$ (where $0 < \epsilon \ll 1$) is used. The limit follows since, $\coth^{-1}(-(1 + \epsilon)) \rightarrow -\infty$ as $\epsilon \rightarrow 0$; and $\coth^2(x) \rightarrow 1$ as $x \rightarrow -\infty$. Further, for the case $\sigma = 0$,

$$\coth^2 \left(\frac{r_H (r_{s*} + \sigma)}{l^2} \right) = \coth^2 \left(\frac{r_H r_{s*}}{l^2} \right) = \coth^2 \left(\coth^{-1} \left(-\frac{r_s}{r_H} \right) \right) \xrightarrow{(\epsilon \rightarrow 0)} 1$$

where the first equality follows from the definition for r_{s*} , Eq.(4.47).

Using Eqs.(4.85, 5.52), Eq.(5.53) can be easily solved in Mathematica⁸⁵ to yield

$$B_\omega = e^{i2\omega(r_{s*} + \sigma_f)}. \quad (5.54)$$

Hence, the general solution $f_\omega(\sigma)$ is given by,

$$\begin{aligned} f_\omega(\sigma) &= f_\omega^{(+)}(\sigma) + B_\omega f_\omega^{(-)}(\sigma) \\ &= e^{+i\omega(r_{s*} + \sigma)} + e^{i2\omega(r_{s*} + \sigma_f)} e^{-i\omega(r_{s*} + \sigma)} \\ &= 2e^{i\omega(r_{s*} + \sigma_f)} \cos(\omega(\sigma - \sigma_f)), \end{aligned} \quad (5.55)$$

where Eqs.(5.52, 5.54) are used in the second line; and the third line follows from the trigonometric identity $\cos(x) = (e^{ix} + e^{-ix})/2$. In order to calculate the falling string endpoint's mean-squared transverse displacement in the small virtuality limit, Eq.(5.55) is substituted into Eq.(5.47):

$$\begin{aligned} s_{\text{small}}^2(t) &:= s^2(t)|_{Q^2 \ll T^2} = \frac{\beta^2}{4\pi^2\sqrt{\lambda}} \int_0^\infty \frac{d\omega}{\omega} \frac{1}{e^{\beta\omega} - 1} \left| 2e^{i\omega(r_{s*} + \sigma_f)} \cos(\omega t) - 2e^{i\omega(r_{s*} + \sigma_f)} e^{i\omega t} \right|^2 \\ &= \frac{\beta^2}{4\pi^2\sqrt{\lambda}} \int_0^\infty \frac{d\omega}{\omega} \frac{1}{e^{\beta\omega} - 1} \left| e^{i\omega(r_{s*} + \sigma_f)} (e^{-i\omega t} - e^{i\omega t}) \right|^2 \\ &= \frac{\beta^2}{4\pi^2\sqrt{\lambda}} \int_0^\infty \frac{d\omega}{\omega} \frac{1}{e^{\beta\omega} - 1} \left(e^{i\omega(r_{s*} + \sigma_f)} (e^{-i\omega t} - e^{i\omega t}) \right) \left(e^{-i\omega(r_{s*} + \sigma_f)} (e^{i\omega t} - e^{-i\omega t}) \right) \\ &= \frac{\beta^2}{4\pi^2\sqrt{\lambda}} \int_0^\infty \frac{d\omega}{\omega} \frac{1}{e^{\beta\omega} - 1} (2 - e^{-2i\omega t} - e^{2i\omega t}) \\ &= \frac{\beta^2}{\pi^2\sqrt{\lambda}} \int_0^\infty \frac{d\omega}{\omega} \frac{1}{e^{\beta\omega} - 1} \sin^2(\omega t), \end{aligned} \quad (5.56)$$

where the complex conjugate property $|z|^2 = z\bar{z}$ is used in the third line, and the trigonometric identities $\cos(x) = (e^{ix} + e^{-ix})/2$ and $\sin^2(x) = (1 - \cos(2x))/2$ are used in the final line. The integral in Eq.(5.56) can be solved analytically. Introducing a change of variables

$$x := \beta\omega \quad \text{and} \quad k := \frac{t}{\beta}, \quad (5.57)$$

Eq.(5.56) becomes

$$\begin{aligned} s_{\text{small}}^2(t) &= \frac{\beta^2}{\pi^2\sqrt{\lambda}} \int_0^\infty \frac{dx}{x} e^{-x} \frac{1}{1 - e^{-x}} \sin^2(kx) \\ &= \frac{\beta^2}{\pi^2\sqrt{\lambda}} \sum_{n=1}^\infty \int_0^\infty \frac{dx}{x} \sin^2(kx) e^{-nx} \\ &= \frac{\beta^2}{4\pi^2\sqrt{\lambda}} \sum_{n=1}^\infty \ln \left(1 + \frac{4k^2}{n^2} \right) \\ &= \frac{\beta^2}{4\pi^2\sqrt{\lambda}} \ln \left(\prod_{n=1}^\infty \left(1 + \frac{4k^2}{n^2} \right) \right) \\ &= \frac{\beta^2}{4\pi^2\sqrt{\lambda}} \ln \left(\frac{\beta}{2\pi t} \sinh \left(\frac{2\pi t}{\beta} \right) \right), \end{aligned} \quad (5.58)$$

⁸⁵See Mathematica Notebook [b]: **BrownianMotion.nb**.

where in the second line the geometric series $1/(1-x) = \sum_{n=0}^{\infty} x^n$ is used; and in the third line the integral was performed using Mathematica⁸⁶. In the final line, Mathematica was again used, followed by a change of variables using Eq.(5.57). Notice from Eq.(5.58) that β naturally defines a cross-over time scale between the dynamics of early and late times⁸⁷, and that the cross-over time is independent of the length of the string ℓ_0 .

(I) Asymptotic Early Time Dynamics

Since, in the early time limit $t \ll \beta$, Eq.(5.58) can be expanded in powers of $k = t/\beta$. For small k a Taylor expansion (about $k = 0$) can be performed. Explicitly, $\ln(\sinh(x)/x) = x^2/6 - x^4/180 + x^6/2835 + \mathcal{O}(x^8)$ (where $x = 2k\pi$). Therefore, Eq.(5.58) becomes

$$s_{\text{small}}^2(t) \xrightarrow{(t \ll \beta)} \frac{\beta^2}{4\pi^2\sqrt{\lambda}} \left[\frac{2\pi^2 t^2}{3\beta^2} + \mathcal{O}\left(\frac{t}{\beta}\right)^4 \right] = \frac{t^2}{6\sqrt{\lambda}} + \mathcal{O}\left(\frac{t}{\beta}\right)^4. \quad (5.59)$$

Since $s_{\text{small}}^2(t) \sim t^2$, the early time dynamics exhibit ballistic behaviour⁸⁸ (see Eq.(3.20)).

(II) Asymptotic Late Time Dynamics

At asymptotically late times ($t \gg \beta$) the integral in Eq.(5.58) can be expanded in powers of $1/k = \beta/t$. Specifically,

$$\begin{aligned} s_{\text{small}}^2(t) &= \frac{\beta^2}{4\pi^2\sqrt{\lambda}} \left[\ln(\sinh(2\pi k)) + \ln\left(\frac{1}{2\pi k}\right) \right] \\ &= \frac{\beta^2}{4\pi^2\sqrt{\lambda}} \left[\ln(e^{2\pi k}(1 - e^{-4\pi k})) + \ln\left(\frac{1}{4\pi k}\right) \right] \\ &= \frac{\beta^2}{4\pi^2\sqrt{\lambda}} \left[\frac{2\pi t}{\beta} + \ln(1 - e^{-4\pi k}) + \ln\left(\frac{\beta}{4\pi t}\right) \right] \\ &\xrightarrow{(\beta \ll t)} \frac{\beta t}{2\pi\sqrt{\lambda}} + \frac{\beta^2}{4\pi^2\sqrt{\lambda}} \ln\left(\frac{\beta}{4\pi t}\right) + \mathcal{O}\left(\beta^2 e^{-\frac{4\pi t}{\beta}}\right), \end{aligned} \quad (5.60)$$

where the second line follows from trigonometric identity $\sinh(x) = (e^x - e^{-x})/2$; and, in the final line, the expansion $\ln(1-x) = -x - x^2/2 - x^3/3 + \mathcal{O}(x^4)$ (where $x = e^{-4\pi k}$) is performed, since $e^{-4\pi k} \rightarrow 0$ in the late time regime ($k \gg 1$).

Since $s_{\text{small}}^2(t) \sim t$, the late time dynamics exhibit diffusive behaviour⁸⁹. From Eq.(3.21) it is expected that $s_{\text{small}}^2(t) = 2Dt$ at late times, where D is the diffusion coefficient. Comparing this to Eq.(5.60), it is easy to see that the diffusion coefficient is given by

$$D_{\text{LQ}}^{\text{AdS}_3} = \frac{\beta}{4\pi\sqrt{\lambda}}. \quad (5.61)$$

The diffusion coefficient for the on-mass-shell heavy quark is given by Eq.(4.122). By comparing Eq.(5.61) with Eq.(4.122), notice that an off-mass-shell small virtuality light quark which is initially at rest in a strongly-coupled thermal plasma has a diffusion coefficient related to that of a massive on-mass-shell heavy quark by

$$D_{\text{LQ}}^{\text{AdS}_3} = \frac{1}{2} D_{\text{HQ}}^{\text{AdS}_3}. \quad (5.62)$$

The factor of $1/2$ may arise through the differences in partitioning the worldsheet for the heavy and light quark test strings. This is explored further in subsection (6.2).

⁸⁶See Mathematica Notebook [b]: `BrownianMotion.nb`.

⁸⁷See footnote 68, page 35.

⁸⁸The early time limit of the on-mass-shell heavy quark also displays ballistic behaviour (see Eq.(4.118)).

⁸⁹The late time limit of the on-mass-shell heavy quark also displays diffusive behaviour (see Eq.(4.121)).

5.2.2.2 Arbitrary Virtuality

(I) Asymptotic Early Time Dynamics

Now consider a probe light quark with arbitrary virtuality. The behaviour of $s^2(t)$, Eq.(5.47), at asymptotically early times is considered. Since $t \ll \beta$, Eq.(5.47) can be expanded in powers of $k = t/\beta$,

$$\begin{aligned}
& |f_\omega(\sigma_f - t) - f_\omega(\sigma_f)e^{i\omega t}|^2 \\
& \xrightarrow{(t \ll \beta)} (f_\omega(\sigma_f) - f_\omega(\sigma_f)e^{i\omega t})(f_\omega^*(\sigma_f) - f_\omega^*(\sigma_f)e^{-i\omega t}) \\
& = 2f_\omega(\sigma_f)f_\omega^*(\sigma_f) - f_\omega(\sigma_f)f_\omega^*(\sigma_f)e^{-i\omega t} - f_\omega(\sigma_f)f_\omega^*(\sigma_f)e^{i\omega t} \\
& = |f_\omega(\sigma_f)|^2 (2 - e^{-i\omega t} - e^{i\omega t}) \\
& = |f_\omega(\sigma_f)|^2 \left(2 - \left(1 - i\omega t - \frac{\omega^2 t^2}{2} + \frac{i\omega^3 t^3}{6} \right) - \left(1 + i\omega t - \frac{\omega^2 t^2}{2} - \frac{i\omega^3 t^3}{6} \right) + \mathcal{O}(\omega t)^4 \right) \\
& = |f_\omega(\sigma_f)|^2 (\omega^2 t^2 + \mathcal{O}(\omega t)^4) \\
& = 4 \frac{1 + \nu^2}{1 + \tilde{r}_0 \nu^2} (\omega^2 t^2 + \mathcal{O}(\omega t)^4),
\end{aligned} \tag{5.63}$$

where the second line follows since in the early time regime $t \ll \beta$ implies $f_\omega(\sigma_f - t) \approx f_\omega(\sigma_f)$; and in the fifth line $e^{i\omega t}$ and $e^{-i\omega t}$ are Taylor expanded. The final line follows⁹⁰ from using Eqs.(4.83, 4.85, 4.90) to calculate $|f_\omega(\sigma_f)|^2 = f_\omega(\sigma_f)f_\omega^*(\sigma_f)$. Inputting Eq.(5.63) into Eq.(5.47), yields

$$\begin{aligned}
s^2(t)|_{t \ll \beta} &= \frac{\beta^2 t^2}{\pi^2 \sqrt{\lambda}} \int_0^\infty d\omega \frac{\omega}{e^{\beta\omega} - 1} \frac{1 + \nu^2}{1 + \tilde{r}_0 \nu^2} \\
&= \frac{4t^2}{\sqrt{\lambda}} \int_0^\infty d\nu \frac{\nu}{e^{2\pi\nu} - 1} \frac{1 + \nu^2}{1 + \tilde{r}_0 \nu^2},
\end{aligned} \tag{5.64}$$

where, in the second line, a change of variables was performed using Eqs.(4.35, 4.78). Eq.(5.64) is evaluated by breaking the integral into two parts and recognising that these terms are the series expansion to $\mathcal{O}(k)^0$ (around $k = 0$, where $k = t/\beta$) of the second derivatives with respect to k of the integrals I_1 and I_2 given in Eq.(4.112) and Eq.(4.113) respectively. To clarify, the second derivative of I_1 and I_2 are given by

$$\begin{aligned}
I_1 &= 4 \int_0^\infty \frac{dx}{x(1 + a^2 x^2)} \frac{\sin^2\left(\frac{kx}{2}\right)}{e^x - 1} \\
&\Rightarrow \left. \frac{\partial^2 I_1}{\partial k^2} \right|_{k=0} = 4\pi \int_0^\infty d\nu \frac{\nu}{e^{2\pi\nu} - 1} \frac{1}{1 + \tilde{r}_0^2 \nu^2},
\end{aligned} \tag{5.65}$$

and,

$$\begin{aligned}
I_2 &= 4 \int_0^\infty \frac{dx}{x} \frac{\sin^2\left(\frac{kx}{2}\right)}{e^x - 1} \\
&\Rightarrow \left. \frac{\partial^2 I_2}{\partial k^2} \right|_{k=0} = 4\pi \int_0^\infty d\nu \frac{\nu}{e^{2\pi\nu} - 1},
\end{aligned} \tag{5.66}$$

⁹⁰Mathematica is used to simplify the algebra. This computation (and others in this section) are explicitly shown in Mathematica Notebook [b] (`BrownianMotion.nb`). For access, see appendix (A.7).

where $x = 2\pi\nu$, $a = \tilde{r}_0/(2\pi)$ and $k = t/\beta$. Explicitly rewriting Eq.(5.64) in terms of $\partial_k^2 I_1$ and $\partial_k^2 I_2$ yields

$$\begin{aligned} s^2(t)|_{t \ll \beta} &= \frac{4t^2}{\sqrt{\lambda}} \int_0^\infty d\nu \left(\frac{\tilde{r}_0^2 - 1}{\tilde{r}_0^2} \frac{\nu}{e^{2\pi\nu} - 1} \frac{1}{1 + \tilde{r}_0^2 \nu^2} + \frac{1}{\tilde{r}_0^2} \frac{\nu}{e^{2\pi\nu} - 1} \right) \\ &= \frac{t^2}{\pi\sqrt{\lambda}} \left(\frac{\tilde{r}_0^2 - 1}{\tilde{r}_0^2} \frac{\partial^2 I_1}{\partial k^2} \Big|_{k=0} + \frac{1}{\tilde{r}_0^2} \frac{\partial^2 I_2}{\partial k^2} \Big|_{k=0} \right). \end{aligned} \quad (5.67)$$

The solution to the integrals I_1 and I_2 are given by Eqs.(4.115, 4.116) respectively. Taking the second derivative with respect to k followed by a series expansion to $\mathcal{O}(k)^0$ (around $k = 0$) for each of these solutions, yields

$$\frac{\partial^2 I_1}{\partial k^2} \Big|_{k=0} = \frac{2 \left(-\pi^2 \ln\left(\frac{\tilde{r}_0}{2\pi}\right) + \pi^2 \ln\left(\frac{2\pi}{\tilde{r}_0}\right) + \pi^3 \cot\left(\frac{\pi}{\tilde{r}_0}\right) - \pi^2 \psi\left(1 + \frac{1}{\tilde{r}_0}\right) - \pi^2 \psi\left(1 - \frac{1}{\tilde{r}_0}\right) - 2\pi^2 \ln(2\pi) \right)}{\tilde{r}_0^2}, \quad (5.68)$$

where it was recognised in the early time case⁹¹ that $|k| = k$, and $\psi(z)$ is the digamma function. In addition,

$$\frac{\partial^2 I_2}{\partial k^2} \Big|_{k=0} = \frac{\pi^2}{3}. \quad (5.69)$$

Inputting Eq.(5.68) and Eq.(5.69) into Eq.(5.67), yields⁹²

$$s^2(t)|_{t \ll \beta} = \frac{t^2}{6\tilde{r}_0^4 \sqrt{\lambda}} \left[\tilde{r}_0^2 + 6(1 - \tilde{r}_0^2) \left(2 \ln(\tilde{r}_0) - \pi \cot\left(\frac{\pi}{\tilde{r}_0}\right) + \psi\left(1 + \frac{1}{\tilde{r}_0}\right) + \psi\left(1 - \frac{1}{\tilde{r}_0}\right) \right) \right]. \quad (5.70)$$

The limit of small or large virtuality can now be considered.

(i) **Small Virtuality Limit** ($\tilde{r}_0 \rightarrow 1 + \epsilon$)

Using Mathematica to take the limit of Eq.(5.70) as $\tilde{r}_0 \rightarrow 1 + \epsilon$, yields

$$s^2(t)|_{t \ll \beta} \xrightarrow{(\tilde{r}_0 \rightarrow 1 + \epsilon)} \frac{t^2}{6\sqrt{\lambda}} + \mathcal{O}(\epsilon). \quad (5.71)$$

This agrees exactly with Eq.(5.59), i.e. taking the early time limit followed by the small virtuality limit is equivalent to taking small virtuality limit followed by the early time limit – a necessary consistency check.

(ii) **Large Virtuality Limit** ($\tilde{r}_0 \rightarrow \infty$)

Since $\tilde{r}_0 \gg 0$, define a variable $y = 1/\tilde{r}_0$ (where $y \ll 0$) so that a Taylor expansion in y can be performed. Rewriting Eq.(5.70) in terms of y and performing a series expansion (around $y = 0$) in Mathematica, yields

$$s^2(t)|_{t \ll \beta} \xrightarrow{(\tilde{r}_0 \rightarrow \infty)} \frac{t^2}{\tilde{r}_0 \sqrt{\lambda}} + \mathcal{O}\left(\frac{1}{\tilde{r}_0}\right)^2. \quad (5.72)$$

As expected, the large virtuality early time behaviour corresponds exactly with the early time limit of the on-mass-shell heavy quark (i.e. the static string solution at early times, Eq.(4.121)).

⁹¹For the physically relevant solution $t \geq 0$, the early time limit $t \ll \beta$ implies $\beta > 0$. Hence, $k = t/\beta \geq 0$, and $|k| = k$.

⁹²Eq.(5.70) agrees with Eq.(3.42) in Moerman *et al.*'s [52] if the the digamma function is rewritten in terms of the harmonic numbers. Specifically, $\psi(n) = H_{(n-1)} - \gamma_E$, where γ_E is the Euler-Mascheroni constant and n is a positive integer. It is worth remarking that this form was avoid here since $(1 + \frac{1}{\tilde{r}_0})$ and $(1 - \frac{1}{\tilde{r}_0})$ are not necessarily positive integers.

(II) Asymptotic Late Time Dynamics

The behaviour of $s^2(t)$, Eq.(5.47), at asymptotically late times is considered. Defining two dimensionless quantities

$$u := \frac{\beta}{t} = \frac{1}{k} \quad \text{and} \quad z := \omega t, \quad (5.73)$$

the late time dynamics of $s^2(t)$ can be examined. At asymptotically late times $t \gg \beta$, or equivalently $u \ll 1$. The integral Eq.(5.47) can then be rewritten

$$s^2(t) = \frac{\beta^2}{4\pi^2\sqrt{\lambda}} \int_0^\infty \frac{dz}{z} \frac{1}{e^{zu} - 1} |f_{z/t}(\sigma_f - \beta/u) - f_{z/t}(\sigma_f)e^{iz}|^2. \quad (5.74)$$

Using Eqs.(4.83, 4.85, 4.90) to simplify the integrand, yields

$$\begin{aligned} & |f_{z/t}(\sigma_f - \beta/u) - f_{z/t}(\sigma_f)e^{iz}|^2 \\ &= (f_{z/t}(\sigma_f - \beta/u) - f_{z/t}(\sigma_f)e^{iz}) \left(f_{z/t}^*(\sigma_f - \beta/u) - f_{z/t}^*(\sigma_f)e^{iz} \right) \\ &= f_{z/t}(\sigma_f - \beta/u) f_{z/t}^*(\sigma_f - \beta/u) - f_{z/t}(\sigma_f - \beta/u) f_{z/t}^*(\sigma_f)e^{-iz} - f_{z/t}(\sigma_f) f_{z/t}^*(\sigma_f - \beta/u) e^{iz} \\ &\quad + f_{z/t}(\sigma_f) f_{z/t}^*(\sigma_f) \\ &\stackrel{(u \ll 1)}{\longrightarrow} 4 \sin^2(\omega t) + \mathcal{O}(\beta/t), \end{aligned} \quad (5.75)$$

where the final line is written in terms of ω , β and t using Eq.(5.73). Further, it has also been recognised that at asymptotically late times the test string's falling endpoint is in the near-horizon region, therefore $r \approx r_H$. Substituting Eq.(5.75) into Eq.(5.74), yields

$$s^2(t)|_{t \gg \beta} = \frac{\beta^2}{\pi^2\sqrt{\lambda}} \int_0^\infty \frac{d\omega}{\omega} \frac{1}{e^{\beta\omega} - 1} \sin^2(\omega t) \equiv s_{\text{small}}^2(t). \quad (5.76)$$

Therefore, the late time dynamics of an arbitrary virtuality light quark in a thermal plasma is diffusive $s_{\text{small}}^2(t) \sim t$, and the diffusion coefficient is given by Eq.(5.61). This statement can be made due to a key insight of Moerman *et al.* [52] – that the integral in Eq.(5.76) is identical to $s_{\text{small}}^2(t)$, the string falling endpoint's mean-squared transverse displacement in the limit of small virtualities (see subsection (5.2.2.1)). This allows them to conclude that the behaviour of arbitrary virtuality quarks at asymptotically late times (i.e. in the near-horizon region) is encoded in the small virtuality case. This is intuitive, since the length of the Limp Noodle is arbitrarily short at asymptotically late times⁹³. Since $s_{\text{small}}^2(t; d)$ can be solved for any dimensions $d \geq 3$ in AdS_d -Schwarzschild, the late time behaviour (and therefore the diffusion coefficient) of Limp Noodles with arbitrary length (equivalently, light quarks of arbitrary virtuality) in any number of transverse spatial dimensions are able to be determined. This generalisation to AdS_d -Schwarzschild is presented in the following subsection.

5.3 Generalising to AdS_d -Schwarzschild

To determine $s_{\text{small}}^2(t; d)$ the AdS_d -Schwarzschild metric (Eq.(4.33)) is examined in the near-horizon limit⁹⁴, which surmounts to letting $r = (1 + \tilde{\epsilon})r_H$, where $(0 < \epsilon \leq \tilde{\epsilon} \ll 1)$ and series expanding each term individually around $\tilde{\epsilon} = 0$.

⁹³Comparing Eq.(5.50) with Eq.(A.56) the limit of small virtualities appears to be equivalent to the near-horizon limit.

⁹⁴As discussed in subsection (2.1), ‘dropping the 1’ from the function $H(r)$ in the $\text{AdS}_d \times S^d$ metric corresponds to being in the near-horizon region (or in the ‘deep-throat’) of $\text{AdS}_d \times S^d$ spacetime – see figure (1), page 5. Here, a further limit is considered – letting $r = (1 + \tilde{\epsilon})r_H$ and studying the near-horizon geometry of the black-brane metric – which is the near-horizon limit referred to in this subsection.

Setting $r = (1 + \tilde{\epsilon})r_H$, the AdS_d-Schwarzschild metric Eq.(4.33) becomes

$$ds_d^2 = \frac{r_H^2}{l^2} (1 + \tilde{\epsilon})^2 d\vec{X}_I^2 - \frac{r_H^2}{l^2} (1 + \tilde{\epsilon})^2 \left(1 - \left(\frac{1}{1 + \tilde{\epsilon}} \right)^{d-1} \right) dt^2 + \frac{l^2}{(1 + \tilde{\epsilon})^2} \frac{1}{1 - (1/(1 + \tilde{\epsilon}))^{d-1}} d\tilde{\epsilon}^2, \quad (5.77)$$

where each term is now able to be expanded in $\tilde{\epsilon}$ (around $\tilde{\epsilon} = 0$). Specifically⁹⁵,

$$\frac{r_H^2}{l^2} (1 + \tilde{\epsilon})^2 d\vec{X}_I^2 = \left(\frac{r_H^2}{l^2} + \frac{2r_H^2 \tilde{\epsilon}}{l^2} + \frac{r_H^2 \tilde{\epsilon}^2}{l^2} \right) d\vec{X}_I^2, \quad (5.78)$$

$$\frac{r_H^2}{l^2} (1 + \tilde{\epsilon})^2 \left(1 - \left(\frac{1}{1 + \tilde{\epsilon}} \right)^{d-1} \right) dt^2 \rightarrow \left(-\frac{(d-1)r_H^2 \tilde{\epsilon}}{l^2} + \frac{(d^2 - 5d + 4)r_H^2 \tilde{\epsilon}^2}{2l^2} + \mathcal{O}(\tilde{\epsilon})^3 \right) dt^2, \quad (5.79)$$

$$\frac{l^2}{(1 + \tilde{\epsilon})^2} \frac{1}{1 - (1/(1 + \tilde{\epsilon}))^{d-1}} d\tilde{\epsilon}^2 \rightarrow \left(\frac{l^2}{(d-1)\tilde{\epsilon}} + \frac{(d-4)l^2}{2(d-1)} + \frac{(d^2 - 14d + 36)l^2 \tilde{\epsilon}}{12(d-1)} + \mathcal{O}(\tilde{\epsilon})^2 \right) d\tilde{\epsilon}^2. \quad (5.80)$$

The question now arises as how to truncate the series expansions (Eqs.(5.78)-(5.80)), such that the dt^2 , $d\vec{X}_I^2$ and $d\tilde{\epsilon}^2$ terms in the metric are all to the same $\mathcal{O}(\tilde{\epsilon})$. To help clarify this task of consistent truncation, there are actually only two options available:

(i) assume $dt^2 \sim \mathcal{O}(\tilde{\epsilon})^0$ and $d\vec{X}_I^2 \sim \mathcal{O}(\tilde{\epsilon})^0$, such that the AdS_d-Schwarzschild metric becomes

$$ds_d^2 = \left(\frac{r_H^2}{l^2} + \frac{2r_H^2 \tilde{\epsilon}}{l^2} \right) d\vec{X}_I^2 - \frac{(d-1)r_H^2 \tilde{\epsilon}}{l^2} dt^2 + \frac{l^2}{(d-1)\tilde{\epsilon}} d\tilde{\epsilon}^2 + \mathcal{O}(\tilde{\epsilon})^2, \quad (5.81)$$

(ii) or, assume $dt^2 \sim \mathcal{O}(\tilde{\epsilon})^0$ and $d\vec{X}_I^2 \sim \mathcal{O}(\tilde{\epsilon})$, such that the AdS_d-Schwarzschild metric becomes

$$ds_d^2 = \frac{r_H^2}{l^2} d\vec{X}_I^2 - \frac{(d-1)r_H^2 \tilde{\epsilon}}{l^2} dt^2 + \frac{l^2}{(d-1)\tilde{\epsilon}} d\tilde{\epsilon}^2 + \mathcal{O}(\tilde{\epsilon})^2. \quad (5.82)$$

These are the only options, since if higher order terms in the dt^2 or $d\tilde{\epsilon}^2$ series are included, the different signs in Eqs.(5.79, 5.80) will result in a metric which is not conformally flat in (t, r_*) coordinates. The leading order metric includes only the first term in the $d\tilde{\epsilon}^2$ series expansion (Eq.(5.80)), therefore – to be consistent – all terms in the leading order metric must be of $\mathcal{O}(\tilde{\epsilon})$. One of the ramifications of this is that it can not be assumed that $d\vec{X}_I \sim \mathcal{O}(\tilde{\epsilon})$ (or higher) at leading order, since the $d\vec{X}_I^2$ term in the metric would then disappear.

To decide between options (i) or (ii), establish which option ensures that t , \vec{X}_I , $\tilde{\epsilon}$ are *on equal footing*, and that the dt , $d\vec{X}_I$, $d\tilde{\epsilon}$ terms scale the same way as $\tilde{\epsilon} \rightarrow \lambda \tilde{\epsilon}$. This will ensure the resulting near-horizon AdS_d-Schwarzschild metric has directions which encode transverse fluctuations⁹⁶. For option (ii), considering the scaling $\tilde{\epsilon} \rightarrow \lambda \tilde{\epsilon}$, the $d\tilde{\epsilon}^2$ term in Eq.(5.82) scales as

$$\frac{l^2}{(d-1)\tilde{\epsilon}} d\tilde{\epsilon}^2 \rightarrow \lambda \frac{l^2}{(d-1)\tilde{\epsilon}} d\tilde{\epsilon}^2.$$

Under the same transformation, in order for the dt^2 term in Eq.(5.82) to scale as

$$\frac{-(d-1)r_H^2 \tilde{\epsilon}}{l^2} dt^2 \rightarrow \lambda \frac{-(d-1)r_H^2 \tilde{\epsilon}}{l^2} dt^2,$$

⁹⁵In Eq.(5.79), all terms greater than $\mathcal{O}(\tilde{\epsilon})^2$ disappear when $d = 3$.

⁹⁶It is clear that the near-horizon AdS_d-Schwarzschild metric needs to have transverse directions since these are present in the near-horizon AdS₃-Schwarzschild metric (which was found directly from inverting the tortoise coordinate in $d = 3$, and calculating the transverse string equations of motion without series expanding the parameters – see subsection (5.2)).

the temporal variable needs to scale like $t \rightarrow t$. Similarly, in order for the $d\vec{X}_I^2$ term in Eq.(5.82) to scale as

$$\frac{r_H^2}{l^2} d\vec{X}_I^2 \rightarrow \lambda \frac{r_H^2}{l^2} d\vec{X}_I^2,$$

the transverse variable needs to scale like $\vec{X}_I \rightarrow \sqrt{\lambda} \vec{X}_I$ ⁹⁷. A consistent way to transform t and \vec{X}_I , such that the dt , $d\vec{X}_I$, $d\tilde{\epsilon}$ terms in the AdS_d -Schwarzschild metric scale the same way under the transformation $\tilde{\epsilon} \rightarrow \lambda \tilde{\epsilon}$, can not be found for option (i). This strongly suggests that option (ii) is the correct way to truncate the near-horizon AdS_d -Schwarzschild metric.

Intuitive arguments aside, a rigorous mathematical approach to proving $dt^2 \sim \mathcal{O}(\tilde{\epsilon})^0$ and $d\vec{X}_I^2 \sim \mathcal{O}(\tilde{\epsilon})$ can be applied in the $d = 3$ case. Since in AdS_3 -Schwarzschild the tortoise coordinate is invertible, the transverse string equations of motion and its solution can be exactly found. The equations of motion and its solution can be series expanded in $\tilde{\epsilon}$ in the near-horizon region. Order by order these should match with the equations of motion and its solution derived from the near-horizon AdS_3 -Schwarzschild (found by expanding the metric in $\tilde{\epsilon}$ and assuming $dt^2 \sim \mathcal{O}(\tilde{\epsilon})^0$ and $dx^2 \sim \mathcal{O}(\tilde{\epsilon})$)⁹⁸. If this method of matching terms proves to be consistent, the order of $\tilde{\epsilon}$ of the temporal and transverse directions will be known, and this remains true for a general number of dimensions, d . The near-horizon AdS_d -Schwarzschild metric will, therefore, also be correctly known. The remainder of the subsection will follow the standard method of finding the equations of motion for the transverse fluctuations, its solution, the string falling endpoint's mean-squared transverse displacement $s^2(t)$, and – finally – the diffusion coefficient for the light quark in AdS_d -Schwarzschild.

5.3.1 Expanding the AdS_3 -Schwarzschild Transverse Equations of Motion and its Solution in the Near-Horizon Region

The AdS_3 -Schwarzschild metric, the resulting transverse equation of motion, and its solution are given by Eqs.(4.41, 4.74, 4.76) respectively⁹⁹. In the near-horizon region (which corresponds to setting $r = (1 + \tilde{\epsilon})r_H$), Eq.(4.41) becomes

$$ds_3^2 = -\frac{r_H^2}{l^2} \tilde{\epsilon} (2 + \tilde{\epsilon}) dt^2 + \frac{r_H^2}{l^2} (1 + \tilde{\epsilon}^2) dx^2 + \frac{l^2}{\tilde{\epsilon} (2 + \tilde{\epsilon})} d\tilde{\epsilon}^2, \quad (5.83)$$

which is equivalent to Eq.(5.77) when $d = 3$; Eq.(4.74) becomes

$$\begin{aligned} 0 &= -\partial_t^2 X(t, \tilde{\epsilon}) + \frac{r_H^2}{l^4} \frac{\tilde{\epsilon} (2 + \tilde{\epsilon})}{(1 + \tilde{\epsilon})^2} \partial_{\tilde{\epsilon}} (\tilde{\epsilon} (1 + \tilde{\epsilon})^2 (2 + \tilde{\epsilon}) \partial_{\tilde{\epsilon}} X(t, \tilde{\epsilon})) \\ &= -\partial_t^2 X_{\text{reg}}(t, \tilde{\epsilon}) + \frac{(\tilde{\epsilon} + 2)}{4l^4(\tilde{\epsilon} + 1)} \left[-l^2 \omega (l^2 \omega (\tilde{\epsilon} + 1)(\tilde{\epsilon} + 2) - 2ir_H \tilde{\epsilon} (3\tilde{\epsilon} + 5)) X_{\text{reg}}(t, \tilde{\epsilon}) \right. \\ &\quad \left. + 4r_H \tilde{\epsilon} (il^2 \omega (\tilde{\epsilon} + 1)(\tilde{\epsilon} + 2) + 4r_H \tilde{\epsilon} (\tilde{\epsilon} + 2) + 2r_H) \partial_{\tilde{\epsilon}} X_{\text{reg}}(t, \tilde{\epsilon}) + 4r_H^2 \tilde{\epsilon}^2 (\tilde{\epsilon} + 1)(\tilde{\epsilon} + 2) \partial_{\tilde{\epsilon}}^2 X_{\text{reg}}(t, \tilde{\epsilon}) \right], \end{aligned} \quad (5.84)$$

where $r = (1 + \tilde{\epsilon})r_H$ and $\partial_{\tilde{\epsilon}} = r_H \partial_r$ are used in the first line; and Eq.(4.76) becomes

$$X(t, \tilde{\epsilon}) = \left(\frac{\tilde{\epsilon}}{\tilde{\epsilon} + 2} \right)^{\frac{il^2 \omega}{2r_H}} \frac{il^2 \omega + r_H \tilde{\epsilon} + r_H}{(\tilde{\epsilon} + 1)(r_H + il^2 \omega)} e^{-i\omega t} =: \tilde{\epsilon}^{-\frac{il^2 \omega}{2r_H}} X_{\text{reg}}(t, \tilde{\epsilon}), \quad (5.85)$$

where $f_{\omega}(r) = f_{\omega}^{(+)}(r)$ (which is defined in Eq.(4.80)), and the regular part of the solution is given by $X_{\text{reg}}(t, \tilde{\epsilon})$. The regular equation of motion (Eq.(5.84)) can now be series expanded in $\tilde{\epsilon}$ (around $\tilde{\epsilon} = 0$).

⁹⁷Accepting that t and \vec{X}_I scale differently isn't far-fetched considering this is the near-horizon region of the black-brane.

⁹⁸This is done in detail Mathematica Notebook [c] (`NearHorizonAdSd.nb`) – see appendix (A.7) for access.

⁹⁹The full solution to the transverse equation of motion is given by Eq.(4.85), where the constant B_{ω} is defined in Eq.(4.90) and the modes $f_{\omega}^{(\pm)}(r)$ are given in Eq.(4.80). The linearly independent solutions $f_{\omega}^{(+)}(r)$ or $f_{\omega}^{(-)}(r)$ are sufficient to work with; since, if an ODE is solved by $f_{\omega}^{(+)}(r)$ or $f_{\omega}^{(-)}(r)$, it will also be solved by the superposition of those solutions, $f_{\omega}(r)$. Therefore, in order to simplify the algebra, take $f_{\omega}(r) = f_{\omega}^{(+)}(r)$ (equivalently $f_{\omega}(r) = f_{\omega}^{(-)}(r)$ could have been chosen).

However, in order to perform this expansion, an ansatz for the expansion of $X_{\text{reg}}(t, \tilde{\epsilon})$ is required. Up to $\mathcal{O}(\tilde{\epsilon})^2$, the simple ansatz $X_{\text{reg}}(t, \tilde{\epsilon}) = x_0(t) + \tilde{\epsilon} x_1(t) + \tilde{\epsilon}^2 x_2(t)$ can be used. The regular equation of motion then becomes

$$0 = (-x_0''(t) - \omega^2 x_0(t)) + \tilde{\epsilon} \left(\frac{\omega(-l^2\omega + 5ir_H)}{l^2} x_0(t) + \frac{(2r_H + il^2\omega)^2}{l^4} x_1(t) - x_1''(t) \right) + \tilde{\epsilon}^2 \left(-\frac{\omega(l^2\omega - 2ir_H)}{4l^2} x_0(t) + \frac{(-l^4\omega^2 + 9il^2r_H\omega + 14r_H^2)}{l^4} x_1(t) + \frac{(4r_H + il^2\omega)^2}{l^4} x_2(t) - x_2''(t) \right) + \mathcal{O}(\tilde{\epsilon})^3, \quad (5.86)$$

where $x''(t) = d^2x/dt^2$. Series expanding the regular part of the solution (Eq.(5.85)) in $\tilde{\epsilon}$ (around $\tilde{\epsilon} = 0$), yields

$$X_{\text{reg}}(t, \tilde{\epsilon}) = e^{-it\omega} 2^{-\frac{il^2\omega}{2r_H}} \left(1 - \frac{il^2\omega(l^2\omega - 5ir_H)}{4r_H(l^2\omega - ir_H)} \tilde{\epsilon} - \frac{l^2\omega(l^4\omega^2 - 11il^2r_H\omega - 34r_H^2)}{32r_H^2(l^2\omega - ir_H)} \tilde{\epsilon}^2 + \mathcal{O}(\tilde{\epsilon})^3 \right) \\ =: x_0(t) + \tilde{\epsilon} x_1(t) + \tilde{\epsilon}^2 x_2(t) + \mathcal{O}(\tilde{\epsilon})^3. \quad (5.87)$$

As a consistency check, notice that the solution Eq.(5.87) solves the transverse equation of motion Eq.(5.86) at each respective order of $\tilde{\epsilon}$.

5.3.2 Expanding the AdS₃-Schwarzschild Metric in the Near-Horizon Region

The transverse equation of motion and its solution which have been derived from the AdS₃-Schwarzschild metric and then series expanded to yield the near-horizon limit (Eqs.(5.86, 5.87)) should match exactly with the transverse equation of motion and its solution derived from the series expanded, near-horizon AdS₃-Schwarzschild metric. Going on physical intuition, it seems like a good starting point would be to assume $dt^2 \sim \mathcal{O}(\tilde{\epsilon})^0$ and $dx^2 \sim \mathcal{O}(\tilde{\epsilon})$ and check if the transverse equation of motion and its solution derived from expanding this metric in the near-horizon limit match with those found in the previous subsection. To this end, assuming $dt^2 \sim \mathcal{O}(\tilde{\epsilon})^0$ and $dx^2 \sim \mathcal{O}(\tilde{\epsilon})$ results in an AdS₃-Schwarzschild metric

$$ds_3^2 = \frac{r_H^2}{l^2} dx^2 - \frac{2r_H^2\tilde{\epsilon}}{l^2} dt^2 + \frac{l^2}{2\tilde{\epsilon}} d\tilde{\epsilon}^2 + \mathcal{O}(\tilde{\epsilon})^2, \quad (5.88)$$

where Eq.(5.82) for $d = 3$ has been used. The near-horizon tortoise coordinate, defined by setting $r = (1 + \tilde{\epsilon})r_H$ in the definition of the tortoise coordinate Eq.(4.38), can also be expanded and truncated around $\tilde{\epsilon} = 0$. To leading order it is sufficient to take¹⁰⁰

$$\tilde{\epsilon}_* := \frac{l^2}{2r_H^2} \ln(\tilde{\epsilon}), \quad (5.89)$$

where $r_* = r_H \tilde{\epsilon}_*$, and the number of dimensions $d = 3$ has been set posthumously. Barring an integration constant of $\mathcal{O}(\tilde{\epsilon})^0$ (specifically $-l^2/(2r_H) \ln(2)$), Eq.(5.89) agrees with expanding and truncating Eq.(4.39) after setting $r = (1 + \tilde{\epsilon})r_H$ ¹⁰¹. Inverting and calculating the differential yields

$$\tilde{\epsilon} = e^{\frac{2r_H^2}{l^2} \tilde{\epsilon}_*}, \quad \text{and} \quad d\tilde{\epsilon} = \frac{2r_H^2}{l^2} e^{\frac{2r_H^2}{l^2} \tilde{\epsilon}_*} d\tilde{\epsilon}_*. \quad (5.90)$$

Eqs.(5.89, 5.90) are used to transform the expanded and truncated metric into $(t, \tilde{\epsilon}_*)$ coordinates. The metric Eq.(5.88) becomes

$$ds_3^2 = 2 \frac{r_H^2}{l^2} e^{\frac{2r_H^2}{l^2} \tilde{\epsilon}_*} (-dt^2 + r_H^2 d\tilde{\epsilon}_*^2) + \frac{r_H^2}{l^2} dx^2 \\ = 2 \frac{r_H^2}{l^2} e^{\frac{2r_H r_*}{l^2}} (-dt^2 + dr_*^2) + \frac{r_H^2}{l^2} dx^2, \quad (5.91)$$

¹⁰⁰It's proven that the leading order tortoise coordinate is given by Eq.(5.89) in appendix (A.6).

¹⁰¹See Mathematica Notebook [c] (`NearHorizonAdSd.nb`) for details: access in appendix (A.7).

where the final line is a conformally flat description of near-horizon AdS₃-Schwarzschild in (t, r_*) coordinates. It follows from the near-horizon definition $r = (1 + \tilde{\epsilon})r_H$, and Eqs.(5.89, 5.90) that

$$r = r_H \left(1 + e^{\frac{2r_H r_*}{l^2}} \right), \quad \text{and} \quad r_* = \frac{l^2}{2r_H} \ln \left(\frac{r}{r_H} - 1 \right). \quad (5.92)$$

As discussed in subsection (5.1.3), in the conformally flat (t, r_*) coordinate system the boundary conditions for the Limp Noodle in AdS₃-Schwarzschild are given by Eqs.(4.46, 4.48), which are respectively analogous to the boundary conditions for the Limp Noodle in \mathbb{R}^{1+1} , Eqs.(4.25, 4.26). Hence, the leading order solution for the Limp Noodle in AdS₃-Schwarzschild in conformal (t, r_*) coordinates can be written down (Eq.(5.39)). Converting then to (t, r) coordinates, the string solution for the $d = 3$ Limp Noodle in the near-horizon limit at leading order is given by

$$X_{\text{AdS}_3\text{-Sch}}^\mu(t, \sigma) = \left(t, \left\{ \begin{array}{ll} r_H \left(1 + e^{\frac{2r_H}{l^2} (r_{s*} + \sigma)} \right), & \text{if } (t, \sigma) \in \mathcal{M}_1 \\ r_H \left(1 + e^{\frac{2r_H}{l^2} (r_{s*} + \sigma_f - t)} \right), & \text{if } (t, \sigma) \in \mathcal{M}_2 \end{array} \right\}, 0 \right)^\mu, \quad (5.93)$$

where Eq.(5.92) is used. The position of the fixed string endpoint attached to the stretched horizon is given by

$$r_{s*} = \frac{l^2}{2r_H} \ln \left(\frac{r_s}{r_H} - 1 \right) \quad \text{or, equivalently} \quad \tilde{\epsilon}_{s*} = \frac{l^2}{2r_H^2} \ln(\epsilon), \quad (5.94)$$

since the stretched horizon is defined as $r_s = (1 + \epsilon)r_H$, where $0 < \epsilon \leq \tilde{\epsilon} \ll 1$. The length of the string in tortoise coordinates is given by

$$\sigma_f = \frac{l^2}{2r_H} \ln \left(\frac{r_s + \ell_0}{r_H} - 1 \right) - r_{s*} \quad \text{or, equivalently} \quad \sigma_f = \frac{l^2}{2r_H} \ln \left(\epsilon + \frac{\ell_0}{r_H} \right) - r_H \tilde{\epsilon}_{s*}, \quad (5.95)$$

and the \mathcal{M}_1 and \mathcal{M}_2 parameter space regions are still given by Eq.(5.33). Using the definition of the near-horizon limit ($r = (1 + \tilde{\epsilon})r_H$) and $r_* = r_H \tilde{\epsilon}_{s*}$, the leading order string solution Eq.(5.93) can be converted into $(t, \tilde{\epsilon})$ coordinates. Specifically,

$$X_{\text{AdS}_3\text{-Sch}}^\mu(t, \sigma) = \left(t, \left\{ \begin{array}{ll} e^{\frac{2r_H}{l^2} (r_H \tilde{\epsilon}_{s*} + \sigma)}, & \text{if } (t, \sigma) \in \mathcal{M}_1 \\ e^{\frac{2r_H}{l^2} (r_H \tilde{\epsilon}_{s*} + \sigma_f - t)}, & \text{if } (t, \sigma) \in \mathcal{M}_2 \end{array} \right\}, 0 \right)^\mu. \quad (5.96)$$

Therefore, the identification $\tilde{\epsilon} = e^{\frac{2r_H}{l^2} (r_H \tilde{\epsilon}_{s*} + \sigma)}$ is made. The equation of motion for the transverse fluctuations in the near-horizon limit of AdS₃-Schwarzschild can be derived from Eq.(4.69),

$$\begin{aligned} 0 &= \partial_a \left(-\frac{1}{2\pi\alpha'} (\sqrt{-g} g^{ab} G_{IJ}) \Big|_{X_0^\mu} \partial_b X^J \right) \\ &= \partial_a \left(\left(\sqrt{-g} g^{ab} \frac{r_H^2}{l^2} \right) \Big|_{X_0^\mu} \partial_b X(t, \tilde{\epsilon}) \right), \end{aligned} \quad (5.97)$$

where the spacetime metric in the near-horizon limit $G_{\mu\nu}$ is given explicitly by

$$G_{\mu\nu} = \begin{bmatrix} -\frac{2r_H^2 \tilde{\epsilon}}{l^2} & 0 & 0 \\ 0 & \frac{l^2}{2\tilde{\epsilon}} & 0 \\ 0 & 0 & \frac{r_H^2}{l^2} \end{bmatrix}, \quad (5.98)$$

where μ, ν index over the directions $(t, \tilde{\epsilon}, x)$. The explicit entries of the induced worldsheet metric are calculated from Eq.(4.2)¹⁰². In the near-horizon limit, for $d = 3$, the leading order induced metric in $(t, \tilde{\epsilon})$ coordinates is given by

$$g_{ab}|_{X_0^\mu} := \left[\begin{array}{cc} g_{tt} & g_{t\sigma} \\ g_{\sigma t} & g_{\sigma\sigma} \end{array} \right] \Big|_{X_0^\mu} = \left[\begin{array}{cc} G_{tt} & 0 \\ 0 & \tilde{\epsilon}'^2 G_{\tilde{\epsilon}\tilde{\epsilon}} \end{array} \right] = \left[\begin{array}{cc} -\frac{2r_H^2 \tilde{\epsilon}}{l^2} & 0 \\ 0 & \tilde{\epsilon}'^2 \frac{l^2}{2\tilde{\epsilon}} \end{array} \right], \quad (5.99)$$

where Eq.(5.98) is used, and $\tilde{\epsilon}' = \partial_\sigma \tilde{\epsilon}$. Hence, its inverse is given by

$$g^{ab}|_{X_0^\mu} := \left[\begin{array}{cc} g^{tt} & g^{t\sigma} \\ g^{\sigma t} & g^{\sigma\sigma} \end{array} \right] \Big|_{X_0^\mu} = \frac{1}{\det(g_{ab}|_{X_0^\mu})} \left[\begin{array}{cc} \tilde{\epsilon}'^2 G_{\tilde{\epsilon}\tilde{\epsilon}} & 0 \\ 0 & G_{tt} \end{array} \right] = \left[\begin{array}{cc} -\frac{l^2}{2r_H^2 \tilde{\epsilon}} & 0 \\ 0 & \frac{2\tilde{\epsilon}}{l^2 \tilde{\epsilon}'^2} \end{array} \right], \quad (5.100)$$

where $\det(g_{ab}|_{X_0^\mu})$ is calculated from Eq.(5.99),

$$g|_{X_0^\mu} \equiv \det(g_{ab}|_{X_0^\mu}) = \tilde{\epsilon}'^2 G_{\tilde{\epsilon}\tilde{\epsilon}} G_{tt} = \left(\tilde{\epsilon}'^2 \frac{l^2}{2\tilde{\epsilon}} \right) \left(-\frac{2r_H^2}{l^2} \tilde{\epsilon} \right) = -r_H^2 \tilde{\epsilon}'^2. \quad (5.101)$$

Expanding the indices of Eq.(5.97) using Eqs.(5.99)-(5.101), the transverse equation of motion become

$$\begin{aligned} 0 &= \partial_\sigma \left(\left(\sqrt{-g} g^{\sigma\sigma} \frac{r_H^2}{l^2} \right) \Big|_{X_0^\mu} \partial_\sigma X(t, \sigma) \right) + \partial_t \left(\left(\sqrt{-g} g^{tt} \frac{r_H^2}{l^2} \right) \Big|_{X_0^\mu} \partial_t X(t, \sigma) \right) \\ &= \partial_\sigma \left(r_H \tilde{\epsilon}' \left(\frac{2\tilde{\epsilon}}{l^2 \tilde{\epsilon}'^2} \right) \frac{r_H^2}{l^2} \partial_\sigma X(t, \sigma) \right) + \partial_t \left(r_H \tilde{\epsilon}' \left(-\frac{l^2}{2r_H^2 \tilde{\epsilon}} \right) \frac{r_H^2}{l^2} \partial_t X(t, \sigma) \right) \\ &= -\partial_t^2 X(t, \sigma) + \frac{4r_H^2}{l^4} \tilde{\epsilon} \frac{1}{\partial_\sigma \tilde{\epsilon}} \partial_\sigma \left(\frac{1}{\partial_\sigma \tilde{\epsilon}} \tilde{\epsilon} \partial_\sigma X(t, \sigma) \right) \\ &= -\partial_t^2 X(t, \tilde{\epsilon}) + \frac{4r_H^2}{l^4} \tilde{\epsilon} \partial_{\tilde{\epsilon}} (\tilde{\epsilon} \partial_{\tilde{\epsilon}} X(t, \tilde{\epsilon})). \end{aligned} \quad (5.102)$$

where the last line is written completely in terms of near-horizon spacetime coordinates $(t, \tilde{\epsilon})$ by differentiating the identification $\tilde{\epsilon} = e^{\frac{2r_H}{l^2} (r_H \tilde{\epsilon}_{s*} + \sigma)}$,

$$\begin{aligned} d\tilde{\epsilon} &= 2 \frac{r_H}{l^2} e^{2\frac{r_H}{l^2} (r_H \tilde{\epsilon}_{s*} + \sigma)} d\sigma \\ \Rightarrow \partial_\sigma &= 2 \frac{r_H}{l^2} e^{2\frac{r_H}{l^2} (r_H \tilde{\epsilon}_{s*} + \sigma)} \partial_{\tilde{\epsilon}} \\ \Rightarrow \partial_\sigma &= 2 \frac{r_H}{l^2} \tilde{\epsilon} \partial_{\tilde{\epsilon}}. \end{aligned} \quad (5.103)$$

In terms of $X_{\text{reg}}(t, \tilde{\epsilon})$ the equation of motion is given by

$$0 = -\partial_t^2 X_{\text{reg}}(t, \tilde{\epsilon}) + \frac{4r_H \tilde{\epsilon} (r_H \tilde{\epsilon} \partial_{\tilde{\epsilon}}^2 X_{\text{reg}}(t, \tilde{\epsilon}) + (r_H + il^2 \omega) \partial_{\tilde{\epsilon}} X_{\text{reg}}(t, \tilde{\epsilon}))}{l^4} - \omega^2 X_{\text{reg}}(t, \tilde{\epsilon}), \quad (5.104)$$

where the definition of the regular solution in Eq.(5.85) has been used. In order to check whether, at leading order, the regular equation of motion agrees with the series expanded regular equation of motion (Eq.(5.86)), the leading order ansatz $X_{\text{reg}}(t, \tilde{\epsilon}) = x_0(t)$ should be used. The leading order contribution to Eq.(5.104) then becomes

¹⁰²This calculation is similar to Eq.(A.34) where the induced metric is calculated explicitly in (t, r) coordinates (see appendix (A.3)).

$$0 = -x_0''(t) - \omega^2 x_0(t), \quad (5.105)$$

which agrees exactly with the leading order contribution of Eq.(5.86). This proves that the expanded near-horizon metric is equivalent to the near-horizon metric at leading order in AdS₃-Schwarzschild. The expanded near-horizon metric given in Eq.(5.88) is therefore correct, and $dt^2 \sim \mathcal{O}(\tilde{\epsilon})^0$ and $dx^2 \sim \mathcal{O}(\tilde{\epsilon})$. As a final check, the calculations in this subsection are repeated assuming $dt^2 \sim \mathcal{O}(\tilde{\epsilon})^0$ and $dx^2 \sim \mathcal{O}(\tilde{\epsilon})^0$. The equation of motion found is,

$$\begin{aligned} 0 &= -\partial_t^2 X(t, \tilde{\epsilon}) + \frac{4r_H^2}{l^4} \frac{\tilde{\epsilon}}{(1+2\tilde{\epsilon})} \partial_{\tilde{\epsilon}}(\tilde{\epsilon}(1+2\tilde{\epsilon}) \partial_{\tilde{\epsilon}} X(t, \tilde{\epsilon})) \\ &= -\partial_t^2 X_{\text{reg}}(t, \tilde{\epsilon}) + \frac{4r_H^2}{l^4} \tilde{\epsilon}^2 \partial_{\tilde{\epsilon}}^2 X_{\text{reg}}(t, \tilde{\epsilon}) + \frac{4r_H \tilde{\epsilon} \partial_{\tilde{\epsilon}} X_{\text{reg}}(t, \tilde{\epsilon}) (il^2 \omega(2\tilde{\epsilon}+1) + 4r_H \tilde{\epsilon} + r_H)}{l^4(2\tilde{\epsilon}+1)} \\ &\quad - \frac{\omega X_{\text{reg}}(t, \tilde{\epsilon}) (l^2 \omega(2\tilde{\epsilon}+1) - 4ir_H \tilde{\epsilon})}{l^2(2\tilde{\epsilon}+1)} \\ &\xrightarrow{LO} -x_0''(t) + \left(-\omega + \frac{4ir_H}{l^2} \frac{\tilde{\epsilon}}{(2\tilde{\epsilon}+1)} \right) \omega x_0(t), \end{aligned} \quad (5.106)$$

which does not match the leading order contribution of Eq.(5.86).

5.3.3 The Diffusion Constant in AdS_d-Schwarzschild

In the previous two subsections it was proven that in order for a near-horizon expansion of the metric to be consistent, the leading order metric is taken to $\mathcal{O}(\tilde{\epsilon})$ – where $dt^2 \sim \mathcal{O}(\tilde{\epsilon})^0$ and $dx^2 \sim \mathcal{O}(\tilde{\epsilon})$ (equivalently $t \sim \mathcal{O}(\tilde{\epsilon})^0$ and $x \sim \mathcal{O}(\sqrt{\tilde{\epsilon}})$). Generalising to d dimensions this holds true, where X_I (instead of x) denotes the transverse directions in AdS_d-Schwarzschild. Hence the leading order, near-horizon AdS_d-Schwarzschild metric is given by Eq.(5.82).

From the near-horizon metric, which is conformal in (t, r_*) coordinates, the leading order string solution followed by the transverse equations of motion can be found. A similar method to subsection (5.3.2) is followed. The near-horizon tortoise coordinate, defined by setting $r = (1 + \tilde{\epsilon})r_H$ in the definition of the tortoise coordinate Eq.(4.38), can be expanded and truncated around $\tilde{\epsilon} = 0$. To leading order it is sufficient to take¹⁰³

$$\tilde{\epsilon}_* := \frac{l^2}{r_H^2} \frac{\ln(\tilde{\epsilon})}{(d-1)}, \quad (5.107)$$

where $r_* = r_H \tilde{\epsilon}_*$. Inverting and calculating the differential yields

$$\tilde{\epsilon} = e^{\frac{r_H^2}{l^2} (d-1) \tilde{\epsilon}_*}, \quad \text{and} \quad d\tilde{\epsilon} = \frac{r_H^2}{l^2} (d-1) e^{\frac{r_H^2}{l^2} (d-1) \tilde{\epsilon}_*} d\tilde{\epsilon}_*. \quad (5.108)$$

The definition of the near-horizon tortoise coordinate, its inverse and differential (Eqs.(5.107, 5.108)) can be used to convert the metric Eq.(5.82) into $(t, \tilde{\epsilon}_*)$ coordinates

$$\begin{aligned} ds_d^2 &= \frac{r_H^2}{l^2} (d-1) e^{\frac{r_H^2}{l^2} (d-1) \tilde{\epsilon}_*} (-dt^2 + r_H^2 d\tilde{\epsilon}_*^2) + \frac{r_H^2}{l^2} d\vec{X}_I^2 \\ &= \frac{r_H^2}{l^2} (d-1) e^{\frac{r_H r_*}{l^2} (d-1)} (-dt^2 + dr_*^2) + \frac{r_H^2}{l^2} d\vec{X}_I^2. \end{aligned} \quad (5.109)$$

¹⁰³It's proven that the leading order tortoise coordinate is given by Eq.(5.107) in appendix (A.6).

From the final line in Eq.(5.109) notice that the metric – like the near-horizon AdS₃-Schwarzschild metric (Eq.(5.91)) – is conformal in (t, r_*) coordinates. It follows from the near-horizon definition $r = (1 + \tilde{\epsilon})r_H$, and Eqs.(5.107, 5.108) that

$$r = r_H \left(1 + e^{\frac{r_H r_*}{l^2} (d-1)} \right), \quad \text{and} \quad r_* = \frac{l^2}{(d-1)r_H} \ln \left(\frac{r}{r_H} - 1 \right), \quad (5.110)$$

which reduces down to Eq.(5.92) for $d = 3$. From the metric Eq.(5.109) the method laid out in subsection (5.1.3) can be followed in order to write down the leading order solution for the Limp Noodle in AdS_d-Schwarzschild in conformal (t, r_*) coordinates, which is given by Eq.(5.39)¹⁰⁴. Converting then to (t, r) coordinates, the string solution for the Limp Noodle in the near-horizon limit at leading order is given by

$$X_{\text{AdS}_d\text{-Sch}}^\mu(t, \sigma) = \left(t, \left\{ \begin{array}{ll} r_H \left(1 + e^{\frac{r_H}{l^2} (d-1) (r_{s*} + \sigma)} \right), & \text{if } (t, \sigma) \in \mathcal{M}_1 \\ r_H \left(1 + e^{\frac{r_H}{l^2} (d-1) (r_{s*} + \sigma_f - t)} \right), & \text{if } (t, \sigma) \in \mathcal{M}_2 \end{array} \right\}, 0 \right)^\mu, \quad (5.111)$$

where Eq.(5.110) is used¹⁰⁵. The position of the fixed string endpoint attached to the stretched horizon is given by

$$r_{s*} = \frac{l^2}{(d-1)r_H} \ln \left(\frac{r_s}{r_H} - 1 \right) \quad \text{or, equivalently} \quad \tilde{\epsilon}_{s*} = \frac{l^2}{(d-1)r_H} \ln(\epsilon), \quad (5.112)$$

since the stretched horizon is defined as $r_s = (1 + \epsilon)r_H$, where $0 < \epsilon \leq \tilde{\epsilon} \ll 1$. The length of the string in tortoise coordinates is given by

$$\sigma_f = \frac{l^2}{(d-1)r_H} \ln \left(\frac{r_s + \ell_0}{r_H} - 1 \right) - r_{s*} \quad \text{or, equivalently} \quad \sigma_f = \frac{l^2}{(d-1)r_H} \ln \left(\epsilon + \frac{\ell_0}{r_H} \right) - r_H \tilde{\epsilon}_{s*}, \quad (5.113)$$

and the \mathcal{M}_1 and \mathcal{M}_2 parameter space regions are still given by Eq.(5.33). Using the definition of the near-horizon limit ($r = (1 + \tilde{\epsilon})r_H$) and $r_* = r_H \tilde{\epsilon}_{s*}$, the leading order string solution Eq.(5.111) can be converted into $(t, \tilde{\epsilon})$ coordinates. Specifically,

$$X_{\text{AdS}_d\text{-Sch}}^\mu(t, \sigma) = \left(t, \left\{ \begin{array}{ll} e^{\frac{r_H}{l^2} (d-1) (r_H \tilde{\epsilon}_{s*} + \sigma)}, & \text{if } (t, \sigma) \in \mathcal{M}_1 \\ e^{\frac{r_H}{l^2} (d-1) (r_H \tilde{\epsilon}_{s*} + \sigma_f - t)}, & \text{if } (t, \sigma) \in \mathcal{M}_2 \end{array} \right\}, 0 \right)^\mu, \quad (5.114)$$

where $\tilde{\epsilon}_{s*}$ and σ_f are defined in Eqs.(5.112, 5.113). Therefore, the identification $\tilde{\epsilon} = e^{\frac{r_H}{l^2} (d-1) (r_H \tilde{\epsilon}_{s*} + \sigma)}$ is made. The equations of motion for the transverse fluctuations in the near-horizon limit of AdS_d-Schwarzschild can be derived from Eq.(4.66), and are equivalent to Eq.(5.97) with the generalised spacetime metric in the near-horizon limit ($G_{\mu\nu}$) given by

$$G_{\mu\nu} = \begin{bmatrix} -\frac{r_H^2}{l^2} (d-1) \tilde{\epsilon} & 0 & 0 & 0 & 0 & 0 \\ 0 & \frac{l^2}{(d-1)} \frac{1}{\tilde{\epsilon}} & 0 & 0 & 0 & 0 \\ 0 & 0 & \frac{r_H^2}{l^2} & 0 & 0 & 0 \\ 0 & 0 & 0 & \frac{r_H^2}{l^2} & \ddots & 0 \\ 0 & 0 & 0 & \ddots & \ddots & 0 \\ 0 & 0 & 0 & 0 & 0 & \frac{r_H^2}{l^2} \end{bmatrix}, \quad (5.115)$$

¹⁰⁴This equation – derived from the worldsheet parameter space partitioning of the test string in $\mathbb{R}^{1,1}$, Eq.(5.34) – is independent of d , the number of spacetime dimensions.

¹⁰⁵It will be much harder to find next-to-leading order corrections to the string solution in the near-horizon limit, since if the near-horizon metric includes higher order terms ($\mathcal{O}(\tilde{\epsilon})^2$ terms) it will no longer be conformal in (t, r_*) coordinates.

where μ, ν index over $(t, r, 2, \dots, d-1)$. The explicit entries of the induced worldsheet metric are calculated from Eq.(4.2). In the near-horizon limit, the leading order induced metric in $(t, \tilde{\epsilon})$ coordinates is given by

$$g_{ab}|_{X_0^\mu} := \begin{bmatrix} g_{tt} & g_{t\sigma} \\ g_{\sigma t} & g_{\sigma\sigma} \end{bmatrix} \Big|_{X_0^\mu} = \begin{bmatrix} G_{tt} & 0 \\ 0 & \tilde{\epsilon}'^2 G_{\tilde{\epsilon}\tilde{\epsilon}} \end{bmatrix} = \begin{bmatrix} -\frac{r_H^2}{l^2} (d-1) \tilde{\epsilon} & 0 \\ 0 & \tilde{\epsilon}'^2 \frac{l^2}{(d-1)} \frac{1}{\tilde{\epsilon}} \end{bmatrix}, \quad (5.116)$$

where Eq.(5.115) is used, and $\tilde{\epsilon}' = \partial_\sigma \tilde{\epsilon}$. Hence, its inverse is given by

$$g^{ab}|_{X_0^\mu} := \begin{bmatrix} g^{tt} & g^{t\sigma} \\ g^{\sigma t} & g^{\sigma\sigma} \end{bmatrix} \Big|_{X_0^\mu} = \frac{1}{\det(g_{ab}|_{X_0^\mu})} \begin{bmatrix} \tilde{\epsilon}'^2 G_{\tilde{\epsilon}\tilde{\epsilon}} & 0 \\ 0 & G_{tt} \end{bmatrix} = \begin{bmatrix} -\frac{l^2}{(d-1)r_H^2 \tilde{\epsilon}} & 0 \\ 0 & \frac{(d-1)\tilde{\epsilon}}{l^2 \tilde{\epsilon}'^2} \end{bmatrix}, \quad (5.117)$$

where $\det(g_{ab}|_{X_0^\mu})$ is calculated from Eq.(5.116),

$$g|_{X_0^\mu} \equiv \det(g_{ab}|_{X_0^\mu}) = \tilde{\epsilon}'^2 G_{\tilde{\epsilon}\tilde{\epsilon}} G_{tt} = \left(\tilde{\epsilon}'^2 \frac{l^2}{(d-1)} \frac{1}{\tilde{\epsilon}} \right) \left(-\frac{r_H^2}{l^2} (d-1) \tilde{\epsilon} \right) = -r_H^2 \tilde{\epsilon}'^2. \quad (5.118)$$

Expanding the indices of Eq.(5.97) using Eqs.(5.116)-(5.118), the transverse equation of motion become

$$\begin{aligned} 0 &= \partial_\sigma \left(\left(\sqrt{-g} g^{\sigma\sigma} \frac{r_H^2}{l^2} \right) \Big|_{X_0^\mu} \partial_\sigma X^I(t, \sigma) \right) + \partial_t \left(\left(\sqrt{-g} g^{tt} \frac{r_H^2}{l^2} \right) \Big|_{X_0^\mu} \partial_t X^I(t, \sigma) \right) \\ &= \partial_\sigma \left(r_H \tilde{\epsilon}' \left(\frac{(d-1)\tilde{\epsilon}}{l^2 \tilde{\epsilon}'^2} \right) \frac{r_H^2}{l^2} \partial_\sigma X^I(t, \sigma) \right) + \partial_t \left(r_H \tilde{\epsilon}' \left(-\frac{l^2}{(d-1)r_H^2} \frac{1}{\tilde{\epsilon}} \right) \frac{r_H^2}{l^2} \partial_t X^I(t, \sigma) \right) \\ &= -\partial_t^2 X^I(t, \sigma) + \frac{r_H^2}{l^4} (d-1)^2 \tilde{\epsilon} \frac{1}{\partial_\sigma \tilde{\epsilon}} \partial_\sigma \left(\frac{1}{\partial_\sigma \tilde{\epsilon}} \tilde{\epsilon} \partial_\sigma X^I(t, \sigma) \right) \\ &= -\partial_t^2 X^I(t, \tilde{\epsilon}) + \frac{r_H^2}{l^4} (d-1)^2 \tilde{\epsilon} \partial_{\tilde{\epsilon}} (\tilde{\epsilon} \partial_{\tilde{\epsilon}} X^I(t, \tilde{\epsilon})), \end{aligned} \quad (5.119)$$

where X^I denotes the transverse direction ($I \in (2, 3, \dots, d-1)$); and the last line is written completely in terms of near-horizon spacetime coordinates $(t, \tilde{\epsilon})$ by differentiating the identification $\tilde{\epsilon} = e^{\frac{r_H}{l^2} (d-1) (r_H \tilde{\epsilon}_{s*} + \sigma)}$,

$$\begin{aligned} d\tilde{\epsilon} &= (d-1) \frac{r_H}{l^2} e^{\frac{r_H}{l^2} (d-1) (r_H \tilde{\epsilon}_{s*} + \sigma)} d\sigma \\ \Rightarrow \partial_\sigma &= (d-1) \frac{r_H}{l^2} e^{\frac{r_H}{l^2} (d-1) (r_H \tilde{\epsilon}_{s*} + \sigma)} \partial_{\tilde{\epsilon}} \\ \Rightarrow \partial_\sigma &= (d-1) \frac{r_H}{l^2} \tilde{\epsilon} \partial_{\tilde{\epsilon}}. \end{aligned} \quad (5.120)$$

Eq.(5.120) can also be used to convert the equations of motion Eq.(5.119) to parameter space coordinates (t, σ) ,

$$\begin{aligned} 0 &= -\partial_t^2 X^I(t, \sigma) + \frac{r_H^2}{l^4} (d-1)^2 \tilde{\epsilon} \frac{l^2}{(d-1)r_H} \frac{1}{\tilde{\epsilon}} \partial_\sigma \left(\tilde{\epsilon} \frac{l^2}{(d-1)r_H} \frac{1}{\tilde{\epsilon}} \partial_\sigma X^I(t, \sigma) \right) \\ &= -\partial_t^2 X^I(t, \sigma) + \partial_\sigma^2 X^I(t, \sigma). \end{aligned} \quad (5.121)$$

The near-horizon string equations of motion for the transverse fluctuations on the Limp Noodle is given by wave equation. Remember that the small virtuality limit of the $d = 3$ Limp Noodle also yielded

the wave equation as the transverse equation of motion (Eq.(5.51))¹⁰⁶. Since this is true, repeating the calculations laid out in subsection (5.2.2.1) is sufficient to calculate $s^2(t; d)$. The only change is that β scales with the number of spacetime dimensions, so Eq.(5.56) needs to be adapted by adding in the appropriate dimensionally dependent factor. In order to calculate this, notice that β enters the calculation of $s_{\text{small}}^2(t)$ in subsection (5.2.2.1) through the use of the normalization constant A_ω . For $d \geq 3$, Eq.(4.100) is generalised

$$A_\omega(d) := \frac{l}{r_H} \sqrt{\frac{\pi \alpha'}{\omega}} = \frac{(d-1)\beta}{4\sqrt{\pi\omega}\lambda^{1/4}} \equiv \frac{(d-1)}{2} A_\omega, \quad (5.122)$$

where the second equality follows from using the definition of the AdS radius of curvature l (Eq.(4.64)) and the Hawking temperature (Eq.(4.35)). Using the generalised normalization constant $A_\omega(d)$, the expectation value of the position of the boundary endpoint at two different times (Eq.(5.43)) becomes¹⁰⁷

$$\begin{aligned} \langle :\hat{X}_{\text{end}}(t_1; d) \hat{X}_{\text{end}}(t_2; d): \rangle &= \frac{(d-1)^2 \beta^2}{16\pi^2 \sqrt{\lambda}} \int_0^\infty \frac{d\omega}{\omega} \frac{1}{e^{\beta\omega} - 1} \text{Re} \left(f_\omega(\sigma_f - t_1) f_\omega^*(\sigma_f - t_2) e^{-i\omega(t_1 - t_2)} \right) \\ &\equiv \frac{(d-1)^2}{4} \langle :\hat{X}_{\text{end}}(t_1) \hat{X}_{\text{end}}(t_2): \rangle, \end{aligned} \quad (5.123)$$

while the string falling endpoint's mean-squared transverse displacement, Eq.(5.47), becomes

$$\begin{aligned} s^2(t; d) &= \frac{(d-1)^2 \beta^2}{16\pi^2 \sqrt{\lambda}} \int_0^\infty \frac{d\omega}{\omega} \frac{1}{e^{\beta\omega} - 1} |f_\omega(\sigma_f - t) - f_\omega(\sigma_f) e^{i\omega t}|^2 \\ &\equiv \frac{(d-1)^2}{4} s^2(t), \end{aligned} \quad (5.124)$$

due to the factors of $A_\omega A_{\omega'}$ appearing in the calculations of both $\langle :\hat{X}_{\text{end}}(t_1; d) \hat{X}_{\text{end}}(t_2; d): \rangle$ and $s^2(t; d)$.

In subsection (5.2.2.1), the general solution to the wave equation, $f_\omega(\sigma)$, is given by Eqs.(5.52)-(5.55). In order to calculate the falling string endpoint's mean-squared transverse displacement in the small virtuality limit, Eq.(5.55) is substituted into Eq.(5.124). Specifically,

$$\begin{aligned} s^2(t; d) &= \frac{(d-1)^2 \beta^2}{16\pi^2 \sqrt{\lambda}} \int_0^\infty \frac{d\omega}{\omega} \frac{1}{e^{\beta\omega} - 1} \left| 2e^{i\omega(r_{s*} + \sigma_f)} \cos(\omega t) - 2e^{i\omega(r_{s*} + \sigma_f)} e^{i\omega t} \right|^2 \\ &= \frac{(d-1)^2 \beta^2}{4\pi^2 \sqrt{\lambda}} \int_0^\infty \frac{d\omega}{\omega} \frac{1}{e^{\beta\omega} - 1} \sin^2(\omega t) \\ &\equiv \frac{(d-1)^2}{4} s_{\text{small}}^2(t) \\ &= \frac{(d-1)^2 \beta^2}{16\pi^2 \sqrt{\lambda}} \ln \left(\frac{\beta}{2\pi t} \sinh \left(\frac{2\pi t}{\beta} \right) \right), \end{aligned} \quad (5.125)$$

where Eq.(5.56) is used in the third line, and Eq.(5.58) in the final line. In order to calculate the diffusion coefficient, the late time dynamics of Eq.(5.125) must be explored. Expanding in powers of $1/k = \beta/t$ yields

¹⁰⁶The solution to Eq.(5.121) is therefore given by Eq.(5.52), or alternatively by $f_\omega^{(\pm)}(\tilde{\epsilon}) = \tilde{\epsilon}^{\pm \frac{1}{(d-1)}} \frac{il^2 \omega}{r_H}$, where the identification $\tilde{\epsilon} = e^{\frac{r_H}{l^2} (d-1) (r_H \tilde{\epsilon}_{s*} + \sigma)}$ is used to convert from parameter space coordinates (t, σ) to near-horizon spacetime coordinates $(t, \tilde{\epsilon})$. Notice when $f_\omega^{(+)}(\tilde{\epsilon})$ is used as the solution (as in subsection (5.3.1)), $f_\omega^{(-)}(\tilde{\epsilon})$ is used in the definition of $X_{\text{reg}}(t, \tilde{\epsilon})$, Eq.(5.85).

¹⁰⁷Note that the Bose-Einstein distribution Eq.(4.102) does not carry any dimensional dependence.

$$\begin{aligned}
s^2(t; d) &= \frac{(d-1)^2 \beta^2}{16\pi^2 \sqrt{\lambda}} \left[\ln(\sinh(2\pi k)) + \ln\left(\frac{1}{2\pi k}\right) \right] \\
&\xrightarrow{(\beta \ll t)} \frac{(d-1)^2 \beta t}{8\pi \sqrt{\lambda}} + \frac{(d-1)^2 \beta^2}{16\pi^2 \sqrt{\lambda}} \ln\left(\frac{\beta}{4\pi t}\right) + \mathcal{O}\left(\beta^2 e^{\frac{-4\pi t}{\beta}}\right),
\end{aligned} \tag{5.126}$$

where the calculation steps in Eq.(5.60) have been followed closely. Since $s^2(t; d) \sim t$, the late time dynamics exhibit diffusive behaviour. From Eq.(3.21) it is expected that $s_{\text{small}}^2(t) = 2D t$ at late times, where D is the diffusion coefficient. Comparing this to Eq.(5.126) it is easy to see that the diffusion coefficient is given by

$$D_{\text{LQ}}^{\text{AdS}d}(d) = \frac{(d-1)^2 \beta}{16\pi \sqrt{\lambda}}. \tag{5.127}$$

For $d = 3$, this reduces down to Eq.(5.61) as expected.

Moerman *et al.* in [52] present an expression for the light quark diffusion coefficient in d dimensions which agrees with Eq.(5.127). However, their method of expanding the near-horizon AdS_d -Schwarzschild metric (described in subsection (3.3) of [52]) is inconsistent. The near-horizon AdS_d -Schwarzschild metric given in Eq.(3.48) of [52] is dimensionally incorrect^{108,109}. Using the near-horizon tortoise coordinate Eq.(5.107) (no attempt is made to explain how the order of truncation is consistent with the leading order near-horizon metric¹¹⁰), the metric in Eq.(3.48) of [52] is converted to $(t, \tilde{\epsilon}_*)$ coordinates, and found to be conformal in this system¹¹¹. Hence, the leading order string solution can be written down in $(t, \tilde{\epsilon}_*)$ coordinates, from which Moerman *et al.* proceeded to finding the transverse equations of motion – this, coincidentally, being the wave equation. Therefore, although there is agreement between the final results, Eq.(5.127) and the diffusion coefficient in d dimensions derived by Moerman *et al.*, the author concludes that the calculations in this subsection arriving at Eq.(5.127), present the first complete, consistent derivation of the light quark diffusion coefficient in d dimensions.

¹⁰⁸Since r_H^2 , $l^2 dx_{d-2}^2$ and dt^2 all go like Energy^{-1} , and $\tilde{\epsilon}$ (as well as $d\tilde{\epsilon}^2$) are defined as dimensionless quantities; the first term in the metric Eq.(3.48) of [52] goes like Energy^{-2} , the second term also goes like Energy^{-2} , but the third term is dimensionless. In juxtaposition, all terms in the correct, leading order near-horizon AdS_d -Schwarzschild metric given in this subsection (Eq.(5.82)) consistently go like Energy^{-2} .

¹⁰⁹A note on terminology: ϵ in [52] corresponds to $\tilde{\epsilon}$ in this dissertation.

¹¹⁰The paper [52] simply states "Expanding (and truncating) each term in the AdS_d metric, Eq.(2.32), to lowest non-vanishing order in ϵ ". There does not appear to have been an attempt to examine if each term is consistently taken to the same order of ϵ ($\tilde{\epsilon}$ – see footnote 109).

¹¹¹The correct near-horizon AdS_d -Schwarzschild metric (Eq.(5.82)) is actually conformal in (t, r_*) coordinates (as shown in Eq.(5.109)).

6 Drag Force in AdS/CFT

Besides the test string set-ups depicted in figures (2) and (3) (see section (4), page 16, and section (5), page 37, respectively), there are many other string set-ups – illuminating various aspects or properties of the thermal plasma in the boundary theory – that could be considered. One such set-up is a trailing string in AdS_5 -Schwarzschild which models an infinitely massive probe quark¹¹² moving with a constant velocity v in a $\mathcal{N} = 4$ SYM thermal plasma¹¹³. This was considered by Gubser [22] and Herzog *et al.* [35] independently in 2006, who aimed to approximately explain jet-quenching – the phenomenon whereby energy loss is experienced by high-energy quarks travelling through the quark-gluon plasma¹¹⁴. The succeeding subsection follows the calculations of [22, 35] in using the AdS/CFT correspondence to calculate the drag force experienced by a massive probe quark in the $\mathcal{N} = 4$ SYM thermal medium. The string set-up used is depicted in figure (9). Further, in subsection (6.2), the set-up is generalised to AdS_d -Schwarzschild.

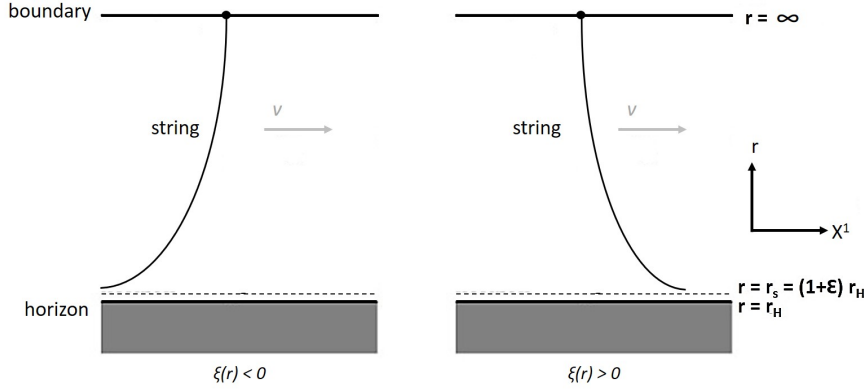


Figure 9: A fundamental open string used as a probe in an AdS black hole background to model an infinitely massive quark moving through a thermal plasma at a constant velocity v on the boundary. One endpoint of the test string is attached to the boundary of anti-de Sitter spacetime at infinity ($r = \infty$), from which the string hangs down to a *stretched horizon* ($r_s = (1 + \epsilon) r_H$ where $0 < \epsilon \ll 1$) placed just above the Schwarzschild black hole horizon. Left: A string which trails behind its boundary endpoint moving with velocity v in the X^2 direction. This is the physical solution. Energy flows from the boundary, down the string, and towards the horizon. Right: A string which trails in front of its boundary endpoint moving with velocity v in the X^2 direction. This solution is unphysical. Energy would need to be flowing away from the horizon, up the string, and towards the boundary.

6.1 Test Strings in AdS_5 -Schwarzschild

Consider a static open string in AdS_5 -Schwarzschild, with one endpoint attached to the boundary at $r = \infty$ and the other allowed to hang down towards the horizon. Since the string is infinitely long (which models an infinitely massive quark in the boundary theory), the transverse fluctuations that the string experiences due to the presence of the black hole horizon never reach the boundary, i.e. the infinitely massive quark does not experience Brownian motion in the thermal medium. Regardless of its length, this test string is still a classical relativistic string and, as such, is described by the standard Polyakov action (Eq.(4.1)) or Nambu-Goto action (Eq.(4.53)). It is convenient to use the Nambu-Goto action here¹¹⁵.

¹¹²Due to its infinite mass such a quark would not undergo Brownian motion in thermal plasma.

¹¹³The constant velocity is measured with respect to the rest frame of the plasma.

¹¹⁴Around the same time, studies examining trailing strings in the AdS spacetime in order to investigate the dissipative and diffusive behaviour of a massive quark moving through a field theory plasma were common (see [36–41]).

¹¹⁵The Nambu-Goto action given in Eq.(4.53) is defined in the String Frame. In the Einstein Frame, the Nambu-Goto action is constructed with an added dilaton factor $e^{\phi/2}$,

$$S_{NG}^E := -\frac{1}{2\pi\alpha'} \int_{\mathcal{M}} d^2\sigma e^{\phi/2} \sqrt{-g},$$

where $g := \det(g_{ab})$ and the induced worldsheet metric g_{ab} is given by Eq.(4.2). In [22] the Einstein Frame is chosen for the proceeding calculations. The phenomenologically relevant case of AdS_5 -Schwarzschild is considered. In this spacetime the dilaton factor can be ignored, since $e^{\phi/2} = H^{(5-d)/4}$ (where H is the warping factor and $e^{\phi/2}$ disappears when $d = 5$). It is worth a footnote to remark, however, that the Einstein Frame is related to the String Frame by a conformal rescaling of the metric, and that the frames are considered interchangeable when describing the physics of massless modes on the string [109]. The calculations in this dissertation are in the String Frame.

From Eq.(4.33), the AdS₅-Schwarzschild metric is given by

$$ds_5^2 = \frac{r^2}{l^2} \left(-h(r) dt^2 + d\vec{X}_I^2 \right) + \frac{l^2}{r^2} \frac{dr^2}{h(r)}, \quad \text{where} \quad h(r) = 1 - \left(\frac{r_H}{r} \right)^4 \in [0, 1] \quad (6.1)$$

is the blackening factor of the Schwarzschild black hole situated at the horizon; $t \in [0, \infty)$ is the temporal coordinate; $r \in [0, \infty)$ is the radial coordinate; and the transverse spatial directions along which the D3-brane is extended are denoted by $\vec{X}_I = (X^2, X^3, X^4) \in \mathbb{R}^3$. Further, $l \in \mathbb{R}^+$ is the curvature radius of AdS_d and S^d .

Following [22, 35], a gauge choice is made where $\tau = t$ and $\sigma = r$ are the worldsheet coordinates. The target spacetime metric $G_{\mu\nu}$ – where μ, ν index over the spacetime directions $(t, r, 2, 3, 4)$ – is given explicitly in Eq.(A.32); and the induced worldsheet metric g_{ab} , defined in Eq.(4.2), takes the form Eq.(A.33). The explicit entries of the metric g_{ab} , its inverse g^{ab} , and its determinant $g := \det(g_{ab})$ are given by Eqs.(A.34, A.35, A.36) respectively. Using the target spacetime metric $G_{\mu\nu}$ and remembering the gauge choice $\tau = t$ and $\sigma = r$, the determinant of the induced metric becomes

$$g = - \left(1 - \frac{1}{h(r)} \dot{X}_I^2 + \frac{r^4}{l^4} h(r) X_I'^2 \right), \quad (6.2)$$

where $\dot{X} \equiv \partial_\tau X = \partial_t X$ and $X' \equiv \partial_\sigma X = \partial_r X$ (in both definitions the second equality follows from the worldsheet gauge choice). Inputting Eq.(6.2), into the definition of the Nambu-Goto action Eq.(4.53) yields

$$S_{NG} = - \frac{1}{2\pi\alpha'} \int_{\mathcal{M}} d^2\sigma \sqrt{1 - \frac{1}{h} \dot{X}_I^2 + \frac{r^4}{l^4} h X_I'^2}, \quad (6.3)$$

where the notational adjustment $h(r) \equiv h$ is used for brevity. The Lagrangian density, also defined in Eq.(4.53), is therefore given by

$$\mathcal{L} = - \sqrt{1 - \frac{1}{h} \dot{X}_I^2 + \frac{r^4}{l^4} h X_I'^2}. \quad (6.4)$$

To proceed, consider movement of the test string with a constant velocity v in one of the transverse directions, the X^2 direction¹¹⁶. Following [22], an ansatz to describe the late-time behaviour of the string is made. Specifically¹¹⁷,

$$X^2(t, r) = vt + \xi(r) + o(t), \quad (6.5)$$

where, at late times, all other motions are damped out and the $o(t)$ term disappears. The ansatz Eq.(6.5) relies on the assumption that steady state behaviour of the string's motion is achieved at late times. Substituting this ansatz into the Lagrangian density Eq.(6.4) – remembering that X^2 is the only direction in which the string is considered to move – yields

$$\begin{aligned} \mathcal{L} &= - \sqrt{1 - \frac{1}{h} \left[\frac{\partial}{\partial t} (vt + \xi) \right]^2 + \frac{r^4}{l^4} h \left[\frac{\partial}{\partial r} (vt + \xi) \right]^2} \\ &= - \sqrt{1 - \frac{v^2}{h} + \frac{r^4}{l^4} h \xi'^2}, \end{aligned} \quad (6.6)$$

where $\xi(r) \equiv \xi$ is implied, and $\xi' = \partial_r \xi$. In order to determine $\xi(r)$, the Euler-Lagrange equations are derived from the Lagrangian density (Eq.(6.6)), and are given by

¹¹⁶Due to a symmetry of anti-de Sitter spacetime all transverse directions are identical. Therefore any of the transverse directions can be chosen – considering motion in either the X^2 , X^3 or X^4 directions would be equivalent.

¹¹⁷To clarify the notation: the mapping function for the second transverse direction will be denoted X^2 , while squaring this mapping function (if necessary) will be denoted $(X^2)^2$.

$$\frac{\partial}{\partial t} \frac{\partial \mathcal{L}}{\partial \xi'} - \frac{\partial \mathcal{L}}{\partial \xi} = 0, \quad (6.7)$$

where the quantity π_ξ can be defined as

$$\pi_\xi := \frac{\partial \mathcal{L}}{\partial(\partial_r \xi)}. \quad (6.8)$$

Since the Lagrangian density (Eq.(6.6)) does not depend on ξ (i.e. $\partial \mathcal{L}/\partial \xi = 0$), the Euler-Lagrange equations become

$$\begin{aligned} \pi_\xi &:= \frac{\partial \mathcal{L}}{\partial \xi'} = \mathcal{C} \\ &= -\frac{r^4}{l^4} h \xi' \left(1 - \frac{v^2}{h} + \frac{r^4}{l^4} h \xi'^2 \right)^{-\frac{1}{2}}, \end{aligned} \quad (6.9)$$

where Eq.(6.6) is used in the second line. Hence, the equation of motion of the string is π_ξ being a constant of motion. Solving Eq.(6.9) yields a defining relation for $\xi'(r)$. Mathematica's `Solve` function is used¹¹⁸, to find

$$\xi'(r) = \pm \pi_\xi \frac{l^4}{r^4 h} \sqrt{\frac{h - v^2}{h - \frac{l^4}{r^4} \pi_\xi^2}}. \quad (6.10)$$

Finding $\xi(r)$ will involve integrating Eq.(6.10) with respect to r . However, $\xi(r)$ is required to be real everywhere, and the square root in Eq.(6.10) is not necessarily always real. The only variable which can be adjusted is π_ξ . Defining π_ξ such that $(h - v^2)/(h - \frac{l^4}{r^4} \pi_\xi^2)$ is always positive (thereby ensuring the square root is always real) is equivalent to setting the appropriate boundary conditions. Since $h(r) \in [0, 1]$, at some intermediate radius $h = h^*$ the numerator $(h - v^2)$ changes sign. In order for the square root to be real everywhere the denominator must change sign at the same point, i.e. at $h = h^*$,

$$h - \frac{l^4}{r^4} \pi_\xi^2 = h - v^2 = 0. \quad (6.11)$$

Rearranging the first equality leaves

$$\pi_\xi^2 = \frac{r^4}{l^4} v^2. \quad (6.12)$$

While the second equality in Eq.(6.11) is rearranged to

$$r^4 = \frac{r_H^4}{1 - v^2}. \quad (6.13)$$

where the definition of $h(r)$ (Eq.(6.1)) is used. Inputting Eq.(6.13) into Eq.(6.12) results in an appropriate expression for π_ξ ,

$$\pi_\xi = \pm \frac{v}{\sqrt{1 - v^2}} \frac{r_H^2}{l^2}. \quad (6.14)$$

Plugging this defining relation for π_ξ into Eq.(6.10) guarantees that the square root in Eq.(6.10) is always positive, and $\xi(r)$ is everywhere real. The (\pm) in Eq.(6.14) determines if the quark is moving in the $(+)$ or $(-)$ X^2 direction. Consider the case where $\pi_\xi > 0$ for the remainder of the calculation. Eq.(6.10) becomes,

¹¹⁸Mathematica is used to help simplify the algebra. See Mathematica Notebook [d] (`DragForce.nb`) for details on the calculations presented in section (6): access in appendix (A.7).

$$\xi'(r) = \pm v \frac{r_H^2 l^2}{r^4 - r_H^4}. \quad (6.15)$$

An integrable expression for ξ' has finally been found. Integrating Eq.(6.15) with respect to r yields¹¹⁹

$$\begin{aligned} \xi(r) &= \mp \frac{l^2 v}{2 r_H} \left(\tan^{-1} \left(\frac{r}{r_H} \right) - \frac{\ln(r_H - r)}{2} + \frac{\ln(r + r_H)}{2} \right), \\ &= \mp \frac{l^2 v}{2 r_H} \left(\tan^{-1} \left(\frac{r}{r_H} \right) + \ln \sqrt{\frac{r + r_H}{r - r_H}} \right), \end{aligned} \quad (6.16)$$

where in the second line $\ln(-x) = \ln(x) + i\pi$ for $x > 0$ is used and it is recognised that $i\pi$ can be absorbed into the integration constant, which (if the calculation was entirely rigorous) would be present in Eq.(6.16). The function $\xi(r)$ can take on two values: (i) for $(\xi'(r) > 0, \xi(r) < 0)$ the string trails behind its boundary endpoint which is moving with a velocity v in the $(+)$ X^2 direction, and (ii) for $(\xi'(r) < 0, \xi(r) > 0)$ the string trails in front of its boundary endpoint which is moving with a velocity v in the $(+)$ X^2 direction. The ‘tail wagging the dog’ scenario depicted in (ii) is an unphysical solution [35]; however both of these cases are depicted in figure (9), page 66.

Using the expression for $\xi'(r)$ given in Eq.(6.15) the Lagrangian density (Eq.(6.6)) becomes

$$\mathcal{L} = -\sqrt{1 - v^2}. \quad (6.17)$$

Since the definition of the Nambu-Goto action (Eq.(4.53)) implies $\mathcal{L} = -\sqrt{-g}$, the determinant of the induced metric becomes

$$g = -(1 - v^2). \quad (6.18)$$

To calculate the flow of momentum down the string dp_2/dt , the canonical momentum densities $\Pi_\mu^a(t, \sigma)$ (Eq.(4.5)), and the string equations of motion (Eq.(4.19)) are needed. The conserved charges associated with the momentum densities Π_μ^a are defined [15, 96] for a general curve γ on the worldsheet, as

$$p_\mu^\gamma := \int_\gamma d\sigma^b \tilde{\epsilon}_{ab} \Pi_\mu^a, \quad (6.19)$$

where $\tilde{\epsilon}_{ab}$ is the Levi-Civita symbol¹²⁰, and g_{ab} is the induced metric on the worldsheet in curved spacetime (Eq.(4.2)). Since the string moves only in the X^2 direction by construction, the string’s transverse momentum densities are only non-zero in this direction. Using Eq.(6.19) the X^2 component of the spacetime momentum flowing over some general time interval \mathcal{I} of length Δt is

$$\frac{dp_2}{dt} \Delta t = p_2^\mathcal{I} = \int_\mathcal{I} dt \Pi_2^r, \quad (6.20)$$

where the gauge choice $\tau = t$ and $\sigma = r$ is applied, and $\tilde{\epsilon}_{rt} = +1$ from the definition of the Levi-Civita symbol. The radius at which the integral in Eq.(6.20) is evaluated does not matter, since the momentum densities $\Pi_\mu^a(t, \sigma)$ are conserved (Eq.(4.19)). For the physical solution where the string trails behind its boundary endpoint ($\xi'(r) > 0, \xi(r) < 0$), the quantity dp_2/dt is identified as the drag force and the orientation of

¹¹⁹Mathematica is used to easily integrate (see Mathematica Notebook [d]: **DragForce.nb**).

¹²⁰The Levi-Civita symbol is defined in two dimensions as

$$\tilde{\epsilon}_{ab} = \begin{cases} +1, & \text{if } (a, b) = (1, 2) \\ -1, & \text{if } (a, b) = (2, 1) \\ 0, & \text{if } a = b \end{cases}.$$

the integral is chosen such that the drag force is negative (i.e. acts to oppose the motion of the string). Therefore, $dp_2/dt = \Pi_2^r$. According to the definition of the momentum densities Eq.(4.5),

$$\begin{aligned}\frac{dp_2}{dt} &:= \Pi_2^r = -\frac{1}{2\pi\alpha'} \sqrt{-\gamma} \gamma^{rb} G_{2\nu} \partial_b X^\nu \\ &= -\frac{1}{2\pi\alpha'} \sqrt{-g} g^{rb} G_{2\nu} \partial_b X^\nu \\ &= -\frac{1}{2\pi\alpha'} \sqrt{1-v^2} g^{rb} G_{2\nu} \partial_b X^\nu,\end{aligned}\tag{6.21}$$

where the constraint equation Eq.(4.10) is used in the second line and Eq.(6.18) is used in the third line. Expanding the implied summation over repeated indices in Eq.(6.21) yields

$$\begin{aligned}\frac{dp_2}{dt} &= -\frac{1}{2\pi\alpha'} \sqrt{1-v^2} G_{2\nu} (g^{rr} \partial_r X^\nu + g^{rt} \partial_t X^\nu) \\ &= -\frac{1}{2\pi\alpha'} \sqrt{1-v^2} G_{22} \left(\frac{1}{g} (G_{tt} + G_{II} \dot{X}_I \dot{X}_I) \partial_r X^2 + \frac{1}{g} (-G_{II} X'_I \dot{X}_I) \partial_t X^2 \right) \\ &= \frac{1}{2\pi\alpha'} \frac{1}{\sqrt{1-v^2}} G_{22} ((G_{tt} + G_{22} \partial_t X^2 \partial_t X^2) \partial_r X^2 + (-G_{22} \partial_r X^2 \partial_t X^2) \partial_t X^2) \\ &= \frac{1}{2\pi\alpha'} \frac{1}{\sqrt{1-v^2}} G_{22} G_{tt} \partial_r \xi \\ &= -\frac{1}{2\pi\alpha'} \frac{r_H^2}{l^2} \frac{v}{\sqrt{1-v^2}},\end{aligned}\tag{6.22}$$

where, in the second line, it was recognised that $G_{2\nu} = G_{22}$ is the only non-zero possibility since $G_{\mu\nu}$ is a diagonal matrix, and Eq.(A.35) was used to find the explicit entries of the inverse induced metric g^{ab} (remembering that the gauge choice $\tau = t$ and $\sigma = r$ must be made). In the third line Eq.(6.18) was used and it was noted that, by construction, the only non-zero transverse direction was the X^2 direction, while in the fourth line the commutative property of partial derivatives and the ansatz Eq.(6.5) was used. The final line follows from inputting the target spacetime metric entries (Eq.(A.32)) and the defining relation for $\xi'(r)$, Eq.(6.15) (where $\xi'(r) > 0$).

Comparing Eq.(6.14) (where $\pi_\xi < 0$) and Eq.(6.22), notice that π_ξ is understood to be a momentum density, since

$$\Pi_2^r = \frac{1}{2\pi\alpha'} \pi_\xi.\tag{6.23}$$

Eq.(6.23) follows from Eq.(4.5) which gives $\Pi_2^r := \frac{1}{2\pi\alpha'} \partial_{(\partial_\sigma X^2)} \mathcal{L}$; and from the worldsheet gauge choice $\sigma = r$, from which the momentum density becomes $\Pi_2^r = \frac{1}{2\pi\alpha'} \partial_{(\partial_r \xi)} \mathcal{L} = \frac{1}{2\pi\alpha'} \pi_\xi$ (where the ansatz Eq.(6.5) is used in the first equality and Eq.(6.8) in the second equality).

For the phenomenologically relevant $\text{AdS}_5/\mathcal{N} = 4$ SYM case, the 't Hooft coupling is $\lambda \equiv g_{\text{YM}}^2 N_c$, where N_c is the number of colours and the Yang-Mills coupling is related to the string coupling by: $g_{\text{YM}} = 2\sqrt{\pi} \bar{g}_s$. The fundamental string length scale Eq.(4.64) becomes

$$\alpha' = \frac{l^2}{\sqrt{g_{\text{YM}}^2 N_c}}.\tag{6.24}$$

Using Eq.(6.24) and the definition of Hawking temperature (Eq.(4.35)) with $d = 5$, the drag force (Eq.(6.22)) can be expressed in terms of phenomenologically relevant gauge theory variables,

$$\frac{dp_2}{dt} = -\frac{\pi \sqrt{g_{YM}^2 N_c}}{2} T^2 \frac{v}{\sqrt{1-v^2}}. \quad (6.25)$$

Following the formal framework of Gubser [22], in the gauge theory the momentum p_2 of the probe quark can be theoretically¹²¹ related to its mass m through

$$p_2(t) = \frac{v}{\sqrt{1-v^2}} m, \quad (6.26)$$

where the $1/\sqrt{1-v^2} \equiv \gamma$ is identified as the Lorentz factor from special relativity. Eq.(6.26) holds regardless of the dimension of the spacetime. Inserting Eq.(6.26) into Eq.(6.25) yields

$$\frac{dp_2}{dt} = -\frac{\pi T^2}{2} \sqrt{g_{YM}^2 N_c} \frac{p_2(t)}{m}, \quad (6.27)$$

which is a linearly separable differential equation and easily integrable to find $p_2(t)$. Specifically,

$$\begin{aligned} \int_{p_2(0)}^{p_2(t)} \frac{1}{p_2} dp_2 &= - \int_0^t \frac{T^2}{m} \frac{\pi \sqrt{g_{YM}^2 N_c}}{2} dt \\ \Rightarrow p_2(t) &= p_2(0) \text{Exp} \left[-\frac{T^2}{m} \frac{\pi \sqrt{g_{YM}^2 N_c}}{2} t \right] \\ \Rightarrow p_2(t) &= p_2(0) e^{-\frac{t}{t_0}}, \quad \text{where} \quad t_0 = \frac{2}{\pi \sqrt{g_{YM}^2 N_c}} \frac{m}{T^2}. \end{aligned} \quad (6.28)$$

The expression for the drag force experienced by a probe quark in a thermal plasma found in Eq.(6.27) agrees with the central result of Gubser [22], and Herzog *et al.* [35]. Agreement with the later rests on the identification $\xi' = x'_{\text{Herzog}}/l^2$ and $g = -g_{\text{Herzog}}/l^4$.

Recall the Langevin Model discussed in section (3) describes a non-relativistic particle of mass m , undergoing Brownian motion in one spatial dimension. The non-retarded Langevin equation Eq.(3.1) is applicable if – as in the case presented in this section – the Brownian particle is taken to have infinite mass with respect to the constituent fluid particles. Since the infinitely massive probe quark travels at a constant velocity v under the influence of the external force $K(t)$, Newton's First Law of Motion ensures that the random force $F(t)$ present in the system must be of equal and opposite magnitude ($K(t) = -F(t)$). The Langevin equation is adjusted accordingly and becomes $\dot{p}(t) = -\gamma_0 p(t)$, where γ_0 is the friction coefficient. It is therefore apparent, from Eq.(6.27), that in the non-relativistic limit $v \ll 1$ the friction coefficient in AdS₅-Schwarzschild is given by

$$\gamma_0^{\text{AdS}_5} = \frac{\pi T^2}{2m} \sqrt{g_{YM}^2 N_c}. \quad (6.29)$$

Using the Einstein-Sutherland relation Eq.(3.18) an expression for the diffusion coefficient can be obtained. Specifically,

$$D_{\text{HQ}}^{\text{AdS}_5} = \frac{2}{\pi T} \frac{1}{\sqrt{g_{YM}^2 N_c}} = \frac{2\beta}{\pi\sqrt{\lambda}}, \quad (6.30)$$

where the second equality follows from the 't Hooft coupling $\lambda \equiv g_{YM}^2 N_c$, and the definition of Hawking temperature Eq.(4.35).

¹²¹Both the momentum p_2 and the mass m of the external quark are, in fact, infinite.

6.2 Generalising to AdS_d -Schwarzschild

The result for the drag force experienced by a probe quark in a thermal plasma found in Eq.(6.27) can be generalised by repeating the calculation presented in subsection (6.1) in AdS_d -Schwarzschild. The AdS -Schwarzschild metric in d dimensions is given by Eq.(4.33), where the blackening factor of the Schwarzschild black hole situated at the horizon, $h(r; d)$, is defined in Eq.(4.34). Explicitly, the target spacetime metric $G_{\mu\nu}$ is given by Eq.(A.32), where μ, ν index over the spacetime directions $(t, r, 2, \dots, d-1)$. As in subsection (6.1), the reparameterization offered by the gauge choice separates the temporal and radial coordinates such that the worldsheet parameter space coordinates become $\tau = t$ and $\sigma = r$, and the mapping functions between the worldsheet and the target spacetime are specified by $X^\mu(t, r)$.

The Hawking temperature of the black-brane in AdS -Schwarzschild scales with the number of dimensions of the spacetime and – in AdS_d -Schwarzschild – is given by Eq.(4.35). Unchanged as the calculation is generalised to AdS_d , the dynamics of the string are still described by the Nambu-Goto action (Eq.(4.53)); and the induced metric g_{ab} , its inverse g^{ab} , and its determinant $g := \det(g_{ab})$ are still given by Eqs.(A.34, A.35, A.36) respectively. Because of this, Eqs.(6.2)-(6.10) all remain true in AdS_d -Schwarzschild.

Consider movement of the test string in AdS_d -Schwarzschild, again with a constant velocity v in one of the transverse directions, the X^2 direction. Following the same reasoning as for the AdS_5 case, Eq.(6.10) can be solved to yield an expression for π_ξ . Since the blackening factor is now given by Eq.(4.34), π_ξ will depend on the number of dimensions of the spacetime. Rearranging the first equality in Eq.(6.11) leaves

$$\pi_\xi^2 = \frac{r^4}{l^4} v^2. \quad (6.31)$$

While, for AdS_d -Schwarzschild, the second equality in Eq.(6.11) is rearranged to

$$r = \frac{r_H}{(1 - v^2)^{1/(d-1)}}, \quad (6.32)$$

where $h = h(r; d)$ (Eq.(4.34)) is used. Inputting Eq.(6.32) into Eq.(6.31) results in an appropriate expression for π_ξ ,

$$\pi_\xi = \pm \frac{v}{(1 - v^2)^{2/(d-1)}} \frac{r_H^2}{l^2}. \quad (6.33)$$

Plugging this generalised relation for π_ξ into Eq.(6.10) guarantees that the square root in Eq.(6.10) is always positive, and $\xi(r)$ is everywhere real. The (\pm) in Eq.(6.33) determines if the quark is moving in the $(+)$ or $(-)$ X^2 direction. Again consider the case where $\pi_\xi > 0$. In AdS_d -Schwarzschild, Eq.(6.10) becomes¹²²

$$\xi'(r) = \pm \frac{l^2 r_H^3 r^{d-4} v (1 - v^2)^{-\frac{2}{d-1}} \sqrt{\frac{r^4 (r_H (v^2 - 1) r^d + r r_H^d)}{-r_H r^{d+4} + r_H^5 v^2 r^d (1 - v^2)^{-\frac{4}{d-1}} + r^5 r_H^d}}}{r_H r^d - r r_H^d}, \quad (6.34)$$

which reduces down to the familiar Eq.(6.15) for $d = 5$. The function $\xi'(r)$ can take on two values: (i) for $(\xi'(r) > 0, \xi(r) < 0)$ the string trails behind its boundary endpoint which is moving with a velocity v in the $(+)$ X^2 direction, and (ii) for $(\xi'(r) < 0, \xi(r) > 0)$ the string trails in front of its boundary endpoint which is moving with a velocity v in the $(+)$ X^2 direction. Using the expression for $\xi'(r)$ in Eq.(6.34) and the definition for $h(r; d)$ in Eq.(4.34), the Lagrangian density (Eq.(6.6)) becomes

$$\mathcal{L} = - \sqrt{\frac{r^4 (r_H (v^2 - 1) r^d + r r_H^d)}{-r_H r^{d+4} + r_H^5 v^2 r^d (1 - v^2)^{-\frac{4}{d-1}} + r^5 r_H^d}}. \quad (6.35)$$

Since the definition of the Nambu-Goto action (Eq.(4.53)) implies $\mathcal{L} = -\sqrt{-g}$, the determinant of the induced metric becomes

¹²²Mathematica is used to help simplify the algebra (see Mathematica Notebook [d]: **DragForce.nb**).

$$g = - \frac{r^4 (r_H (v^2 - 1) r^d + r r_H^d)}{-r_H r^{d+4} + r_H^5 v^2 r^d (1 - v^2)^{-\frac{4}{d-1}} + r^5 r_H^d}. \quad (6.36)$$

To proceed with calculating the drag force dp_2/dt note that the canonical momentum densities $\Pi_\mu^a(t, \sigma)$ (Eq.(4.5)), the string equations of motion (Eq.(4.19)), and the definition of the conserved charges associated with the momentum densities Eq.(6.19) all remain the same in AdS_d -Schwarzschild. As in the $d = 5$ case, the string moves only in the X^2 direction by construction, and its transverse momentum densities are only non-zero in this direction. The X^2 component of the spacetime momentum flowing over some general time interval \mathcal{I} of length Δt , is still given by Eq.(6.20) in AdS_d -Schwarzschild. For the physical solution where the string trails behind its boundary endpoint ($\xi'(r) > 0$, $\xi(r) < 0$), $dp_2/dt = \Pi_2^r$. According to the definition of the momentum densities Eq.(4.5),

$$\begin{aligned} \frac{dp_2}{dt} &:= \Pi_2^r = -\frac{1}{2\pi\alpha'} \sqrt{-\gamma} \gamma^{rb} G_{2\nu} \partial_b X^\nu \\ &= -\frac{1}{2\pi\alpha'} \sqrt{-g} g^{rb} G_{2\nu} \partial_b X^\nu \\ &= -\frac{1}{2\pi\alpha'} \sqrt{\frac{r^4 (r_H (v^2 - 1) r^d + r r_H^d)}{-r_H r^{d+4} + r_H^5 v^2 r^d (1 - v^2)^{-\frac{4}{d-1}} + r^5 r_H^d}} G_{2\nu} (g^{rr} \partial_r X^\nu + g^{rt} \partial_t X^\nu) \\ &= \frac{1}{2\pi\alpha'} \left(\sqrt{\frac{r^4 (r_H (v^2 - 1) r^d + r r_H^d)}{-r_H r^{d+4} + r_H^5 v^2 r^d (1 - v^2)^{-\frac{4}{d-1}} + r^5 r_H^d}} \right)^{-\frac{1}{2}} G_{22} G_{tt} \partial_r \xi \\ &= -\frac{1}{2\pi\alpha'} \frac{r_H^2}{l^2} \frac{v}{(1 - v^2)^{\frac{2}{d-1}}}, \end{aligned} \quad (6.37)$$

where the constraint equation Eq.(4.10) is used in the second line; while in the third line, the summation over repeated indices is expanded and Eq.(6.36) is used. Following a similar calculation to Eq.(6.22), recognize that $G_{2\nu} = G_{22}$ is the only non-zero possibility, Eq.(A.35) can be used to find the explicit entries of the inverse induced metric g^{ab} and the ansatz Eq.(6.5) can be used to simplify the derivative terms. The final line follows from inputting the target spacetime metric entries (Eq.(A.32)) and the defining relation for $\xi'(r)$, Eq.(6.34) (where $\xi'(r) > 0$).

The drag force given in Eq.(6.37) reduces down to Eq.(6.22) when $d = 5$ – a necessary consistency check. Using the definition of Hawking temperature (Eq.(4.35)) to insert a unit factor $(T^2 \times 1/T^2)$, the drag force can be rewritten

$$\frac{dp_2}{dt} = -\frac{8\pi l^2 T^2}{(d-1)^2 \alpha'} \frac{v}{(1 - v^2)^{\frac{2}{d-1}}}, \quad (6.38)$$

where the momentum $p_2(t)$ is given by Eq.(6.26), which holds regardless of the dimension of the spacetime. From Eq.(6.38), in the non-relativistic limit $v \ll 1$, the friction coefficient in AdS_d -Schwarzschild is given by

$$\gamma_0^{\text{AdS}_d} = \frac{8\pi l^2 T^2}{(d-1)^2 \alpha' m}. \quad (6.39)$$

Using the Einstein-Sutherland relation Eq.(3.18) an expression for the diffusion coefficient in general d dimensions can be obtained. Specifically,

$$D_{\text{HQ}}^{\text{AdS}_d}(d) = \frac{(d-1)^2 \alpha'}{8\pi l^2 T} = \frac{(d-1)^2 \beta}{8\pi \sqrt{\lambda}}, \quad (6.40)$$

where the second equality follows from the fundamental string length scale Eq.(4.64), and the definition of Hawking temperature Eq.(4.35). For $d = 3$, complete agreement is found between this equation and

the diffusion coefficient found in the case of a finite mass heavy quark undergoing Brownian motion in the thermal plasma (subsection (4.4), Eq.(4.122)) – a comforting consistency check for this work¹²³.

The heavy quark diffusion coefficient in general d dimensions (Eq.(6.40)) can be compared to the light quark diffusion coefficient in general d dimensions (Eq.(5.127)), to find

$$D_{\text{LQ}}^{\text{AdS}_d}(d) = \frac{1}{2} D_{\text{HQ}}^{\text{AdS}_d}(d), \quad (6.41)$$

which agrees with Eq.(5.62) for $d = 3$. The factor of $1/2$ in Eq.(6.41) may arise through differences in partitioning the worldsheet for the heavy and light quark test strings. Moerman *et al.* postulated in [52] that by introducing a factor a which determines the fraction of the local speed of light the boundary endpoint of the test string falls at, a general expression can be found for the mean-squared displacement of said endpoint (and therefore the diffusion coefficient) which interpolates between the heavy and light quark results¹²⁴. Explicitly, the string falling endpoint's mean-squared transverse displacement is given by

$$s_{\text{small}}^2(t; a; d) = \frac{1}{\sqrt{\lambda}} \left(\frac{(d-1)\beta}{4\pi} \right)^2 \ln \left(\frac{2a\beta^3}{\pi^3(a^2-1)^2 t^3} \sinh^2 \left(\frac{\pi(a+1)t}{\beta} \right) \sinh^2 \left(\frac{\pi(a-1)t}{\beta} \right) \text{csch} \left(\frac{2\pi a t}{\beta} \right) \right), \quad (6.42)$$

which, at late times, becomes¹²⁵

$$s_{\text{small}}^2(t; a; d) \xrightarrow{(\beta \ll t)} \frac{(d-1)^2 \beta t}{4\pi \sqrt{\lambda}} \left[1 - \frac{a}{2} \right] + \frac{(d-1)^2 \beta^2}{16\pi^2 \sqrt{\lambda}} \begin{cases} 4 \ln \left(\frac{\beta}{2\pi t} \right), & \text{if } a = 0 \\ \ln \left(\frac{a\beta^3}{4\pi^3(a^2-1)^2 t^3} \right), & \text{if } 0 < a < 1 \\ \ln \left(\frac{\beta}{4\pi t} \right), & \text{if } a = 1 \end{cases} + \mathcal{O} \left(\frac{\beta}{t} \right)^0. \quad (6.43)$$

The diffusion coefficient for a quark in a $(d-1)$ -dimensional thermal plasma can be extracted from Eq.(6.43). Specifically,

$$D(a; d) = \left[1 - \frac{a}{2} \right] \frac{(d-1)^2 \beta}{8\pi \sqrt{\lambda}}. \quad (6.44)$$

When $a = 0$, Eq.(6.44) reduces to the heavy quark diffusion coefficient, Eq.(6.40); and when $a = 1$, Eq.(6.44) becomes the light quark diffusion coefficient, Eq.(5.127). Hence Eq.(6.42) provides a natural interpolation between a test string set-up where the boundary endpoint is held stationary, and a test string set-up where the boundary endpoint is allowed to fall at the local speed of light. However, values of $a \notin \{0, 1\}$ correspond to a test string whose boundary endpoint is falling at velocity smaller than the local speed of light. An external force opposing the motion of the falling string must be present in order for this to be the case¹²⁶. This might be realised by the introduction of a flavour D7-brane with a world-volume electric field on it at the boundary^{127, 128}. Considering an external force acting to retard the motion of the falling string's endpoint is a natural and interesting extension of this work – a possible starting point for future research.

¹²³Eq.(6.40) also agrees with the result given in Eq.(3.10) of [42]; the results from subsection (3.3) in [35]; the results from section (3) in [22]; and the result – for $d = 5$ – from section (V) in [38]. The rigorous reader might also be interested in [36], a topical study which computed an ultra-relativistic quark's transverse momentum diffusion.

¹²⁴The heavy and light quark set-ups to study Brownian motion are considered in sections (4) and (5), respectively.

¹²⁵See Mathematica notebook [b] (`BrownianMotion.nb`) for a derivation of Eqs.(6.42)-(6.44) – access in appendix (A.7).

¹²⁶The solution where $a \notin \{0, 1\}$ is not a physically obtainable string solution in the current set-up since the Virasoro constraints (Eq.(4.18)) are violated and, consequently, the late time next-to-leading order behaviour in Eq.(6.43) does not smoothly interpolate between the light and heavy quark results. This can be rectified by adding in an external field which will alter the energy-momentum tensor (Eq.(4.6)) and, by construction, cause T_{ab} to vanish (which ensures the Virasoro constraints are satisfied).

¹²⁷This corresponds to an additional force acting on the external Brownian particle in the boundary theory whose motion can now be characterised by the generalised Langevin model (described in subsection (3.2)).

¹²⁸For the case of the heavy quark, adding forced motion has been studied by de Boer *et al.* [42], subsection (3.2).

7 Conclusions and Future Outlook

The main aim of this work was to present an instructional or pedagogical approach to using the AdS/CFT correspondence to explore the dynamical behaviour of probe heavy and light quarks immersed in a thermal plasma, such as the quark-gluon plasma created in heavy-ion experiments. This was achieved within a rigorous and consistent framework, while correcting previous errors and vague statements in the literature.

To summarise, the gauge/string duality is briefly introduced in section (2). Particular attention is paid to the *throat* construction of anti-de Sitter spacetime as a limit of D3-brane geometry, and the justification of the AdS/CFT conjecture. Section (3) explored the basic theory of Brownian motion and Langevin dynamics in the boundary theory. Specifically, particles undergoing Brownian motion in the absence of an external force can be described by the non-retarded Langevin equation which is parametrized by two constants: (i) the friction coefficient γ_0 , and (ii) the magnitude of the random force κ_0 . The second fluctuation-dissipation theorem relates these two constants. It is possible to calculate the mean-squared displacement (Eq.(3.19)), from which the time dependence of $s^2(t)$ is apparent. At early times, the Brownian particle's behaviour is proportional to time and the motion is expected to be ballistic $s(t) \sim t$; while, at late times, the Brownian particle motion is diffusive, $s(t) \sim \sqrt{t}$. The cross-over time sets the scale for early and late time behaviour and is given by t_{relax} , which represents the time it takes for a Brownian particle which had some initial velocity at $t = 0$ to thermalize in the medium. The section concludes by describing the generalised Langevin model which adapts the friction term to depend on the past trajectory of the Brownian particle and takes an additional external force acting on the system into account. In section (6) it was seen that the generalised Langevin model can be used in a number of applications: to model heavy quark trailing strings or light quark strings whose endpoint falls with a velocity that is less than the local speed of light.

Sections (4), (5) and (6) turn towards the bulk theory. In the bulk theory, the dual description of these probe quarks are realised as test strings in an asymptotically anti-de Sitter-Schwarzschild background. Calculations are computed in AdS-Schwarzschild, and then related to quantities in the boundary theory using the AdS/CFT dictionary. In section (4) an on-mass-shell external heavy quark is modelled as a fundamental open string of length ℓ_0 attached at the boundary of anti-de Sitter spacetime and hanging towards the stretched horizon. At the semiclassical level, the Hawking radiation due to the Schwarzschild black hole environment excites the modes on the string – resulting in the string's boundary endpoint enduring irregular motion. This motion can be related to the Brownian motion of the external heavy quark in the boundary gauge theory. The main results of this section include the derivation of the leading order, static string solution in AdS₃-Schwarzschild (Eq.(4.50)); the transverse equations of motion found by expanding the Nambu-Goto action up to quadratic order and varying this action with respect to the transverse string worldsheet coordinates X^I (Eq.(4.66)); and from there the mean-squared displacement of the test string's boundary endpoint, $s^2(t)$, in AdS₃-Schwarzschild (Eq.(4.109)). The cross-over time from early to late time dynamics is found to be independent of the initial length of the string ℓ_0 and solely dependant on the Hawking temperature $\beta = 1/T$. As expected, in the early time limit ($t \ll \beta$) the motion is ballistic (Eq.(4.118)); while in the late time limit ($t \gg \beta$) the motion is diffusive, and the diffusion coefficient can be extracted from $s^2(t)|_{t \gg \beta}$ (Eq.(4.122)).

An off-mass-shell external light quark is modelled in section (5) as an open string, initially stretched between the AdS boundary and just above the horizon, whose AdS boundary endpoint is released to fall at the local speed of light. The set-up is termed the *Limp Noodle* configuration [52]. Using the Bars *et al.* method [107, 108], the worldsheet of the Limp Noodle is partitioned into two regions and the leading order string solution is found in AdS₃-Schwarzschild (Eq.(5.40)). Again, the transverse fluctuations on the string excited by the Schwarzschild black hole are considered. From the equations of motion of these fluctuations, the string falling endpoint's mean-squared transverse displacement $s^2(t)$ is calculated (Eq.(5.47)). The limiting cases of $s^2(t)$ are then examined. For the small virtuality case (small string lengths ℓ_0 compared to the radial position of the black-brane horizon r_H), $s^2_{\text{small}}(t)$ is analytically evaluated (Eq.(5.58)) and the early and late time behaviour found to be ballistic and diffusive respectively. For the arbitrary virtuality case, $s^2(t)$ can be analytically found in the early time limit (Eq.(5.70)); while the behaviour of arbitrary virtuality quarks at asymptotically late times (i.e. in the near-horizon region) is found to be encoded in the small virtuality case, i.e. $s^2(t)|_{t \gg \beta} = s^2_{\text{small}}(t)$ (Eq.(5.76)). Since $s^2_{\text{small}}(t; d)$ can be solved in any $d \geq 3$ dimensions, this universality of late times motivates the generalisation of the mean-squared displacement $s^2(t)|_{t \gg \beta}$ to AdS_d-Schwarzschild. In terms of original advancement, subsection (5.3) presents a very important part of

this dissertation: correcting Moerman *et al.* [52] by presenting the proper method in which to generalise to $s^2(t; d)$. Finally, the diffusion coefficient in AdS_d -Schwarzschild is extricated from $s^2(t; d)|_{t \gg \beta}$ and given in Eq.(5.127) by

$$D_{\text{LQ}}^{\text{AdS}_d}(d) = \frac{(d-1)^2 \beta}{16\pi\sqrt{\lambda}},$$

which is – to the author’s knowledge – the first complete, consistent derivation of the light quark diffusion coefficient in d dimensions.

In section (6), a trailing string in AdS_5 -Schwarzschild which models an infinitely massive probe quark moving with a constant velocity v in a $\mathcal{N} = 4$ SYM thermal plasma is considered. By making use of the late-time behaviour ansatz (Eq.(6.5)), the drag force on the test string is calculated in the bulk and rewritten – via the AdS/CFT correspondence – in terms of relevant quantities in the gauge theory (Eq.(6.25)). Because the external quark is moving with a constant velocity in the boundary theory, it can be modelled by the Langevin equation adapted such that the external force $K(t)$ acting on the system is of equal and opposite magnitude to the random force ($K(t) = -F(t)$). Hence the friction coefficient γ_0 can be read off from Eq.(6.27), and related – using the Einstein-Sutherland relation – to the diffusion coefficient in $d = 5$ dimensions. In the second subsection, the drag force calculation is generalised to AdS_d -Schwarzschild and the diffusion coefficient is found to be given in Eq.(6.40) by

$$D_{\text{HQ}}^{\text{AdS}_d}(d) = \frac{(d-1)^2 \beta}{8\pi\sqrt{\lambda}},$$

which agrees, for $d = 3$, with the diffusion coefficient found by studying the transverse fluctuations on the heavy quark’s test string in section (4) (Eq.(4.122)).

The heavy and light quark’s diffusion constants in general d dimensions are related by a factor of a $1/2$ (Eq.(6.41)). This disparity may arise through the differences in partitioning the worldsheet for the heavy and light quark test strings. As was briefly discussed towards the end of section (6), in order to understand the physical origin of the $1/2$ factor an interpolation between $D_{\text{LQ}}^{\text{AdS}_d}(d)$ and $D_{\text{HQ}}^{\text{AdS}_d}(d)$ can be sought. This leads to the realisation that considering test strings with boundary endpoints falling slower than the local speed of light will only yield physically valid solutions if an external force is introduced. Considering an external force acting to retard the motion of the falling string’s endpoint is a natural and interesting extension of this work, and a possible starting point for future research. The publications [42, 110–112] might provide a good commencement for this exercise.

The main contribution of this dissertation to the field of AdS/CFT calculations is presenting a definitive, consolidated theoretical derivation of the light and heavy quark diffusion constants in general d dimensions. The work acts as a *springboard* from which students might pursue further research avenues. Some of these that the author has considered – besides the addition of an external electric field – are (i) repeating these calculations using a numerical framework in order to confirm the analytic results; (ii) examining the fluctuation-dissipation theorem in the bulk; (iii) considering next-to-leading order transverse fluctuations on the leading order solution (this would surely prove difficult as the expanded, near-horizon metric in AdS_d -Schwarzschild would no longer be conformal in (t, r_*) coordinates); and (iv) considering different test string configurations to illuminate other aspects of the thermal plasma. With regards to the latter, one such example is studying the quantum fluctuations in the non-transverse directions of a trailing string where the boundary endpoint is allowed to fall.

Acknowledgements

I wish to thank both my supervisors, William Horowitz and Jonathan Shock, for all their help and always being available to discuss physics; as well as my parents and partner for their love and support throughout this dissertation. This work was funded by the Mandela Rhodes Foundation, to whom I am incredibly grateful for an insightful and introspective year. Finally, although I never had the chance to meet him, I wish to acknowledge the role of Steven Gubser in suggesting the study of light quark Brownian motion using strings with falling boundary endpoints. His untimely passing (during the course of this dissertation) leaves a big hole in the AdS/CFT community.

A Appendix

A.1 Polyakov String Equations of Motion

Working in the static gauge, the string equations of motion are derived in this appendix by calculating the functional derivative of the Polyakov Action with respect to the string worldsheet coordinates and setting this variation to zero. The calculation of the string equations of motion presented here follows the layout of appendix (A) in Moerman *et al.*'s exposition on light quark Brownian motion [52].

Using the definition Eq.(4.5), the Polyakov Action Eq.(4.1) is rewritten in terms of the canonical momentum densities

$$S_P = \frac{1}{2} \int_{\mathcal{M}} d^2\sigma \Pi_\mu^a(t, \sigma) \partial_a X^\mu(t, \sigma). \quad (\text{A.1})$$

Determining the functional derivative of S_P with respect to X^μ and setting this variation to vanish, yields

$$\begin{aligned} 0 = \delta_X S_P &= \frac{1}{2} \int_{\mathcal{M}} d^2\sigma \left[(\delta \Pi_\mu^a) \partial_a X^\mu + \Pi_\mu^a \partial_a (\delta X^\mu) \right] \\ &= \frac{1}{2} \int_{\mathcal{M}} d^2\sigma \left[(\delta \Pi_\mu^a) \partial_a X^\mu + \partial_a (\Pi_\mu^a \delta X^\mu) - \delta X^\mu \partial_a (\Pi_\mu^a) \right], \end{aligned} \quad (\text{A.2})$$

where the product rule is used in the second line.

The functional derivative of the momentum densities with respect to X^μ gives two terms

$$\delta_X \Pi_\mu^a = -\frac{1}{2\pi\alpha'} \sqrt{-\gamma} \gamma^{ab} \left[G_{\mu\nu} \partial_b (\delta X^\nu) + \partial_\rho G_{\mu\nu} \delta X^\rho \partial_b X^\nu \right], \quad (\text{A.3})$$

since, in a curved background, the worldsheet coordinates X^μ as well as the spacetime metric $G_{\mu\nu}$ (which also depends on X^μ) are varied. Hence the first term in Eq.(A.2), $(\delta \Pi_\mu^a) \partial_a X^\mu$, becomes

$$\begin{aligned} (\delta_X \Pi_\mu^a) \partial_a X^\mu &= \frac{-1}{2\pi\alpha'} \sqrt{-\gamma} \gamma^{ab} G_{\mu\nu} \partial_b (\delta X^\nu) \partial_a X^\mu + \partial_\rho G_{\mu\nu} \delta X^\rho \left(\frac{-1}{2\pi\alpha'} \sqrt{-\gamma} \gamma^{ab} \partial_b X^\nu \right) \partial_a X^\mu \\ &= \frac{-1}{2\pi\alpha'} \sqrt{-\gamma} \gamma^{ab} G_{\mu\nu} \partial_b X^\nu \partial_a (\delta X^\mu) + \partial_\rho G_{\mu\nu} \delta X^\rho \left(\frac{-1}{2\pi\alpha'} \sqrt{-\gamma} \gamma^{ab} G_{\gamma\nu} \partial_b X^\nu \right) G^{\gamma\mu} \partial_a X^\mu \\ &= \Pi_\mu^a \partial_a (\delta X^\mu) + \partial_\rho G_{\mu\nu} \delta X^\rho \Pi_\gamma^a G^{\gamma\nu} \partial_a X^\mu \\ &= \partial_a (\Pi_\mu^a \delta X^\mu) - \delta X^\mu \partial_a (\Pi_\mu^a) + 2 \delta X^\rho \left(\frac{1}{2} G^{\gamma\nu} \partial_\rho G_{\mu\nu} \right) \Pi_\gamma^a \partial_a X^\mu \\ &= \partial_a (\Pi_\mu^a \delta X^\mu) - \delta X^\mu \partial_a (\Pi_\mu^a) + 2 \delta X^\rho \left(\frac{1}{2} G^{\gamma\nu} (\partial_\rho G_{\mu\nu} + \partial_\mu G_{\rho\nu} - \partial_\nu G_{\rho\mu}) \right) \Pi_\gamma^a \partial_a X^\mu, \end{aligned} \quad (\text{A.4})$$

where the definition of the momentum densities Eq.(4.5) is used in the third line, and the product rule is used in the fourth line. In the final line two extra terms are added. This can be done since

$$\Pi_\gamma^a \partial_a X^\mu (\partial_\mu G_{\rho\nu} - \partial_\nu G_{\rho\mu}) = -\frac{1}{2\pi\alpha'} \sqrt{-\eta} G_{\mu\nu} \left[\eta^{ab} \partial_b X^\nu \partial_a X^\mu (\partial_\mu G_{\rho\nu} - \partial_\nu G_{\rho\mu}) \right] = 0, \quad (\text{A.5})$$

where the first equality holds in the conformal gauge ($\gamma^{ab} = \eta^{ab}$) – which, as discussed in subsection (4.1), is chosen to eliminate the Weyl invariance in the Polyakov action. To prove Eq.(A.5), notice that the Minkowski metric can be expanded

$$\eta^{ab} \partial_a X^\mu \partial_b X^\nu (\partial_\mu G_{\rho\nu} - \partial_\nu G_{\rho\mu}) = \partial_\tau X^\mu \partial_\tau X^\nu (\partial_\mu G_{\rho\nu} - \partial_\nu G_{\rho\mu}) + \partial_\sigma X^\mu \partial_\sigma X^\nu (\partial_\mu G_{\rho\nu} - \partial_\nu G_{\rho\mu})$$

and that for each set of reflective cases ($\mu = 1, \nu = 2$ and $\mu = 2, \nu = 1$), the terms generated by the first case will cancel those generated by the second. For the identical case (which doesn't have a reflective partner case), i.e. $\mu = \nu = 1$ or $\mu = \nu = 2$, the bracket $(\partial_\mu G_{\rho\nu} - \partial_\nu G_{\rho\mu})$ vanishes.

The Christoffel symbols are now able to be defined

$$\Gamma_{\mu\nu}^\alpha := \frac{1}{2} G^{\alpha\gamma} (\partial_\mu G_{\nu\gamma} + \partial_\nu G_{\mu\gamma} - \partial_\gamma G_{\mu\nu}). \quad (\text{A.6})$$

These symbols are a set of numbers which characterise a metric connection. A metric connection defines precisely how distances are measured on a surface, by invoking the notion of consistently transporting data in a parallel manner along a family of curves [96].

With this definition, Eq.(A.4) becomes

$$(\delta_X \Pi_\mu^a) \partial_a X^\mu = \partial_a (\Pi_\mu^a \delta X^\mu) - \delta X^\mu \partial_a (\Pi_\mu^a) + 2 \delta X^\rho \Gamma_{\rho\mu}^\gamma \Pi_\gamma^a \partial_a X^\mu. \quad (\text{A.7})$$

Finally, inputting Eq.(A.7) into Eq.(A.2) returns

$$\begin{aligned} 0 = \delta_X S_P &= \frac{1}{2} \int_{\mathcal{M}} d^2\sigma \left[-2 \delta X^\mu \partial_a (\Pi_\mu^a) + 2 \delta X^\rho \Gamma_{\rho\mu}^\gamma \Pi_\gamma^a \partial_a X^\mu + 2 \partial_a (\Pi_\mu^a \delta X^\mu) \right] \\ &= - \int_{\mathcal{M}} d^2\sigma \delta X^\mu \left[\partial_a \Pi_\mu^a - \Gamma_{\mu\nu}^\gamma \Pi_\gamma^a \partial_a X^\nu \right] + \int_{\mathcal{M}} d^2\sigma \partial_a (\Pi_\mu^a \delta X^\mu) \\ &= - \int_{\mathcal{M}} d^2\sigma \delta X^\mu \left[\partial_a \Pi_\mu^a - \Gamma_{\mu\nu}^\gamma \Pi_\gamma^a \partial_a X^\nu \right] + \int_{\partial\mathcal{M}} d\sigma^b \epsilon_{ba} (\Pi_\mu^a \delta X^\mu) \\ &= - \int_{\mathcal{M}} d^2\sigma \delta X^\mu \left[\partial_a \Pi_\mu^a - \Gamma_{\mu\nu}^\gamma \Pi_\gamma^a \partial_a X^\nu \right] + \int_0^{\tau_f} d\tau \left[\delta X^\mu \Pi_\mu^a \Big|_{\sigma=0}^{\sigma=\sigma_f} \right], \end{aligned} \quad (\text{A.8})$$

where Stokes' Theorem in d-dimensions [96] is used in the third line. In the final line the coordinates on the worldsheet parameter space are chosen to be $\sigma^a = (t, \sigma)^a$ where $\sigma^a \in \mathcal{M} = [0, t_f] \times [0, \sigma_f]$, and one of the integrals of the last term is simplified by using $\delta X^\mu|_{t \in \{0, t_f\}} = 0$.

Choosing the boundary conditions

$$\delta X^\mu \Pi_\mu^a \Big|_{\sigma=0}^{\sigma=\sigma_f} = 0, \quad (\text{A.9})$$

the last term in Eq.(A.8) disappears. Hence, the string equations of motion are given by

$$0 = \partial_a \Pi_\mu^a - \Gamma_{\mu\nu}^\alpha \partial_a X^\nu \Pi_\alpha^a =: \nabla_a \Pi_\mu^a, \quad (\text{A.10})$$

which is the string analogue of the geodesic equation for a point particle [96].

A.2 The Virasoro Constraints and String Equations of Motion in Isothermal Coordinates

Since the metric of any $(1+1)$ -dimensional subspace can be transformed into a conformally flat metric [107, 108] a new, isothermal coordinate system is introduced. These isothermal coordinates $y^{\mu'}(\sigma^+, \sigma^-)$ are given by Eq.(5.2), while the corresponding string mapping functions $Y^{\mu'}(\sigma^+, \sigma^-)$ are defined in Eq.(5.8). Notice that light-cone coordinates have been chosen for the parameter space. In this appendix, the Virasoro constraint equations and the string equations of motion, Eqs.(4.18, 4.19), are rewritten in terms of $Y^{\mu'}(\sigma^+, \sigma^-)$.

In the conformal gauge, the Virasoro constraint equations (Eqs.(4.18)) become

$$\begin{aligned}
0 &= G \eta_{\mu\nu} \partial_{\pm} X^{\mu} \partial_{\pm} X^{\nu} \\
&= -G \partial_{\pm} X^0 \partial_{\pm} X^0 + G \partial_{\pm} X^1 \partial_{\pm} X^1 \\
&= -\frac{G}{2} \left[\partial_{\pm} (Y^{0'} + Y^{1'}) \partial_{\pm} (Y^{0'} + Y^{1'}) \right] + \frac{G}{2} \left[\partial_{\pm} (Y^{0'} - Y^{1'}) \partial_{\pm} (Y^{0'} - Y^{1'}) \right] \\
&= -2G \partial_{\pm} Y^{0'} \partial_{\pm} Y^{1'} \\
&= \partial_{\pm} Y^0 \partial_{\pm} Y^1,
\end{aligned} \tag{A.11}$$

where $\mu, \nu \in \{0, 1\}$ are spacetime coordinates, $\partial_{\pm} := \frac{\partial}{\partial \sigma^{\pm}}$, and the definition of the new mapping functions Eq.(5.8) is used in the third line. In the final line, recognise that G is defined as a non-zero scalar function and that the indices have been renamed ($\mu' = \mu$). This is precisely the Virasoro constraint equations given in subsection (5.1.1), Eq.(5.13).

The string equations of motion, Eq.(4.19), become

$$\partial_{\pm} \Pi_{\mu}^{\pm} - \Gamma_{\mu\nu}^{\alpha} \partial_{\pm} X^{\nu} \Pi_{\alpha}^{\pm} = 0, \tag{A.12}$$

in the light-cone coordinate frame. This breaks into two equations of motion, since $\mu = (0, 1)$. For $\mu = 0$, the string equations of motion are

$$(\partial_+ \Pi_0^+ - \Gamma_{0\nu}^{\alpha} \partial_+ X^{\nu} \Pi_{\alpha}^+) + (\partial_- \Pi_0^- - \Gamma_{0\nu}^{\alpha} \partial_- X^{\nu} \Pi_{\alpha}^-) = 0. \tag{A.13}$$

The first bracket in Eq.(A.13) can be simplified

$$\begin{aligned}
&\partial_+ \Pi_0^+ - \Gamma_{0\nu}^{\alpha} \partial_+ X^{\nu} \Pi_{\alpha}^+ \\
&= \partial_+ \left(-\frac{1}{2\pi\alpha'} G \partial_- X^0 \right) - \Gamma_{0\nu}^{\alpha} \partial_+ X^{\nu} \left(\frac{1}{2\pi\alpha'} G \eta_{\alpha\alpha} \partial_- X^{\alpha} \right) \\
&= \frac{1}{2\pi\alpha'} [-\partial_+ (G \partial_- X^0) + G \eta_{\alpha\alpha} (-\Gamma_{00}^{\alpha} \partial_+ X^0 \partial_- X^{\alpha} - \Gamma_{01}^{\alpha} \partial_+ X^1 \partial_- X^{\alpha})] \\
&= \frac{1}{2\pi\alpha'} [-\partial_+ (G \partial_- X^0) + G (\Gamma_{00}^0 \partial_+ X^0 \partial_- X^0 - \Gamma_{00}^1 \partial_+ X^0 \partial_- X^1 + \Gamma_{01}^0 \partial_+ X^1 \partial_- X^0 - \Gamma_{01}^1 \partial_+ X^1 \partial_- X^1)] ,
\end{aligned} \tag{A.14}$$

where, in the first line, the canonical momentum densities Eq.(5.9) are used and the spacetime metric simplifies due to the conformal gauge choice (i.e. $G_{\mu\nu}(x) = G \eta_{\mu\nu}$, $G^{\mu\nu}(x) = 1/G \eta^{\mu\nu}$). Further, the Christoffel symbols, defined in Eq.(4.20), can be calculated

$$\begin{aligned}
\Gamma_{00}^0 &= \frac{1}{2G} \eta^{0\gamma} (\eta_{0\gamma} \partial_0 G + \eta_{0\gamma} \partial_0 G - \eta_{00} \partial_\gamma G) = \frac{1}{2G} \eta^{00} (-\partial_0 G - \partial_0 G + \partial_0 G) = \frac{1}{2G} (\partial_0 G) \\
\Gamma_{00}^1 &= \frac{1}{2G} \eta^{1\gamma} (\eta_{0\gamma} \partial_0 G + \eta_{0\gamma} \partial_0 G - \eta_{00} \partial_\gamma G) = \frac{1}{2G} \eta^{11} (\partial_1 G) = \frac{1}{2G} (\partial_1 G) \\
\Gamma_{01}^0 &= \frac{1}{2G} \eta^{0\gamma} (\eta_{1\gamma} \partial_0 G + \eta_{0\gamma} \partial_1 G - \eta_{01} \partial_\gamma G) = \frac{1}{2G} \eta^{00} (\partial_1 G) = \frac{1}{2G} (\partial_1 G) \\
\Gamma_{01}^1 &= \frac{1}{2G} \eta^{1\gamma} (\eta_{1\gamma} \partial_0 G + \eta_{0\gamma} \partial_1 G - \eta_{01} \partial_\gamma G) = \frac{1}{2G} \eta^{11} (\partial_0 G) = \frac{1}{2G} (\partial_0 G) .
\end{aligned} \tag{A.15}$$

Hence Eq.(A.14) becomes

$$\frac{1}{2\pi\alpha'} \left[-\partial_+ (G \partial_- X^0) + \frac{1}{2} (\partial_0 G \partial_+ X^0 \partial_- X^0 - \partial_1 G \partial_+ X^0 \partial_- X^1 + \partial_1 G \partial_+ X^1 \partial_- X^0 - \partial_0 G \partial_+ X^1 \partial_- X^1) \right] , \tag{A.16}$$

where $\partial_\mu := \frac{\partial}{\partial X^\mu}$ for $\mu = (0, 1)$. The second bracket in Eq.(A.13) can be similarly simplified

$$\begin{aligned}
&\partial_- \Pi_0^- - \Gamma_{0\nu}^\alpha \partial_- X^\nu \Pi_\alpha^- \\
&= \partial_- \left(-\frac{1}{2\pi\alpha'} G \partial_+ X^0 \right) - \Gamma_{0\nu}^\alpha \partial_- X^\nu \left(\frac{1}{2\pi\alpha'} G \eta_{\alpha\alpha} \partial_+ X^\alpha \right) \\
&= \frac{1}{2\pi\alpha'} [-\partial_- (G \partial_+ X^0) + G \eta_{\alpha\alpha} (-\Gamma_{00}^\alpha \partial_- X^0 \partial_+ X^\alpha - \Gamma_{01}^\alpha \partial_- X^1 \partial_+ X^\alpha)] \\
&= \frac{1}{2\pi\alpha'} [-\partial_- (G \partial_+ X^0) + G (\Gamma_{00}^0 \partial_- X^0 \partial_+ X^0 - \Gamma_{00}^1 \partial_- X^0 \partial_+ X^1 + \Gamma_{01}^0 \partial_- X^1 \partial_+ X^0 - \Gamma_{01}^1 \partial_- X^1 \partial_+ X^1)] \\
&= \frac{1}{2\pi\alpha'} \left[-\partial_- (G \partial_+ X^0) + \frac{1}{2} (\partial_0 G \partial_- X^0 \partial_+ X^0 - \partial_1 G \partial_- X^0 \partial_+ X^1 + \partial_1 G \partial_- X^1 \partial_+ X^0 - \partial_0 G \partial_- X^1 \partial_+ X^1) \right] ,
\end{aligned} \tag{A.17}$$

where the calculated Christoffel symbols (Eq.(A.15)) are used in the final line. Using the simplifications for the first and second brackets (Eqs.(A.16, A.17)), the first string equation of motion Eq.(A.13) becomes

$$-\partial_+ (G \partial_- X^0) - \partial_- (G \partial_+ X^0) + \partial_0 G \partial_+ X^0 \partial_- X^0 - \partial_0 G \partial_+ X^1 \partial_- X^1 = 0 . \tag{A.18}$$

Following a similar calculation as before, the second string equation of motion (where $\mu = 1$) is

$$(\partial_+ \Pi_1^+ - \Gamma_{1\nu}^\alpha \partial_+ X^\nu \Pi_\alpha^+) + (\partial_- \Pi_1^- - \Gamma_{1\nu}^\alpha \partial_- X^\nu \Pi_\alpha^-) = 0 . \tag{A.19}$$

Again, the first bracket in Eq.(A.19) can be simplified

$$\begin{aligned}
&\partial_+ \Pi_1^+ - \Gamma_{1\nu}^\alpha \partial_+ X^\nu \Pi_\alpha^+ \\
&= \partial_+ \left(\frac{1}{2\pi\alpha'} G \partial_- X^1 \right) - \Gamma_{1\nu}^\alpha \partial_+ X^\nu \left(\frac{1}{2\pi\alpha'} G \eta_{\alpha\alpha} \partial_- X^\alpha \right) \\
&= \frac{1}{2\pi\alpha'} [\partial_+ (G \partial_- X^1) + G \eta_{\alpha\alpha} (-\Gamma_{10}^\alpha \partial_+ X^0 \partial_- X^\alpha - \Gamma_{11}^\alpha \partial_+ X^1 \partial_- X^\alpha)] \\
&= \frac{1}{2\pi\alpha'} [\partial_+ (G \partial_- X^1) + G (\Gamma_{10}^0 \partial_+ X^0 \partial_- X^0 - \Gamma_{10}^1 \partial_+ X^0 \partial_- X^1 + \Gamma_{11}^0 \partial_+ X^1 \partial_- X^0 - \Gamma_{11}^1 \partial_+ X^1 \partial_- X^1)] ,
\end{aligned} \tag{A.20}$$

where, in the first line, the canonical momentum densities Eq.(5.9) are used and the spacetime metric simplifies due to the conformal gauge choice. The Christoffel symbols now need to be calculated. However first note that the Christoffel symbols are symmetric on their lower indexes [96], i.e. $\Gamma_{\alpha\beta}^\gamma = \Gamma_{\beta\alpha}^\gamma$. Therefore $\Gamma_{10}^0 = \Gamma_{01}^0$ and $\Gamma_{10}^1 = \Gamma_{01}^1$ (the latter of which have both been calculated in Eq.(A.15)). The remaining two Christoffel symbols can be calculated

$$\begin{aligned}\Gamma_{11}^0 &= \frac{1}{2G} \eta^{0\gamma} (\eta_{1\gamma} \partial_1 G + \eta_{1\gamma} \partial_1 G - \eta_{11} \partial_\gamma G) = \frac{1}{2G} \eta^{00} (-\partial_0 G) = \frac{1}{2G} (\partial_0 G) \\ \Gamma_{11}^1 &= \frac{1}{2G} \eta^{1\gamma} (\eta_{1\gamma} \partial_1 G + \eta_{1\gamma} \partial_1 G - \eta_{11} \partial_\gamma G) = \frac{1}{2G} \eta^{11} (\partial_1 G + \partial_1 G - \partial_1 G) = \frac{1}{2G} (\partial_1 G).\end{aligned}\tag{A.21}$$

Hence Eq.(A.20) becomes

$$\frac{1}{2\pi\alpha'} \left[\partial_+ (G \partial_- X^1) + \frac{1}{2} (\partial_1 G \partial_+ X^0 \partial_- X^0 - \partial_0 G \partial_+ X^0 \partial_- X^1 + \partial_0 G \partial_+ X^1 \partial_- X^0 - \partial_1 G \partial_+ X^1 \partial_- X^1) \right].\tag{A.22}$$

The second bracket in Eq.(A.19) can be similarly simplified

$$\begin{aligned}\partial_- \Pi_1^- &- \Gamma_{1\nu}^\alpha \partial_- X^\nu \Pi_\alpha^- \\ &= \partial_- \left(\frac{1}{2\pi\alpha'} G \partial_+ X^1 \right) - \Gamma_{1\nu}^\alpha \partial_- X^\nu \left(\frac{1}{2\pi\alpha'} G \eta_{\alpha\alpha} \partial_+ X^\alpha \right) \\ &= \frac{1}{2\pi\alpha'} [\partial_- (G \partial_+ X^1) + G \eta_{\alpha\alpha} (-\Gamma_{10}^\alpha \partial_- X^0 \partial_+ X^\alpha - \Gamma_{11}^\alpha \partial_- X^1 \partial_+ X^\alpha)] \\ &= \frac{1}{2\pi\alpha'} [\partial_- (G \partial_+ X^1) + G (\Gamma_{10}^0 \partial_- X^0 \partial_+ X^0 - \Gamma_{10}^1 \partial_- X^0 \partial_+ X^1 + \Gamma_{11}^0 \partial_- X^1 \partial_+ X^0 - \Gamma_{11}^1 \partial_- X^1 \partial_+ X^1)] \\ &= \frac{1}{2\pi\alpha'} \left[\partial_- (G \partial_+ X^1) + \frac{1}{2} (\partial_1 G \partial_- X^0 \partial_+ X^0 - \partial_0 G \partial_- X^0 \partial_+ X^1 + \partial_0 G \partial_- X^1 \partial_+ X^0 - \partial_1 G \partial_- X^1 \partial_+ X^1) \right],\end{aligned}\tag{A.23}$$

where the calculated Christoffel symbols (Eqs.(A.15, A.21)) are used in the final line. Using the simplifications for the first and second brackets (Eqs.(A.22, A.23)), the second string equation of motion Eq.(A.19) becomes

$$\partial_+ (G \partial_- X^1) + \partial_- (G \partial_+ X^1) + \partial_1 G \partial_+ X^0 \partial_- X^0 - \partial_1 G \partial_+ X^1 \partial_- X^1 = 0.\tag{A.24}$$

Now, the two string equations of motion (Eqs.(A.18, A.24)) can be rewritten in terms of the new string embedding functions $Y^{\mu'}(\sigma^+, \sigma^-)$. Combining Eq.(A.18) and Eq.(A.24) yields

$$-\partial_+ (G \partial_- (X^0 - X^1)) - \partial_- (G \partial_+ (X^0 - X^1)) + (\partial_0 G + \partial_1 G) [\partial_+ X^0 \partial_- X^0 - \partial_+ X^1 \partial_- X^1] = 0,\tag{A.25}$$

where the derivatives are defined as $\partial_\mu := \frac{\partial}{\partial X^\mu}$ for $\mu = (0, 1)$. By the chain rule

$$\partial_0 G = (\partial_{0'} G + \partial_{1'} G) \quad \text{and} \quad \partial_1 G = (\partial_{0'} G - \partial_{1'} G),\tag{A.26}$$

where $\partial_{\mu'} := \frac{\partial}{\partial Y^{\mu'}}$ for $\mu' = (0', 1')$. Using Eq.(A.26) and the definition of $Y^{\mu'}(\sigma^+, \sigma^-)$ (Eq.(5.8)), the equation of motion Eq.(A.25) becomes

$$\begin{aligned}
0 &= -\sqrt{2} \left[\partial_+ \left(G \partial_- Y^{1'} \right) + \partial_- \left(G \partial_+ Y^{1'} \right) \right] + \sqrt{2} \partial_0 G \left[\frac{1}{2} \partial_+ \left(Y^{0'} + Y^{1'} \right) \partial_- \left(Y^{0'} + Y^{1'} \right) \right. \\
&\quad \left. - \frac{1}{2} \partial_+ \left(Y^{0'} - Y^{1'} \right) \partial_- \left(Y^{0'} - Y^{1'} \right) \right] \\
&= \partial_+ \left(G \partial_- Y^{1'} \right) + \partial_- \left(G \partial_+ Y^{1'} \right) + \frac{1}{2} \partial_0 G \left[\partial_+ Y^{0'} \partial_- Y^{0'} + \partial_+ Y^{0'} \partial_- Y^{1'} + \partial_+ Y^{1'} \partial_- Y^{0'} + \partial_+ Y^{1'} \partial_- Y^{1'} \right. \\
&\quad \left. - \partial_+ Y^{0'} \partial_- Y^{0'} + \partial_+ Y^{0'} \partial_- Y^{1'} + \partial_+ Y^{1'} \partial_- Y^{0'} - \partial_+ Y^{1'} \partial_- Y^{1'} \right] \\
&= \partial_+ \left(G \partial_- Y^1 \right) + \partial_- \left(G \partial_+ Y^1 \right) - (\partial_0 G) \left[(\partial_+ Y^0) (\partial_- Y^1) + (\partial_+ Y^1) (\partial_- Y^0) \right],
\end{aligned} \tag{A.27}$$

where the indices have been renamed ($\mu' = \mu$) in the last line. This is precisely one of the string equations of motion given in subsection (5.1.1), Eq.(5.13). In order to find the other string equation of motion, subtract Eq.(A.18) from Eq.(A.24) to yield

$$\begin{aligned}
0 &= -\partial_+ \left(G \partial_- (X^0 + X^1) \right) - \partial_- \left(G \partial_+ (X^0 + X^1) \right) + (\partial_0 G - \partial_1 G) \left[\partial_+ X^0 \partial_- X^0 - \partial_+ X^1 \partial_- X^1 \right] \\
&\quad - \sqrt{2} \left[\partial_+ \left(G \partial_- Y^{0'} \right) + \partial_- \left(G \partial_+ Y^{0'} \right) \right] + \sqrt{2} \partial_1 G \left[\frac{1}{2} \partial_+ \left(Y^{0'} + Y^{1'} \right) \partial_- \left(Y^{0'} + Y^{1'} \right) \right. \\
&\quad \left. - \frac{1}{2} \partial_+ \left(Y^{0'} - Y^{1'} \right) \partial_- \left(Y^{0'} - Y^{1'} \right) \right] \\
&= \partial_+ \left(G \partial_- Y^0 \right) + \partial_- \left(G \partial_+ Y^0 \right) - (\partial_1 G) \left[(\partial_+ Y^0) (\partial_- Y^1) + (\partial_+ Y^1) (\partial_- Y^0) \right].
\end{aligned} \tag{A.28}$$

The Virasoro constraints Eq.(A.11) and the string equations of motion Eqs.(A.27, A.28) agree with the equations given by Bars *et al.* in [107, 108] where $u = Y^0$ and $v = Y^1$. Further, using the product and chain rules, Eq.(A.27) becomes

$$\begin{aligned}
0 &= (\partial_+ G) (\partial_- Y^1) + G \partial_+ (\partial_- Y^1) + (\partial_- G) (\partial_+ Y^1) + G \partial_- (\partial_+ Y^1) \\
&\quad - (\partial_0 G) \left[(\partial_+ Y^0) (\partial_- Y^1) + (\partial_+ Y^1) (\partial_- Y^0) \right] \\
&= [(\partial_0 G) (\partial_+ Y^0) + (\partial_1 G) (\partial_+ Y^1)] (\partial_- Y^1) + [(\partial_0 G) (\partial_- Y^0) + (\partial_1 G) (\partial_- Y^1)] (\partial_+ Y^1) + 2 G \partial_+ (\partial_- Y^1) \\
&\quad - (\partial_0 G) \left[(\partial_+ Y^0) (\partial_- Y^1) + (\partial_+ Y^1) (\partial_- Y^0) \right] \\
&= G \partial_+ \partial_- Y^1 + (\partial_1 G) (\partial_+ Y^1) (\partial_- Y^1),
\end{aligned} \tag{A.29}$$

and Eq.(A.28) becomes

$$\begin{aligned}
0 &= (\partial_+ G) (\partial_- Y^0) + G \partial_+ (\partial_- Y^0) + (\partial_- G) (\partial_+ Y^0) + G \partial_- (\partial_+ Y^0) \\
&\quad - (\partial_1 G) \left[(\partial_+ Y^0) (\partial_- Y^1) + (\partial_+ Y^1) (\partial_- Y^0) \right] \\
&= [(\partial_0 G) (\partial_+ Y^0) + (\partial_1 G) (\partial_+ Y^1)] (\partial_- Y^0) + [(\partial_0 G) (\partial_- Y^0) + (\partial_1 G) (\partial_- Y^1)] (\partial_+ Y^0) + 2 G \partial_+ (\partial_- Y^0) \\
&\quad - (\partial_1 G) \left[(\partial_+ Y^0) (\partial_- Y^1) + (\partial_+ Y^1) (\partial_- Y^0) \right] \\
&= G \partial_+ \partial_- Y^0 + (\partial_0 G) (\partial_+ Y^0) (\partial_- Y^0),
\end{aligned} \tag{A.30}$$

which agrees exactly with the string equations of motion given by Moerman *et al.* in [52].

A.3 Energy of a Test String in an AdS-Schwarzschild Background

At $t = 0$ the test string set-up for the heavy quark agrees with the test string set-up for the light quark, since the string is initially static in both cases – i.e. $X^I = 0$ (where $I \in (2, 3, \dots, d-1)$) at time $t = 0$, with embedding functions $X^\mu(t, \sigma) = (t, r(t, \sigma), 0)^\mu$. The on-mass-shell heavy quark's mass or the off-mass-shell light quark's mass¹²⁹ can be calculated by finding the total energy of the relevant test string in AdS_d -Schwarzschild. In order to calculate the string's total energy, the configuration of the string is chosen to be stretched between the radial positions $r = 0$ and $r = \ell_0$. This choice will simplify the calculation.

The AdS_d -Schwarzschild metric in d dimensions is given by

$$\begin{aligned} ds_d^2 &:= G_{\mu\nu} dx^\mu dx^\nu \\ &= G_{tt} dt^2 + G_{rr} dr^2 + G_{II} d\vec{X}_I^2 \\ &= \frac{r^2}{l^2} \left(-h(r; d) dt^2 + d\vec{X}_I^2 \right) + \frac{l^2}{r^2} \frac{dr^2}{h(r; d)}, \end{aligned} \quad (\text{A.31})$$

where $t \in [0, \infty)$ is the temporal coordinate, $r \in [0, \infty)$ is the radial coordinate, and the transverse spatial directions are denoted by $\vec{X}_I = (X^2, X^3, \dots, X^{(d-1)}) \in \mathbb{R}^{d-2}$. Further, $l \in \mathbb{R}^+$ is the curvature radius of AdS_d and S^d , and the blackening factor of the Schwarzschild black hole situated at the horizon, $h(r; d)$, is given by Eq.(4.34). Explicitly, the target spacetime metric $G_{\mu\nu}$ is given by

$$G_{\mu\nu} = \begin{bmatrix} \left(-\frac{r^2}{l^2} h(r; d) \right) & 0 & 0 & 0 & 0 & 0 \\ 0 & \left(\frac{l^2}{r^2} \frac{1}{h(r; d)} \right) & 0 & 0 & 0 & 0 \\ 0 & 0 & \left(\frac{r^2}{l^2} \right) & 0 & 0 & 0 \\ 0 & 0 & 0 & \left(\frac{r^2}{l^2} \right) & \ddots & 0 \\ 0 & 0 & 0 & \ddots & \ddots & 0 \\ 0 & 0 & 0 & 0 & 0 & \left(\frac{r^2}{l^2} \right) \end{bmatrix}, \quad (\text{A.32})$$

where μ, ν index over $(t, r, 2, \dots, d-1)$. The induced worldsheet metric g_{ab} , defined in Eq.(4.2), takes the explicit form

$$g_{ab} = \begin{bmatrix} g_{tt} & g_{t\sigma} \\ g_{\sigma t} & g_{\sigma\sigma} \end{bmatrix}, \quad (\text{A.33})$$

since (t, σ) are the two parameter space coordinates in the static gauge ($\tau = t$). In order to determine the explicit entries of the induced metric g_{ab} , the definition Eq.(4.2) is used to calculate each component. Specifically,

$$g_{ab} = \begin{bmatrix} G_{tt} + G_{II} \dot{X}_I^2 & G_{II} \dot{X}_I X'_I \\ G_{II} X'_I \dot{X}_I & r'^2 G_{rr} + G_{II} X'^2_I \end{bmatrix}, \quad (\text{A.34})$$

where $\dot{X} \equiv \partial_t X$ and $X' \equiv \partial_\sigma X$; I indexes over the transverse directions $X_I = (X^2, X^3, \dots, X^{(d-1)})$; and the fact that $G_{\mu\nu}$ (Eq.(A.32)) is a diagonal matrix is used.

¹²⁹Particles are *on the mass shell*, or simply *on-mass-shell*, if their behaviour satisfies Einstein's energy and momentum relation $E^2 = (pc)^2 + (mc)^2$. Particles whose behaviour violates this relation are known as *off-mass-shell*. In the case of the light quark it starts at $t = 0$ as an off-mass-shell particle (corresponding to the initial static string), radiates energy as it travels through the thermal medium (string contracts as the boundary endpoint falls at the local speed of light), and finally stops radiating as it becomes an on-mass-shell particle. This appendix is focused on calculating the mass (or *virtuality*) of the light quark as an initially off-mass-shell particle; and the mass of an on-mass-shell heavy quark.

For later use, the inverse metric g^{ab} (where $g^{ab} \equiv (g_{ab})^{-1}$) is also written out explicitly

$$g^{ab} = \frac{1}{\det(g_{ab})} \begin{bmatrix} r'^2 G_{rr} + G_{II} X_I'^2 & -G_{II} \dot{X}_I X_I' \\ -G_{II} X_I' \dot{X}_I & G_{tt} + G_{II} \dot{X}_I^2 \end{bmatrix}. \quad (\text{A.35})$$

The determinant of the induced metric is

$$\begin{aligned} g := \det(g_{ab}) &= (r'^2 G_{rr} + G_{II} X_I'^2) (G_{tt} + G_{II} \dot{X}_I^2) - (G_{II}^2 \dot{X}_I^2 X_I'^2) \\ &= r'^2 G_{rr} G_{tt} + r'^2 G_{rr} G_{II} \dot{X}_I^2 + G_{tt} G_{II} X_I'^2 + G_{II}^2 X_I'^2 \dot{X}_I^2 - G_{II}^2 \dot{X}_I^2 X_I'^2 \\ &= G_{rr} G_{tt} \left(r'^2 + \frac{r'^2}{G_{tt}} G_{II} \dot{X}_I^2 + \frac{1}{G_{rr}} G_{II} X_I'^2 \right). \end{aligned} \quad (\text{A.36})$$

Now that the ground work has been laid, the total energy of the static string can be calculated

$$\begin{aligned} E &= \int_0^{\ell_0} d\sigma \Pi_t^\tau \\ &= -\frac{1}{2\pi\alpha'} \int_0^{\ell_0} d\sigma \sqrt{-\gamma} \gamma^{\tau b} G_{t\nu} \partial_b X^\nu \\ &= -\frac{1}{2\pi\alpha'} \int_0^{\ell_0} d\sigma \sqrt{-g} g^{tb} G_{tt} \partial_b X^t \\ &= -\frac{1}{2\pi\alpha'} \int_0^{\ell_0} d\sigma \sqrt{-g} (g^{tt} \partial_t X^t + g^{t\sigma} \partial_\sigma X^t) \left(-\frac{r^2}{l^2} h(r; d) \right) \\ &= \frac{1}{2\pi\alpha'} \int_0^{\ell_0} d\sigma \sqrt{-g} g^{tt} \left(\frac{r^2}{l^2} h(r; d) \right) \\ &= \frac{1}{2\pi\alpha'} \int_0^{\ell_0} d\sigma \sqrt{-g} (r'^2 G_{rr} + G_{II} X_I'^2) \left(\frac{r^2}{l^2} h(r; d) \right) \\ &= \frac{1}{2\pi\alpha'} \int_0^{\ell_0} d\sigma \sqrt{-g} r'^2 \left(\frac{l^2}{r^2} \frac{1}{h(r; d)} \right) \left(\frac{r^2}{l^2} h(r; d) \right), \end{aligned} \quad (\text{A.37})$$

where the constraint equation Eq.(4.10) and the static gauge choice ($\tau = t$) are used in the third line, and Eq.(A.32) is used in the fourth line. The fifth line follows from remembering the string is static ($X_I = 0$), and Eq.(A.35) is used in the sixth line.

Using Eq.(A.36), the total energy of the static string (Eq.(A.37)) becomes

$$\begin{aligned} E &= \frac{1}{2\pi\alpha'} \int_0^{\ell_0} d\sigma r'^2 \sqrt{-G_{rr} G_{tt} \left(r'^2 + \frac{r'^2}{G_{tt}} G_{II} \dot{X}_I^2 + \frac{1}{G_{rr}} G_{II} X_I'^2 \right)} \\ &= \frac{1}{2\pi\alpha'} \int_0^{\ell_0} d\sigma r'^2 \sqrt{-r'^2 G_{rr} G_{tt}} \\ &= \frac{1}{2\pi\alpha'} \int_0^{\ell_0} d\sigma \partial_\sigma^3 r, \end{aligned} \quad (\text{A.38})$$

where Eq.(A.36) is used in the first line, the second line follows again from $X_I = 0$, and Eq.(A.32) is used the final line.

From Eq.(A.38) it is apparent that the energy of the string is contingent on how the radial coordinate r depends on the worldsheet parameter space coordinate σ . In the static gauge (which is employed in sections (4) and (5)) the energy of the test string is easily found in AdS₃-Schwarzschild by using the identification Eq.(4.52) and solving the integral in Eq.(A.38). Since the tortoise coordinate in anti-de Sitter-Schwarzschild spacetime can only be inverted for $d = 3$, an equivalent identification to Eq.(4.52) in AdS _{d} -Schwarzschild can not be found. However, a different gauge choice can be made. Taking, for example, the gauge choice¹³⁰ in section (6) where $\tau = t$ and $\sigma = r$ are the worldsheet coordinates, Eq.(A.38) becomes

$$E = \frac{1}{2\pi\alpha'} [\ell_0 - 0], \quad (\text{A.39})$$

in AdS _{d} -Schwarzschild. Therefore

$$E^2 \equiv m_q^2 = \frac{\ell_0^2}{4\pi^2\alpha'^2}, \quad (\text{A.40})$$

where the first equivalence follows from the AdS/CFT correspondence: the energy of a test string in the bulk theory is equivalent to the mass of the given probe quark in the boundary theory. Notice that Eq.(A.40) agrees with Eq.(4.31), which is a reflection of the fact that the spacetime in the bulk theory is curved precisely along the additional radial direction r , and not along the temporal or transverse directions. Since the boundary theory does not include this radial direction, from the perspective of the probe quark its mass will be the same whether the string is in Minkowski or AdS-Schwarzschild spacetime¹³¹. Considering that

$$\sqrt{\alpha'} \equiv \frac{l}{\lambda^{1/4}}, \quad (\text{A.41})$$

where $l \in \mathbb{R}^+$ is the radius of curvature of AdS _{d} and $\lambda = g_{YM}^2 N_c$ is the 't Hooft coupling (see table (1), page 6); the quark's mass¹³² becomes

$$m_q^2 = \frac{\lambda \ell_0^2}{4\pi^2 l^4}. \quad (\text{A.42})$$

Alternatively, Eq.(A.42) can be rewritten as

$$m_q = \frac{\sqrt{\lambda} \ell_0}{\beta r_H} = \frac{\sqrt{\lambda}}{\beta} \frac{(r_s + \ell_0 - r_s)}{r_H} = \frac{\sqrt{\lambda}}{\beta} \left(\tilde{r}_0 - \frac{r_s}{r_H} \right) \approx \frac{\sqrt{\lambda}}{\beta} \tilde{r}_0, \quad (\text{A.43})$$

where the first equality follows from using the definition of the Hawking temperature Eq.(4.35); the second equality from Eq.(4.88); and the approximation from the definition of the stretched horizon $r_s = (1 + \epsilon)r_H$ (where $0 < \epsilon \ll 1$). Using the definition of the Hawking temperature yields $m_q = \sqrt{\lambda} \tilde{r}_0 T$. Eq.(A.43) might be a convenient form of the quark mass m_q in some cases.

¹³⁰This gauge choice is also made in [22, 35].

¹³¹In an AdS/CFT context, this implies that the energy of the string is equivalent in Minkowski or AdS-Schwarzschild spacetime.

¹³²Remembering this is either the initial, off-mass-shell mass for the light quark or the on-mass-shell mass for the heavy quark.

A.4 Nambu-Goto String Equations of Motion for Transverse Fluctuations

The calculation of the string equations of motion for the transverse fluctuations presented in this appendix, follows the layout of appendix (B) in Moerman *et al.*'s exposition on light quark Brownian motion [52]. Working in the static gauge, the transverse string equations of motion are derived by varying the effective action for the transverse fluctuations with respect to the transverse string worldsheet coordinates, and setting this functional variation to zero.

Using the definition Eq.(4.5), the effective transverse action Eq.(4.61) can be written in terms of the transverse canonical momentum densities

$$S_{NG}^{(2)} = \frac{1}{2} \int_{\mathcal{M}} d^2\sigma \Pi_I^a(t, \sigma) \partial_a X^I(t, \sigma). \quad (\text{A.44})$$

Determining the functional derivative of $S_{NG}^{(2)}$ with respect to X^I and setting this variation to vanish, results in

$$\begin{aligned} 0 = \delta_X S_{NG}^{(2)} &= \frac{1}{2} \int_{\mathcal{M}} d^2\sigma \left[(\delta \Pi_I^a) \partial_a X^I + \Pi_I^a \partial_a (\delta X^I) \right] \\ &= \frac{1}{2} \int_{\mathcal{M}} d^2\sigma \left[(\delta \Pi_I^a) \partial_a X^I + \partial_a (\Pi_I^a \delta X^I) - \partial_a (\Pi_I^a) \delta X^I \right], \end{aligned} \quad (\text{A.45})$$

where the product rule is used in the second line.

The functional derivative of the momentum densities with respect to X^I is given by

$$\delta_X \Pi_I^a = -\frac{1}{2\pi\alpha'} (\sqrt{-g} g^{ab} G_{IJ})|_{X_0^\mu} \partial_b (\delta X^J), \quad (\text{A.46})$$

where the spacetime metric $G_{\mu\nu}$ does not need to be varied since it is independent of the transverse directions X^I (Eq.(A.32)). Hence the first term in Eq.(A.45), $(\delta \Pi_I^a) \partial_a X^I$, becomes

$$\begin{aligned} (\delta_X \Pi_I^a) \partial_a X^I &= \left(-\frac{1}{2\pi\alpha'} (\sqrt{-g} g^{ab} G_{IJ})|_{X_0^\mu} \partial_b (\delta X^J) \right) \partial_a X^I \\ &= \left(-\frac{1}{2\pi\alpha'} (\sqrt{-g} g^{ab} G_{IJ})|_{X_0^\mu} \partial_a X^\mu \right) \partial_b (\delta X^J) \\ &= \Pi_J^b \partial_b (\delta X^J) \\ &= \partial_b (\Pi_J^b \delta X^J) - (\partial_b \Pi_J^b) \delta X^J, \end{aligned} \quad (\text{A.47})$$

where the definition of the momentum densities Eq.(4.65) are used in the third line, and the product rule is used in the final line. Inputting Eq.(A.47) into Eq.(A.45), yields

$$\begin{aligned} 0 = \delta_X S_{NG}^{(2)} &= \frac{1}{2} \int_{\mathcal{M}} d^2\sigma \left[\partial_b (\Pi_J^b \delta X^J) - (\partial_b \Pi_J^b) \delta X^J + \partial_a (\Pi_I^a \delta X^I) - \partial_a (\Pi_I^a) \delta X^I \right] \\ &= - \int_{\mathcal{M}} d^2\sigma \delta X^I (\partial_a \Pi_I^a) + \int_{\mathcal{M}} d^2\sigma \partial_a (\Pi_I^a \delta X^I) \\ &= - \int_{\mathcal{M}} d^2\sigma \delta X^I (\partial_a \Pi_I^a) + \int_{\partial\mathcal{M}} d\sigma^b \epsilon_{ba} (\Pi_I^a \delta X^I) \\ &= - \int_{\mathcal{M}} d^2\sigma \delta X^I (\partial_a \Pi_I^a) + \int_0^{\tau_f} d\tau \left[\Pi_I^a \delta X^I \Big|_{\sigma=0}^{\sigma=\sigma_f} \right], \end{aligned} \quad (\text{A.48})$$

where, in the second line, the indices have been renamed and the terms grouped; and Stokes's Theorem in d-dimensions [96] has been used in the third line. In the final line the coordinates on the worldsheet parameter space are chosen to be $\sigma^a = (t, \sigma)^a$ where $\sigma^a \in \mathcal{M} = [0, t_f] \times [0, \sigma_f]$, and one of the integrals of the last term is simplified by using $\delta X^I|_{t \in \{0, t_f\}} = 0$.

Choosing the boundary conditions

$$\Pi_I^a \delta X^I \Big|_{\sigma=0}^{\sigma=\sigma_f} = 0, \quad (\text{A.49})$$

the last term in Eq.(A.48) disappears. Hence, the string equations of motion for the transverse fluctuations are given by

$$0 = \partial_a \Pi_I^a = \nabla_a \Pi_I^a, \quad (\text{A.50})$$

which agrees with Eq.(4.66). The second equality follows because $\nabla_a \Pi_\mu^a := \partial_a \Pi_\mu^a - \Gamma_{\mu\nu}^\alpha \partial_a X^\nu \Pi_\mu^a$ in curved spacetime, but the second term vanishes since the Christoffel symbols are identically zero ($\Gamma_{IJ}^\alpha = 0$) due to symmetry between each of the transverse X^I directions.

A.5 Canonical Commutation Relations and Normalised Basis

This appendix aims to fix the normalization constant A_ω , thereby completely determining the general solution for the transverse equations of motion (Eq.(4.91)) discussed in subsection (4.3.2). In order to determine A_ω the theory is quantized: the scalar field $X(t, \sigma)$ and its canonically conjugate momentum $P^t(t, \sigma)$ are promoted to operators (Eqs.(4.92, 4.93) respectively), and suitable commutation relations are imposed

$$\begin{aligned} \left[\hat{X}(t, \sigma), n_t \hat{P}^t(t, \sigma') \right]_\Sigma &= i \delta(\sigma, \sigma') = i \frac{\delta(\sigma - \sigma')}{\sqrt{\tilde{g}}|\Sigma|}, \\ \left[\hat{X}(t, \sigma), \hat{X}(t, \sigma') \right]_\Sigma &= \left[n_t \hat{P}^t(t, \sigma), n_t \hat{P}^t(t, \sigma') \right]_\Sigma = 0, \end{aligned} \quad (\text{A.51})$$

where Σ is a Cauchy hypersurface in the $x^\mu = (t, r)^\mu$ part of spacetime that is chosen to be a constant time surface¹³³, \tilde{g} is the induced metric on Σ , and n_μ is the future pointing normal to Σ (where $n_\mu = \delta_{\mu t} / \sqrt{-\tilde{g}_{tt}}$). The commutation relations described in Eq.(A.51) are known as equal time commutation relations – they encode the expectation that simultaneous measurements at different points on the string do not interfere with each other [92].

Additionally, canonical creation and annihilation commutation relations on the Fourier coefficient operators ($\hat{a}_\omega, \hat{a}_\omega^\dagger$) are enforced:

$$\begin{aligned} \left[\hat{a}_\omega, \hat{a}_{\omega'}^\dagger \right]_\Sigma &= 2\pi \delta(\omega - \omega'), \\ \left[\hat{a}_\omega, \hat{a}_{\omega'} \right]_\Sigma &= \left[\hat{a}_\omega^\dagger, \hat{a}_{\omega'}^\dagger \right]_\Sigma = 0. \end{aligned} \quad (\text{A.52})$$

Consistency between the commutation relations Eq.(A.51) and Eq.(A.52) is required¹³⁴. To this end, the commutator bracket $\left[\hat{X}(t, \sigma), n_t \hat{P}^t(t, \sigma') \right]_\Sigma$ is calculated from the definitions Eqs.(4.92, 4.93), and the result is equated to the relevant right hand side of Eq.(A.51). Specifically,

$$\begin{aligned} \left[\hat{X}(t, \sigma), n_t \hat{P}^t(t, \sigma') \right]_\Sigma &= \hat{X}(t, \sigma)|_\Sigma n_t \hat{P}^t(t, \sigma')|_\Sigma - n_t \hat{P}^t(t, \sigma')|_\Sigma \hat{X}(t, \sigma)|_\Sigma, \\ &= -\frac{i}{2\pi\alpha'} \frac{r^2}{l^2} \frac{\delta_{tt}}{\sqrt{\tilde{g}}|\Sigma|} \int_0^\infty \frac{d\omega d\omega'}{(2\pi)^2} \omega A_\omega A_{\omega'} \times \\ &\quad \left([f_\omega(\sigma) e^{-i\omega t} \hat{a}_\omega + f_\omega^*(\sigma) e^{i\omega t} \hat{a}_\omega^\dagger] [f_{\omega'}(\sigma') e^{-i\omega' t} \hat{a}_{\omega'} - f_{\omega'}^*(\sigma') e^{i\omega' t} \hat{a}_{\omega'}^\dagger] \right. \\ &\quad \left. - [f_{\omega'}(\sigma') e^{-i\omega' t} \hat{a}_{\omega'} - f_{\omega'}^*(\sigma') e^{i\omega' t} \hat{a}_{\omega'}^\dagger] [f_\omega(\sigma) e^{-i\omega t} \hat{a}_\omega + f_\omega^*(\sigma) e^{i\omega t} \hat{a}_\omega^\dagger] \right) \\ &= -\frac{i}{2\pi\alpha'} \frac{r^2}{l^2} \frac{1}{\sqrt{\tilde{g}}|\Sigma|} \int_0^\infty \frac{d\omega d\omega'}{(2\pi)^2} \omega A_\omega A_{\omega'} \times \\ &\quad \left(-f_\omega(\sigma) f_{\omega'}^*(\sigma') e^{i(\omega' - \omega)t} \hat{a}_\omega \hat{a}_{\omega'}^\dagger + f_\omega^*(\sigma) f_{\omega'}(\sigma') e^{i(\omega - \omega')t} \hat{a}_\omega^\dagger \hat{a}_{\omega'} \right. \\ &\quad \left. - f_{\omega'}(\sigma') f_\omega^*(\sigma) e^{i(\omega - \omega')t} \hat{a}_{\omega'} \hat{a}_\omega^\dagger + f_{\omega'}^*(\sigma') f_\omega(\sigma) e^{i(\omega' - \omega)t} \hat{a}_{\omega'}^\dagger \hat{a}_\omega \right) \\ &= -\frac{i}{2\pi\alpha'} \frac{r^2}{l^2} \frac{1}{\sqrt{\tilde{g}}|\Sigma|} \int_0^\infty \frac{d\omega d\omega'}{2\pi} \omega A_\omega A_{\omega'} \times \\ &\quad \left(-f_\omega(\sigma) f_{\omega'}^*(\sigma') e^{i(\omega' - \omega)t} \delta(\omega - \omega') - f_{\omega'}(\sigma') f_\omega^*(\sigma) e^{i(\omega - \omega')t} \delta(\omega' - \omega) \right), \end{aligned} \quad (\text{A.53})$$

¹³³Giving initial conditions on this hypersurface determines the future (and past) evolution uniquely.

¹³⁴In order to ensure consistent quantization of the theory.

where the third line follows because the cross terms $(\hat{a}_\omega \hat{a}_{\omega'} - \hat{a}_{\omega'} \hat{a}_\omega)$ and $(\hat{a}_\omega^\dagger \hat{a}_{\omega'}^\dagger - \hat{a}_{\omega'}^\dagger \hat{a}_\omega^\dagger)$ vanish (using the second commutation relation in Eq.(A.52)); and the fourth line follows from using the first commutation relation in Eq.(A.52). Collecting terms, and converting to (t, r_*) coordinates using Eq.(4.52), yields

$$\begin{aligned} \therefore \left[\hat{X}(t, \sigma), n_t \hat{P}^t(t, \sigma') \right]_\Sigma &= -\frac{i}{2\pi\alpha'} \frac{r^2}{l^2} \frac{1}{\sqrt{\tilde{g}}|\Sigma} \int_0^\infty \frac{d\omega}{2\pi} \omega A_\omega^2 (-f_\omega(\sigma) f_\omega^*(\sigma') - f_\omega(\sigma') f_\omega^*(\sigma)) \\ &= \frac{i}{2\pi\alpha'} \frac{r_H^2}{l^2} \coth^2 \left(\frac{r_H(r_{s*} + \sigma')}{l^2} \right) \frac{1}{\sqrt{\tilde{g}}|\Sigma} \int_0^\infty \frac{d\omega}{2\pi} \omega A_\omega^2 (f_\omega(\sigma) f_\omega^*(\sigma') + f_\omega(\sigma') f_\omega^*(\sigma)) . \end{aligned} \quad (\text{A.54})$$

Inputting Eqs.(4.83, 4.85, 4.90), the commutator becomes¹³⁵

$$\left[\hat{X}(t, \sigma), n_t \hat{P}^t(t, \sigma') \right]_\Sigma = \frac{1}{\sqrt{\tilde{g}}|\Sigma} \frac{i}{\pi\alpha'} \frac{r_H^2}{l^2} \int_0^\infty \frac{d\omega}{2\pi} \omega A_\omega^2 \left(e^{-i(\sigma+\sigma')\omega} + e^{i(\sigma-\sigma')\omega} + e^{i(\sigma+\sigma')\omega} + e^{i(\sigma'-\sigma)\omega} \right), \quad (\text{A.55})$$

where the near-horizon limit ($r \rightarrow r_H \equiv r_{s*} \rightarrow -\infty \equiv \tilde{r}_0 \rightarrow 1$) has been taken after multiplication¹³⁶. Note that in the near-horizon limit,

$$\coth^2 \left(\frac{r_H(r_{s*} + \sigma)}{l^2} \right) \rightarrow 1, \quad \text{as } r_{s*} \rightarrow -\infty. \quad (\text{A.56})$$

The commutator Eq.(A.55) can be further simplified

$$\begin{aligned} &\left[\hat{X}(t, \sigma), n_t \hat{P}^t(t, \sigma') \right]_\Sigma \\ &= \frac{1}{\sqrt{\tilde{g}}|\Sigma} \frac{i}{\pi\alpha'} \frac{r_H^2}{l^2} \left(\int_0^\infty \frac{d\omega}{2\pi} \omega A_\omega^2 \left[e^{-i(\sigma+\sigma')\omega} + e^{-i(\sigma-\sigma')\omega} \right] + \int_0^\infty \frac{d\omega}{2\pi} \omega A_\omega^2 \left[e^{i(\sigma+\sigma')\omega} + e^{i(\sigma-\sigma')\omega} \right] \right) \\ &= \frac{1}{\sqrt{\tilde{g}}|\Sigma} \frac{i}{\pi\alpha'} \frac{r_H^2}{l^2} \left(-\int_{-\infty}^0 \frac{d\omega}{2\pi} \omega A_\omega^2 \left[e^{-i(\sigma+\sigma')\omega} + e^{-i(\sigma-\sigma')\omega} \right] + \int_0^\infty \frac{d\omega}{2\pi} \omega A_\omega^2 \left[e^{i(\sigma+\sigma')\omega} + e^{i(\sigma-\sigma')\omega} \right] \right) \\ &= \frac{1}{\sqrt{\tilde{g}}|\Sigma} \frac{i}{\pi\alpha'} \frac{r_H^2}{l^2} \left(-\int_{-\infty}^0 \frac{(-d\omega)}{2\pi} (-\omega) (-A_\omega^2) \left[e^{i(\sigma+\sigma')\omega} + e^{i(\sigma-\sigma')\omega} \right] + \int_0^\infty \frac{d\omega}{2\pi} \omega A_\omega^2 \left[e^{i(\sigma+\sigma')\omega} + e^{i(\sigma-\sigma')\omega} \right] \right) \\ &= \frac{1}{\sqrt{\tilde{g}}|\Sigma} \frac{i}{\pi\alpha'} \frac{r_H^2}{l^2} \int_{-\infty}^\infty \frac{d\omega}{2\pi} \omega A_\omega^2 \left[e^{i(\sigma+\sigma')\omega} + e^{i(\sigma-\sigma')\omega} \right]. \end{aligned} \quad (\text{A.57})$$

In order for Eq.(A.57) to be consistent with the definition of the commutation relation Eq.(A.51), the normalization constant needs to be defined as

$$A_\omega := \frac{l}{r_H} \sqrt{\frac{\pi\alpha'}{\omega}} = \frac{\beta}{2\sqrt{\pi\omega} \lambda^{1/4}}, \quad (\text{A.58})$$

¹³⁵Mathematica is used to be spared from the tedious multiplication (see Mathematica Notebook [b]: **BrownianMotion.nb**).

¹³⁶If the commutation relations hold in the near-horizon limit (i.e. for a specific value of (t, σ)) then they hold $\forall (t, \sigma)$. In [42] de Boer *et al.* determine the normalization constant A by demanding the normalization of the modes through the Klein-Gordon inner product. The near-horizon limit is taken during this calculation. In a later work [46], Appendix A, a similar collaboration Atmaja *et al.* argue that the inner product contribution from the near-horizon region can be thought of as the overall inner product. There is a contribution to the inner product from regions away from the horizon; however, the near-horizon region is semi-infinite in the tortoise coordinate r_* ($r \rightarrow r_H \equiv r_{s*} \rightarrow -\infty$); and as such the normalization can be completely fixed by the near-horizon regime. Therefore, the near-horizon limit can be taken here without concern.

where the second equality follows from using the definition of the AdS radius of curvature l (Eq.(4.64)), and the relation $l = \beta r_H^2 / 2\pi$ from Eq.(4.35).

To prove that the commutation relations Eq.(A.51) now hold, input the newly defined A_ω into Eq.(A.57). Explicitly,

$$\begin{aligned}
\left[\hat{X}(t, \sigma), n_t \hat{P}^t(t, \sigma') \right]_\Sigma &= \frac{1}{\sqrt{\tilde{g}}|_\Sigma} \frac{i}{\pi \alpha'} \frac{r_H^2}{l^2} \int_{-\infty}^{\infty} \frac{d\omega}{2\pi} \omega \left(\frac{l^2}{r_H^2} \frac{\pi \alpha'}{\omega} \right) \left[e^{i(\sigma + \sigma')\omega} + e^{i(\sigma - \sigma')\omega} \right] \\
&= \frac{i}{\sqrt{\tilde{g}}|_\Sigma} \int_{-\infty}^{\infty} \frac{d\omega}{2\pi} \omega \left[e^{i(\sigma + \sigma')\omega} + e^{i(\sigma - \sigma')\omega} \right] \\
&= \frac{i}{\sqrt{\tilde{g}}|_\Sigma} [\delta(\sigma + \sigma') + \delta(\sigma - \sigma')] \\
&= \frac{i}{\sqrt{\tilde{g}}|_\Sigma} \delta(\sigma - \sigma'),
\end{aligned} \tag{A.59}$$

where the third line follows from the Dirac delta function property $\delta(y - x) = \frac{1}{2\pi} \int_{-\infty}^{\infty} dk e^{-ik(y-x)}$; and, in the final line, the first Dirac delta function has disappeared since $\sigma, \sigma' \in [0, \sigma_f]$. Hence, the scalar field and conjugate momentum commutation relations (Eq.(A.51)) and the Fourier coefficient creation and annihilation commutation relations (Eq.(A.57)) are consistent; proving that the normalization constant A_ω is correctly given by Eq.(A.58).

A.6 Leading Order Contributions of the Near-Horizon Tortoise Coordinate

The tortoise coordinate r_* is defined in Eq.(4.38). In the near-horizon limit ($r = (1+\tilde{\epsilon})r_H$) the tortoise coordinate can be expanded and truncated around $\tilde{\epsilon} = 0$, in order to yield the near-horizon tortoise coordinate, $\tilde{\epsilon}_*$. This coordinate is given – for general d dimensions – by

$$\begin{aligned}\tilde{\epsilon}_* &:= \frac{l^2}{r_H^2(d-1)} \ln(\tilde{\epsilon}) + \frac{(d-4)l^2}{2r_H^2(d-1)} \tilde{\epsilon} + \frac{(d^2-14d+36)l^2}{24r_H^2(d-1)} \tilde{\epsilon}^2 - \frac{(5d^2-46d+96)l^2}{72r_H^2(d-1)} \tilde{\epsilon}^3 + \mathcal{O}(\tilde{\epsilon})^4 \\ &= a_0 \ln(\tilde{\epsilon}) + a_1 \tilde{\epsilon} + a_2 \tilde{\epsilon}^2 + a_3 \tilde{\epsilon}^3 + \mathcal{O}(\tilde{\epsilon})^4 ,\end{aligned}\tag{A.60}$$

where $r_* = r_H \tilde{\epsilon}_*$, and a_0, a_1, a_2, a_3 are constants. To leading order, the near-horizon AdS_d -Schwarzschild metric is given by

$$ds_d^2 = \frac{r_H^2}{l^2} d\vec{X}_I^2 - \frac{(d-1)r_H^2 \tilde{\epsilon}}{l^2} dt^2 + \frac{l^2}{(d-1)\tilde{\epsilon}} d\tilde{\epsilon}^2 ,\tag{A.61}$$

where all terms are $\mathcal{O}(\tilde{\epsilon})$. To be consistent, at leading order $\tilde{\epsilon}_*$ must be considered to $\mathcal{O}(\tilde{\epsilon})$ – hence, it has the form $\tilde{\epsilon}_* = a_0 \ln(\tilde{\epsilon}) + a_1 \tilde{\epsilon} + \mathcal{O}(\tilde{\epsilon})^2$.

The near-horizon tortoise coordinate is used to convert the near-horizon metric into $(t, \tilde{\epsilon}_*)$ coordinates, thereby arriving at a conformally flat description of near-horizon AdS_d -Schwarzschild, from which the leading order string solution and the transverse equations of motion can be found. Considering Eq.(5.109) it is clear that the metric conversion factor between $(t, \tilde{\epsilon})$ and $(t, \tilde{\epsilon}_*)$ coordinates is

$$\begin{aligned}e^{\frac{r_H^2(d-1)\tilde{\epsilon}_*}{l^2}} &= e^{\frac{r_H^2(d-1)}{l^2}(a_0 \ln(\tilde{\epsilon}) + a_1 \tilde{\epsilon} + \mathcal{O}(\tilde{\epsilon})^2)} \\ &= e^{c a_0 \ln(\tilde{\epsilon})} e^{c a_1 \tilde{\epsilon}} e^{\mathcal{O}(\tilde{\epsilon})^2} \\ &= \tilde{\epsilon}^{c a_0} \left(1 + c a_1 \tilde{\epsilon} + \mathcal{O}(\tilde{\epsilon})^2\right) \left(1 + \mathcal{O}(\tilde{\epsilon})^2\right) \\ &= \tilde{\epsilon} \left(1 + \frac{(d-4)}{2} \tilde{\epsilon} + \mathcal{O}(\tilde{\epsilon})^2\right) \left(1 + \mathcal{O}(\tilde{\epsilon})^2\right) \\ &= \tilde{\epsilon} + \mathcal{O}(\tilde{\epsilon})^2 ,\end{aligned}\tag{A.62}$$

where the relevant leading order form of $\tilde{\epsilon}_*$ is used in the first equality, the constant $c = r_H^2(d-1)/l^2$ is defined in the second line, and in the third line the terms $e^{c a_1 \tilde{\epsilon}}$ and $e^{\mathcal{O}(\tilde{\epsilon})^2}$ are series expanded around $\tilde{\epsilon} = 0$. While inputting the values for c, a_0 , and a_1 (from Eq.(A.60)) into the fourth line, notice that $c a_0 = 1$ by construction. All terms of $\mathcal{O}(\tilde{\epsilon})^2$ are disregarded, in order to be consistent with the leading order near-horizon AdS_d -Schwarzschild metric. Hence, from Eq.(A.62), the inverse near-horizon tortoise coordinate is given by

$$\tilde{\epsilon} := e^{\frac{r_H^2(d-1)\tilde{\epsilon}_*}{l^2}} ,\tag{A.63}$$

at leading order; while the near-horizon tortoise coordinate is given by

$$\tilde{\epsilon}_* := \frac{l^2}{r_H^2(d-1)} \ln(\tilde{\epsilon}) ,\tag{A.64}$$

at leading order. Claims that Eq.(A.64) is the leading order contribution to the near-horizon tortoise coordinate have been made in [52]. This is, however, the first time to the author's knowledge a proof to this effect (even a heuristic one) has been provided.

A.7 Accessing the Mathematica Code

The Mathematica code used to generate all the analytic results and plots in this dissertation is provided as supplementary material.

The code is organised into four comprehensively annotated Mathematica notebooks containing: (a) the mapping of the heavy and light quark test string solutions between the worldsheet parameter space and target spacetime (`MappingWorldSheetToTarget.nb`); (b) calculations pertaining to the analysis of heavy and light quark test strings undergoing Brownian motion (`BrownianMotion.nb`); (c) the expansion of the AdS_d -Schwarzschild metric in the near-horizon region for the light quark's test string configuration (`NearHorizonAdSd.nb`); and (d) drag force calculations in AdS/CFT (`DragForce.nb`).

For readers please always check for the latest versions of the notebooks in the GitHub repository:

<https://github.com/AlexesMes/brownian-motion-of-quarks>.

This repository holds the work of A. Mes in AdS/CFT Brownian motion and contains additional resources which would be of interest.

AlexesMes / brownian-motion-of-quarks

Unwatch 1 Star 0 Fork 0

Code Issues 0 Pull requests 0 Actions Projects 0 Wiki Security 0 Insights Settings

Understanding Heavy and Light Quark Brownian Motion from AdS/CFT Edit

Manage topics

3 commits 1 branch 0 packages 0 releases 1 contributor

Branch: master New pull request Create new file Upload files Find file Clone or download

AlexesMes Uploaded Mathematica notebooks and thesis Latest commit 860afef 1 hour ago

publications	Uploaded Mathematica notebooks and thesis	1 hour ago
BrownianMotion.nb	Uploaded Mathematica notebooks and thesis	1 hour ago
DragForce.nb	Uploaded Mathematica notebooks and thesis	1 hour ago
MappingWorldSheetToTarget.nb	Uploaded Mathematica notebooks and thesis	1 hour ago
NearHorizonAdSd.nb	Uploaded Mathematica notebooks and thesis	1 hour ago
README.md	Uploaded Mathematica notebooks and thesis	1 hour ago

README.md

Understanding Heavy and Light Quark Brownian Motion from AdS/CFT

This repository holds the work of Alexes Mes in AdS/CFT Brownian Motion. The latest versions of all documents are kept here.

There is a dissertation which can be found in the publications folder of this repository.

The code is organised into four comprehensively annotated Mathematica notebooks containing: (a) the mapping of the heavy and light quark test string solutions between the worldsheet parameter space and target spacetime (`MappingWorldSheetToTarget.nb`); (b) calculations pertaining to the analysis of heavy and light quark test strings undergoing Brownian motion (`BrownianMotion.nb`); (c) the expansion of the AdS_d -Schwarzschild metric in the near-horizon region for the light quark's test string configuration (`NearHorizonAdSd.nb`); and (d) drag force calculations in AdS/CFT (`DragForce.nb`).

References

- [1] A. Aronson and T. Ludlam. Hunting the Quark Gluon Plasma: Results from the First 3 Years at the Relativistic Heavy Ion Collider (RHIC). *Upton, New York: Brookhaven National Laboratory. Formal Report: BNL-73847*, (2005). Available at [http://www.bnl.gov/npp/docs/Hunting the QGP.pdf](http://www.bnl.gov/npp/docs/Hunting_the_QGP.pdf).
- [2] U. Heinz and P. Kolb. Early Thermalization at RHIC. *Nuclear Physics A*, 702(1-4), (2002). doi: 10.1016/S0375-9474(02)00714-5. [arXiv:hep-ph/0111075](#).
- [3] M. Gyulassy. The QGP discovered at RHIC. In *Structure and Dynamics of Elementary Matter (NATO Advanced Study Institute)*, pages 159–182. Springer, (2004). [arXiv:nuc1-th/0403032](#).
- [4] U. Heinz and R. Snellings. Collective Flow and Viscosity in Relativistic Heavy-Ion Collisions. *Annual Review of Nuclear and Particle Science*, 63(1), (2013). doi: 10.1146/annurev-nucl-102212-170540. [arXiv:1301.2826 \[nuc1-th\]](#).
- [5] C. Gale, S. Jeon, and B. Schenke. Hydrodynamic Modeling of Heavy-Ion Collisions. *International Journal of Modern Physics A*, 28(11), (2013). doi: 10.1142/S0217751X13400113. [arXiv:1301.5893 \[nuc1-th\]](#).
- [6] A. Majumder and M. van Leeuwen. The Theory and Phenomenology of Perturbative QCD based Jet Quenching. *Progress in Particle and Nuclear Physics*, 66(1), (2011). doi: 10.1016/j.ppnp.2010.09.001. [arXiv:1002.2206 \[hep-ph\]](#).
- [7] W. Horowitz. Heavy Quark Production and Energy Loss. *Nuclear Physics A*, 904-905, (2013). doi: 10.1016/j.nuclphysa.2013.01.061. [arXiv:1210.8330 \[nuc1-th\]](#).
- [8] M. Djordjevic, M. Djordjevic, and B. Blagojevic. RHIC and LHC Jet Suppression in Non-central Collisions. *Physics Letters B*, 737, (2014). [arXiv:1405.4250 \[nuc1-th\]](#).
- [9] T. Hirano, P. Huovinen, and Y. Nara. Elliptic Flow in Pb+Pb Collisions at $\sqrt{s_{NN}} = 2.76$ TeV: Hybrid Model Assessment of the First Data. *Physical Review C*, 84(1), (2011). doi: 10.1103/physrevc.84.011901. [arXiv:1012.3955 \[nuc1-th\]](#).
- [10] C. Shen, U. Heinz, P. Huovinen, and H. Song. Radial and Elliptic Flow in Pb+Pb Collisions at Energies Available at the CERN Large Hadron Collider from Viscous Hydrodynamics. *Physical Review C*, 84(4), (2011). doi: 10.1103/physrevc.84.044903. [arXiv:1105.3226 \[nuc1-th\]](#).
- [11] Z. Qiu, C. Shen, and U. Heinz. Hydrodynamic Elliptic and Triangular flow in Pb–Pb Collisions at $\sqrt{s} = 2.76$ ATeV. *Physics Letters B*, 707(1), (2012). doi: 10.1016/j.physletb.2011.12.041. [arXiv:1110.3033 \[nuc1-th\]](#).
- [12] C. Gale, S. Jeon, B. Schenke, P. Tribedy, and R. Venugopalan. Event-by-event Anisotropic Flow in Heavy-Ion Collisions from Combined Yang-Mills and Viscous Fluid Dynamics. *Physical Review Letters*, 110(1), (2013). doi: 10.1103/physrevlett.110.012302. [arXiv:1209.6330 \[nuc1-th\]](#).
- [13] S. Gubser, I. Klebanov, and A. Peet. Entropy and Temperature of Black 3-Branes. *Physical Review D*, 54(6), (1996). doi: 10.1103/physrevd.54.3915. [arXiv:hep-th/9602135](#).
- [14] J. Casalderrey-Solana, H. Liu, D. Mateos, K. Rajagopal, and U. Wiedemann. *Gauge/String Duality, Hot QCD and Heavy Ion Collisions*. Cambridge University Press, (2014). [arXiv:1101.0618 \[hep-th\]](#).
- [15] R. Morad and W. Horowitz. Strong-coupling Jet Energy Loss from AdS/CFT. *Journal of High Energy Physics*, 2014(11), (2014). doi: 10.1007/jhep11(2014)017. [arXiv:1409.75455 \[hep-th\]](#).
- [16] J. Casalderrey-Solana, D. Gulhan, J. Milhano, D. Pablos, and K. Rajagopal. A Hybrid Strong/Weak Coupling Approach to Jet Quenching. *Journal of High Energy Physics*, 2014(10), (2014). doi: 10.1007/jhep10(2014)019. [arXiv:1405.3864 \[hep-ph\]](#).
- [17] W. Horowitz. Fluctuating Heavy Quark Energy Loss in a Strongly Coupled Quark-Gluon Plasma. *Physical Review D*, 91(8), (2015). doi: 10.1103/physrevd.91.085019. [arXiv:1501.04693 \[hep-ph\]](#).

- [18] G. 't Hooft. A Planar Diagram Theory for Strong Interactions. *Nuclear Physics. B*, 72(3):461–473, (1974).
- [19] I. Klebanov. TASI Lectures: Introduction to the AdS/CFT Correspondence. *Strings, Branes and Gravity*, (2001). doi: 10.1142/9789812799630_0007. arXiv:hep-th/0009139.
- [20] M. Natsuume. *AdS/CFT Duality User Guide*, volume 903. Springer, (2015). arXiv:1409.3575 [hep-th].
- [21] J. Maldacena. The large-N Limit of Superconformal Field Theories and Supergravity. *International Journal of Theoretical Physics*, 38(4):1113–1133, (1999). doi: 10.1023/a:1026654312961. arXiv:hep-th/9711200.
- [22] S. Gubser. Drag force in AdS/CFT. *Physical Review D*, 74(12), (2006). doi: 10.1103/physrevd.74.126005. arXiv:hep-th/0605182.
- [23] D. Bak, A. Karch, and L. Yaffe. Debye Screening in Strongly Coupled $\mathcal{N} = 4$ Supersymmetric Yang-Mills Plasma. *Journal of High Energy Physics*, 2007(08), (2007). doi: 10.1088/1126-6708/2007/08/049. arXiv:0705.0994 [hep-th].
- [24] E. Witten. Anti-de Sitter Space and Holography. *Advances in Theoretical and Mathematical Physics*, 2:253–291, (1998). arXiv:hep-th/9802150.
- [25] S. Gubser, I. Klebanov, and A. Polyakov. Gauge Theory Correlators from Non-critical String Theory. *Physics Letters B*, 428(1-2):105–114, (1998). doi: 10.1016/s0370-2693(98)00377-3. arXiv:hep-th/9802109.
- [26] O. Aharony and E. Witten. Anti-de Sitter Space and the Center of the Gauge Group. *Journal of High Energy Physics*, 1998(11):018–018, (1998). doi: 10.1088/1126-6708/1998/11/018. arXiv:hep-th/9807205.
- [27] O. Aharony, S. Gubser, J. Maldacena, H. Ooguri, and Y. Oz. Large N Field Theories, String Theory and Gravity. *Physics Reports*, 323(3-4):183–386, (2000). doi: 10.1016/s0370-1573(99)00083-6. arXiv:hep-th/9905111.
- [28] G. Policastro, D. Son, and A. Starinets. Shear Viscosity of Strongly Coupled $\mathcal{N} = 4$ Supersymmetric Yang-Mills Plasma. *Physical Review Letters*, 87(8), (2001). doi: 10.1103/physrevlett.87.081601. arXiv:hep-th/0104066.
- [29] **PHENIX** Collaboration, S. Adler, and et al. Elliptic Flow of Identified Hadrons in Au+Au Collisions at $\sqrt{s_{NN}} = 200$ GeV. *Physical Review Letters*, 91(18), (2003). doi: 10.1103/physrevlett.91.182301. arXiv:nucl-ex/0305013.
- [30] **STAR** Collaboration, J. Adams, and et al. Azimuthal Anisotropy in Au+Au collisions at $\sqrt{s_{NN}} = 200$ GeV. *Physical Review C*, 72(1), (2005). doi: 10.1103/physrevc.72.014904. arXiv:nucl-ex/0409033.
- [31] P. Kovtun, D. Son, and A. Starinets. Holography and Hydrodynamics: Diffusion on Stretched Horizons. *Journal of High Energy Physics*, 2003(10):064–064, (2003). doi: 10.1088/1126-6708/2003/10/064. arXiv:hep-th/0309213.
- [32] P. Kovtun, D. Son, and A. Starinets. Viscosity in Strongly Interacting Quantum Field Theories from Black Hole Physics. *Physical Review Letters*, 94(11), (2005). doi: 10.1103/physrevlett.94.111601. arXiv:hep-th/0405231.
- [33] A. Buchel and J. Liu. Universality of the Shear Viscosity from Supergravity Duals. *Physical Review Letters*, 93(9), (2004). doi: 10.1103/physrevlett.93.090602. arXiv:hep-th/0311175.
- [34] A. Buchel. On Universality of Stress-Energy Tensor Correlation Functions in Supergravity. *Physics Letters B*, 609(3-4):392–401, (2005). doi: 10.1016/j.physletb.2005.01.052. arXiv:hep-th/0408095.
- [35] C. Herzog, A. Karch, P. Kovtun, C. Kozcaz, and L. Yaffe. Energy Loss of a Heavy Quark Moving through $\mathcal{N} = 4$ Supersymmetric Yang-Mills Plasma. *Journal of High Energy Physics*, 2006(07):013, (2006). doi: 10.1088/1126-6708/2006/07/013. arXiv:hep-th/0605158.

- [36] H. Liu, K. Rajagopal, and U. Wiedemann. Calculating the Jet Quenching Parameter. *Physical Review Letters*, 97(18), (2006). doi: 10.1103/physrevlett.97.182301. [arXiv:hep-ph/0605178](#).
- [37] C. Herzog. Energy Loss of a Heavy Quark from Asymptotically AdS Geometries. *Journal of High Energy Physics*, 2006(09):032–032, (2006). doi: 10.1088/1126-6708/2006/09/032. [arXiv:hep-th/0605191](#).
- [38] J. Casalderrey-Solana and D. Teaney. Heavy Quark Diffusion in Strongly Coupled $\mathcal{N} = 4$ Yang Mills. *Physical Review D*, 74(8), (2006). doi: 10.1103/physrevd.74.085012. [arXiv:hep-ph/0605199](#).
- [39] H. Liu, K. Rajagopal, and U. Wiedemann. Wilson Loops in Heavy Ion Collisions and their Calculation in AdS/CFT. *Journal of High Energy Physics*, 2007(03):066–066, (2007). doi: 10.1088/1126-6708/2007/03/066. [arXiv:hep-ph/0612168](#).
- [40] J. Casalderrey-Solana and D. Teaney. Transverse Momentum Broadening of a Fast Quark in a $\mathcal{N} = 4$ Yang-Mills Plasma. *Journal of High Energy Physics*, 2007(04):039–039, (2007). doi: 10.1088/1126-6708/2007/04/039. [arXiv:hep-th/0701123](#).
- [41] S. Gubser. Momentum Fluctuations of Heavy Quarks in the Gauge-String Duality. *Nuclear Physics B*, 790(1-2):175–199, (2008). doi: 10.1016/j.nuclphysb.2007.09.017. [arXiv:hep-th/061214](#).
- [42] J. de Boer, V. Hubeny, M. Rangamani, and M. Shigemori. Brownian Motion in AdS/CFT. *Journal of High Energy Physics*, 2009(07):094–094, (2009). doi: 10.1088/1126-6708/2009/07/094. [arXiv:0812.5112 \[hep-th\]](#).
- [43] D. Son and D. Teaney. Thermal Noise and Stochastic Strings in AdS/CFT. *Journal of High Energy Physics*, 2009(07), (2009). doi: 10.1088/1126-6708/2009/07/021. [arXiv:0901.2338 \[hep-th\]](#).
- [44] W. Fischler, J. Pedraza, and W. Tangarife Garcia. Holographic Brownian Motion in Magnetic Environments. *Journal of High Energy Physics*, 2012(12), (2012). doi: 10.1007/jhep12(2012)002. [arXiv:1209.1044 \[hep-th\]](#).
- [45] A. Atmaja. Holographic Brownian Motion in Two Dimensional Rotating Fluid. *Journal of High Energy Physics*, 2013(4), (2013). doi: 10.1007/jhep04(2013)021. [arXiv:1212.5319 \[hep-th\]](#).
- [46] A. Atmaja, J. de Boer, and M. Shigemori. Holographic Brownian Motion and Time Scales in Strongly Coupled Plasmas. *Nuclear Physics B*, 880:23–75, (2014). doi: 10.1016/j.nuclphysb.2013.12.018. [arXiv:1002.2429 \[hep-th\]](#).
- [47] P. Banerjee and B. Sathiapalan. Holographic Brownian Motion in $1 + 1$ Dimensions. *Nuclear Physics B*, 884, (2014). doi: 10.1016/j.nuclphysb.2014.04.016. [arXiv:1308.3352 \[hep-th\]](#).
- [48] S. Chakraborty, S. Chakraborty, and N. Haque. Brownian Motion in Strongly Coupled, Anisotropic Yang-Mills Plasma: A Holographic Approach. *Physical Review D*, 89(6), (2014). doi: 10.1103/physrevd.89.066013. [arXiv:1311.5023 \[hep-th\]](#).
- [49] J. Sadeghi, F. Pourasadollah, and H. Vaez. Holographic Brownian Motion in Three-Dimensional Gödel Black Hole. *Advances in High Energy Physics*, 2014, (2014). doi: 10.1155/2014/762151. [arXiv:1308.2483 \[hep-th\]](#).
- [50] J. Sadeghi, B. Pourhassan, and F. Pourasadollah. Holographic Brownian motion in $2 + 1$ Dimensional Hairy Black Holes. *The European Physical Journal C*, 74(3), (2014). doi: 10.1140/epjc/s10052-014-2793-7. [arXiv:1312.4906 \[hep-th\]](#).
- [51] W. Fischler, P. Nguyen, J. Pedraza, and W. Tangarife. Fluctuation and Dissipation in de Sitter Space. *Journal of High Energy Physics*, 2014(8), (2014). doi: 10.1007/jhep08(2014)028. [arXiv:1404.0347 \[hep-th\]](#).
- [52] R. Moerman and W. Horowitz. A Semi-classical Recipe for Wobbly Limp Noodles in Partonic Soup. *arXiv preprint*, (2016). [arXiv:1605.09285 \[hep-th\]](#).
- [53] R. Brown. A Brief Account of Microscopical Observations made in the Months of June, July and August 1827, on the Particles contained in the Pollen of Plants; and on the General Existence of Active Molecules in Organic and Inorganic Bodies. *The Philosophical Magazine*, 4(21):161–173, (1828).

- [54] A. Karch and E. Katz. Adding Flavor to AdS/CFT. *Journal of High Energy Physics*, 2002(06), (2002). doi: 10.1088/1126-6708/2002/06/043. [arXiv:hep-th/0205236](#).
- [55] A. Polyakov. String Theory and Quark Confinement. *Nuclear Physics B*, 68(1-3):1–8, (1998). doi: 10.1016/S0920-5632(98)00135-2. [arXiv:hep-th/9711002](#).
- [56] G. 't Hooft. Dimensional Reduction in Quantum Gravity. *Salamfestschrift: a collection of talks*, 4 (A):1, (1993). [arXiv:gr-qc/9310026](#).
- [57] L. Susskind. The World as a Hologram. *Journal of Mathematical Physics*, 36(11):6377–6396, (1995). doi: 10.1063/1.531249. [arXiv:hep-th/9409089](#).
- [58] C. Thorn. Reformulating String Theory with the $1/N$ Expansion. In *Proceedings of the first international Sakharov conference on physics*, (1992). [arXiv:hep-th/9405069](#).
- [59] G. Gibbons and K. Maeda. Black Holes and Membranes in Higher-Dimensional Theories with Dilaton Fields. *Nuclear Physics B*, 298(4):741–775, (1988).
- [60] G. Horowitz and A. Strominger. Black Strings and P-branes. *Nuclear Physics B*, 360(1):197–209, (1991).
- [61] D. Garfinkle, G. Horowitz, and A. Strominger. Charged Black Holes in String Theory. *Physical Review D*, 43(10):3140, (1991).
- [62] C. Ballón Bayona and N. Braga. Anti-de Sitter Boundary in Poincaré Coordinates. *General Relativity and Gravitation*, 39(9), (2007). doi: 10.1007/s10714-007-0446-y. [arXiv:hep-th/0512182](#).
- [63] D. Mateos. String Theory and Quantum Chromodynamics. *Classical and Quantum Gravity*, 24(21), (2007). doi: 10.1088/0264-9381/24/21/s01. [arXiv:0709.1523 \[hep-th\]](#).
- [64] E. Witten. Anti-de Sitter Space, Thermal Phase Transition, and Confinement in Gauge Theories. *Adv. Theor. Math. Phys.*, 2(IASSNS-HEP-98-21):89–117, (1998). [arXiv:hep-th/9803131](#).
- [65] M. Douglas and D. Taylor. Branes in the Bulk of Anti-de Sitter Space, (1998). [arXiv:hep-th/9807225](#).
- [66] S. Das. Holograms of Branes in the Bulk and Acceleration terms in SYM Effective Action. *Journal of High Energy Physics*, 1999(06), (1999). doi: 10.1088/1126-6708/1999/06/029. [arXiv:hep-th/9905037](#).
- [67] F. Gonzalez-Rey, B. Kulik, I. Park, and M. Roček. Self-dual Effective Action of $\mathcal{N} = 4$ super-Yang-Mills. *Nuclear Physics B*, 544(1-2), (1999). doi: 10.1016/S0550-3213(99)00046-2. [arXiv:hep-th/9810152](#).
- [68] M. Tanabashi et al. Particle Data Group Review. *Physical Review D*, 98:030001, (2018).
- [69] L. Alday and J. Maldacena. Gluon Scattering Amplitudes at Strong Coupling. *Journal of High Energy Physics*, 2007(06):064, (2007). [arXiv:0705.0303 \[hep-th\]](#).
- [70] S. Hartnoll, C. Herzog, and G. Horowitz. Building a Holographic Superconductor. *Physical Review Letters*, 101(3), (2008). doi: 10.1103/physrevlett.101.031601. [arXiv:0803.3295 \[hep-th\]](#).
- [71] S. Gubser. Breaking an Abelian Gauge Symmetry Near a Black Hole Horizon. *Physical Review D*, 78 (6), (2008). doi: 10.1103/physrevd.78.065034. [arXiv:0801.2977 \[hep-th\]](#).
- [72] K. Maeda, M. Natsuume, and T. Okamura. Universality Class of Holographic Superconductors. *Physical Review D*, 79(12), (2009). doi: 10.1103/physrevd.79.126004. [arXiv:0904.1914 \[hep-th\]](#).
- [73] S. Hartnoll. Lectures on Holographic Methods for Condensed Matter Physics. *Classical and Quantum Gravity*, 26(22):224002, (2009). [arXiv:0903.3246 \[hep-th\]](#).
- [74] A. Einstein. On the Motion of Small Particles Suspended in Liquids at Rest Required by the Molecular-Kinetic Theory of Heat. *Annalen der physik*, 17(549-560):208, (1905).
- [75] M. Smoluchowski. On the Kinetic Theory of the Brownian Molecular Motion and of Suspensions. *Annalen der Physik*, 21:756–780, (1906).

- [76] S. Brush. A History of Random Processes: I. Brownian Movement from Brown to Perrin. *Archive for History of Exact Sciences*, 5(1):1–36, (1968).
- [77] L. Bachelier. Theory of Speculation. *Dimson, E. and M. Mussavian (1998), A brief history of market efficiency, European Financial Management*, 4(1):91–193, (1990).
- [78] N. Wiener. Differential-Space. *Journal of Mathematics and Physics*, 2(1-4):131–174, (1923).
- [79] P. Langevin. “On the theory of Brownian Motion” (“Sur la Théorie du Mouvement Brownien,” *cr acad. sci.(paris)* 146, 530–533 (1908)). *American Journal of Physics*, 65(11):1079–1081, (1997).
- [80] G. Uhlenbeck and L. Ornstein. On the Theory of the Brownian Motion. *Physical Review*, 36(5):823, (1930).
- [81] N. Pottier. *Nonequilibrium Statistical Physics: Linear Irreversible Processes*. Oxford University Press, (2010).
- [82] R. Kubo. The Fluctuation-Dissipation Theorem. *Reports on progress in physics*, 29(1):255, (1966).
- [83] L. Ornstein. On the Brownian Motion. *Acad. Amst*, 26:1005, (1917).
- [84] H. Mori. Transport, Collective Motion, and Brownian motion. *Progress of theoretical physics*, 33(3): 423–455, (1965).
- [85] N. Wiener. Generalised Harmonic Analysis. *Acta mathematica*, 55:117–258, (1930).
- [86] M. Wang and G. Uhlenbeck. On the Theory of the Brownian Motion II. *Reviews of modern physics*, 17(2-3):323, (1945).
- [87] J. Dunkel and P. Hänggi. Relativistic Brownian Motion. *Physics Reports*, 471(1):1–73, (2009). doi: 10.1016/j.physrep.2008.12.001. [arXiv:0812.1996](https://arxiv.org/abs/0812.1996) [hep-th].
- [88] R. Kubo, M. Toda, and N. Hashitsume. *Statistical Physics II: Nonequilibrium Statistical Mechanics*, volume 31. Springer Science & Business Media, (2012).
- [89] L. Brink, P. Di Vecchia, and P. Howe. A Locally Supersymmetric and Reparametrization Invariant Action for the Spinning String. *Physics Letters B*, 65(5):471–474, (1976).
- [90] S. Deser and B. Zumino. A Complete Action for the Spinning String. *Physics Letters B*, 65(4): 369–373, (1976).
- [91] A. Polyakov. Quantum Geometry of Bosonic Strings. In *Supergravities in Diverse Dimensions: Commentary and Reprints (In 2 Volumes)*, pages 1197–1200. World Scientific, (1989).
- [92] B. Zwiebach. *A First Course in String Theory*. Cambridge University Press, (2004).
- [93] J. Polchinski. *String Theory: Volume 1, An Introduction To The Bosonic String*. Cambridge University Press, (1998).
- [94] Y. Nambu. Duality and Hadrodynamics, Lectures at the Copenhagen High Energy Symposium, 1970. In *Broken Symmetry: Selected Papers of Y Nambu*, pages 280–301. World Scientific, (1995).
- [95] T. Gotō. Relativistic Quantum Mechanics of One-dimensional Mechanical Continuum and Subsidiary Condition of Dual Resonance Model. *Progress of Theoretical Physics*, 46(5):1560–1569, (1971).
- [96] S. Carroll. *Spacetime and Geometry: An Introduction to General Relativity*. Addison Wesley, (2004).
- [97] Wolfram Research, Inc. Mathematica, Version 11.3, (2018). Champaign, IL.
- [98] A. Rich, P. Scheibe, and N. Abbasi. Rule-based Integration: An Extensive System of Symbolic Integration Rules. *Journal of Open Source Software*, 3(32):1073, (2018). doi: 10.21105/joss.01073. Available at <https://doi.org/10.21105/joss.01073>.
- [99] M. Bañados, C. Teitelboim, and J. Zanelli. Black Hole in Three-Dimensional Spacetime. *Physical Review Letters*, 69(13):1849–1851, (1992). doi: 10.1103/physrevlett.69.1849. [arXiv:hep-th/9204099](https://arxiv.org/abs/hep-th/9204099).

- [100] W. Bardeen, I. Bars, A. Hanson, and R. Peccei. Study of the Longitudinal Kink Modes of the String. *Physical Review D*, 13(8):2364, (1976).
- [101] S. Gubser, D. Gulotta, S. Pufu, and F. Rocha. Gluon Energy Loss in the Gauge-String Duality. *Journal of High Energy Physics*, 2008(10):052–052, (2008). doi: 10.1088/1126-6708/2008/10/052. arXiv:0803.1470 [hep-th].
- [102] P. Chesler, K. Jensen, and A. Karch. Jets in Strongly Coupled $\mathcal{N} = 4$ Yang-Mills Theory. *Physical Review D*, 79(2), (2009). doi: 10.1103/physrevd.79.025021. arXiv:0804.3110 [hep-th].
- [103] P. Chesler, K. Jensen, A. Karch, and L. Yaffe. Light Quark Energy Loss in Strongly Coupled $\mathcal{N} = 4$ Supersymmetric Yang-Mills Plasma. *Physical Review D*, 79(12), (2009). doi: 10.1103/physrevd.79.125015. arXiv:0810.1985 [hep-th].
- [104] A. Ficnar. AdS/CFT Energy Loss in Time-Dependent String Configurations. *Physical Review D*, 86(4), (2012). doi: 10.1103/physrevd.86.046010. arXiv:1201.1780 [hep-th].
- [105] A. Ficnar, J. Noronha, and M. Gyulassy. Falling Strings and Light Quark Jet Quenching at LHC. *Nuclear Physics A*, 910-911:252–255, (2013). doi: 10.1016/j.nuclphysa.2012.12.030. arXiv:1208.0305 [hep-th].
- [106] A. Ficnar and S. Gubser. Finite Momentum at String Endpoints. *Physical Review D*, 89(2), (2014). doi: 10.1103/physrevd.89.026002. arXiv:1306.6648 [hep-th].
- [107] I. Bars. Classical Solutions of 2D String Theory in any Curved Spacetime. In *Second Paris Cosmology Colloquium*, page 399. World Scientific, (1994). arXiv:hep-th/9411217.
- [108] I. Bars and J. Schulze. Folded Strings Falling into a Black Hole. *Physical Review D*, 51(4):1854–1868, (1995). doi: 10.1103/physrevd.51.1854. arXiv:hep-th/9405156.
- [109] E. Álvarez and J. Conde. Are the String and Einstein Frames Equivalent? *Modern Physics Letters A*, 17(07):413–420, (2002). doi: 10.1142/s0217732302006606. arXiv:gr-qc/0111031.
- [110] T. Matsuo, D. Tomino, and W. Wen. Drag Force in SYM Plasma with B Field from AdS/CFT. *Journal of High Energy Physics*, 2006(10), (2006). doi: 10.1088/1126-6708/2006/10/055. arXiv:hep-th/0607178.
- [111] K. Kim, J. Shock, and J. Tarrío. The Open String Membrane Paradigm with External Electromagnetic Fields. *Journal of High Energy Physics*, 2011(6), (2011). doi: 10.1007/jhep06(2011)017. arXiv:1103.4581 [hep-th].
- [112] M. Cederwall, A. von Gussich, A. Mikovic, B. Nilsson, and A. Westerberg. On the Dirac-Born-Infeld Action for D-branes. *Physics Letters B*, 390(1-4), (1997). doi: 10.1016/s0370-2693(96)01367-6. arXiv:hep-th/9606173.